

MATERIAL PROPERTIES TO MINIMIZE DISTRESS IN ZERO-MAINTENANCE PAVEMENTS

Vol. 2. Parameter Study

March 1981

Final Report



Document is available to the public through
the National Technical Information Service,
Springfield, Virginia 22161



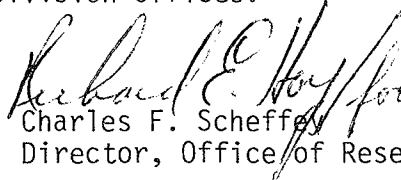
REPRODUCED BY
**NATIONAL TECHNICAL
INFORMATION SERVICE**
U.S. DEPARTMENT OF COMMERCE
SPRINGFIELD, VA 22161

Prepared for
FEDERAL HIGHWAY ADMINISTRATION
Offices of Research & Development
Structures and Applied Mechanics Division
Washington, D.C. 20590

FOREWORD

In Volume 2 of this report the results of a study to optimize currently available pavement materials were presented. Possible material properties were developed for input to mechanistic predictive design procedures. The dependent variables were certain modes of distress which had to be kept below acceptable levels for "Zero-Maintenance" performance. The major output was ranges of material properties necessary to control the pavement damage requiring maintenance.

Sufficient copies of this report are being distributed by FHWA Bulletin to provide a minimum of one copy to each Regional office, one copy to each Division office, and one copy to each State highway agency. Direct distribution is being made to the Division offices.


Charles F. Scheffey
Director, Office of Research

NOTICE

This document is disseminated under the sponsorship of the Department of Transportation in the interest of information exchange. The United States Government assumes no liability for its contents or use thereof.

The contents of this report reflect the views of Austin Research Engineers, Inc., which is responsible for the facts and the accuracy of the data presented herein. The contents do not necessarily reflect the official views or policy of the Department of Transportation. This report does not constitute a standard, specification, or regulation.

The United States Government does not endorse products or manufacturers. Trade or manufacturer's names appear herein only because they are considered essential to the object of this document.

1. Report No. FHWA/RD-80/156		2. Government Accession No.		3. Recipient's Catalog No. PB82 1 1291 3	
4. Title and Subtitle MATERIAL PROPERTIES TO MINIMIZE DISTRESS IN ZERO-MAINTENANCE PAVEMENTS VOLUME 2. PARAMETER STUDY				5. Report Date March 1981	
				6. Performing Organization Code 35E4-032 U287017	
7. Author(s) Freddy L. Roberts, Thomas W. Kennedy, Gary E. Elkins				8. Performing Organization Report No.	
9. Performing Organization Name and Address Austin Research Engineers Inc 2600 Dellana Lane Austin, Texas 78746				10. Work Unit No. (TRAIS) 35E4-032	
				11. Contract or Grant No. DOT-FH-11-9349	
12. Sponsoring Agency Name and Address Federal Highway Administration Office of Research Structures and Applied Mechanics Division Washington, D.C. 20590				13. Type of Report and Period Covered Final Report	
				14. Sponsoring Agency Code 801150	
15. Supplementary Notes Mr. Kenneth C. Clear (HRS-22) FHWA Contract Manager					
16. Abstract <p>This second volume provides a summary of a detailed study to 1) identify distresses that cause significant loss of serviceability and/or maintenance in pavements; 2) identify material properties that significantly influence the occurrence of distress; 3) select the best theoretical or empirical models for predicting distress using material properties and other engineering parameters; and 4) utilize the selected models to study the effects of the significant distresses and to optimize material properties for zero maintenance pavements.*</p> <p>The emphasis of this second volume was a discussion of the results of a parameter study with selected models using a range of material properties available in conventional and nonconventional pavement materials. The effects of varying these material properties on various distresses were evaluated and the tradeoffs required were discussed. The result from these studies was the development of a set of material properties that the models indicate were adequate to ensure design of zero maintenance flexible, rigid, and composite pavements.</p> <p>*Volume 1 published as FHWA/RD-80/155.</p>					
17. Key Words zero-maintenance, distress, fatigue cracking, low-temperature cracking, reflection cracking, pavement models, pavement response, rutting, shrinkage cracking, material properties, pavements			18. Distribution Statement No restrictions. This document is available to the public through the National Technical Information Service, Springfield, Virginia 22161		
19. Security Classif. (of this report) Unclassified		20. Security Classif. (of this page) Unclassified		21. No. of Pages 180	22. Price

PREFACE

This is the second of two volumes for this research report. The overall project goal is to develop a set of material properties for use in design of zero-maintenance pavements. In the first volume, project staff (1) identified significant material properties for each distress and pavement type, (2) selected the best distress models to use in studying the effect of these material properties on distress, and (3) recommended a research approach for the remaining project work.

The results of the model studies and analyses are presented in this second volume. The effect of variations in the material properties on distress are included and discussed. Finally, an analysis was conducted to evaluate the tradeoffs of material properties and distress production in order to develop a recommended set of material properties for use in design of zero-maintenance pavements.

TABLE OF CONTENTS

	Page
CHAPTER 1. INTRODUCTION	1
OUTLINE OF TASK	1
RESEARCH APPROACH	2
OVERVIEW OF REPORT	2
 CHAPTER 2. BACKGROUND AND DESCRIPTION OF PREVIOUS PROJECT WORK	 6
DISTRESS	6
PAVEMENT RESPONSE AND DISTRESS MODELS	7
Pavement Structural Models Utilizing	
Elastic Theory	8
Distress Models for Flexible Pavements	9
Distress Models for Composite Pavements	18
Distress Models for Rigid Pavements	19
Selected Models	22
MATERIAL PROPERTIES	22
 CHAPTER 3. DESCRIPTION OF MODEL INPUTS	 30
COMMON INPUTS	30
Environmental Factors	30
Drainage	32
Substructure	32
Environmental Layer	33
Traffic Levels	34
FLEXIBLE PAVEMENT INPUTS	34
Pavement Thickness	34
Material Properties - VESYS	38
Material Properties - Low Temperature Cracking	59
Material Properties - Loss of Skid Resistance	62
RIGID PAVEMENT INPUTS	62
Pavement Thickness	66
Material Properties - JCP and JRCP	66
Material Properties - CRCP	72
COMPOSITE PAVEMENT INPUTS	74
Pavement Thickness	74
Fatigue Cracking	74
Reflection Cracking	78
 CHAPTER 4. FLEXIBLE PAVEMENT STUDY	 81
FATIGUE CRACKING	81
RUTTING	87
LOW TEMPERATURE CRACKING	96
SKID RESISTANCE	108

TABLE OF CONTENTS (Continued)

CHAPTER 5. RIGID PAVEMENT STUDY 112
 DISTRESS STUDIES OF JRCP AND JCP 112
 Fatigue Cracking 112
 Joint or Crack Faulting 116
 Joint Spalling 117
 Low Temperature and Shrinkage Cracking 118
 DISTRESS STUDIES OF CRCP 118
 Fatigue Cracking 118
 Punchouts and Crack Spalling 120
 Low Temperature and Shrinkage Cracking 128

CHAPTER 6. COMPOSITE PAVEMENT STUDY 140
 FATIGUE CRACKING 140
 RUTTING 142
 REFLECTION CRACKING 142
 Horizontal Tensile Strain 146
 Vertical Shear 146

CHAPTER 7. DISCUSSION, RECOMMENDATIONS, AND CONCLUSIONS 157
 DISCUSSION AND RECOMMENDATIONS 157
 Flexible Pavements 157
 Rigid Pavements 160
 Composite Pavements 161
 CONCLUSIONS 162

REFERENCES 164

LIST OF TABLES

Table 1. Significant distresses selected for further study 3
 Table 2. Models selected for parameter studies for each distress type. 4
 Table 3. Distress, related material properties and distress models
 selected for flexible pavements 23
 Table 4. Distress, related material properties and distress models
 selected for jointed reinforced concrete pavement 24
 Table 5. Distress, related material properties and distress models
 selected for jointed concrete pavement. 25
 Table 6. Distress, related material properties and distress models
 selected for continuously reinforced concrete pavement. 26
 Table 7. Distress, related material properties and distress models
 selected for composite pavements. 27

LIST OF TABLES (continued)

Table 8.	Material properties considered to affect distresses in premium pavements	28
Table 9.	Studies from which K_1 , K_2 values were obtained.	39
Table 10.	Test data for fatigue coefficients vs. temperature.	43
Table 11.	Log K_1 (70°F) and K_2 (70°F) values selected for use in the parameter study ¹ for flexible ² pavements.	47
Table 12.	Fatigue constants selected for the four environmental zones and the four seasons.	48
Table 13.	Combination of ALPHA and GNU selected for the flexible pavement parameter study	58
Table 14.	Material property ranges for future pavement low temperature cracking studies.	60
Table 15.	Environmental zone dependent input variables for low temperature cracking study.	63
Table 16.	Input variables held constant throughout low temperature cracking analysis	64
Table 17.	Material property values for reduced skid resistance model study.	65
Table 18.	Material properties varied in PCC pavement studies.	73
Table 19.	Values of factors held constant during JCP and JRCP analysis.	73
Table 20.	Combinations of material properties selected for CRCP studies	75
Table 21.	Constant inputs for CRCP low temperature and shrinkage cracking studies.	76
Table 22.	Inputs for composite pavement reflection cracking study	79
Table 23.	Material properties varied for each environment used in the reflection cracking study	80
Table 24.	Time required in years for 5 percent fatigue cracking to occur.	86
Table 25.	Predicted low temperature cracking, ft/1000 ft ²	102
Table 26.	Required asphalt properties to prevent low temperature cracking using the Shahin-McCullough aging models	109
Table 27.	Summary of fatigue cracking results for JRCP and JCP.	113

LIST OF TABLES (continued)

Table 28.	Summary of fatigue cracking results for CRCP	121
Table 29.	Effects of unit changes in input variables on crack spacing and crack width.	139
Table 30.	Summary of times at which rutting reached 0.5 in (13mm) for composite pavements thickness and material combinations	143
Table 31.	Summary of times at which rutting reached 0.5 in (13mm) for flexible pavement material property combinations	145
Table 32.	Horizontal strain results from reflection cracking study	147
Table 33.	Stress results from reflection cracking study, psi	148
Table 34.	Fatigue equations based on indirect tensile and beam specimens .	154
Table 35.	Maximum mix stiffness for selecting asphalt cement grade	159

LIST OF FIGURES

Figure 1.	Freezing index map of the United States	31
Figure 2.	Cross section optimization based on SAMP6	36
Figure 3.	ACP surface vs. granular base thickness	37
Figure 4.	Individual relationships between K_2 and $\log K_1$ for various mixtures and test procedures.	41
Figure 5.	Combined relationships between K_1 and K_2 from various studies, as reported by Kennedy	42
Figure 6.	Relation between normalized K_1 and temperature.	44
Figure 7.	Relationship between normalized K_2 and temperature.	45
Figure 8.	Relationship selected for modifying stiffness as a function of temperature	50
Figure 9.	Assumed logarithmic relationship between permanent strain and number of load repetitions	52
Figure 10.	Range of practical GNU and ALPHA values for asphalt concrete. .	53
Figure 11.	Relationship between ALPHA and stress difference for different test methods.	54

LIST OF FIGURES (continued)

Figure 12. Relationship between GNU and stress difference for various test methods 55

Figure 13. Relationship between GNU and ALPHA for different test methods. . 57

Figure 14. Comparison of several fatigue curves based on field performance. 67

Figure 15. Fatigue relationships for concrete based on various laboratory test procedures. 68

Figure 16. Stress factors versus distance from edge of rigid slab 70

Figure 17. Predicted damage ratios versus distance from rigid pavement edge.71

Figure 18. Fatigue in flexible pavements for various K_1 , K_2 combinations and surface thicknesses, -zone: wet-freeze¹ 82

Figure 19. Fatigue in flexible pavements for various K_1 , K_2 combinations and surface thicknesses, -zone: dry-freeze¹ 83

Figure 20. Fatigue in flexible pavements for various K_1 , K_2 combinations and surface thicknesses, -zone: wet-no freeze² 84

Figure 21. Fatigue in flexible pavements for various K_1 , K_2 combinations and surface thicknesses, -zone: dry-no freeze² 85

Figure 22. Effect of fatigue constants on fatigue life of flexible pavements, -zone: wet-freeze. 88

Figure 23. Effect of fatigue constants on fatigue life of flexible pavements, -zone: dry-no freeze 89

Figure 24. Effect of fatigue constants on fatigue life of flexible pavements, -zone: wet-no freeze 90

Figure 25. Effect of fatigue constants on fatigue life of flexible pavements, -zone: dry-freeze 91

Figure 26. Rutting versus time for ALPHA 0.7, all GNUs, and 13 in (330 mm) surface 92

Figure 27. Rutting versus time for ALPHA 0.7, all GNUs, and 18 in (457 mm) surface 93

Figure 28. Rutting versus time for ALPHA 0.8, all GNUs, and 13 in (330 mm) surface 94

Figure 29. Rutting versus time for ALPHA 0.8, all GNUs, and 18 in (457 mm) surface 95

LIST OF FIGURES (continued)

Figure 30.	Effect of permanent deformation parameters on rutting in flexible pavements: zone: wet-freeze	97
Figure 31.	Effect of permanent deformation parameters on rutting in flexible pavements: zone: dry-freeze	98
Figure 32.	Effect of permanent deformation parameters on rutting in flexible pavements: zone: wet-no freeze	99
Figure 33.	Effect of permanent deformation parameters on rutting in flexible pavements: zone: dry-no freeze	100
Figure 34.	Parameter combinations meeting zero maintenance criteria by environmental zone	101
Figure 35.	Low temperature cracking versus the assumed asphalt cement type	104
Figure 36.	Low temperature cracking versus mix tensile strength	105
Figure 37.	Low temperature cracking versus AC thermal coefficient	106
Figure 38.	Low temperature cracking versus asphalt concrete stiffness	107
Figure 39.	Range of acceptable combinations of SN_{40} and B_{field} for Steittle-McCullough skid resistance model	110
Figure 40.	Influence of concrete modulus of elasticity on JRCP and JCP fatigue cracking	114
Figure 41.	Influence of subbase modulus of elasticity on JRCP and JCP fatigue cracking	115
Figure 42.	A comparison between the tensile strength of concrete at the surface for spalled and non-spalled areas.	119
Figure 43.	Influence of concrete modulus of elasticity on CRCP fatigue cracking	122
Figure 44.	Influence of subbase modulus of elasticity on CRCP fatigue cracking	123
Figure 45.	Stress in X and Y direction versus crack spacing for a 279 mm (11 in) thick slab	124
Figure 46.	A comparison between the crack widths for spalled and non-spalled areas	126

LIST OF FIGURES (continued)

Figure 47.	Allowable crack width for control of spalling	127
Figure 48.	Effects of concrete strength, shrinkage characteristics and thermal coefficients on crack spacing and crack width in the dry-freeze zone	129
Figure 49.	Effects of concrete strength, shrinkage characteristics and thermal coefficients on crack spacing and crack width in the wet-freeze zone	130
Figure 50.	Effects of concrete strength, shrinkage and thermal coefficients on steel stress at the crack for CRCP	131
Figure 51.	Effects of material property variables on crack width by crack spacing for the dry-freeze zone	133
Figure 52.	Crack spacing and crack width versus magnitude of temperature drop for low-strength concrete	134
Figure 53.	Summary of crack spacing and crack width showing regions of acceptability for zero maintenance pavements	136
Figure 54.	Summary of crack spacing and steel stresses showing regions of acceptability for zero maintenance pavements	137
Figure 55.	Composite pavement fatigue cracking results for a 6 inch (152 mm) asphalt concrete over an 8 inch (203 mm) slab and an 8 inch (203 mm) base	141
Figure 56.	Rutting versus time for ALPHA, GNU combinations - composite pavement in wet-freeze zone	144
Figure 57.	Induced horizontal tensile stress in unbound asphalt concrete layer: zone: wet-freeze	149
Figure 58.	Effect of bond on horizontal tensile stress: zone: wet-freeze .	150
Figure 59.	Shear strain in asphalt concrete surface layer as a function of ACP dynamic modulus and percent load transfer of the underlying joint	152
Figure 60.	Shear strain in asphalt concrete surface layer as a function of the ACP dynamic modulus and percent load transfer of the joint	156

CHAPTER 1. INTRODUCTION

The Federal Highway Administration has pursued for several years multiple research studies aimed at producing premium pavement structures for heavily traveled routes. The objectives of the efforts have been to minimize pavement maintenance, which disrupts traffic flow and thus creates hazards and high user costs. This general research effort has been designated as "Premium Pavements for Zero Maintenance." Its goal is the development of pavement structures that will be maintenance-free for a minimum of 20 years and will require only routine maintenance for 10 to 20 years thereafter.

Research is underway for upgrading conventional structures by use of improved paving materials or new materials such as sulphur-asphalt and sulflex. Field surveys have been conducted to study the nature of existing pavements that have performed satisfactorily with essentially zero maintenance. These studies have produced valuable information for use on this and other zero maintenance research projects.

This Research Project entitled "Material Property Requirements for Zero-Maintenance Pavements" has as its goal the identification of material properties that will provide optimal performance in flexible, rigid, and composite premium, or zero maintenance, pavements.

OUTLINE OF TASKS

This effort was subdivided into the following tasks:

1. Develop a complete list of distresses for each pavement type, engineering properties related to these distress types, and factors affecting the engineering properties of the materials,
2. Assess the relative importance of distress types in terms of frequency of occurrence and to evaluate their effect on pavement serviceability, i.e., does it result in a need for immediate or long-term maintenance or does the distress produce secondary distresses,
3. Assess the relative importance of material properties on each of the important distresses in Task 2,
4. Summarize the distresses and related material properties having sufficient impact on pavement performance and maintenance requirements to warrant further consideration,
5. Review the analytical models capable of modeling distresses and select those best suited to an evaluation of the effect of material properties on the production of distress,

6. Establish ranges of material properties and evaluate the effect of the material properties on the production of distress, and
7. Develop ranges of properties most suited to the production of zero maintenance pavements.

RESEARCH APPROACH

The terms used to describe categories of distress, specific forms of distress, distress mechanisms, distress manifestations, response mechanisms, responses, material properties, and other descriptors were clearly and concisely defined. Distresses affecting the performance of the five types of pavement structures, i.e., flexible, jointed concrete, jointed reinforced concrete, continuously reinforced concrete, and composite, were identified from a combination of literature review and experience of staff and consultants. The primary source of published information was from field surveys which identify the types of distress observed and the frequency of occurrence (References 1¹, 2²). The material properties that have had a significant effect on each of the observed distresses were also generated based on a combination of literature review and the experience of the staff and consultants. The distresses selected for study for each pavement type are included in Table 1.

A complete literature survey was conducted to review all analytical models available to predict pavement distress. The models reviewed include those based on linear elasticity and those based on Westergaard equation, discrete element slab theory, finite element theory, and elastic layer theory. These various models were classified and compared for capability of predicting distress with the final model selection results as shown in Table 2. These models were used with selected material properties and the results analyzed to develop recommendations on material property ranges suitable for use in the design of zero maintenance pavements.

OVERVIEW OF REPORT

Chapter 2 contains a brief description of the analytical models selected for use in the parameter studies and the range of material properties selected for evaluation. Chapter 3 contains a description of all

¹Darter, M.I. and E.J. Barenberg, "Zero-Maintenance Pavements Requirements and Capabilities of Conventional Pavement Systems", Interim Report No FHWA-RD-76-105, Federal Highway Administration, April 1976.

²McCullough, B.F., A. Abou-Ayyash, W.R. Hudson, and J.P. Randall, "Design of Continuously Reinforced Concrete Pavements for Highways", NCHRP 1-15, National Cooperative Highway Research Program, 1975.

TABLE 1. SIGNIFICANT DISTRESSES SELECTED FOR FURTHER STUDY (REFERENCE 3)

<u>Flexible</u>	<u>Rigid Pavements</u>			<u>Composite Pavements</u>
	<u>JCP</u>	<u>JRCP</u>	<u>CRCP</u>	
Fatigue Cracking	Fatigue Cracking	Low-Temp. and Shrinkage Cracking	Crack Spalling	Reflection Cracking
Rutting	Joint Faulting	Fatigue Cracking	Fatigue Cracking	Fatigue Cracking
Low-Temp. Cracking	Joint Spalling	Crack Faulting	Low-Temp. Cracking	Rutting
Reduced Skid Resistance		Joint Spalling	Shrinkage Cracking	Reduced Skid Resistance
			Punchouts	

TABLE 2. MODELS SELECTED FOR PARAMETER STUDIES FOR EACH DISTRESS TYPE (REFERENCE 3)

<u>PAVEMENT TYPE</u>	<u>Fatigue Cracking</u>	<u>Low-Temp Cracking</u>	<u>Rutting</u>	<u>Reduced Skid Resistance</u>	<u>Faulting</u>	<u>Spalling</u>	<u>Shrinkage Cracking</u>	<u>Reflection Cracking</u>	<u>Punchouts</u>
Flexible	VESYS	Shahin-McCullough	VESYS	-*	-	-	-	-	-
JCP	ELSYM5	-	-	-	-*	-*	-	-	-
CONCRETE	JRCP	ELSYM5	JRCP2	-	-*	-*	JRCP2	-	-
	CRCP	ELSYM5	CRCP2	-	-	-*	CRCP2	-	-*
Composite	VESYS	-	VESYS	-*	-	-	-	RFLCR1	-

*Analytical models are not available for these distresses, therefore, separate qualitative studies have been conducted to evaluate the effects of material properties on these distresses.

input data required for use in the parameter study using the models selected in Chapter 2. Chapters 4, 5, and 6 contain discussions of the results from the model studies and general observations made from the analysis of the results.

Chapter 7 contains a discussion of the zero maintenance potential for materials used in each of the pavement types and the ranges of properties necessary to secure performance compatible with the zero maintenance requirements. Chapter 8 contains a summary of the conclusions and recommendations.

CHAPTER 2. BACKGROUND AND DESCRIPTION OF PREVIOUS PROJECT WORK

This chapter summarizes a study to select contemporary mathematical models capable of predicting the important distresses in terms of the significant material properties. It includes a brief description of the significant distresses by pavement type, the material properties considered to affect each distress, the distress models considered, and the distress model selected to predict each distress.

DISTRESS

The basic approach used to identify the various distresses and the engineering material properties which affect these distresses involved several steps of review and refinement. The first step involved identifying and categorizing various distresses based on the experience of the research team. At the same time, those material properties affecting each distress were identified. Then an additional review, expansion, and refinement of the lists was conducted. Previous identifications of distress from the literature and inputs from this research were introduced at this stage to insure that all pertinent distress types and related material properties had been considered. This study also identified those environmental, mixture design, construction, and traffic factors that influence material properties.

In the second step, careful consideration was given to each of the previously proposed distresses to ascertain whether it was a distress or a secondary effect. In addition, more definitive relationships between distress and related material properties were developed and a preliminary assessment of the relative importance of the various distresses and their related material properties was made. Finally, the results of this study were carefully reviewed to insure that all pertinent distresses were considered and that the list of related material properties was complete.

The first two steps produced a complete set of distresses for each pavement type, a complete set of material properties affecting the specific distresses, and a reasonably complete set of independent mixture and construction factors, e.g., type of aggregate, cement factor, and mixing temperature, which affect these material properties. The final step involved establishing the relative importance of the distresses and their related material properties. The basis for these decisions were:

1. The results of field surveys and the combined experience of the project staff and consultants which were used to establish distresses warranting consideration. The primary sources of field survey information were References 1 and 2.
2. The results of the field surveys, sensitivity analyses on both regression and theoretical models, and the combined experience of the project staff and consultants were used to rank the material properties in order of their importance to specific distresses.

From the previous tables of various distresses, it was necessary to select those distresses that are of primary concern in producing premium pavements and that must be considered in the analysis or design of the pavement structures in order to minimize their occurrence and associated effects. Distresses not included in this list either have been eliminated through improvements in existing design procedures, proper selection of materials, or proper construction practices including quality control.

The results from condition surveys reported in References 1 and 2 were used extensively along with the experience of project engineers and consultants to rank the pavement distresses. The resulting priority ranking of pavement distresses is shown in Table 1. The models used to predict the occurrence of these distresses typically have included variables such as material properties, traffic, and environmental effects.

PAVEMENT RESPONSE AND DISTRESS MODELS

Numerous pavement response models that predict stresses and strains in a pavement structure have been developed. These models generally assume linear elasticity and fall into two categories. One category basically considers analysis of an elastic plate supported by springs (or a semi-dense liquid) while the other considers a layered system with individual elastic properties. Included in this group of models are the Westergaard equations, elastic layer theory, discrete element slab theory, and finite element theory. Some versions of these models also consider nonlinearity in materials response through iteration on nonlinear stress-strain curves furnished as input. Environmental effects are also considered by some of the models in terms of their effects on the input variables. While capable of predicting pavement behavior under loads and environmental effects, none of these models can predict distress or performance.

In addition, more sophisticated models such as VESYS A (References 3¹ and 4²) and PDMAP (Reference 5³) for flexible pavements, and RPOD (Reference 6⁴) and JCP-1 (Reference 7⁵) for rigid pavements have been developed

¹Rauhut, J.F., F.L. Roberts, and T.W. Kennedy, "Models and Significant Material Properties for Predicting Distresses in Zero-Maintenance Pavements", Report No FHWA-RD-78-84, Federal Highway Administration, September 1978.

²Rauhut, J.B. and P.R. Jordahl, "Effects on Flexible Highways of Increased Legal Vehicle Weights Using VESYS IIM", Final Report No FHWA-RD-77-116, Federal Highway Administration, January 1978.

³Finn, F.N., C. Saraf, R. Kulkarni, K. Nair, W. Smith, and A. Abdullah, "Development of Pavement Structural Subsystems", Final Report, NCHRP Project 1-10B, National Cooperative Highway Research Program, February 1977.

⁴Treybig, H.J., B.F. McCullough, P. Smith, and H. Von Quintus, "Overlay Design and Reflection Cracking Analysis for Rigid Pavements, Volume 1, Development of New Design Criteria", Final Report No FHWA-RD-77-66, Federal Highway Administration, January 1978.

to relate load-induced stresses or strains to distress and thus become predictive models for distress. These models generally can predict either fatigue cracking or rutting for flexible and composite pavements, and fatigue cracking for rigid pavements. Other computer-based analytical procedures (References 2, 5, and 8¹ have been developed for predicting thermal cracking.

All practical analytical models were studied along with the identification of significant distresses and related material properties. The more promising models were evaluated and used to determine the importance of various material properties. Models that best predicted each type of distress were selected for use in more detailed studies.

Five types of pavements, i.e., flexible, composite, plain jointed concrete pavement (JCP), jointed reinforced concrete pavement (JRCP), and continuously reinforced concrete pavement (CRCP) were considered in this study. A detailed discussion of the various theoretical types of models can be found in Reference 3. All pavement structure models included in this study are based on elastic or quasi-elastic theory and are discussed in following sections.

Pavement Structure Models Utilizing Elastic Theory

The three general types of computer programs or pavement structure models available are based on elastic layer theory, plate theory (Wester-gaard, discrete element SLAB and two-dimensional finite-element models), and three-dimensional finite element theory are discussed and compared in References 3 and 9². Elastic layer theory has the capability of analyzing many pavement systems, but edge or corner stresses for rigid slabs can not be directly modeled due to the inherent assumption that wheel loads are applied to a surface with infinite horizontal dimensions. This is generally a satisfactory assumption for flexible pavements and for interior wheel loadings for rigid pavements.

⁵Darter, M.I., "Design of Zero-Maintenance Plain Jointed Concrete Pavement, Vol 1 - Development of Design Procedures", Report ZM-2-77, prepared by the Department of Civil Engineering, University of Illinois at Urbana-Champaign, prepared for the FHWA, June 8, 1977.

¹Shahin, M.Y., "Prediction of Low-Temperature and Thermal Fatigue Cracking of Bituminous Pavements", University of Texas, Ph.D. Dissertation, August 1972.

²Crawford, J.E. and M.G. Katrona, "State-of-the-Art for Prediction of Pavement Response", Report No FAA-RD-75-183, U.S. Army Engineer Waterways Experiment Station, September 1975.

Elastic layer theory can characterize all of the layers in the pavement structure and study their separate effects on pavement response. The predicted stresses and strains vary with depth in a more realistic fashion than for the plate models, and the programs are considerably more economical to operate. The primary limitations of elastic layer theory are its inability to define any horizontal boundaries and to simulate the existence of variations in stiffness in the pavement structure, cracks in the surface, or voids under the surface layer. Despite these limitations, however, elastic layer theory and those distress models using it as a pavement structure model provide a useful tool for a comprehensive study of the various layer materials.

Since elastic layer theory is one of the models to be used, it was necessary to compare the various computer codes and to select those most suited to project needs. Schnitter (Reference 10¹) compared computer output from ELSYM5, LAYER5, LAYER15, LAYIT, and BISAR for several typical problems over a range of conditions and obtained essentially the same results from all programs. The most economical program for use was LAYER5, but it is capable of handling only one wheel load at a time. ELSYM5 and BISAR can handle multiple loads. ELSYM5 is more economical to operate than BISAR and five layers are generally sufficient for most problems. BISAR, however, can consider both variable friction at its interfaces and a horizontal load applied at the surface, so it may have utility for special studies.

ELSYM5 serves as the pavement structure model for the rutting prediction system by Monismith, et al (Reference 11²) and for RPOD (Reference 6). PDMAP (Reference 5) uses an elastic layer program called NLAYER, which as the name implies may consider any reasonable number of layers desired. The Shell Method utilized BISAR as its structural model. VESYS (Reference 4) initially used an elastic layer code limited to three layers derived from an early CHEVRON program but later versions of VESYS can analyze up to seven layers.

Distress Models for Flexible Pavements

The distress models studied and considered for use in this project for flexible pavements were:

¹Schnitter, O., "Comparison of Stresses, Strains, and Deflections Calculated with Various Layer Programs", Pavement Design Course Term Project, University of Texas at Austin, Spring 1977.

²Monismith, C.L., K. Inkabi, C.R. Freena, and D.E. McLean, "A Subsystem to Predict Rutting in Asphalt Concrete Pavement Structures", Proceedings, Fourth International Conference on Structural Design of Asphalt Pavements, Vol 1, August 1977.

1. Rutting Distress
 - a. The Shell Method (Reference 12¹)
 - b. VESYS A (Reference 4)
 - c. PDMAP (Reference 5)
 - d. Rutting Subsystem - Monismith, et al (Reference 11)
 - e. DEVPAV (Reference 13²)
 - f. OPAC (Reference 14³) and WATMODE (Reference 15⁴), and
 - g. The Huschek Rutting Prediction Method (Reference 16⁵)
2. Fatigue Cracking Distress
 - a. The Shell Method
 - b. VESYS A
 - c. PDMAP, and
 - d. OPAC and WATMODE

¹Classen, A.I.M., J.M. Edwards, P. Sommer, and P. Uge, "Asphalt Pavement Design - The Shell Method", Proceedings, Fourth International Conference on Structural Design of Asphalt Pavement, Vol 1, August 1977.

²Kirwan, R.W., M.N. Snaith, and T.E. Glynn, "A Computer-Based Subsystem for the Prediction of Pavement Deformation", Proceedings, Fourth International Conference on Structural Design of Asphalt Pavements", Vol 1, August 1977.

³Meyer, F.R.P. and R.C.G. Haas, "A Working Design Subsystem for Pavement Deformation in Asphalt Pavements", Proceedings, Fourth International Conference on Structural Design of Asphalt Pavements, Vol I, August 1977.

⁴Meyer, F.R.P., A. Cheetham, and R.C.G. Haas, "A Coordinated Method for Structural Distress Predictions in Asphalt Pavements", Proceedings, Meeting of the Association of Asphalt Paving Technologists, Vol 47, February 1978.

⁵Huschek, S., "Evaluation of Rutting Due to Viscous Flow in Asphalt Pavements", Proceedings, Fourth International Conference on Structural Design of Asphalt Pavements, Vol I, August 1977.

3. Low-Temperature Cracking

- a. VESYS A
- b. PDMAP
- c. Shahin-McCullough Model (References 8 and 17¹), and
- d. OPAC and WATMODE

4. Reduced Skid Resistance

- a. Steitle-McCullough Studies (Reference 18²), and
- b. Rauhut-McCullough Studies (Reference 19³).

Of the above models, VESYS A, PDMAP, OPAC, and WATMODE consider rutting, fracture cracking, and low-temperature cracking while the Shell Method considers rutting and fatigue cracking. All of the others consider only the distress under which they are listed.

Shell Method. The Shell Method was specifically developed as a design procedure to be exercised by hand calculations and thus is highly simplified. All rutting is assumed to occur in the asphalt concrete layer and is proportional to surface layer thickness. This assumption is in conflict with results from Shell's own research program. These research results indicate that rutting is limited to surface layers when the surface thickness exceeds about 5 inches (127 mm) while some rutting occurs in underlying layers for thicknesses less than 5 inches (127 mm) (Reference 20⁴). Results from the Shell circular test track indicated that even though the rutting is limited to the surface layer (Reference 21⁵) for surface thicknesses greater than 5 inches (127 mm), the rut depth is not a function of thickness. In addition, all strains in base, subbase, and subgrade are assumed to be elastic.

¹Shahin, M.Y., "Design System for Minimizing Asphalt Concrete Thermal Cracking", Proceedings, Fourth International Conference on Structural Design of Asphalt Pavements, August 1977.

²Steitle, D.C. and B.F. McCullough, "Skid Resistance Considerations in the Flexible Pavement Design System", Research Report 123-9, published jointly by Texas Highway Department; Texas Transportation Institute; Texas A&M University; and Center for Highway Research, The University of Texas at Austin, April 1972.

³Rauhut, J.B. and B.F. McCullough, "Development of Guideway Skid Control Requirements for Dual Mode Vehicle Systems", submitted to ABAM Engineers by ARE Inc, January 1974.

⁴Uge, P. and P.J. Van de Loo, "Permanent Deformation of Asphalt Mixes", Proceedings, Canadian Technical Asphalt Association, Vol 19, 1974.

The Shell research on fatigue cracking of asphalt concrete materials (Reference 22¹) compared the results of "wheel tracking tests" on instrumented asphalt concrete slabs supported by elastic subgrade and beam fatigue tests for a variety of mixes. It and the work reported in Reference 23² provide valuable data on the energy approach to prediction of fatigue life. Shell's approach was to provide a design procedure for limiting radial strain in the bottom of the asphalt concrete layer to an acceptable level using hand computations. While fatigue characterizations of materials using the energy approach are arrived at differently from those obtained from standard laboratory testing, linear summation of cycle ratios (Miner's Hypothesis) is used as in other models to estimate the percent of the fatigue life that has been consumed at any point in time. Consequently, there appears to be no advantage to utilizing the analytical procedures in the Shell Method for predicting fatigue life. References 12, 22, and 23 contain extensive information for developing the fatigue characterizations of the materials.

VESYS. VESYS A is an improved version of Program VESYS IIM, a distress model that has been discussed in great detail in the literature (References 24³ and 25⁴). The capabilities added to VESYS IIM to produce VESYS A were:

⁵Pfeiffer, J. and P.M. Van Doormaal, "The Rheological Properties of Asphaltic Bitumen", Journal, Institute of Petroleum Technologists, No 22, 1963.

¹Van Dijk, W., "Practical Fatigue Characterization of Bituminous Mixes", Proceedings, Association of Asphalt Paving Technologists, Vol 44, February, 1975.

²Van Kijk, W. and W. Visser, "The Energy Approach to Fatigue for Pavement Design", Proceedings, Association of Asphalt Paving Technologists, Vol 46, February 1977.

³Rauhut, J.B., J.C. O'Quin, and W.R. Hudson, "Sensitivity Analysis of FHWA Structural Model VESYS II", Report No FHWA-RD-76-23 and FHWA-RD-76-24, Federal Highway Administration, March 1976.

⁴Kenis, W.J., "Predicted Design Procedures - Design Method for Flexible Pavements Using the VESYS Structural Subsystem", Proceedings, Fourth International Conference on Structural Design of Asphalt Pavements, Vol I, August 1977.

1. Seasonal modification of material properties,
2. Incremental breakdown of the axle load distribution by tire radius and corresponding tire pressure, and
3. Addition of a low-temperature cracking model.

The details of these revisions and the improvements in the idealization of flexible pavements are discussed in Reference 4.

VESYS A is a sophisticated computer code that accepts some 23 control variables and 44 independent variables describing a flexible pavement structure, the traffic loading, through input of pavement temperatures, and seasonal materials characterization of the environment in which it exists. Using this input, it then predicts fatigue cracking, rut depth, slope variance, present serviceability index, and expected life as functions of time.

Fatigue cracking distress is predicted using the classical fatigue equation and linear summation of cycle ratios, i.e., Miner's Hypothesis, to predict the damage at any time due to an established axle load distribution and traffic rate. The primary difference between the VESYS formulations and others using Miner's Hypothesis is that the VESYS formulation utilizes probability theory in order to consider variability of the input parameters in the predictions. Because cracking generally occurs for conditions other than the mean condition of the pavement, the statistical formulation is a definite improvement.

Rutting is calculated as the difference between the predicted total and elastic displacements at the surface. This is accomplished by separate sets of solutions from the elastic layer structural model, one with the normal elastic moduli and the other with the moduli modified by permanent deformation characterizations to delete the permanent strains. This procedure is very similar in effect to that proposed by Monismith, et al (Reference 11). In VESYS A, the permanent strains in the layers are accumulated through separate solutions with the layer stiffnesses modified, while the permanent deformations in the layers are calculated separately and added together to predict the change in displacement at the surface in the Monismith procedure.

VESYS III is a modified version of the VESYS G program that was received by the FHWA as part of a recent contract. VESYS III contains an N-layer probabilistic package using a quasi-elastic treatment with a maximum of seven layers and an assignable Poisson's ratio in the place of the original three-layer package employing visco-elastic theory, convolution integrals and a fixed Poisson ratio of 0.5. The FHWA removed the probabilistic N-layer section of VESYS G and inserted it into VESYS A thereby keeping all the desirable features of VESYS A. The combination of VESYS G and VESYS A was named VESYS III by the FHWA. Upon receipt of VESYS III by ARE, several modifications were made that reduced the running time by a factor of 10 compared to the running time as received. In addition,

modifications were made to permit input of only seasonal values for asphalt concrete modulus based on the average seasonal pavement temperature. One other modification was made to provide the capability of analyzing fatigue in composite structures by examining the stress at the bottom of a stiff stabilized layer. This modified version of VESYS III was called VESYS IIIA and has been referred to as VESYS in the text of this report. VESYS was used for all model studies in flexible and composite pavements for fatigue and rutting.

VESYS is perhaps the most complete flexible pavement distress model in existence today and considers a broad range of material properties in its distress subsystems. Some of the input variables, such as those for the permanent deformation characterization of materials, are relatively new to the engineering profession; however, considerable data for these have been accumulated for a variety of materials from several sources.

PDMAP. The term PDMAP stands for Probabilistic Distress Models for Asphalt Pavement. The distress models included are for fatigue cracking and rutting. The low temperature cracking distress model is a separate computer program COLD. Both the fatigue cracking distress and the rutting models in PDMAP are based on multiple regressions on data from the AASHO Road Test, but depend on predictions of pavement response from an elastic layer structural model.

The rutting model for PDMAP predicts seasonal rate of rutting for permanent deformation per equivalent load application. Seasonal changes in the elastic constants used for the various layers are considered as rutting accumulates with time. The rutting predictions are displayed at different confidence levels on the basis of the stochastic characteristics of the elastic materials characterizations. The fatigue distress model is very similar to that used in most fatigue predictions, except that an additional term has been added to consider the effects of asphalt concrete stiffness.

The rutting distress model has some limitations that restrict its value to research. These are:

1. The regression model is based entirely on elastic material properties and elastic responses and includes no permanent deformation characterization of the materials. The consideration of the permanent deformation characteristics of materials in this regression model are applicable directly only to those materials in the pavements of the AASHO Road Test.
2. The three regression coefficients in the rate of rutting prediction model are based entirely on AASHO Road Test materials and conditions and require reestablishment for use under other conditions (Reference 26¹).

¹Christison, J.T., "Response of Asphalt Pavements to Low Temperatures", Ph.D. Dissertation, University of Alberta, 1972.

Monismith Subsystem. The design subsystem presented by Monismith, et al (Reference 11) estimates the amount of permanent deformation or rutting resulting from repeated traffic loading. Relationships between applied stress and permanent strain defined by repeated load triaxial compression tests are used for fine grained soils, granular materials, and asphalt concrete. Stresses resulting from the wheel loads are estimated through use of one of the ELSYM computer programs. The stresses are used to estimate permanent deformation in each pavement layer by computing the permanent strain at a number of points within the layer sufficient to define the strain variations with depth, and then summing the products of the average permanent strains and the corresponding differences in depths between the locations at which the strains were determined. Total rut depth is estimated by summing the permanent deformation contributions from each layer.

While this is a fairly straightforward method and indicates promise, the two serious drawbacks that limit its use are:

1. The materials characterizations are complex and require a very detailed test program to arrive at the values of the many parameters included in the equations, and
2. Laborious hand calculations are required for use in large studies.

Since both this rutting prediction model and that of VESYS A effectively accumulate the permanent deformations in each layer as permanent displacement at the surface, similar results are to be expected if the permanent deformation characterizations were based on the same test data.

DEVPAV. DEVPAV is a finite element program that has been under development by Kirwan, et al (Reference 13) for some years in Ireland. In addition to the usual loading information, the permanent deformation characterizations are apparently based on multiple regression studies.

The equation for permanent strain contains temperature, number of load cycles, and applied stress as independent variables. Kirwan, et al compared, calculated and measured rut depths for the Shell Test Track (Reference 27¹) and the Nottingham Test Track and reported that the computed rut depths were in all cases substantially higher than those actually measured, but that the shapes of the plots of rut depth versus applications were similar. General use of this model is limited because materials characterizations for permanent deformations are available only for the two materials recorded in Reference 13, and the finite element program has been revised so that the lateral strain of one column of elements is prevented from affecting the adjoining column.

¹Hofstra, A. and A.J.G. Klomp, "Permanent Deformation of Flexible Pavements Under Simulated Road Traffic Conditions", Proceedings, Third International Conference on the Structural Design of Asphalt Pavements, Vol I, London, 1972.

OPAC. OPAC is a pavement design system developed for the Province of Ontario (Reference 16). It has been further developed into a later form called WATMODE (Reference 18) (Waterloo Model of Distress Estimation). Both models predict rutting, fatigue cracking, and low temperature cracking.

These models are generally based on statistical correlations between laboratory tests on materials from the Brampton and St. Anne's Road Tests in Ontario and measured roadway responses. The correlations between predicted and measured distress are very good for those road tests, but may not be generally applicable to more temperate climates. These procedures can only be used in other locations and with different materials after careful validation. Useful developments in WATMODE are discussed in References 3 and 14.

Huschek Method. The Huschek method (Reference 16) is very similar to that described above for Monismith, et al, except that the structural model is the elastic layer program BISAR and the permanent deformation characterization for the asphalt concrete is based on cyclic creep compliance tests. The rutting is again predicted by summing the permanent deformations in the separate layers as is done by Monismith and indirectly by VESYS A. Calculated results from this procedure compared reasonably well to measured rutting on a test road in Switzerland.

Shahin-McCullough Model. The Shahin-McCullough model for prediction of low temperature or thermal cracking includes separate models for pavement temperature, thermal stress, low temperature cracking, and thermal fatigue cracking (References 8 and 17).

The Shahin-McCullough low temperature cracking model was selected for the study of low temperature cracking in flexible pavements (Reference 3). The materials properties required to complete this analysis are asphalt concrete mix stiffness, asphalt concrete tensile strength, and asphalt concrete thermal coefficient. The program calculates stiffness of the asphaltic concrete using a computerized version of the Van der Poel nomographs as modified by Heukelom and Klomp (Reference 28¹). The asphalt cement properties used to characterize the bitumen stiffness include: original asphalt cement penetration, penetration test temperature, percent change in penetration after the thin film oven test, and the ring and ball softening point. A thermal loading time is also input to calculate the asphalt cement stiffness. The required concrete mix properties include percent asphalt, specific gravity of asphalt, specific gravity of aggregate, and density of the compacted mix. Using these properties, the computer program estimates the effect of aging on the asphalt properties with time and then calculates the mix stiffness as a function of temperature during the analysis period.

¹Heukelom, W. and A.J.G. Klomp, "Road Design and Dynamic Loading, Proceedings, Association of Asphalt Paving Technologists, Vol 33, February 1964.

A thermal-fatigue cracking model was developed also because thermal cracking of asphalt concrete pavements occurs in temperate zones as well as northern zones having relatively low temperatures. This was attributed to the fatigue effects of daily temperature cycling. Thus, by comparison, the cracking predicted by COLD might be thought of as "one cycle fatigue cracking" at a much higher strain level than those which produce failure under repetitive loading considered in the Shahin-McCullough model.

Comparisons between measured and calculated low-temperature cracking from the Shahin-McCullough model for the St. Anne test road, Ontario, AASHO test road, and a runway in Fairbanks, Alaska were reasonable considering the variability in occurrence of low-temperature cracking in the field; i.e., significant differences in amount of cracking are generally found between apparently identical sections for the same environmental conditions.

Skid Resistance. Most of the literature on skid resistance is concerned with the magnitudes of skid number for different types of pavements and the reductions in measured skid numbers over periods of time. Steitle and McCullough (Reference 18) reported statistical relationships between measured skid numbers, number of vehicle applications with trucks and cars counted equally, a "field constant" for each aggregate that depends on its traffic polishing characteristics, and a skid number taken after a specific number of vehicle applications.

The most suitable form of the skid decay model was determined by Steitle and McCullough (Reference 18) to be that shown below:

$$N = N_1 \left[\frac{SN_{40@N_1}}{SN_{40@N}} \right]^{1/b_{field}}$$

The equation represented a straight line in a log-log plot of traffic polish data versus time or SN versus traffic applications. The value $SN_{40@N_1}$ represented the skid number at 40 mph (64 kph) measured at a time in which the pavement had been subjected to N_1 applications. The value $SN_{40@N}$ represented the minimum allowable skid number measured at 40 mph (64 kph) before the pavement surface required maintenance to improve the skid resistance. Because of the form of the relationship between SN_{40} and traffic applications, the value of N_1 selected was 50,000 applications to ensure that the straight line portion of the relationship was used to determine the exponent. Limited data were reported in Reference 18 and was used to evaluate the zero maintenance potential for asphalt concrete surface pavements and for considering the general effects on skid resistance produced by abrasive wear of surface aggregates.

Selection of Predictive Models for Flexible Pavements. A careful evaluation indicates that none of the models discussed above can predict rutting and fatigue cracking distress as well as VESYS. Thus, the VESYS system was selected because it predicts both distresses and because considerable information on permanent deformation characterizations for a range of materials is available for use in this study.

The Shahin-McCullough model was selected for low-temperature cracking because it has a much more thorough theoretical base and offers much more general applicability than other available models.

The Steitle-McCullough model based on the effects of aggregate polishing was selected for use to study loss of skid resistance, but the amount of field data available limited its use so that only qualitative results were derived.

Distress Models for Composite Pavements

The choice of models for prediction of distress in composite pavements is much more limited than for flexible pavements. A composite pavement is considered to be one having a flexible surface over a very stiff subbase, composed of either a portland cement concrete pavement layer or a portland cement treated granular base layer. Thus, special modeling was required since the strongest pavement layer does not occur at the surface. Rutting and reduced skid resistance may be studied with the same models as for flexible pavements, but the fatigue model must be capable of considering fatigue in the more rigid underlying layer. Also, the serious problem of reflection cracking in the surface layer, induced by movements of the underlying layer at the joints or cracks, must be evaluated with an entirely different model.

The distress models reviewed and considered for use in studying composite pavements are as follows:

1. Rutting Distress - VESYS
2. Fatigue Cracking Distress:
 - a. Computer program ELSYM5 for predicting stresses and strains at the bottom of the flexible and rigid layers, supplemented by fatigue relationships or a modification of VESYS to handle the fatigue in the PCC layer below the asphalt surface.
 - b. RPOD (References 6 and 29¹).
3. Reflection Cracking Distress - RFLCR1 (Reference 6)

¹Treybig, H.J., B.F. McCullough, P. Smith, and H. Von Quintus, "Overlay Design and Reflection Cracking Analysis for Rigid Pavements, Vol 2, Design Procedures", Report No FHWA-RD-77-67, Federal Highway Administration, August 1977.

4. Reduced Skid Resistance - Studied concurrently with the flexible pavement study.

Rutting Distress Model. No available models were developed specifically for predicting rutting in composite pavements; so VESYS was used.

RPOD. Program RPOD was developed by Austin Research Engineers specifically for the design of either flexible or rigid overlays of rigid pavements, and includes a fatigue cracking distress model utilizing ELSYM5 as a pavement structure model. The alternatives for study of fatigue cracking distress are:

1. Modify ELSYM5 to add a fatigue cracking distress model to the present pavement structure model, or
2. Bypass most of RPOD's subroutines to use only the ELSYM5 pavement structure model and its fatigue cracking distress model. An analysis indicated that it would be more economical to modify ELSYM5.

RFLCR1. RFLCR1 is the only available model for predicting reflection cracking. It includes analysis of two types of distress mechanisms. One is a form of reflection cracking in the overlay due to horizontal movements of the rigid slab caused by temperature and moisture changes. The second is shear cracking due to differential vertical movements at joints or cracks in the underlying rigid pavements.

Selection of Prediction Model for Composite Pavements. A review of available models indicates that VESYS is the best available model for predicting rutting in composite pavements. VESYS can also be utilized to predict the fatigue life of the underlying PCC layer with a modification to the program. Since both RPOD and VESYS utilize elastic layered programs for the analysis of stresses and strains in static solutions, VESYS was modified and utilized for both the rutting and fatigue analysis of composite pavements. RFLCR1 was chosen for analysis of the reflection cracking in composite pavements and the results from the skid resistance study of flexible pavements are directly applicable to composite pavement.

Distress Models for Rigid Pavements

The types of rigid pavements were JCP, JRCP, and CRCP. Since the steel provided in JRCP or CRCP is neither positioned properly nor of sufficient quantity to provide additional structural capacity, a common pavement structure model was used for the prediction of stresses and strains in JRCP, CRCP and JCP. Thus, the study of fatigue cracking can be done simultaneously for all three pavement types. The distress mechanisms for faulting at cracks and joints, and joint spalling are also essentially the same for JRCP and JCP; so these distresses can also be studied simultaneously.

Thermal and shrinkage cracking are generally not serious problems for JCP if the joint spacings are short. Future designs should not include joint spacing any greater than 15 feet (4.57m)(Reference 7). Since longer joint spacings are sometimes used for JRCP, thermal and shrinkage cracking should be considered. The only models available for predicting this distress in a JRCP were a computer program called JRCP-1 (Reference 30¹), and an improved version called JRCP-2, unless the classical subgrade drag theory was considered.

The fatigue cracking model for JRCP may also be utilized for CRCP, but CRCP's distinctive nature also requires special distress models for thermal and shrinkage cracking. The only relatively complete models were CRCP-1, developed by McCullough, et al (Reference 2), and CRCP-2 developed by Ma (Reference 31²), which is an improved version of CRCP-1. Follow-on studies by Strauss (Reference 32³) and others offer additional statistical insight into the effects of material properties on CRCP distress.

There are many pavement structure models, several of which were discussed previously, that could be used to predict stresses and strains for the fatigue cracking analysis. Because of the limitations of plate theory, elastic layer theory was considered to be the appropriate pavement structure model when consideration of all pavement layers was desired, but the special capabilities of the discrete element and finite element models could also be used for special studies.

JCP-1. Although subject to the same limitations as the Huang and Wang model (Reference 33⁴) upon which it was based, Computer Program JCP-1 was also considered as a potential fatigue cracking model. Program JCP-1 provides fatigue and serviceability data for a design procedure for JCP developed by Darter and Barenberg (Reference 7). Multiple regression equations based on analytical solutions from the Huang and Wang finite element program predict pavement stress for an 18-kip (80 kN) axle load with the outside tire on the outer 6 inches (152mm) of the slab. The procedure also included prediction of day time and night time curling stresses and their superposition with stresses created by wheel loads. A very detailed fatigue cracking model was then applied to predict fatigue damage.

¹Rivero-Vallejo and B.F. McCullough, "Drying Shrinkage and Temperature Drop Stresses in Jointed Reinforced Concrete Pavement", Report 177-1, Center for Highway Research, The University of Texas at Austin, August 1975.

²Ma, J.C.M., "CRCP-2, An Improved Computer Program for the Analysis of Continuously Reinforced Concrete Pavement", University of Texas at Austin, Master Thesis, August 1977.

³Strauss, P., B.F. McCullough, and W.R. Hudson, "Continuously Reinforced Concrete Pavements; Structural Performance and Design Construction Variables", Research Report 177-7, Center for Highway Research, The University of Texas at Austin, May 1977.

The approach of including the effect of curling and accumulating fatigue damage separately by day and by night to more accurately apply the effects of curling during these periods was considered to be excellent. The emphasis given to the greater importance of wheel loads near the edge because of the magnitudes of stresses they create was also significant. However, the procedure was based on certain "built-in" assumptions that limit its general applicability for these studies, so it was not selected as a primary model. A detailed discussion of JCP-1 and reasons for its limited use appear in Reference 3.

CRCP-2. The dimensional changes in a continuously reinforced concrete pavement caused by drying shrinkage of the concrete and temperature variation after curing were investigated by McCullough, et al and the design method utilizing Program CRCP-1 was developed (Reference 2). This computer program was subsequently improved by Ma (Reference 31) and designated Program CRCP-2.

The spacing of transverse cracks that occur naturally in CRCP was perhaps the most important variable affecting the behavior of the pavement. Relatively large distances between cracks result in a higher accumulation of drag forces from the subgrade due to frictional resistance, thus high steel stress at the crack and wide crack widths are produced. Closer crack spacing reduces the frictional restraint, the steel stress, and the crack width. It was clear that the transverse cracks in CRCP were due to the thermal contraction and shrinkage of the concrete slab. The one-dimensional axial model used in this method was the only rational model available which considers the internal forces caused by the difference in thermal coefficient between the concrete and the steel material and therefore was a valuable tool for the analysis of CRC pavements.

In 1959, the Texas Highway Department began the Falls-McClennan County Project to evaluate the performance of continuously reinforced concrete pavements. Intensive crack spacing surveys were conducted at ages varying from 20 days to 15 years. The results obtained from the survey were compared to the CRCP-2 computer prediction, and the good correlation indicates that this method gives reasonable predictions.

JRCP-2. Program JRCP-2 was developed by Rivero-Vallejo and McCullough (Reference 30) and used many of the concepts developed for CRCP-1. However, the geometry and boundary conditions for this were considerably different from CRCP-2. JRCP-2 also considered the stresses in the concrete and reinforcing steel with time and location. These stresses were affected by the frictional resistance of the subbase; the stiffness, tensile strength, and the shrinkage coefficient of the concrete; the temperature drop anticipated in time; the slab length; the percent reinforcement; the bar diameter; the yield stress of the steel; the elastic modulus of the steel; the unit weight of the concrete; and the ages at which cracking was to be considered. Given this information, JRCP-2 theoretically would proceed with analysis until the first crack forms and then would restructure the problem for

⁴Huang, Y.H. and S.T. Wang, "Finite-Element Analysis of Concrete Slab and Its Implications for Rigid Pavement Design", Highway Research Record 466, Highway Research Board, 1973.

subsequent consideration for the formation of a second crack between the joint and the first crack. The output included the time when the first crack was formed, concrete stress, steel stress, joint width, and crack width as a function of time, and the same data for second cracks if they were formed.

Program JRCP-2 was the only thorough model available for the study of the effects of material properties on drying shrinkage and thermal cracking in JRCP. Unfortunately, use of the model indicated that the computer program was not completely "debugged" and that it did not predict cracking, nor did it correctly predict stresses in concrete and steel. Consequently, predictions for crack widths were questionable. Even though JRCP-2 appeared to be theoretically correct and was the only suitable model for JRCP, corrections were not made to the model and these studies were not conducted.

Selected Models

The available pavement structure response and pavement distress models for the distresses to be considered have been discussed and those models that best predict distress identified. Tables 3 through 7 show the distresses, material properties and models selected for flexible pavements, composite pavements, JRCP, JCP, and CRCP.

Because no suitable mathematical models were found for prediction of certain distresses, these were not assigned a specific model, but were studied separately from the parameter study.

MATERIAL PROPERTIES

Engineering material properties are defined as those properties that may be used with a constitutive equation to predict the physical behavior of a material in a particular environment. Material properties then are those engineering properties that are used to represent the materials in mathematical models and equations or in decision criteria. These, in turn, are used to evaluate the behavior and the suitability of materials for particular application.

The materials properties initially identified as having important effects on distresses in premium pavements are contained in Table 8. Each of the properties included was considered by the project team to affect the occurrence and magnitude of a distress. Detailed tables were prepared in which the independent material properties affecting a particular distress was coded so that the types of material and layer for which the property applies could be identified (Reference 3).

Factors believed to affect the magnitude of the various materials properties were also identified and appear in Appendix A of Reference 3. This information provided valuable insight for evaluating the relative significance of material properties for this project. All factors having

TABLE 3. DISTRESS, RELATED MATERIAL PROPERTIES AND DISTRESS MODELS
SELECTED FOR FLEXIBLE PAVEMENTS (REFERENCE 3)

Distresses that have Significant Effects on Pavement Performance and/or Maintenance Requirement	FATIGUE CRACKING	RUTTING	LOW-TEMPERATURE CRACKING	REDUCED SKID RESISTANCE
Material Properties that have significant effects on the distresses	1) Fatigue Constants $K_1(T)$, $K_1(T)$ for AC Surface. 2) Stiffness Modulus for AC Surface. 3) Stiffness Modulus for Base Materials.	1) Stiffness Modulus for AC Surface. 2) Permanent Deformation Parameters for AC Surface. 3) Stiffness Modulus for Subgrade Soil. 4) Permanent Deformation parameters for Subgrade Soil.	1) Coefficient of Thermal Expansion for AC. 2) Stiffness Modulus for AC. 3) Tensile Strength for AC.	1) Abrasive Wear Potential.
Models Selected for Distress Studies	VESYS	VESYS	SHAHIN-MCCULLOUGH "Low-Temperature Cracking Model"	Study Separately

TABLE 4. DISTRESS, RELATED MATERIAL PROPERTIES AND DISTRESS MODELS
SELECTED FOR JOINTED REINFORCED CONCRETE PAVEMENT (REFERENCE 3)

Distresses that have Significant Effects on Pavement Performance and/or Maintenance Requirements	LOW-TEMPERATURE AND SHRINKAGE CRACKING	FATIGUE (TRANSVERSE OR CORNER CRACKING)	FAULTING AT CRACKS	JOINT SPALLING
Material Properties that have Significant Effects on the Distresses	<ol style="list-style-type: none"> 1) Tensile Strength for PCC. 2) Thermal Coefficient. 3) Shrinkage Coefficient. 	<ol style="list-style-type: none"> 1) Fatigue Constants for PCC. 2) Stiffness Modulus for PCC. 3) Stiffness Modulus for Subbase Material. 		<ol style="list-style-type: none"> 1) Volume change Characteristics for PCC Surface. 2) Tensile Strength for PCC. 3) Stiffness Modulus for PCC.
Models Selected for Distress Studies	JRCP-2	ELSYM5*	Study Separatly	Study Separatly

*The stresses predicted by ELSYM5 are essentially "Interior Slab Stresses," and were multiplied by a stress factor to approximate "Slab Edge Stresses."

TABLE 5. DISTRESS, RELATED MATERIAL PROPERTIES AND DISTRESS MODELS
SELECTED FOR JOINTED CONCRETE PAVEMENT (REFERENCE 3)

Distresses that have Significant Effects on Pavement Performance and/or Maintenance Requirement	FATIGUE CRACKING	JOINT FAULTING	JOINT SPALLING
Material Properties that have Significant Effects on the Distresses	1) Fatigue Constants for PCC. 2) Stiffness Modulus for PCC. 3) Stiffness Modulus for Sub-base Materials.	1) Erodability of Subbase. 2) Erodability of Subgrade. 3) Tensile Strength of PCC.	
Models Selected for Distress Studies	ELSYM5*(Concurrent with Studies for JRCP & CRCP)	Study Separatly	Concurrent with Study for JRCP

*The stresses predicted by ELSYM5 are essentially "Interior Slab Stresses," and were multiplied by a stress factor to approximate "Slab Edge Stresses."

TABLE 6. DISTRESS, RELATED MATERIAL PROPERTIES AND DISTRESS MODELS SELECTED FOR CONTINUOUSLY REINFORCED CONCRETE PAVEMENT (REFERENCE 3)

Distresses that have Significant Effects on Pavement Performance and/or Maintenance Requirements	FATIGUE CRACKING	LOW TEMPERATURE AND SHRINKAGE CRACKING	PUNCHOUTS CRACK SPALLING STEEL RUPTURE		
			Responses to Thermal and Shrinkage Strains that may be Optimized to Minimize Distresses	- -	- -
Material Properties that have Significant Effects on the Distresses	1) Fatigue Constants for PCC. 2) Stiffness Modulus for PCC. 3) Stiffness Modulus for Subbase.	2) Thermal Coefficient for PCC. 2) Shrinkage Coefficient for PCC. 3) Tensile Strength for PCC.	Same as for Low Temperature and Shrinkage Cracking.		
Model Selected for Distress Studies	ELSYM5*(Concurrent with Study for JRCP)	CRCP-2	CRCP-2 (Concurrent with Study for Low Temperature and Shrinkage Cracking for CRCP).		

*The stresses predicted by ELSYM5 are essentially "Interior Slab Stresses," and were multiplied by a stress factor to approximate "Slab Edge Stresses."

TABLE 7. DISTRESS, RELATED MATERIAL PROPERTIES AND DISTRESS MODELS SELECTED FOR COMPOSITE PAVEMENTS (REFERENCE 3)

Distress that have Significant Effects on Pavement Performance and/or Maintenance Requirement	REFLECTION • CRACKING	FATIGUE CRACKING	RUTTING	REDUCED SKID RESISTANCE
Material Properties that have Significant Effects on the Distresses	1) Stiffness Modulus for AC Overlay. 2) Thermal Coefficient for Existing Pavement. 3) Creep Modulus for AC Overlay.	1) Stiffness Modulus for PCC or Cement Treated base. 2) Fatigue Constants for AC Overlay or PCC. 3) Stiffness Modulus for AC Overlay.	1) Permanent Deformation Parameters for AC Overlay. 2) Stiffness Modulus for AC Overlay.	1) Abrasive Wear
Model Selected for Distress Studies	RFLCRI	ELSYM5* or VESYS	VESYS	Study Concurrently with Flexible Pavement

The stresses predicted by ELSYM5 are essentially "Interior Slab Stress" and were multiplied by a stress factor to approximate "Slab Edge Stresses"

TABLE 8. MATERIAL PROPERTIES CONSIDERED TO AFFECT DISTRESSES IN PREMIUM PAVEMENTS (REFERENCE 3)

Pavement Type			MATERIAL PROPERTY
Rigid	Flexible	Composite	
X	X	X	Constants of the Fatigue Equation
X	X	X	Tensile Strength
X		X	Shrinkage Characteristics
X	X	X	Coefficient of Thermal Expansion
X	X	X	Aggregate Characteristics
X	X	X	Compaction-Volume Change Characteristics
X			Erodability of Subbase and Subgrade Materials
X	X	X	Frost Susceptibility of Subgrade Soil
X	X	X	Mixture Stiffness*
	X	X	Permanent Deformation Characteristics
X	X	X	Bond (Adhesion)

*Includes stability, creep compliance, and elastic properties.

an effect on the various materials properties were listed for each property and categorized to indicate whether the factor related to environment, mixture design and materials, construction, traffic, or time.

In order to evaluate the available models for inclusion of the most significant material properties, a second priority ranking was performed. These priority rankings of material properties affecting distress in premium pavements by layer resulted in the material properties selected for inclusion in the model studies as shown in Tables 3, 4, 5, 6 and 7. In developing the priority rankings for material properties within a particular distress, the rankings were based on total effect with no consideration given to whether the material property could be controlled during design.

CHAPTER 3. DESCRIPTION OF MODEL INPUTS

The use of the models selected for the distress studies outlined in Chapter 2 require the development of input values for each variable that occurs in each of the models. There are several categories of input variables that are discussed in the following sections.

COMMON INPUTS

Several categories of factors are common to all pavements and models and are independent of the pavement material properties themselves. These factors are the environment in which the pavement occurs, the traffic level to which the pavement is subjected, and the thickness of the pavement layers. Other factors, or inputs, are dependent on the model used and the pavement type.

Environmental Factors

In order to consider the effect of the environment upon pavement response, the FHWA required that the parameter studies incorporate characteristics of four environmental zones. These environmental zones were selected to be representative of regions with similar combinations of temperature and moisture conditions. The four zones were designated as wet-freeze, dry-freeze, wet-no freeze, and dry-no freeze. The approximate locations of these regions are shown in Figure 1.

The environment in which a pavement system exists has a significant effect upon the response of the pavement to the traffic loads imposed upon it. In order to consider this important parameter, four interstate highway sections were selected as being typical of zero maintenance pavements for this study, one from a cold climate with generally high humidity and rainfall and designated as wet-freeze, one from a cold climate with little rainfall and low humidity and designated as dry-freeze, one from a relatively warm climate with high rainfall and humidity and designated as wet-no freeze, and one from a relatively warm climate with little rainfall and low humidity and designated as dry-no freeze. A previous study (Reference 34¹) also utilized the same environmental designations and provided valuable information for a range of flexible pavements that were being considered for this study. Sections of interstate highways representing each zone were chosen after coordination with several Federal Highway Administration personnel including the contract manager, and other knowledgeable persons. The sections chosen for use in this study were:

1. Wet-freeze - IH-80 in Illinois (part of the original AASHO Road Test)

¹Darter, M.I., E.J. Barenberg, and J.S. Sarvan, "Maintenance-Free Life of Heavily Trafficked Flexible Pavements", a paper presented at the 55th Annual Meeting of the Transportation Research Board, January 1976.

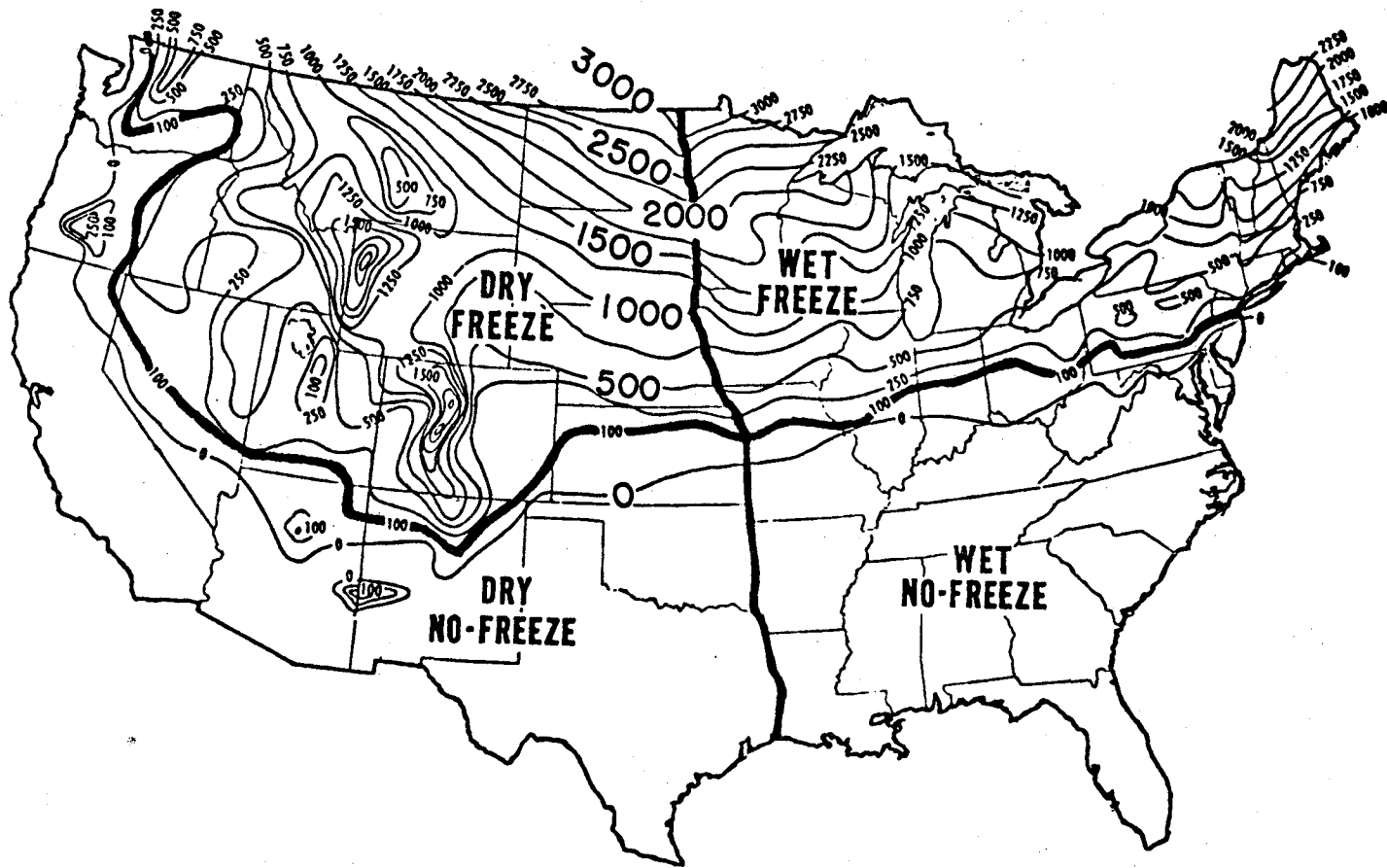


FIGURE 1. FREEZING INDEX MAP OF THE UNITED STATES

2. Dry-freeze - IH-80N in northern Utah (near Snowville)
3. Wet-no freeze - IH-10 in Florida (near Madison)
4. Dry-no freeze - IH-20 in Texas (between Midland and Odessa).

Drainage

Positive drainage courses were provided for all pavements considered. Historically pavements have not been designed for the rapid elimination of water. However, as water enters the structure, increased pore pressures occur with the result that erosion and deterioration of the pavement structural layers can occur. Therefore, drainage systems have been incorporated into all cross sections to minimize this possibility. Drainage systems may also be required to lower a high water table or to rapidly remove surface moisture infiltration from the pavement structure. References 35¹, 36², 37³, and 38⁴ provide extensive information on the construction and purpose of several drainage systems. The base or subbase layer was assumed to be waterproofed by treatment with an asphalt coating and the modulus was assumed to remain constant with season. In addition, the subgrade materials were assumed to be compacted at optimum moisture content and the moisture level is assumed to remain constant with season so that uniform support for the surfacing layer is ensured.

Substructure

This substructure of the pavement consists of all materials below the base layer, i.e., subbase, improved subgrade and/or subgrade. The materials chosen for these layers are dependent on the environment (i.e., frost penetration, temperature variations, precipitation, etc.) and existing soil conditions (i.e., water table level, soil type, swelling potential, frost susceptibility, etc.). In order to ensure that a pavement structure will provide zero maintenance, the substructure must be constructed to the highest obtainable standards. In addition, the subbase and subgrade materials will probably require stabilization to ensure that the support to the surface is not affected significantly by the changes from season to

¹"Drainage of Asphalt Pavement Structures", MS-15, The Asphalt Institute, May 1966.

²Cedergren, H.R., J.A. Arman, and K.H. O'Brien, "Development of Guidelines for the Design of Subsurface Drainage Systems for Highway Pavement Structural Sections", Report No FHWA-RD-73-14, Federal Highway Administration, February 1973.

³"Implementation Package for a Drainage Blanket in Highway Pavement Systems", Federal Highway Administration, May 1972.

⁴Cedergren, H.R., Drainage of Highway and Airfield Pavements, John Wiley and Sons, 1974.

season. This may require special considerations for treatment of these materials, use of special environmental layers, etc.

Environmental Layer

Pavement structures must be protected from the effects of expansive or frost susceptible soils. Techniques for identification of these soils have been presented in References 39¹, 40², 41³, and 42⁴. Treatment of frost susceptible soils to attain performance compatible with zero maintenance requirements can be realized using two techniques where selection depends on the total frost penetration into the pavement structure. The first is encapsulating the material in a membrane to maintain the same moisture content during construction. This technique should be used in areas where the frost penetration is generally less than three feet (0.914 m). The in-service and laboratory performance and construction of encapsulated materials are presented in References 43⁵, 44⁶, 45⁷, and 46⁸. In areas where the frost penetration is much greater than three feet (0.914m) use of an insulating material may be warranted to provide protection from differential

¹Snethen, D.R., L.D. Johnson, and D.M. Patrick, "An Evaluation of Expedient Methodology for Identification of Potentially Expansive Soils", Report No FHWA-RD-77-94, Federal Highway Administration, June 1977.

²McKeen, R.G., "Design and Construction of Airport Pavements on Expansive Soils", Report No FAA-RD-76-66, Federal Aviation Administration, June 1976.

³Soils and Geology - Pavement Design for Frost Conditions, TM 5-818-2, Department of the Army Technical Manual, Headquarters, Department of the Army, July 1965.

⁴McKeen, R.G. and J.P. Nielsen, "Characterization of Expansive Soils for Airport Pavement Design", Interim Report No FAA-RD-78-59, Federal Aviation Administration, August 1978.

⁵Smith, N., R.A. Eaton, and J.M. Stubstab, "Repetitive Loading Tests on Membrane-Enveloped Road Sections During Freeze-Thaw Cycles", CRREL Report 78-12, Cold Regions Research and Engineering Laboratory, May 1978.

⁶Sayward, J.M., "Evaluation of MESL Membrane-Puncture, Stiffness, Temperature, Solvents", CRREL Report 72-22, Cold Regions Research and Engineering Laboratory, June 1976.

⁷Smith, N. and D.A. Pazzint, "Field Test of a MESL (Membrane-Enveloped Soil Layer) Road Section in Central Alaska", CRREL Technical Report 260, Cold Regions Research and Engineering Laboratory, July 1975.

⁸Webster, S.L., "Implementation Package 74-2, Users' Manual for Membrane Encapsulated Pavement Sections (MEPS)", Federal Highway Administration, June 1974.

frost heave. Penner (Reference 47¹) discusses the effects of the resulting frost heave on pavements. All pavements designed to be zero maintenance should consider both swelling and frost susceptibility characteristics of the subgrade soils and design to eliminate their effect.

Traffic Levels

Reasonable traffic levels in terms of 18-kip (80 kN) equivalent single axle loads were selected for each of the types of pavement considered. Since no predictions exist for traffic to be carried by premium pavements, it was necessary to consider past data and to extrapolate forward to arrive at the values used in this study. Previously reported traffic information (References 1, 4, and 48²) indicated:

1. Some rigid pavements are experiencing over 2 million 18-kip (80 kN) ESAL annually and 1 to 1.25 million are relatively common.
2. Most composite pavement (Reference 1) are experiencing 750 thousand to 1 million 18-kip (80 kN) ESAL annually.
3. Most flexible pavements were experiencing less than 500 thousand 18-kip (80 kN) ESAL.

The same traffic level could have been used for all pavement types, but because different levels occur in practice, the following traffic levels were established for use based on experience and past records:

1. Rigid Pavements - 2 million 18-kip (80 kN) ESAL
2. Composite Pavements - 1.5 million 18-kip (80 kN) ESAL
3. Flexible Pavements - 1 million 18-kip (80 kN) ESAL

These traffic levels were used in all parameter studies and were also used for thickness design of the different pavement sections considered.

FLEXIBLE PAVEMENT INPUTS

Pavement Thickness

SAMP is a computer based design procedure that was based on the AASHTO design procedures that select flexible pavement design and management strategies using a serviceability related failure criterion (Reference 48). Designs are generated and an optimal design is selected based on the

¹Penner, E., "Insulated Road Study", Transportation Research Record No 612, Transportation Research Board, 1976.

²Lytton, R.L., W.F. McFarland, and D.L. Schaefer, "Flexible Pavement Design and Management, Systems Approach Implementation", NCHRP Report 160, National Cooperative Highway Research Program, 1975.

lowest total cost over a prescribed analysis period. The initial thickness designs for flexible pavement were selected based on SAMP6 computer runs. Inputs for SAMP6 were developed using the traffic and environmental data associated with each zone, available structural and soil data, and 1977 material costs.

The cross sections determined by SAMP6 as the most economical appear in Figure 2 along with their estimated cost per square yard and predicted life before terminal PSI occurred. A review of the data in Figure 2 indicated that sections with crushed stone or gravel base and/or subbase were generally the most economical, while those having bases treated with asphalt or cement were more expensive.

It must be noted that in SAMP6 fatigue cracking, which is the most prevalent cause of failure in flexible pavements was not considered directly. To check fatigue cracking, an elastic layer analysis using ELSYMS was conducted. The strains at the bottom of the asphalt concrete layer were calculated using ELSYMS for various asphalt concrete surfaces and base thicknesses and for different base stiffness moduli. These resulting strains were used with a fatigue relationships to consider failure by way of fatigue fracture as well as serviceability.

Numerous fatigue relationships are available to relate strain to the number of load applications required to produce fatigue failure. The Austin Research Engineers equation (Reference 6), which was based on 5 percent cracking as the failure condition, is:

$$N_f = 9.73 \times 10^{-15} (\epsilon)^{-5.16}$$

for N_f equal to the design traffic. The fatigue model developed by Finn (Reference 7), which was based on cracking equal to or less than 10 percent, is:

$$\log N_f = 15.947 + 3.291 \log (\epsilon/10^{-6}) - .854 \log (|E^*|/10^3)$$

for N_f equal to the design traffic.

Using these two fatigue relationships and the relationships between strains, asphalt concrete thickness, base modulus, and base thickness, the design asphalt concrete thicknesses were calculated and plotted against design base thicknesses for a base having a conservative stiffness modulus of 20,000 psi (137,896 kPa) in Figure 3. For a given base thickness, Finn's (10 percent cracking) relationship requires approximately 0.75 inch (19 mm) less asphalt concrete surface than the ARE (5 percent cracking) relationship and either requires between 12.5 to 14.25 inches (318 to 362 mm) of asphalt concrete surface across the range of base thicknesses. Thus, it appears that only "deep-strength" or "full-depth" asphalt concrete pavement could be expected to survive the 25,000,000 18-kip (80 kN) ESAL without fatigue damage.

Regional Factor = 1

<p>6" ACP</p> <p>21" Crushed Stone</p> <p>8" Gravel</p> <p>Tot. Cost \$15 Life 20 yrs.</p>	<p>12" ACP</p> <p>9" CTB</p> <p>\$25 34 yrs.</p>	<p>8" ACP</p> <p>5" CTB</p> <p>18" Gravel</p> <p>\$20.30 29 yrs.</p>	<p>11" ACP</p> <p>5" ATB</p> <p>\$20.30 28 yrs.</p>	<p>6" ACP</p> <p>5" ATB</p> <p>20" Gravel</p> <p>\$18.30 28 yrs.</p>
--	--	--	---	--

Regional Factor = 1.5

<p>7" ACP</p> <p>27" Crushed Stone</p> <p>\$15.90 29 yrs.</p>	<p>6" ACP</p> <p>27" Crushed Stone</p> <p>4" S.G.</p> <p>\$15.53 29 yrs.</p>	<p>12" ACP</p> <p>9" CTB</p> <p>\$25.90 25 yrs.</p>	<p>9" ACP</p> <p>5" CTB</p> <p>18" Gravel</p> <p>\$21.50 27.5 yrs.</p>	<p>7" ACP</p> <p>11" ATB</p> <p>\$22.30 30 yrs.</p>
---	--	---	--	---

Regional Factor = 2.0

<p>7" ACP</p> <p>29" Crushed Stone</p> <p>\$16.40 29 yrs.</p>	<p>6" ACP</p> <p>27" Crushed Stone</p> <p>6" S.G.</p> <p>\$15.90 30 yrs.</p>	<p>12" ACP</p> <p>9" CTB</p> <p>\$26.10 30 yrs.</p>	<p>9" ACP</p> <p>5" CTB</p> <p>20" Gravel</p> <p>\$22.00 28 yrs.</p>	<p>10" ACP</p> <p>9" ATB</p> <p>\$23.50 28 yrs.</p>
---	--	---	--	---

ACP: Asphalt Concrete Pavement
 CTB: Cement Treated Base
 ATB: Asphalt Treated Base

CS: Crushed Stone
 SG: Sandy Gravel

FIGURE 2. CROSS SECTION OPTIMIZATION BASED ON SAMP'6.

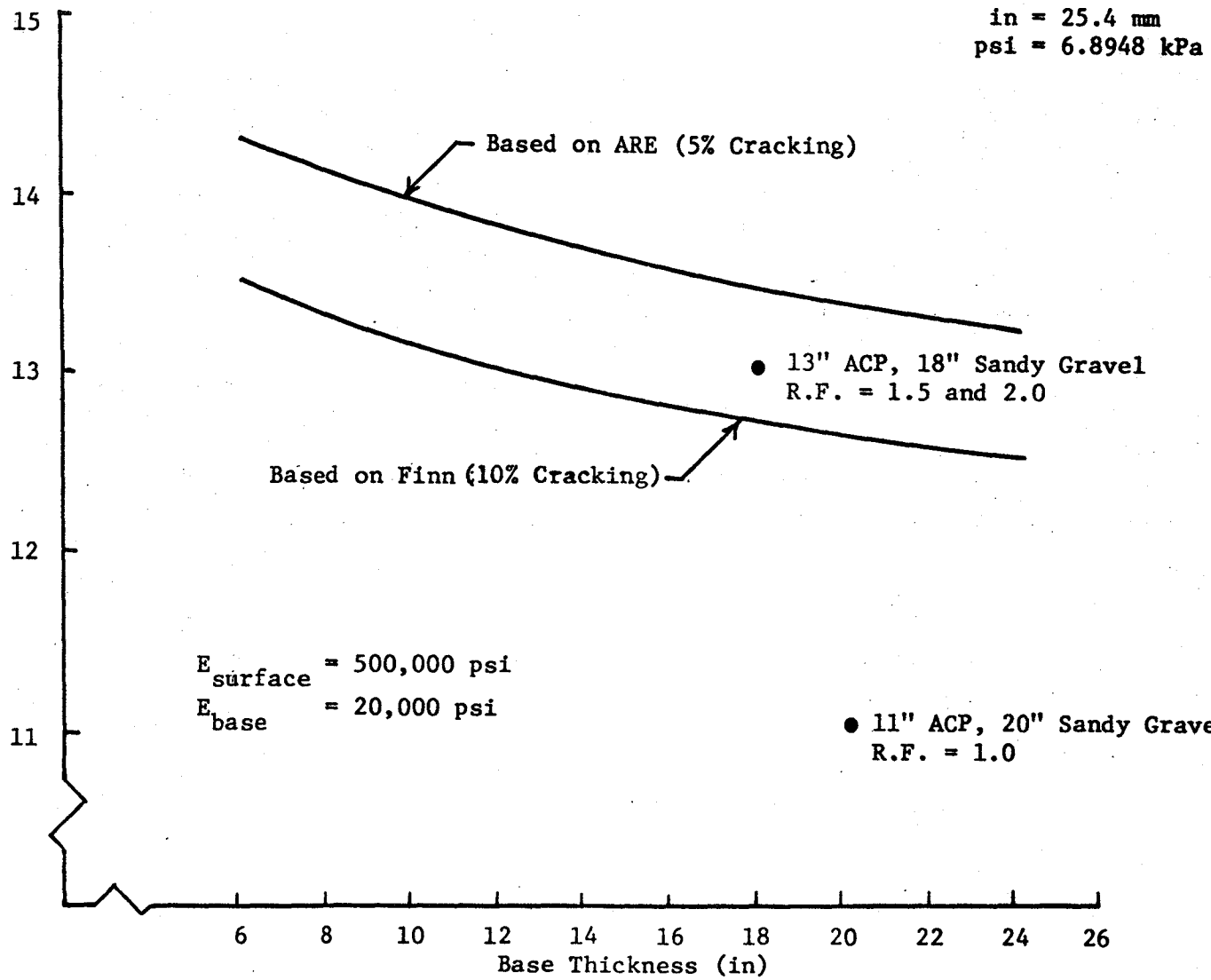


FIGURE 3. ACP SURFACE VS. GRANULAR BASE THICKNESS

Utilizing the cost optimization information based on serviceability, SAMP6, and these fatigue relationships, the minimum cross section at thicknesses selected for the study of flexible pavements were 13 inches (330 mm) of asphalt concrete materials and 8 inches (203 mm) of granular base. The granular base served primarily as a drainage layer and thus was open graded and asphalt treated for waterproofing, which minimized changes in modulus between seasons and provided constant support to the surface layer.

In order to generate a more complete analysis of the effects of the fatigue properties on pavement performance, two additional thickness combinations were selected for the flexible pavement analysis. A combined asphalt concrete thickness of 18 inches (457 mm) over an 8 inch (203 mm) open graded, asphalt treated base was selected for a complete analysis and a surface thickness of 16 inches (406 mm) was selected for partial analysis for fatigue cracking.

Material Properties - VESYS

The basic properties required for input to the analysis of flexible pavements were fatigue constants, stiffness, permanent deformation characteristics, and low temperature cracking factors. Properties for each of these categories are discussed in detail and the values selected for use in the factorial studies presented.

Fatigue Constants. The primary sources (References 49¹, 50², 51³, 52⁴, and 53⁵) of data upon which the fatigue constant selections were made are included in Table 9. Investigators (References 49 and 52) have proposed

¹Adedimila, A.S. and T.W. Kennedy, "Fatigue and Resilient Characteristics of Asphalt Mixtures by Repeated-Load Indirect Tensile Test", Research Report 183-5, Center for Highway Research, The University of Texas at Austin, August 1975.

²Monismith, C.L., J.A. Epps, D.A. Kasianchuk, and D.B. McLean, "Asphalt Mixture Behavior in Repeated Flexure", Report No TE-70-5, Office of Research Services, University of California, Berkeley, December 1970.

³Kallas, B.F. and V.P. Puzinauskas, "Flexural Fatigue Tests on Asphalt Paving Mixtures", ASTM STP 508, American Society for Testing and Materials, 1972.

⁴Pell, P.S. and K.E. Cooper, "The Effect of Testing and Mix Variables on the Fatigue Performance of Bituminous Materials", Proceedings, Association of Asphalt Paving Technologists, Vol 44, 1975.

⁵Navarro, D. and T.W. Kennedy, "Fatigue and Repeated-Load Elastic Characteristics of In-Service Asphalt-Treated Materials", Research Report 183-2, Center for Highway Research, The University of Texas at Austin, January 1975.

TABLE 9. STUDIES FROM WHICH K_1 , K_2 VALUES WERE OBTAINED (REFERENCE 49)

Test	Group	Source	Mix*
Flexure (Beam)	1	Monismith, et al. (Reference 50)	British, California Gonzales, Morro Bay and Folsom
	2	Kallas and Puzinauskas (Reference 51)	Colorado, Ontario, Washington State Test Track and Laboratory Study asphalt concrete
Flexure (Rotating Cantilever)	3	Pell and Cooper (Reference 52)	Hot rolled asphalt, Dense bitumen macadam, Dense tar macadam, Asphalt concrete, and Mastic asphalt
Axial Load	4		Hot rolled asphalt
	5**	Navarro and Kennedy (Reference 53)	Inservice blackbase and asphalt concrete
Indirect Tension	6**	Adedimila and Kennedy (Reference 49)	Asphalt concrete or blackbase

*See references for details of mix and testing temperatures.

**Based on deviator distress.

a relationship between K_1 and K_2 as shown in Figure 4. The data included in Table 9 were plotted and a regression analysis performed to determine the nature of and correlation coefficients for a relationship between K_1 and K_2 . Kennedy (Reference 49) reported an excellent correlation coefficient and standard error for K_2 as a function of K_1 (Figure 5). The linear regression relationships obtained by Kennedy from combined data are given below:

- (1) K_2 as dependent variable

$$K_2 = 1.350 - 0.252 \log K_1, (R = 0.95, S_e = 0.29)$$

- (2) K_2 as independent variable

$$\log K_1 = 3.977 - 3.609 K_2, (R = 0.95, S_e = 1.09)$$

The 95 percent confidence interval for R was between 0.92 and 0.97. Figure 5 illustrates the positions of the above relationships relative to all data points. The high correlation coefficients associated with the above expressions indicates that a linear relationship exists between K_2 and $\log K_1$, irrespective of mixture properties and test procedures.

Since the values of K_1 and K_2 vary with temperature, it was necessary to modify K_1 and K_2 to reflect the temperature range of each environment zone.

Rauhut et al (Reference 24) surveyed available information on fatigue constants at various temperatures (Table 10). These data were normalized to a 70°F (21°C) curve for ease of comparison. Values of $K_1(T)$ and $K_2(T)$ were divided by $K_1(70^\circ\text{F})$ and $K_2(70^\circ\text{F})$, respectively to arrive at comparable normalized values as shown in Table 10. Where tests were not performed at 70°F (21°C), values were estimated from the relationships between $\log K_1$ and temperature.

The normalized values of K_1 for the data reported in Table 10 are shown in Figure 6a. If the slope of the fatigue curve is assumed constant with temperature (variations are usually minor), fatigue life at a specific level of initial strain is then directly proportional to $K_1(T)$, which is simply $K_1(70^\circ\text{F})$ multiplied by the normalized value. As shown in Figure 6a, the fatigue life varies across at least seven orders of magnitude as the temperature increases from 0°F to 100°F (-18 to 38°C).

Envelopes of normalized values appear as dashed lines in Figure 6b. The solid line in Figure 6b was recommended by Rauhut (Reference 24) and was the relation selected for use to develop values of $K_1(T)$ in this study. Values of $K_1(T)$ were obtained by multiplying $K_1(70^\circ\text{F})$ by the normalized value for the desired temperature T.

Figure 7 provides similar normalized plots for $K_2(T)$ versus temperature. K_2 is the inverse of the absolute value of the slope of the fatigue relation; therefore, a normalized value of 1.00 implies that the fatigue curves at the various temperatures are parallel on a log-log plot.

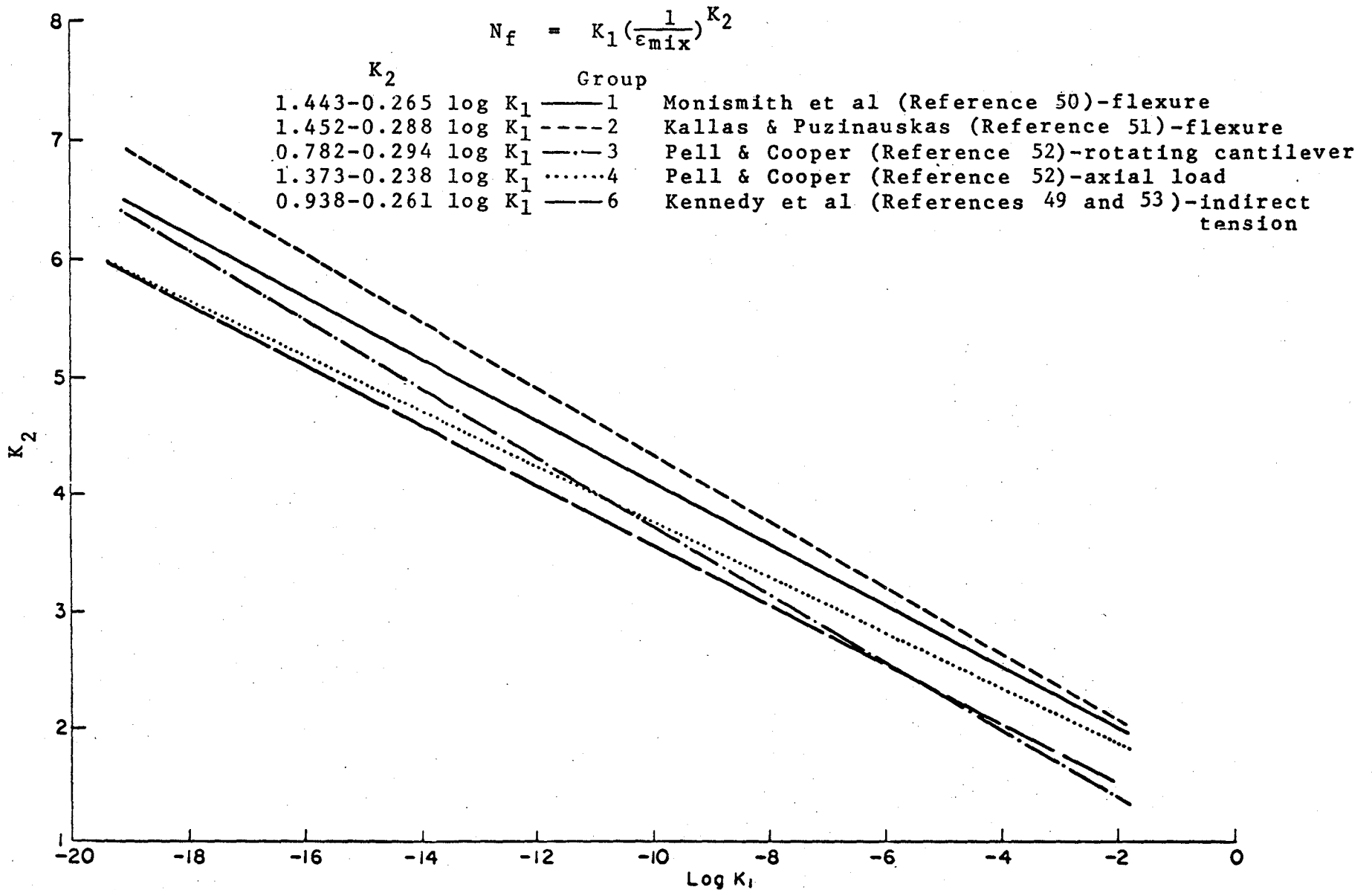


FIGURE 4. INDIVIDUAL RELATIONSHIPS BETWEEN K_2 AND $\log K_1$ FOR VARIOUS MIXTURES AND TEST PROCEDURES (REFERENCE 49).

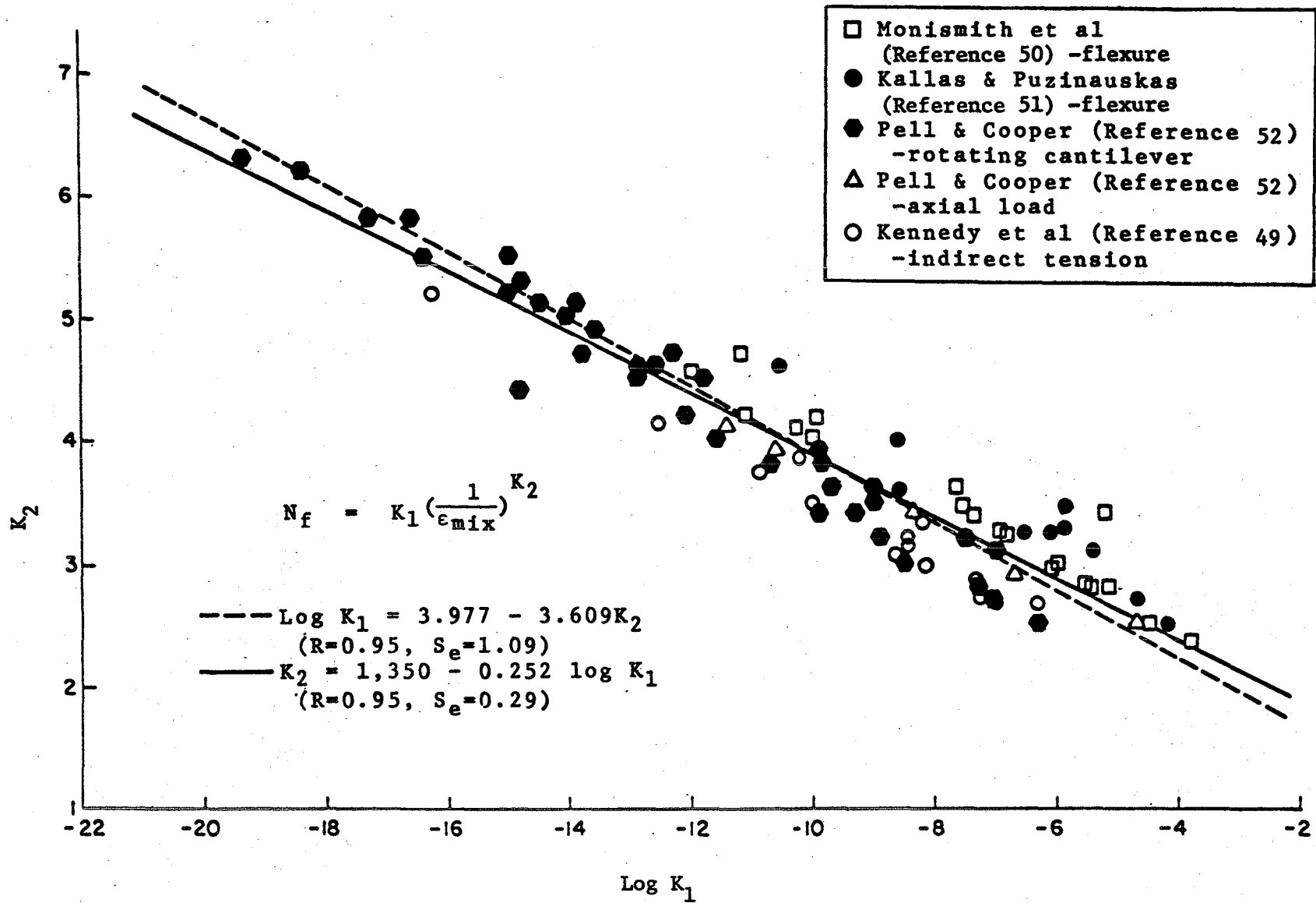
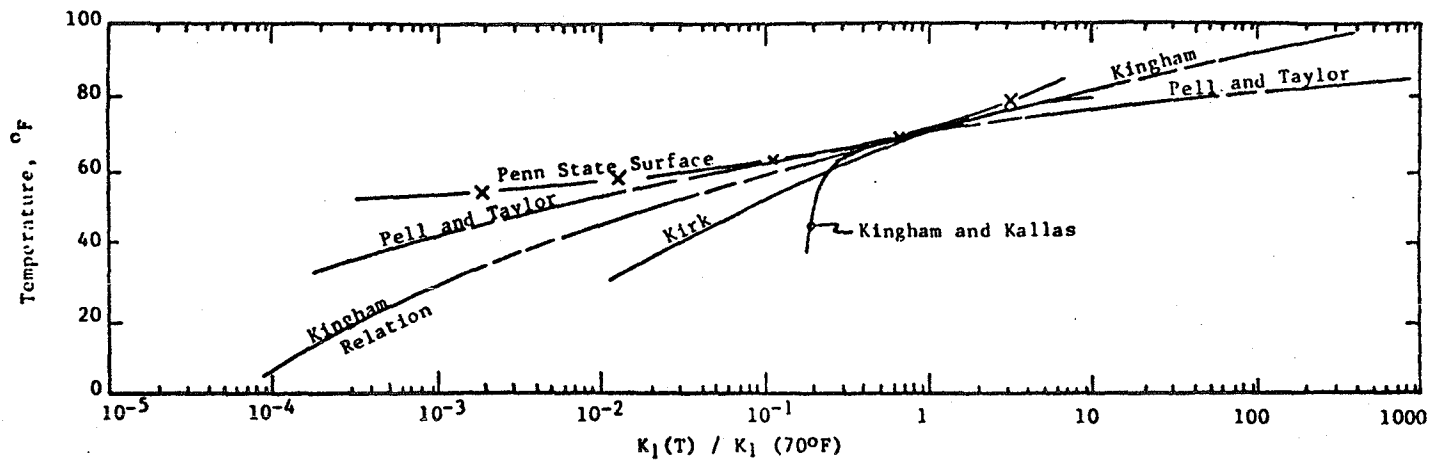


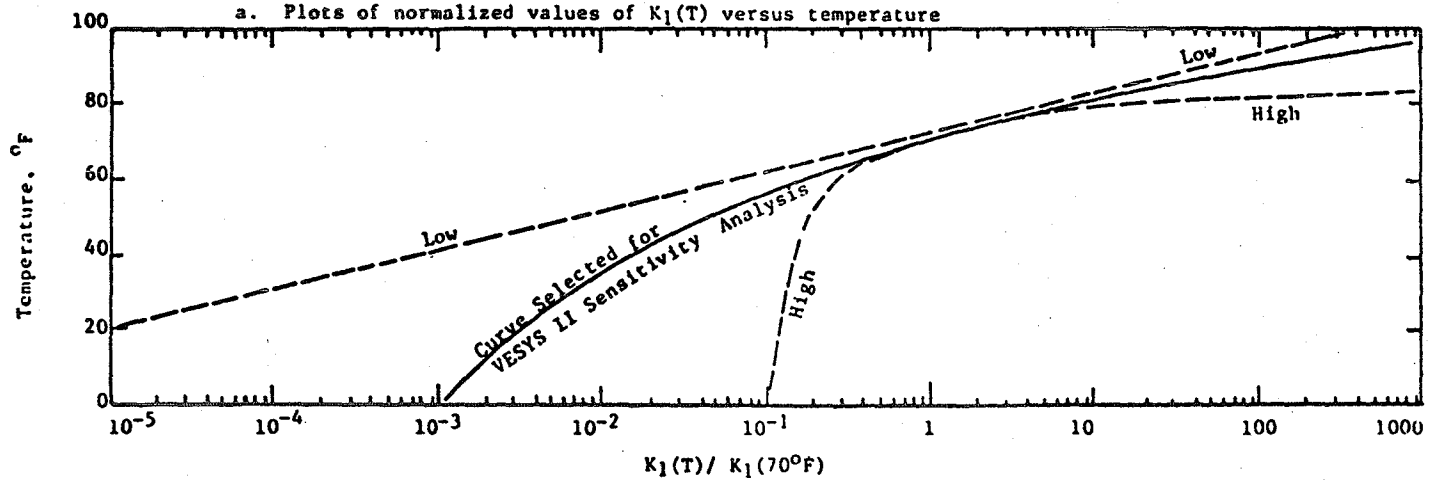
FIGURE 5. COMBINED RELATIONSHIPS BETWEEN K_1 AND K_2 FROM VARIOUS STUDIES, AS REPORTED BY KENNEDY (REFERENCE 49)

TABLE 10. TEST DATA FOR FATIGUE COEFFICIENTS VS. TEMPERATURE (REFERENCE 24)

Source	Type Material	(°F)	K_1	K_2	$\frac{K_1(T)}{K_1(70)}$	$\frac{K_2(T)}{K_2(70)}$	
Kingham & Kallas	A.C. Surface	40	$5.45(10^{-11})$	4.32	.19	1.03	
		60	$6.31(10^{-11})$	4.32	.22	1.02	
		80	$3.12(10^{-9})$	4.14	11.1	.98	
	Asphalt treated Base	40	$2.25(10^{-18})$	6.44	.05	1.00	
		60	$8.84(10^{-18})$	6.44	.18	1.00	
	Sand Asphalt Base	40	$8.83(10^{-10})$	3.83	.05	1.01	
		60	$7.49(10^{-9})$	3.81	.41	1.00	
	Pell & Taylor	Mix G.	32	$4.55(10^{-16})$	5.29	.00018	1.20
		Base Course	50	$4.50(10^{-14})$	4.83	.018	1.10
		6% Asphalt	68	$3.90(10^{-13})$	4.52	.16	1.02
		Cap Graded	86	$2.63(10^{-9})$	3.80	1047	0.86
	Kirk	A.C. Surface, Crushed Granite & Limestone (same curve) Filler	32	$1.87(10^{-18})$	6.43	.013	1.04
50-59			$2.58(10^{-17})$	6.24	.131	1.01	
77			$6.72(10^{-16})$	6.16	4.70	1.00	
Kingham Relation Based on AASHO Road Test Data	Developed from AASHO data	5	$2.60(10^{-17})$	5.00	.00009	1.0	
		25	$1.48(10^{-16})$	5.00	.0005	1.0	
		45	$2.53(10^{-15})$	5.00	.009	1.0	
		65	$9.50(10^{-14})$	5.00	.338	1.0	
		70	$2.81(10^{-13})$	5.00	1.0	1.0	
		85	$4.63(10^{-12})$	5.00	16.5	1.0	
		105	$4.03(10^{-10})$	5.00	1434	1.0	
Penn State Data	A.C. Surface	55	6.28×10^{-9}	3.92	0.0135	1.09	
		70	4.66×10^{-9}	3.92	1.0	1.0	
		85	2.90×10^{-6}	3.51	6.22	0.97	



a. Plots of normalized values of $K_1(T)$ versus temperature



b. Plots of normalized values of $K_1(T)$ to use for modifying $K_1(70^\circ\text{F})$ in VESYS II sensitivity analysis

FIGURE 6. RELATION BETWEEN NORMALIZED K_1 AND TEMPERATURE (REFERENCE 24)

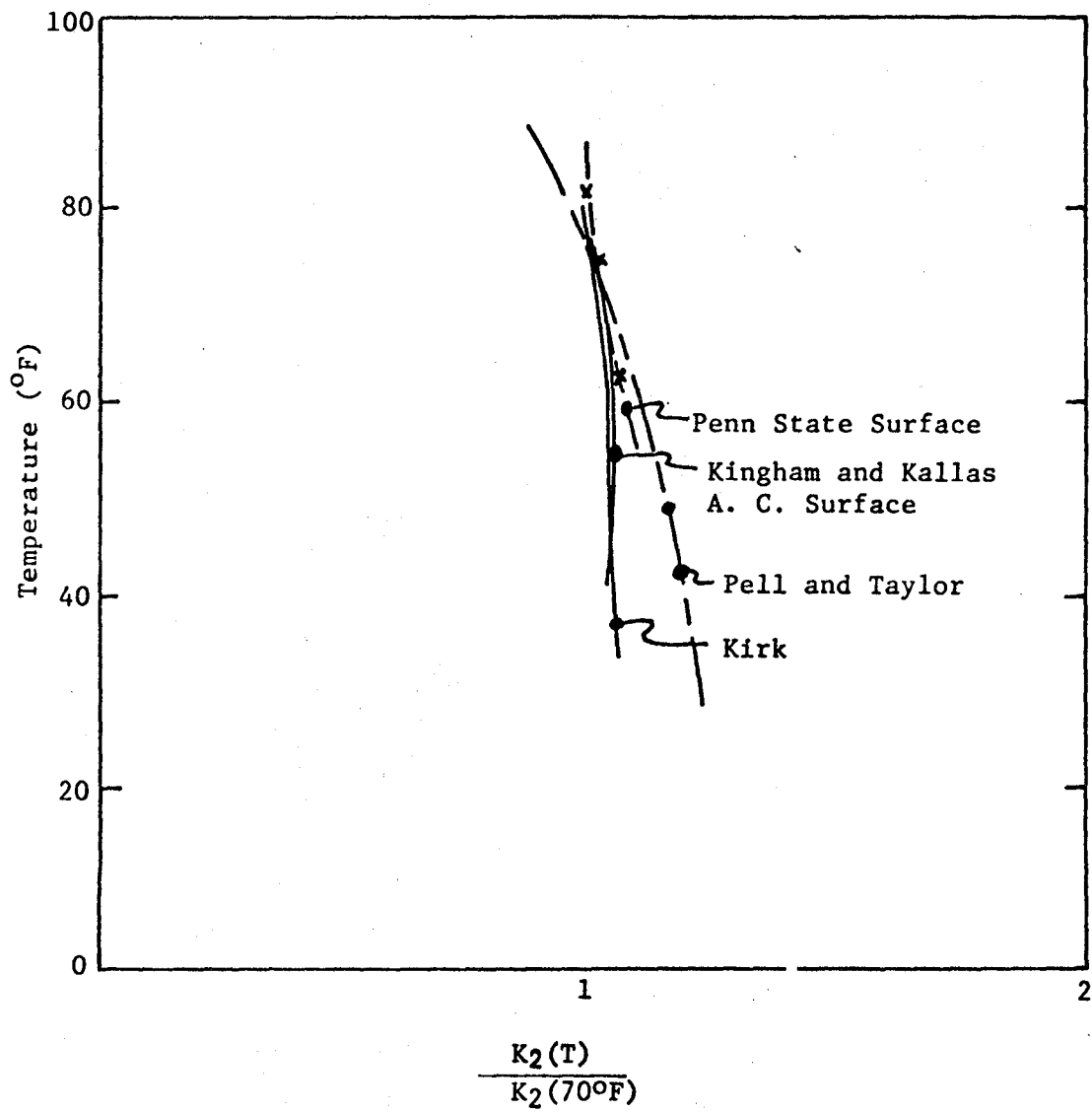


FIGURE 7. RELATIONSHIP BETWEEN NORMALIZED K_2 AND TEMPERATURE (REFERENCE 24)

Much of the data indicates a trend toward a slight decrease in the exponent K_2 with increasing temperature, although some of the data indicates no variation with temperature. Since the value of the exponent has a significant effect on the fatigue life, it seemed desirable to permit a slight variation in the normalized value. Rauhut (Reference 24) suggested a variation of -0.001 per $^{\circ}\text{F}$ ($.0018$ per $^{\circ}\text{C}$) increase in temperature, which resulted in an equation for this variation:

$$K_2(T) = K_2(70^{\circ}\text{F})[1 - 0.001 (T - 70)]$$

Values for $\log K_1$ were selected to span the range of reported values and K_2 was computed using the correlation developed by Kennedy (Reference 49). The values selected for inclusion in the parameter study for the K_1 and K_2 at 70°F (21°C) are included in Table 11.

The relationships previously described were utilized to calculate $K_1(T)$ and $K_2(T)$ for the temperature representing the seasonal average in each of the four zones. The range of fatigue curves selected and the $K_1(T)$ and $K_2(T)$ utilized in the study are shown in Table 12.

Stiffness. Seasonal multipliers were used to establish the stiffness of the asphalt concrete materials appropriate for the various seasonal temperatures. These multipliers were developed primarily using the results of a study conducted by The Asphalt Institute (Reference 54¹) which involved 41 mixes at three levels of loading frequency and temperature and provided a data base of 369 points and were checked with results from a study by Hudson and Kennedy (Reference 55²). These data were plotted and are included in Figure 8 along with the line representing the multipliers selected for use in this analysis.

Permanent Deformation Parameters. The procedures for calculating permanent deformations at the pavement surface used in VESYS and the derivation of the terms ALPHA and GNU are discussed in Reference 24. Since these terms are relatively new to the engineering profession, only a limited amount of testing has been reported for use in evaluating ALPHA and GNU. The most extensive testing programs conducted to summarize ALPHA and

¹Witczak, M.W., "Development of Regression Models for Asphalt Concrete Modulus for Use in MS-1 Study", unpublished report dated January 1978, The Asphalt Institute, College Park, Maryland.

²Hudson, W.R. and T.W. Kennedy, "An Indirect Tensile Test for Stabilized Materials", CFHR Research Report 98-1, Center for Highway Research The University of Texas at Austin, January 1968.

TABLE 11. LOG K_1 (70°F) and K_2 (70°F) VALUES SELECTED FOR
USE IN THE PARAMETER STUDY FOR FLEXIBLE PAVEMENTS

Log K_1 (70°F)	K_2 (70°F)
-5	2.61
-10	3.87
-15	5.13
-20	6.39

TABLE 12. FATIGUE CONSTANTS SELECTED FOR THE FOUR ENVIRONMENTAL ZONES AND THE FOUR SEASONS

Environmental Zone	Seasons	Pavement Temperature of	$K_1(T)/K_2(T)^*$ for $K_1(70)/K_2(70)^{**}$ of:			
			$10^{-5}/(2.61)$	$10^{-10}/(3.87)$	$10^{-15}/(5.13)$	$10^{-20}/(6.39)$
Wet Freeze	Winter	35	$1.0 \times 10^{-7}/2.70$	$1.0 \times 10^{-12}/4.01$	$1.0 \times 10^{-17}/5.13$	$1.0 \times 10^{-22}/6.61$
	Spring	65	$3.9 \times 10^{-6}/2.62$	$3.9 \times 10^{-11}/3.89$	$3.9 \times 10^{-16}/5.16$	$3.9 \times 10^{-21}/6.42$
	Summer	95	$4.8 \times 10^{-3}/2.54$	$4.8 \times 10^{-8}/3.77$	$4.8 \times 10^{-13}/5.00$	$4.8 \times 10^{-18}/6.73$
	Fall	60	$1.8 \times 10^{-6}/2.64$	$1.8 \times 10^{-11}/3.91$	$1.8 \times 10^{-16}/5.18$	$1.8 \times 10^{-21}/6.45$
Dry Freeze	Winter	35	$1.0 \times 10^{-7}/2.70$	$1.0 \times 10^{-12}/4.01$	$1.0 \times 10^{-17}/5.31$	$1.0 \times 10^{-22}/6.61$
	Spring	60	$1.8 \times 10^{-6}/2.14$	$1.8 \times 10^{-11}/3.91$	$1.8 \times 10^{-16}/5.18$	$1.8 \times 10^{-21}/6.45$
	Summer	90	$1.1 \times 10^{-3}/2.56$	$1.1 \times 10^{-8}/3.79$	$1.1 \times 10^{-13}/5.03$	$1.1 \times 10^{-18}/6.26$
	Fall	50	$4.0 \times 10^{-7}/2.66$	$4.0 \times 10^{-12}/13.95$	$4.0 \times 10^{-17}/5.23$	$4.0 \times 10^{-22}/6.52$
Wet-No Freeze	Winter	75	$2.7 \times 10^{-5}/2.60$	$2.7 \times 10^{-10}/3.85$	$2.7 \times 10^{-15}/5.10$	$2.7 \times 10^{-20}/6.36$
	Spring	95	$4.8 \times 10^{-3}/2.54$	$4.8 \times 10^{-8}/3.77$	$4.8 \times 10^{-13}/5.00$	$4.8 \times 10^{-18}/6.23$
	Summer	105	$1.1 \times 10^{-1}/2.52$	$1.1 \times 10^{-6}/3.73$	$1.1 \times 10^{-11}/4.95$	$1.1 \times 10^{-16}/6.17$
	Fall	95	$4.8 \times 10^{-3}/2.54$	$4.8 \times 10^{-8}/3.77$	$4.8 \times 10^{-13}/5.00$	$4.8 \times 10^{-18}/6.23$

* $K_1(T)$ and $K_2(T)$ adjusted for each seasonal temperature using relationships obtained from Reference 24.

** $K_2(70)$ for each $K_1(70)$ computed using relationship obtained from Reference 49.

TABLE 12. FATIGUE CONSTANTS SELECTED FOR THE FOUR ENVIRONMENTAL ZONES AND THE FOUR SEASONS (Continued)

Environmental Zone	Seasons	Pavement Temperature of	$K_1(T)/K_2(T)^*$ for $K_1(70)/K_2(70)^{**}$ of:			
			$10^{-5}/(2.61)$	$10^{-10}/(3.87)$	$10^{-15}/(5.13)$	$10^{-20}/(6.39)$
Dry-No Freeze	Winter	55	$8.0 \times 10^{-7}/2.65$	$8.0 \times 10^{-12}/3.93$	$8.0 \times 10^{-17}/5.21$	$8.0 \times 10^{-22}/6.49$
	Spring	75	$2.7 \times 10^{-5}/2.60$	$2.7 \times 10^{-10}/3.85$	$2.7 \times 10^{-15}/5.10$	$2.7 \times 10^{-20}/6.49$
	Summer	95	$4.8 \times 10^{-3}/2.56$	$4.8 \times 10^{-8}/3.79$	$4.8 \times 10^{-13}/5.03$	$4.8 \times 10^{-18}/6.26$
	Fall	75	$2.7 \times 10^{-5}/2.60$	$2.7 \times 10^{-10}/3.85$	$2.7 \times 10^{-15}/5.10$	$2.7 \times 10^{-20}/6.36$

* $K_1(T)$ and $K_2(T)$ adjusted for each seasonal temperature using relationships obtained from Reference 24.

** $K_2(70)$ for each $K_1(70)$ computed using relationship obtained from Reference 49.

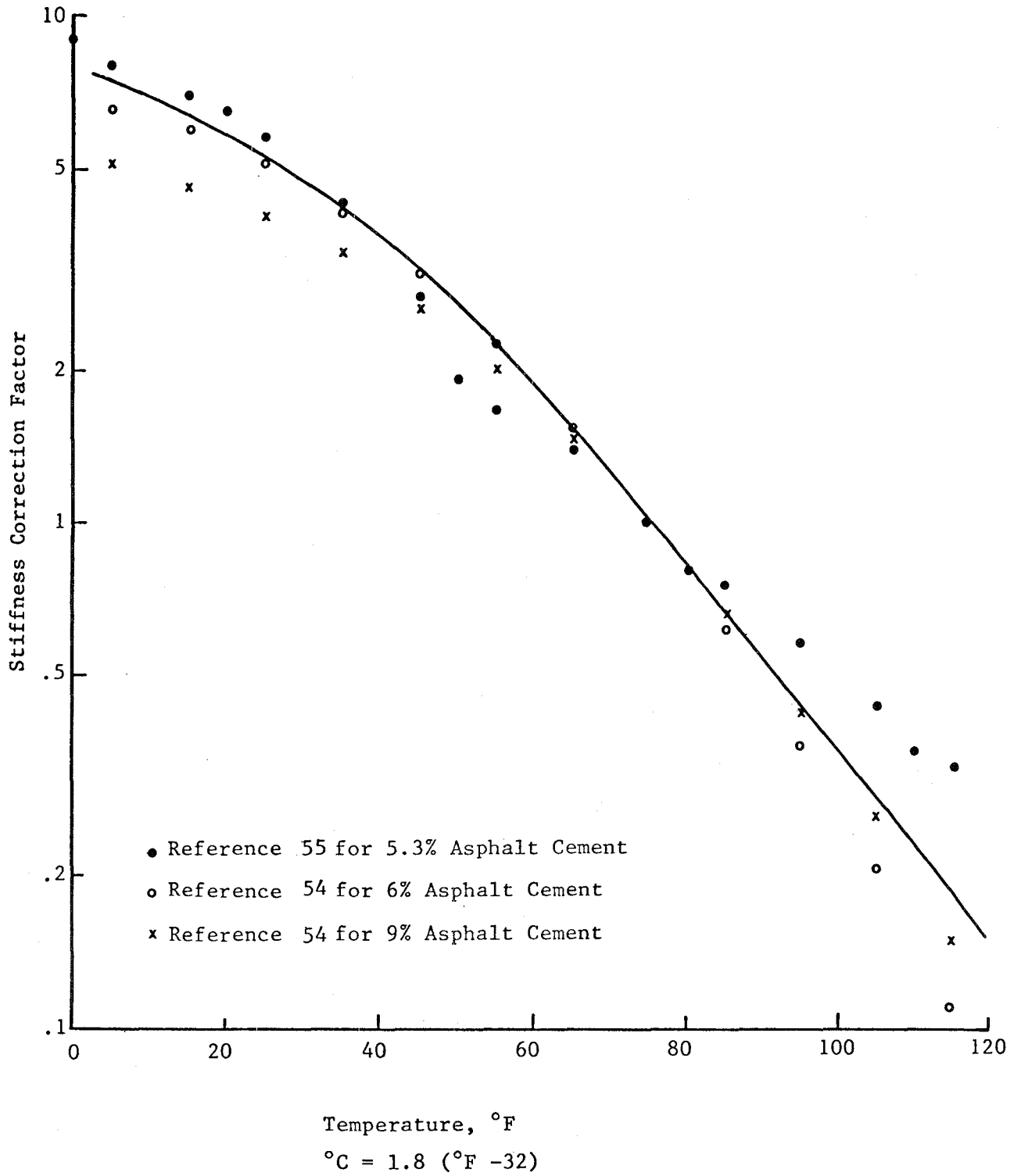


FIGURE 8. RELATIONSHIP SELECTED FOR MODIFYING STIFFNESS AS A FUNCTION OF TEMPERATURE

GNU are reported in References 4, 24, and 56¹. ALPHA and GNU are defined by the intercept and slope of the relationship between the logarithm of permanent strain and the logarithm of the number of load applications as shown in Figure 9 and are defined as

$$\text{GNU} = \frac{IS}{\epsilon_r}$$

and

$$\text{ALPHA} = 1 - S$$

where:

I = arithmetic value of the intercept (not a logarithm) as shown in Figure 9,

S = slope of the linear portion of the logarithmic relationship, and

ϵ_r = resilient strain.

Rauhut (Reference 24) established a range of GNU and ALPHA values which when used as an input to VESYS resulted in reasonable predictions of rut depths for asphalt pavements. He concluded that only values of GNU and ALPHA falling near or within the shaded band in Figure 10 were typical of asphalt concretes used in practice and that while mixtures represented by combinations of GNU and ALPHA substantially outside the band could be obtained, such mixtures and values were not to be expected using modern mixture and pavement thickness design procedures. Thus, ALPHA values ranging from 0.7 to 0.9 and GNU values ranging from 0.2 to 1.4 were considered to be realistic and were selected for use in this study.

Figure 11 compares ALPHA values for different tests and illustrates the relationship between ALPHA and stress difference for the different types of tests and testing temperatures. The relationship between GNU and stress difference for different test methods and testing temperatures were plotted as shown in Figure 12. The range of values for all tests except the indirect tensile test was from 0.12 to 4.80. Rauhut (Reference 24) proposed that values greater than 1.80 not be considered since these values occur only when low stress difference occur. Stress difference appeared to have very little effect on the magnitude of either ALPHA or GNU.

¹Vallejo, J., T.W. Kennedy, and R. Haas, "Permanent Deformation Characteristics of Asphalt Mixtures by Repeated-Load Indirect Tensile Test", CFHR Research Report 183-7, Center for Highway Research, The University of Texas at Austin, June 1976.

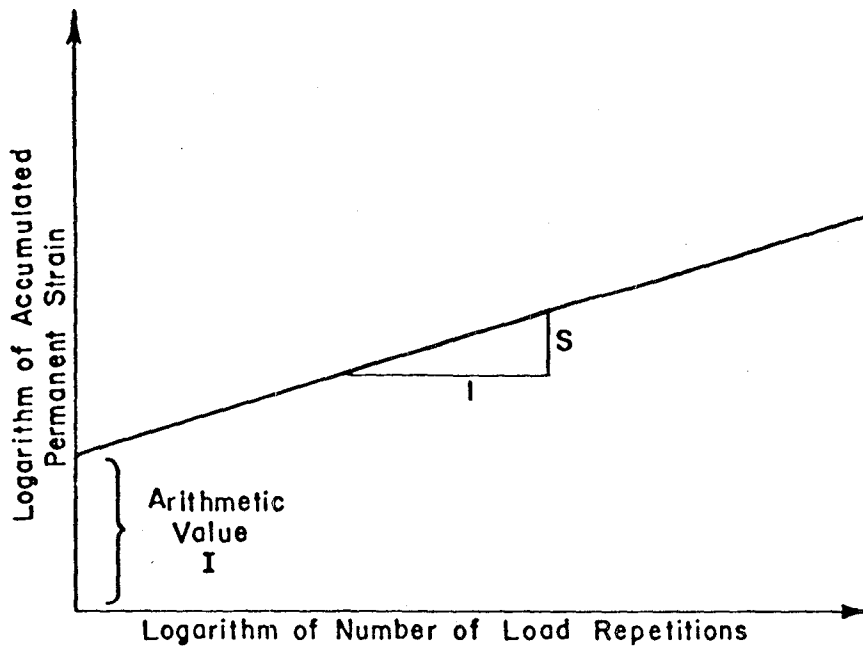


FIGURE 9. ASSUMED LOGARITHMIC RELATIONSHIP BETWEEN PERMANENT STRAIN AND NUMBER OF LOAD REPETITIONS (REFERENCE 57).

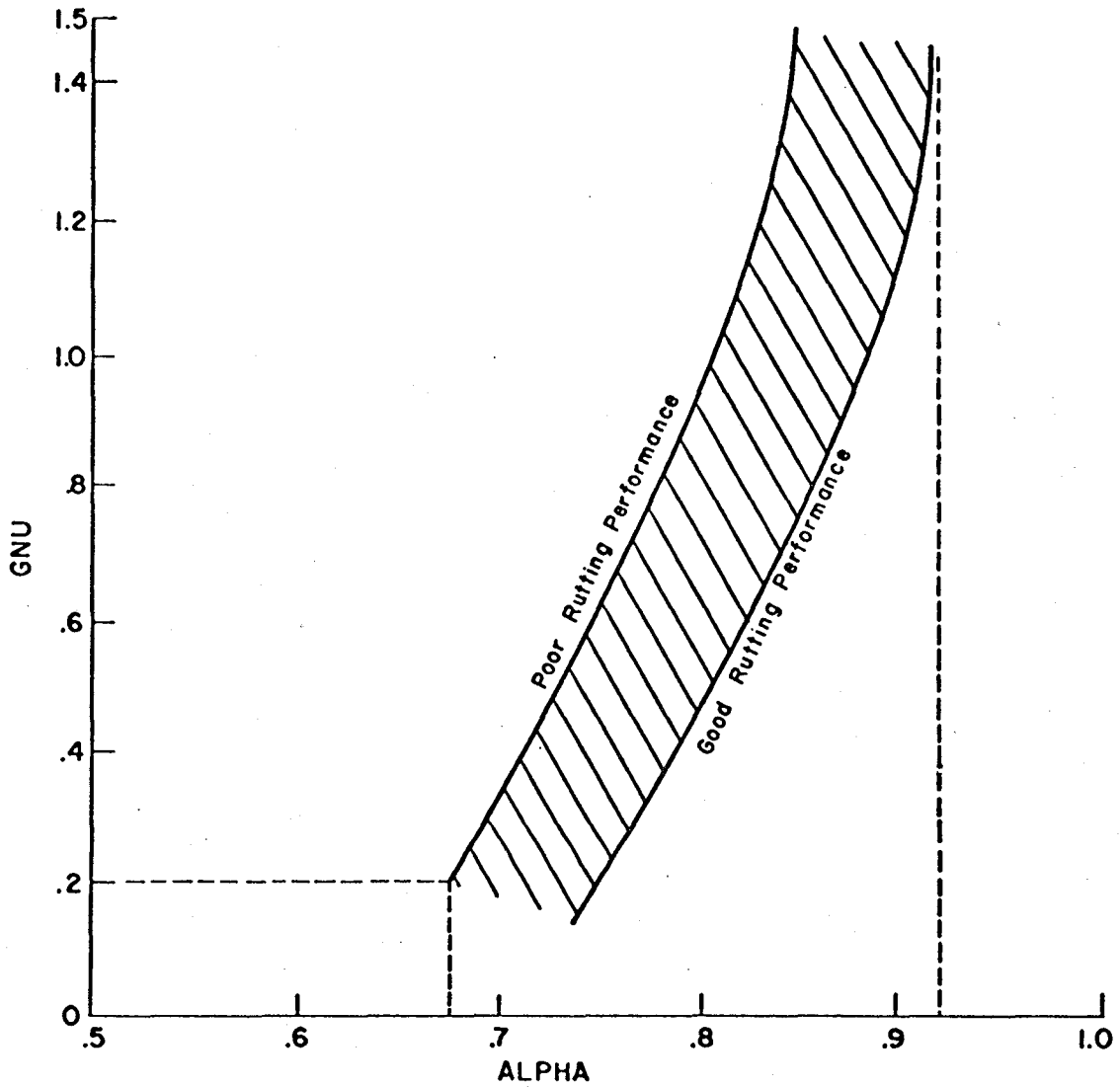


FIGURE 10. RANGE OF PRACTICAL GNU AND ALPHA VALUES FOR ASPHALT CONCRETE (REFERENCE 24).

The relationship between GNU and ALPHA was also analyzed. Rauhut (Reference 24) plotted all ALPHA and GNU data available at that time (Figure 13). A region was defined by A, B, C, D, and E corresponding to GNU and ALPHA values tested under stress differences between 20 and 90 psi (138 and 621 kPa). It was concluded that these data could be separated into three distinct groups, depending on stress difference, and that the indirect tensile test values fell into a high stress difference region. Unfortunately, values from the indirect tensile test were the only ones in that region, and therefore, it was concluded that stress level was the reason for the observed difference. An analysis of more current data showed that values determined from indirect tensile testing are not in a separate group and substantiate the observation that the values cannot be grouped according to stress difference.

Since the traffic levels for this study require very heavy duty pavements, ALPHA greater than 0.7 for pavements with a surface thickness greater than 10 inches (254 mm) was assumed as recommended by Rauhut (Reference 24). The combinations of ALPHA and GNU selected for use in this study are contained in Table 13. Solutions for all combinations were performed for pavement surface thicknesses of 13 inches (330 mm) and 18 inches (451 mm) with limited runs conducted for 16 inches (406 mm).

To eliminate the effects of variation in the permanent deformation characterizations of the base and subgrade materials, one set of values were selected for each layer and these were assumed to remain constant. The same ALPHA and GNU values for the base and subgrade were utilized for each environmental zone and each season of the year. The values selected for the base and subgrade are also contained in Table 13.

Stochastic Parameters. Because the traffic for zero maintenance pavements was considered to be very heavy and because the project mileages were expected to be small, extraordinary high quality control was believed to be necessary during construction of these pavements. The requirements under development for the Design of Zero Maintenance Flexible and Composite Pavements, FHWA Contract No. DOT-FH-11-9348, were considered while developing the values for quality control type stochastic variables used in this project. The level of quality control requirements selected for use was considered to match closely that exercised during the construction of the AASHO Road Test pavements. Rauhut discussed the AASHO Road Test quality control and presented typical values for the coefficients of variation for the various strength, stiffness, and permanent deformation parameters (Reference 24). The values selected for use in this study are compatible with the objectives of providing zero maintenance pavements were:

<u>Variable</u>	<u>Description</u>	<u>Input Value</u>
VARCOEF	Coefficient of Variation in Material Properties for	
	(a) Surface	0.10
	(b) Base	0.15
	(c) Subgrade	0.15

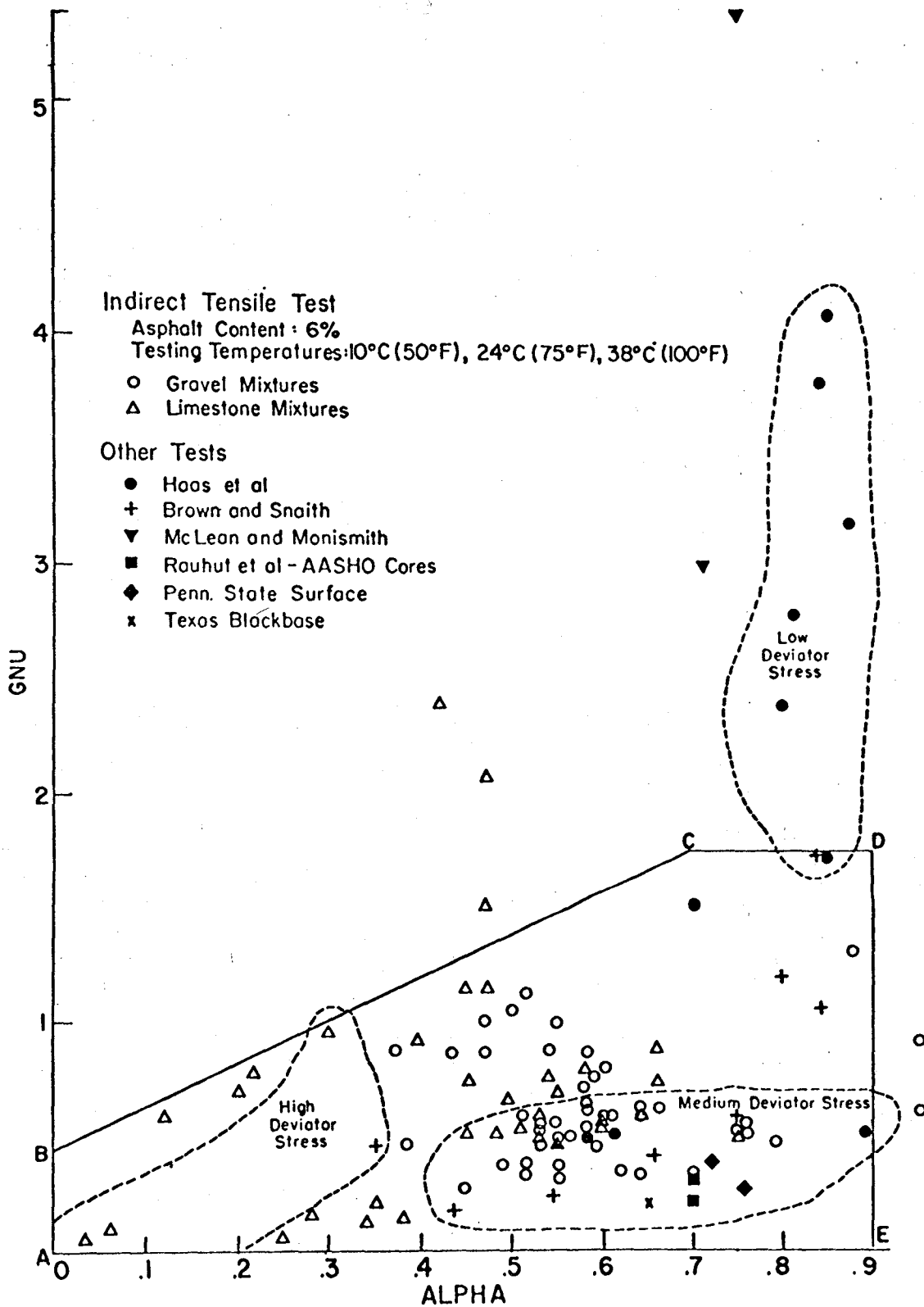


FIGURE 13. RELATIONSHIP BETWEEN GNU AND ALPHA FOR DIFFERENT TEST METHODS (REFERENCE 56).

TABLE 13. COMBINATION OF ALPHA AND GNU SELECTED FOR THE FLEXIBLE PAVEMENT PARAMETER STUDY

LAYER	Permanent Deformation Characteristics				
	ALPHA	GNU			
SURFACE		0.2	0.5	0.8	1.4
	0.7	X	X	X	X
	0.8	X	X	X	X
	0.9	X	X	X	X
BASE	0.92	0.25			
SUBGRADE	0.90	0.15			

COEFK1	Coefficient of Variation in K_1	0.20
COEFK2	Coefficient of Variation in K_2	0.04
K1K2CorL	Correlation Coefficient Between K_1 and K_2	-0.9

Material Properties - Low Temperature Cracking

The material properties required to complete this analysis are asphalt concrete mix stiffness, asphalt concrete tensile strength, and asphalt concrete thermal coefficient. The values selected for use are listed in Table 14. The mixture stiffness range for the parameter study was determined from typical properties for an AC-40 and AC-10 asphalt cement. To ensure a proper comparison of cracking with respect to stiffness, the material properties for an asphalt cement used to calculate the stiffness were made comparable in terms of temperature susceptibility. The properties selected for the asphalt cements (Table 14) were developed to ensure that the resulting mixtures had similar penetration indices. The appropriate material properties were established using information obtained from References 58¹, 59², 60³, 61⁴, 62⁵, 63⁶, 64⁷, 65⁸, 66⁹, and 67¹⁰.

¹Hveem, F.N., E. Zube, and J. Skog, "Progress Report on the Zaca-Wigmore Experimental Asphalt Test Project", Symposium on Paving Materials, American Society for Testing Materials, Special Technical Publication No 277, 1959.

²Witczak, M.W., "Development of Regression Model for Asphalt Concrete Modulus for Use in MS-1 Study", January, 1978.

³Gotolski, W.H., S.K. Ciesielski, and L.N. Heagy, "Progress Report on Changing Asphalt Properties of In-Service Pavements in Pennsylvania", Proceedings, Association of Asphalt Paving Technologists, Vol 33, February, 1964.

⁴Kenis, W.J., Sr., "Progress Report on Changes in Asphaltic Concrete in Service", Bulletin 333, Highway Research Board, Washington, D.C., 1962.

⁵Simpson, W.C., R.L. Griffin, and T.K. Miles, "Correlation of the Microfilm Durability Test with Field Hardening Observed in the Zaca-Wigmore Experimental Project", Symposium on Paving Materials, American Society for Testing Materials, Special Technical Publication No 277, 1959.

⁶Skog, J., "Results of Cooperative Test Series on Asphalts from the Zaca-Wigmore Experimental Project", Symposium on Paving Materials, American Society for Testing Materials, Special Technical Publication No 277, 1959.

TABLE 14. MATERIAL PROPERTY RANGES FOR FUTURE PAVEMENT
LOW TEMPERATURE CRACKING STUDIES

MATERIAL PROPERTY	LOW LEVEL	HIGH LEVEL
Mix Stiffness:		
Original Penetration 100 gms, 5 sec, 77°F, D mm	120	50
Original Softening Point, °F (°C)	115 (46)	125 (52)
% of Original Penetration After thin-film oven test	67	70
Specific Gravity of Asphalt	1.040	1.015
Maximum Tensile Strength, psi (kPa)	300 (2,068)	600 (4,136)
Thermal Coefficient of Asphalt Concrete $10^{-6}/^{\circ}\text{F}$ ($10^{-6}/^{\circ}\text{C}$)	11 (20)	17 (31)

The values shown in Table 14 for tensile strength represent the maximum that was expected to occur at a bitumen stiffness of approximately 10,000 psi (68,948 kPa). A range in tensile strength from 300 to 600 psi (2,068 to 4,136 kPa) was selected for use in this study.

The range in thermal coefficients (Table 14) were derived from Reference 62 and were checked for reasonableness with the author of Reference 8. Although the thermal coefficient of asphalt concrete does vary with temperature, they were held constant for this analysis.

The characterization of the environmental zones in this analysis required the following additional information:

1. air temperature
2. wind velocity, and
3. solar radiation

The required temperature inputs were the average air temperature, annual temperature range, and the daily temperature range. The pavement temperature at a specified depth was calculated from the air temperatures and the following inputs:

1. solar radiation,
2. wind velocity,
3. surface absorbtivity,
4. mixture conductivity,
5. mixture specific heat, and
6. mixture density.

⁷Zube, E. and J. Skog, "Final Report on the Zaca-Wigmore Asphalt Test Road", a progress report presented to the Materials and Research Department of the California Division of Highways, 1959.

⁸Corbett, L.W. and R.E. Merz, "Asphalt Binder Hardening in the Michigan Test Road after 18 Years of Service", Transportation Research Record No 544, Transportation Research Board, 1975.

⁹Schmidt, R.J., "Use of ASTM Tests to Predict Low-Temperature Stiffness of Asphalt Mixes", Transportation Research Record No 544, Transportation Research Board, 1975.

¹⁰Johnson, T.C., M.Y. Shahin, B.J. Dempsey, and J. Ingersoll, "Projected Thermal and Load-Associated Distress in Pavements Incorporating Different Grades of Asphalt Cement", Proceedings, Association of Asphalt Paving Technologists, Vol 48, February 1979.

The average annual air temperature, average daily temperature range, solar radiation, and wind velocity were obtained from climatological data from selected cities in each environmental zone to develop a composite set of data representative of each zone (Reference 68¹). The annual air temperature range was developed so that the lowest calculated air temperature over the analysis period was approximately the lowest 20 year extreme. The input variables that were different for each zone are listed in Table 15.

The low temperature model inputs that were held constant throughout the analysis are shown in Table 16. In most cases these values were set at values typical for asphalt pavements. In some cases, the inputs for which limited information were available were set equal to the values used in the model development.

Material Properties - Loss of Skid Resistance

The material properties required to complete this analysis were the values of the initial skid number, $SN_{40@N_1}$ and the exponent, b_{field} , for several values of skid number to define the region of acceptable values. Values for five Texas aggregates are listed in Table 17. These values were used in the Steittle-McCullough model to predict skid numbers for the heavy zero-maintenance pavement traffic levels.

In order to utilize the Steittle-McCullough model, it was necessary to convert 18 kip (80 kN) ESAL applications to volume of vehicles in the design lane. This conversion was accomplished using typical loadometer results for Texas Interstate highways and highway capacity manual adjustments to take into account vehicle size. These calculations led to the use of a total design volume of 300 million vehicles for a 30 year design life.

Since it was assumed that there would be no significant use of studded tires, all environmental zones were assumed to exhibit an equivalent loss rate of skid number.

RIGID PAVEMENT INPUTS

Because most of the distress models for JRCP and JCP are virtually equivalent, these two pavement types will be discussed together and differences which exist will be discussed appropriately.

¹National Oceanic and Atmospheric Administration, et al, "Local Climatological Data: Annual Summaries for 1977."

TABLE 15. ENVIRONMENTAL ZONE DEPENDENT INPUT VARIABLES FOR LOW TEMPERATURE CRACKING STUDY

VARIABLE	ENVIRONMENTAL ZONE			
	Wet Freeze	Dry Freeze	Wet No Freeze	Dry No Freeze
Annual Average Temperature, °F	50	50	70	65
Average Annual Temperature Range °F	118	135	112	89
Average Daily Temperature Range °F	20	25	20	25
Average Annual Wind Speed, mph	10	9	7	11
Average Annual Solar Radiation, langleys	350	375	400	500
July Average Solar Radiation, langleys	525	625	500	625

$$^{\circ}\text{F} = 1.8^{\circ}\text{C} + 32$$

$$1 \text{ mph} = 1.609 \text{ kph}$$

$$\text{langley} = 4.184 \times 10^4 \text{ joules/m}^2$$

TABLE 16. INPUT VARIABLES HELD CONSTANT THROUGHOUT
LOW TEMPERATURE CRACKING ANALYSIS

<u>INPUT VARIABLE</u>	<u>VALUE</u>
Thermal Loading Time, Sec	3,600
Mixture Density, pcf(kg/m ²)	150 (2,403)
Mixture Specific Heat, BTU/(lb-°F)[Joule/(kg-°C)]	0.22 (921)
Mixture Conductivity, BTU/(ft-hr-°F)[Joule/(sec-m-°C)]	0.7 (1.2)
Absortivity of Surface to Solar Radiation, %	95
Coefficient of Variation of Thermal Coefficient	0.1
Coefficient of Variation of Max. Tensile Strength	0.2
Design Period, yrs	10
% Asphalt by Aggregate Weight	5.5
Specific Gravity of Aggregate	2.6
% Air Voids	5.0

TABLE 17. MATERIAL PROPERTY VALUES FOR REDUCED SKID
RESISTANCE MODEL STUDY (REFERENCE 18)

Skid Resistance Parameters	AGGREGATE TYPE				
	Expanded Shale	Burnet Dolomite	Knippa Trap Rock	Georgetown Limestone	Iron Slag
SN^*_i	67	58	58	52	56
b_{field}	0.041	0.121	0.096	0.136	0.063

* SN_i measured at an N_i estimated to be approximately 50,000 applications.

Pavement Thickness

The AASHTO design procedures were used to generate the thickness design for rigid pavements. A small study using two types of subbase, three subbase thicknesses, and their corresponding moduli was performed using load transfer values of 2.2, 3.0, and 3.2 for CRCP, JCP, and JRCP respectively. An analysis was then conducted to select the rigid pavement cross sections. This analysis utilized the serviceability index equation for zero maintenance jointed concrete pavements which was developed by Darter and Barenberg using data from the site of the AASHTO Road Test.

For a medium range of subbase moduli, the following rigid pavement cross sections were selected:

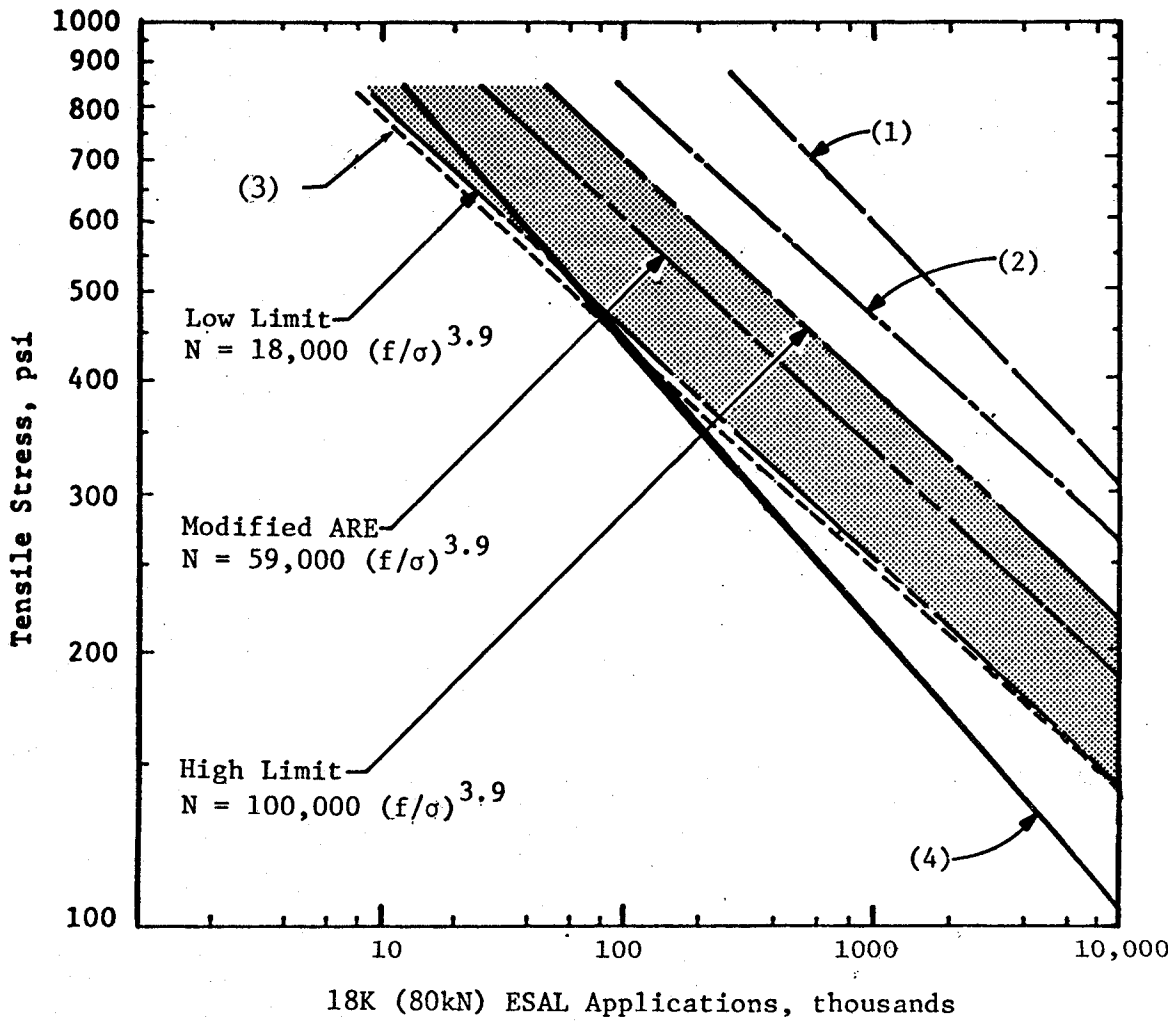
Pavement Type	JRCP	JCP	CRCP
PCC Surface thickness, in (mm)	13 (330)	13 (330)	11 (279)
Subbase thickness, in (mm)	8 (203)	8 (203)	8 (203)

Material Properties - JCP and JRCP

Fatigue curves that have been developed from evaluations of AASHTO Road Test and other data are included in Figure 14. The curves in Figure 14 represent fatigue relationships based on the field performance of pavement slabs while the curves in Figure 15 show relationships that were developed from laboratory beam or indirect tension tests.

One of the difficulties in the use of curves such as the PCA curve (Figure 15) is the basic assumption that no fatigue failure would occur at stress levels below 50 percent of the flexural strength. Darter presents another curve based on a large sample of laboratory beam tests as reported in Reference 7 and shown in Figure 15 as "Darter". That was not selected for the design of zero maintenance plain jointed concrete pavement, since the design curve was selected at a 25 percent probability level. As can be seen, the beam test data reported in Reference 7 indicate that there should be no fatigue cracking for the low stresses that should occur in thick zero maintenance pavements.

The fatigue relationships used in this study are also shown on Figure 15. The relationship designated as "All Sections ARE Curve" in Figure 14 was developed from interior stresses predicted by elastic layer theory, on a slab with a flexural strength of 700 psi (4826 kPa), and using the initial occurrence of Class 3 and 4 cracking as a failure criterion. Class 3 or 4 cracking was selected on the basis of a comparison of deflections between the uncracked and cracked condition. No significant difference was found between the edge deflections of uncracked slabs and slabs exhibiting class 1 and 2 cracking as measured with the Benkelman Beam at the AASHTO Road Test. However, a significant difference did exist between the uncracked slab deflections and the deflections on slabs exhibiting class 3 or 4 cracking. On the basis of this series of comparisons, uncracked slabs



- (1) Liddle, et al (Ref 69) $N = 615,000 (f/\sigma)^{3.42}$
- (2) Vesic (Ref 72) $N = 225,000 (f/\sigma)^{4.00}$
- (3) Treybig, et al (Ref 71) $N = 17,000 (f/\sigma)^{4.0}$
- (4) All Sections ARE Curve $N = 23,440 (f/\sigma)^{3.21}$

FIGURE 14. COMPARISON OF SEVERAL FATIGUE CURVES BASED ON FIELD PERFORMANCE (REFERENCE 6)

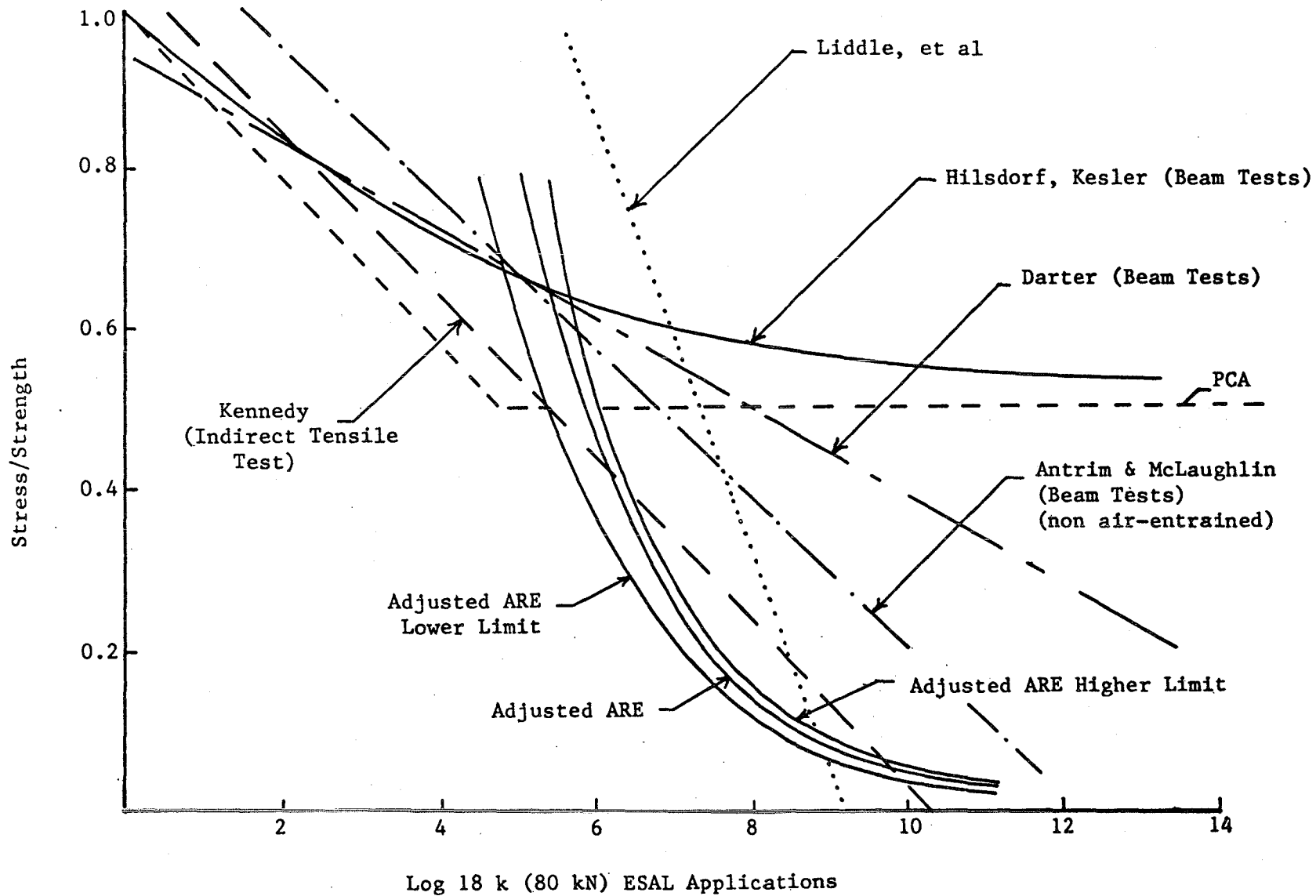


FIGURE 15. FATIGUE RELATIONSHIPS FOR CONCRETE BASED ON VARIOUS LABORATORY TEST PROCEDURES (REFERENCE 6)

and slabs with only class 1 and 2 cracking were considered to be structurally the same; however, slabs exhibiting class 3 or 4 cracking were considered to be structurally different. These data were used in a multiple regression analysis to develop the fatigue curve. A detailed discussion of the development of this relationship is contained in Reference 6, however, a brief description was included in the next section.

Interior stresses were used in developing the ARE relationship because that is the most economical way to consider the effects of all layers of the pavement structure on fatigue life. Even though edge loads can not be modeled using layered theory, it was assumed that the error was not serious since the center of the wheel path was 29 inches in from the edge of the pavement and the stresses at that location vary only about 10 to 15 percent from interior stresses. However, studies reported in Reference 7 indicate that the small percent of the traffic wandering toward the edge may induce more fatigue damage than the preponderance of the traffic farther from the edge. The ARE Curve was then modified as shown in Figure 14. Data from Reference 7 was utilized in this study to evaluate the differences between edge and interior stresses induced by the distribution of traffic in the wheel path. That data indicate that the wheel load distribution was approximately normal with a standard deviation of 10 inches (254 mm). The average distance from the pavement edge to the outside of the tire tread was 17 inches (432 mm) and represented traffic typical of rural four-lane interstate highways. Since elastic layer theory was selected for predicting stresses for the fatigue analysis, it is necessary to correct these interior stresses to appropriate stresses near the edge of the slab. For the slabs of interest for this study, the approximate relationship between stress factors and distance from the edge of the slab are plotted in Figure 16. The stress factor for use in the analysis can be selected once the critical tensile stress location has been identified. This critical tensile stress was defined as that induced stress where the predicted damage ratio was the largest. Therefore, the location of that critical stress was a function of both the magnitude of the stress, the distribution of axle loads, and the form of the fatigue relationship. To determine that critical stress location, the wheel path was divided into increments, the traffic applications for that interval were determined, the stress computed, the damage ratio using a fatigue relationship calculated, and the critical increment determined. This procedure was applied for discrete increments of 3, 6, and 8 inches (76, 152 and 203 mm) for a PCC slab 11 inches (279 mm) thick, having a subbase 8 inches (203 mm) thick. The subbase had a modulus of elasticity of 15,000 psi (103, 422 kPa) and the subgrade had a modulus of 20,000 psi (137, 896 kPa). The low-strength PCC had a modulus of elasticity of 3,000,000 psi (20,684,400 kPa) a modulus of rupture f_R of 560 psi (3,861 kPa) and a fatigue relationship as follows:

$$N = 18,000 (f_R/\sigma)^{3.9}$$

The results are plotted in Figure 17. As can be seen, these curves reach a maximum at around 16 to 17 inches (406 to 432 mm) from the edge, so a distance of 16.5 inches (419 mm) was selected. From Figure 16, this results in a stress factor of 1.23.

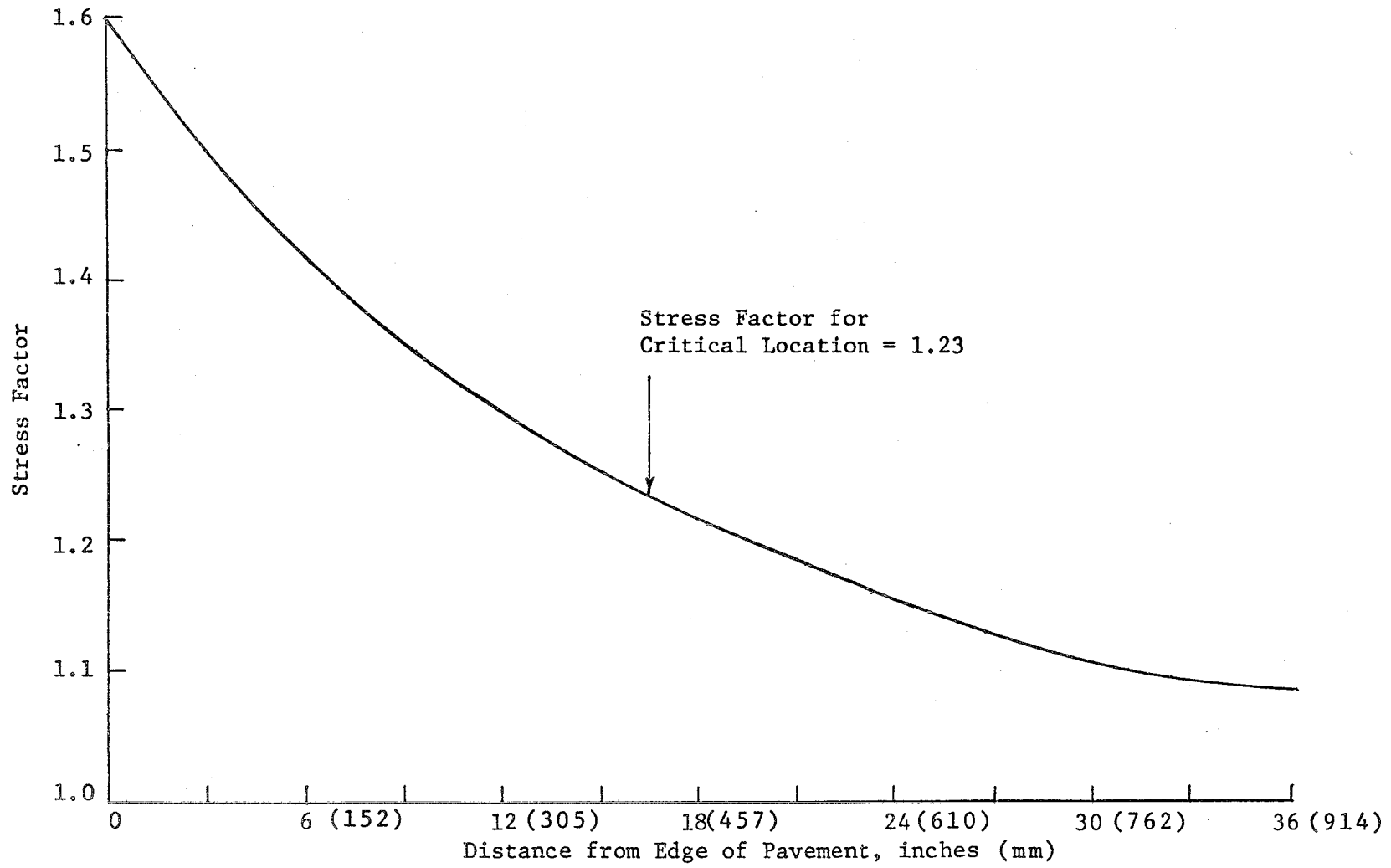


FIGURE 16. STRESS FACTORS VERSUS DISTANCE FROM EDGE OF RIGID SLAB

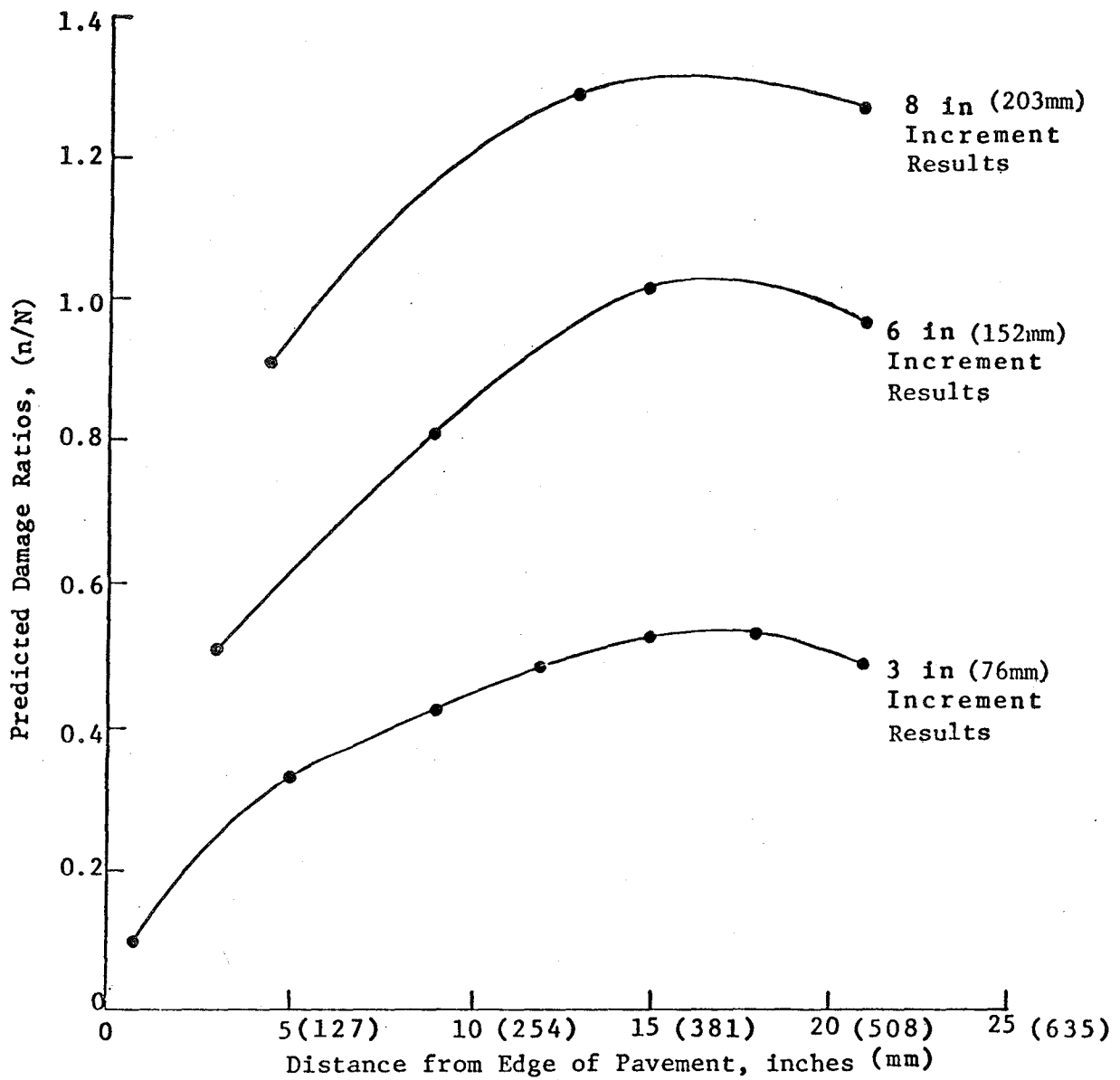


FIGURE 17. PREDICTED DAMAGE RATIOS VERSUS DISTANCE FROM RIGID PAVEMENT EDGE

Similar studies were also conducted for a 13 inch (330 mm) rigid pavement with a high subbase modulus of 1,000,000 psi (6,894,800 kPa). The location producing the highest damage ratio was approximately the same as for the 11 inch (279 mm) slab so a stress factor of 1.23 was used throughout the rigid pavement fatigue studies.

The range of material property variables selected for this study are included in Table 18.

In addition to the values included in Table 18, intermediate levels for PCC and subbase modulus of elasticity were investigated in a subsequent analysis. Values of 5,250,000 and 500,000 psi (36,197,700 and 3,447,400 kPa) were selected for the PCC and subbase moduli of elasticity, respectively. The other factors held constant throughout this analysis are included in Table 19.

The subgrade modulus of elasticity of 20,000 psi (137,896 kPa) was selected to realistically take into account the very low stress typical of the entire subgrade and the stress sensitivity of typical clay soils. The use of a single 9 kip (20 kN) load to represent dual tires for rigid pavements in the analysis using ELSYM5 produces a very small difference in stress when compared with the stress generated using 2, 4.5 kip (10 kN) wheel loads. Therefore, the simple configuration of a single load was selected.

Material Properties - CRCP

The significant CRCP distresses selected for study were fatigue cracking, punchouts, crack spalling, steel rupture, and low temperature and shrinkage cracking.

The occurrence of punchouts, crack spalling and steel rupture are closely related to the low temperature and shrinkage characteristics of the CRCP. The material properties that affect the low temperature and shrinkage distresses in CRCP are the same as those previously identified for JCP and JRCP. The influence of these distresses were introduced into the analysis by setting limits on the response parameters derived from the low temperature shrinkage cracking parameter study.

The CRCP pavement models whose inputs are discussed in this section include ELSYM5 for fatigue cracking, and CRCP-2 (Reference 31) for low temperature shrinkage cracking.

Fatigue Cracking. The fatigue analysis input selections are identical to those selected for the JRCP and JCP studies as included in Tables 18 and 19. The only difference between the two analyses was the thickness of the concrete layer which was 11 inches (279 mm) for the CRCP pavement.

Low Temperature and Shrinkage Cracking. Computer Program CRCP-2 (Reference 31) was used to predict the responses of CRCP to changes in material properties. The effects of thermal coefficient, shrinkage and tensile strength were of primary interest in this study. Values of each of

TABLE 18. MATERIAL PROPERTIES VARIED IN PCC PAVEMENT STUDIES

MATERIAL PROPERTY	LOW VALUE	HIGH VALUE
PCC Modulus, 10^{-6} psi (kPa)	3.5 (24)	7.0 (48)
Subbase Modulus, 10^{-3} psi (kPa)	15 (103)	1,000 (6,895)
Subbase Poisson Ratio	0.20	0.40
Fatigue Relationship: Coef	18,000	100,000
N = Coef $(f_r/\sigma)^{Exp}$ Exp	3.9	3.9
Modulus of Rupture, psi (kPa)	560 (3,861)	1,000 (6,895)

TABLE 19. VALUES OF FACTORS HELD CONSTANT DURING JCP AND JRCP ANALYSIS.

FACTOR	VALUE
Traffic Application per year 18 kip ESAL (80 kN ESAL)	2,000,000
PCC Thickness, in (mm)	13 (330)
PCC Poisson Ratio	0.15
Subgrade Poisson Ratio	0.45
Subgrade Modulus, 10^3 psi (10^3 kPa)	20 (138)
Wheel Loads, kips (kN)	2 @ 9 (2 @ 40)
Tire Pressure, psi (kPa)	75 (517)

the material property combinations are shown in Table 20. Other material property inputs selected are listed in Table 21 and remained constant throughout this analysis. The difference between the four environmental zones was the temperature drop expected after the concrete gained full strength. The temperature drops selected as typical for each zone were 55 °F (13°C) for wet-freeze, 51°F (11°C) for dry freeze, 34°F (1°C) for dry-no freeze and 24°F (-4°C) for the wet-no freeze. Although a constant curing temperature of 80°F (27°C) was used for each environmental zone, the model used only the temperature drop in the calculations.

COMPOSITE PAVEMENT INPUTS

Since the properties of the asphalt and portland cement concrete materials available for use in construction of composite pavements are the same as previously discussed, only those elements of the analysis that are different are discussed.

Pavement Thickness

The critical stresses in the rigid layer component of a composite pavement were determined using the elastic layer program ELSYM5 for various asphalt concrete surface and PCC base thicknesses. Although fatigue curves developed by several agencies were available, the ARE curve was used to develop the minimum cross section for the composite pavement. For low stress level, the ARE curve predicts a lower fatigue life than from other fatigue relationships.

Using a traffic rate of 1.5 million 18 kip (80 kN) ESAL per year, and modulus of rupture for PCC equal to 650 psi, (4,482 kPa), the maximum allowable stress for the composite pavement was calculated to be 125 psi (862 kPa). At that stress level, a 6-inch (152 mm) asphalt concrete surface over an 8-inch (203 mm) PCC slab would provide adequate fatigue life for the composite pavement. Therefore, the basic thickness combination selected for the composite analysis was 6 inches (152 mm) of asphalt concrete surface over 8 inches (203 mm) of PCC over 8 inches (203 mm) of a granular subbase. A limited set of runs were made with a 9 inch (229 mm) surface course.

Fatigue Cracking

The material properties and relationships previously discussed and summarized in Table 18 were also utilized in the composite pavement study. In addition to the two sets of values for the fatigue relationship contained in Table 18 an intermediate value for the coefficient of 80,000 with a modulus of rupture of 750 psi (5,171 kPa) was selected for comparisons on the high value side of the study. A fatigue coefficient of 40,000 with a modulus of rupture of 750 psi (5,171 kPa) was selected for comparisons on the low value side of the study.

Since the asphalt concrete surfacing in the composite pavement was in compression, no fatigue failure for that layer was considered. Therefore, no asphalt concrete fatigue properties were included in the composite pavement study.

TABLE 20. COMBINATIONS OF MATERIAL PROPERTIES SELECTED FOR CRCP STUDIES

Amount of Steel Reinforcement Percent	CONCRETE PROPERTIES		
	Ultimate Tensile Strength, psi	Thermal Coefficients $10^{-6}/^{\circ}\text{F}$	Shrinkage
0.60	400	4.5	.0002
			.0008
		9.0	.0002
			.0008
	450	6.0	.0005
			.00065
		6.5	.0006
			7.0
		.0007	
	500	5.5	.0005
	500	5.0	.0004
	600	5.0	.0003
	800	4.5	.0002
			.0008
9.0		.0002	
	.0008		
0.75	450	6.5	.0006
	500	5.5	.0005
	550	5.0	.0004
0.9	500	5.5	.0005
	550	5.0	.0004

psi = 6.89 kPa

$10^{-6}/^{\circ}\text{F} = 1.8 \times 10^{-6}/^{\circ}\text{C}$

TABLE 21. CONSTANT INPUTS FOR CRCP LOW TEMPERATURE AND SHRINKAGE CRACKING STUDIES

STEEL PROPERTIES

Reinforcement Type:	Deformed Bars
Bar Diameter, in (mm):	.625 (15.88)
Yield Stress, psi (kPa):	60,000 (413,700)
Elastic Modulus psi (kPa):	29.0×10^{-6} (200×10^{-6})
Thermal Coefficient, °F(°C):	6.0×10^{-6} (10.8×10^{-6})

CONCRETE PROPERTIES

Slab Thickness, in (mm):	11.0 (279)
Unit Weight, pcf (kg/m ²):	150 (2,403)
Ratio Between Tensile Strength and Flexural Strength:	.86 (STRNMUL)
Concrete Moduli = 33.0 (W)	$1.5 \frac{\text{Tensile Strength}}{\text{STRNMUL} \times 7.5}$

SLAB-BASE FRICTION CHARACTERISTICS

Concrete Movement, in(mm)	Friction Stress (kPa)
0.0 (0.0)	0.0 (0.0)
0.01 (0.25)	0.21 (1.45)
0.10 (2.54)	0.63 (4.34)
0.15 (3.81)	0.80 (5.52)
0.20 (5.08)	0.94 (6.48)
0.3 (7.62)	0.97 (6.69)

TEMPERATURE DATA

Curing Temperature, °F(°C):	80 (27)
Constant Temp. Drop Over First 28 Days, °F(°C):	20 (-7)
Time Before Reaching Minimum Temperature:	28 Days

DESIGN LOW TEMPERATURE

Wet Freeze, °F(°C) -	25 (-4)
Dry Freeze, °F(°C) -	29 (-2)
Wet-No Freeze, °F(°C) -	56 (13)
Dry-No Freeze, °F(°C) -	46 (8)

TABLE 21. CONSTANT INPUTS FOR CRCP LOW TEMPERATURE
AND SHRINKAGE CRACKING STUDIES (continued)

WHEEL LOAD

Wheel Load, lb (N):	9000 (40,000)
Effective Tire Radius, in (mm):	6.18 (57)
Modulus of Subgrade Reaction, psi (kPa/m):	600 (162,869)
Time of Load Application:	28th Day

ITERATION AND TOLERANCE CONTROL

Maximum No. of Iterations:	60
Relative Closure Tolerance:	5%

Reflection Cracking

Program RFLCR1 (Reference 6) was the only analytical model currently available and was therefore selected for use in this study. Program RFLCR1 predicts tensile and shear strains in the asphaltic concrete surface over joints constructed in the underlying rigid layer; however, the program does not directly predict the point at which cracking occurs in the surface material. Since an elastic model of the asphalt concrete was utilized in calculating the induced strains, the results may be represented in terms of either stress or strain. This elastic model does not account for the viscous characteristics of the asphaltic concrete.

A description of inputs for the composite model studies are summarized in Tables 22 and 23. The composite cross section selected for use in this study consists of a 6 inch (152 mm) asphaltic surface layer over an 8 inch (203 mm) portland cement concrete layer. The PCC layer was modeled as an uncracked plain jointed pavement with a 15 foot (4.57 m) joint spacing.

The environmental zones were characterized by the design temperature drops. The design temperature drop for this analysis was set equal to the difference between the average high temperature and the lowest expected temperature over a 20 year interval. The temperature at the bottom of the asphalt concrete layer was estimated using the procedure proposed by the Asphalt Institute. The design temperature drop for the asphalt concrete layer was the difference between the average of the high temperatures on the top and bottom of this layer and the average of the low temperature on the top and bottom of this layer. The design temperature drop for the concrete layer was the difference between the high and low temperature at the bottom of the asphalt concrete layer. These temperatures are shown in Table 23.

TABLE 22. INPUTS FOR COMPOSITE PAVEMENT REFLECTION CRACKING STUDY

A. MATERIAL PROPERTIES HELD CONSTANT

LAYER	MATERIAL PROPERTY	VALUE
Portland Cement Concrete	Modulus of Elasticity, 10 ⁶ psi (10 ⁶ kPa)	4.0 (28)
	Thickness, in (mm)	8 (203)
	Density, Pcf (kg/m ²)	150 (2,403)
	Joint Spacing, ft (m)	15 (4.57)
	Movement at Sliding, in (mm)	0.15 (3.8)
Asphaltic Concrete	Thermal Coefficient, 10 ⁻⁶ /°F (10 ⁻⁶ /°C)	12 (22)
	Thickness, in (mm)	6 (152)
	Density, pcf (kg/m ²)	140 (2,243)
	Poisson's Ratio	.3

B. RANGE OF MATERIAL PROPERTIES VARIED WITHOUT REGARD TO ZONE

Material Property	Low Value	High Value
Dynamic Modulus of Asphalt Concrete 10 ³ psi (10 ³ kPa)	10 (69)	5,000 (34,474)
Creep Modulus of Asphalt Concrete 10 ³ psi (10 ³ kPa)	5 (34)	500 (3,447)
Thermal Coefficient of concrete 10 ⁶ /°F (10 ⁶ /°C)	4.5 (8.1)	9.0 (16.2)

TABLE 23. MATERIAL PROPERTIES VARIED FOR EACH ENVIRONMENT USED IN THE REFLECTION CRACKING STUDY

Material Property	Input Value by Environmental Zone				
	Wet-Freeze	Dry-Freeze	Wet-No Freeze	Dry-No Freeze	
Mean high temperature, °F (°C)	75(24)	78(26)	80(27)	82(28)	
Joint width at high temperature, in (mm)	.01(.25)	.01(.25)	.01(.25)	.01(.25)	
Mean low temperature, °F (°C)	20(-7)	27(-3)	56(13)	48(9)	
Joint width at low temp. inches (mm)	Low α_c *	.05(1.3)	.05(1.3)	.025(.64)	.035(.89)
	High α_c *	.095(2.4)	.09(2.3)	.045(1.1)	.062(1.6)
Design temperature change of ACP layer, °F (°C)	77.5 (25)	85 (29)	69 (21)	66 (19)	
Design temperature change of PCC layer, °F (°C)	60 (16)	62 (17)	58 (14)	55 (13)	

* Low $\alpha_c = 4.5 \times 10^{-6}/^{\circ}\text{F}$ ($8.1 \times 10^{-6}/^{\circ}\text{C}$)

High $\alpha_c = 9.0 \times 10^{-6}/^{\circ}\text{F}$ ($16.2 \times 10^{-6}/^{\circ}\text{C}$)

CHAPTER 4. FLEXIBLE PAVEMENT STUDY

Results from the parameter studies for flexible pavement using the distress models described in Chapter 2 and the inputs described in Chapter 3 are summarized in this chapter.

FATIGUE CRACKING

The relationships between percent fatigue cracking and time for each environmental zone are shown in Figures 18 through 21. Time was selected as the independent variable rather than equivalent axle loads, since the traffic was assumed to be uniform at 1,000,000 18-kip (80 kN) ESAL per year. These relationships show the percent cracking for each K_1 , K_2 and thickness combination. It is quite apparent that surface thickness has a very significant effect on development of fatigue cracking. Until the total thickness exceeded some critical value which was adequate to serve the traffic during the analysis period, the effects of varying the fatigue coefficients and exponents were not important. For the lowest K_1 value, which produces the longest value of fatigue life, the 13 inch (330 mm) pavement experienced fatigue cracking exceeding tolerable levels in all zones in from 5 to 13 years. No set of material properties met the zero-maintenance criteria for a surface thickness of 13 inches (330 mm) over an 8 inch (203 mm) base (Table 24).

As the pavement thickness was increased to 16 inches (406 mm) and 18 inches (457 mm), the asphalt concrete began to perform in a manner compatible with zero-maintenance requirements. As can be seen in Figures 18 through 21, at a log K_1 of -10 for 18 inch (457 mm) surface, the fatigue cracking for all environmental zones was at an acceptable level after 20 years. It should be noted, however, that once fatigue cracking was initiated, only a few years at this very high traffic rate were required for the fatigue cracking to advance to an unacceptable level. It can also be seen that the effect of fatigue properties of the materials were not important except at larger thicknesses which again emphasizes the importance of the surface thickness.

The development of fatigue cracking occurred in a similar pattern for the wet-freeze, dry-freeze, and dry-no freeze zones. However, in the wet-no freeze zone the fatigue life was substantially longer than for all other zones. This was attributed to the interaction of the strain-stiffness-fatigue relationship produced by the higher seasonal temperatures and the smaller temperature range between seasons for the wet-no freeze zone. Table 12 showed the average seasonal temperatures for each zone. It should also be noted that the fatigue life relationships are more closely spaced for the wet-no freeze zone than any of the other zones indicating that in higher temperature zones the difference between the fatigue constants are not nearly as important as in the lower temperature zones where the range of stiffnesses during a year were larger.

From this analysis it can be concluded that:

- Legend:
- ... 10 in ACP/8 in base
 - - - 13 in ACP/8 in base
 - · - 16 in ACP/8 in base
 - 18 in ACP/8 in base

Numbers on curves are $\log K_1$

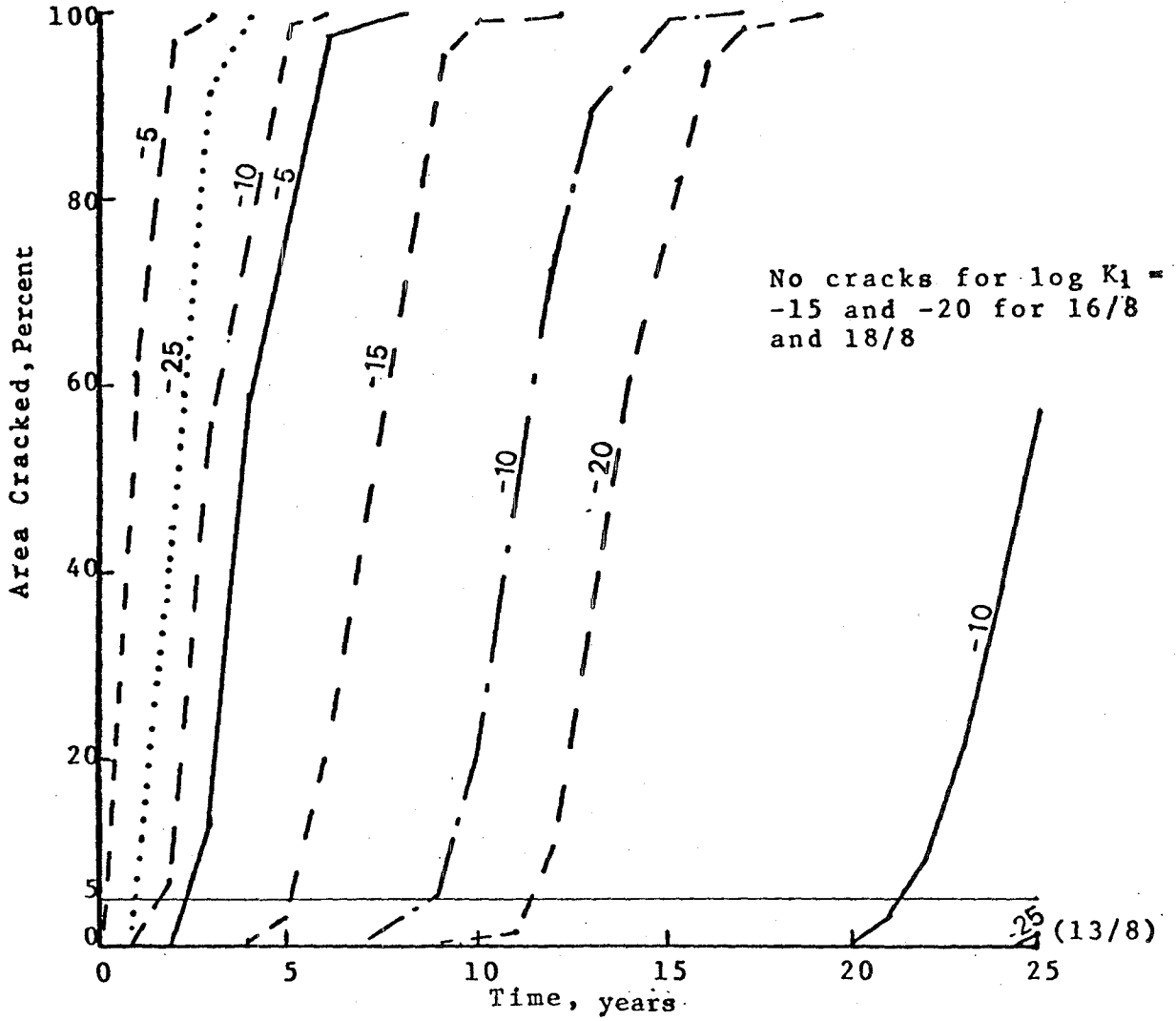


FIGURE 18. FATIGUE IN FLEXIBLE PAVEMENTS FOR VARIOUS K_1 , K_2 COMBINATIONS AND SURFACE THICKNESSES, ZONE: WET - FREEZE

- Legend:
- . . . 10 in ACP/8 in base
 - - - 13 in ACP/8 in base
 - · - 16 in ACP/8 in base
 - 18 in ACP/8 in base

Numbers on curves are $\log K_1$

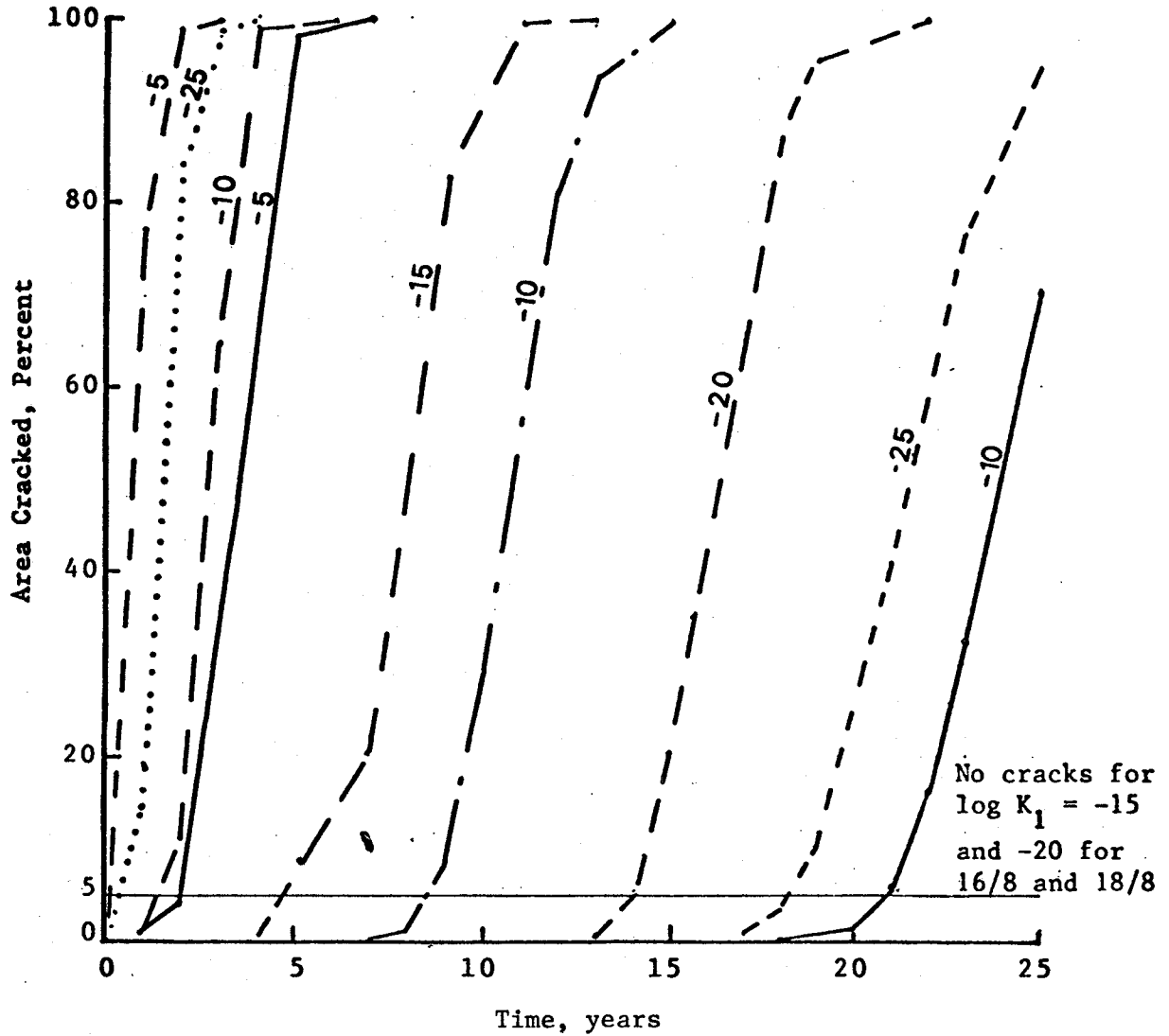


FIGURE 19. FATIGUE IN FLEXIBLE PAVEMENTS FOR VARIOUS K_1 , K_2 COMBINATIONS AND SURFACE THICKNESSES, ZONE: DRY - FREEZE

Legend: . . . 10 in ACP/8 in base
 - - - 13 in ACP/8 in base
 - - 16 in ACP/8 in base
 — 18 in ACP/8 in base
 Numbers on curves are $\log K_1$

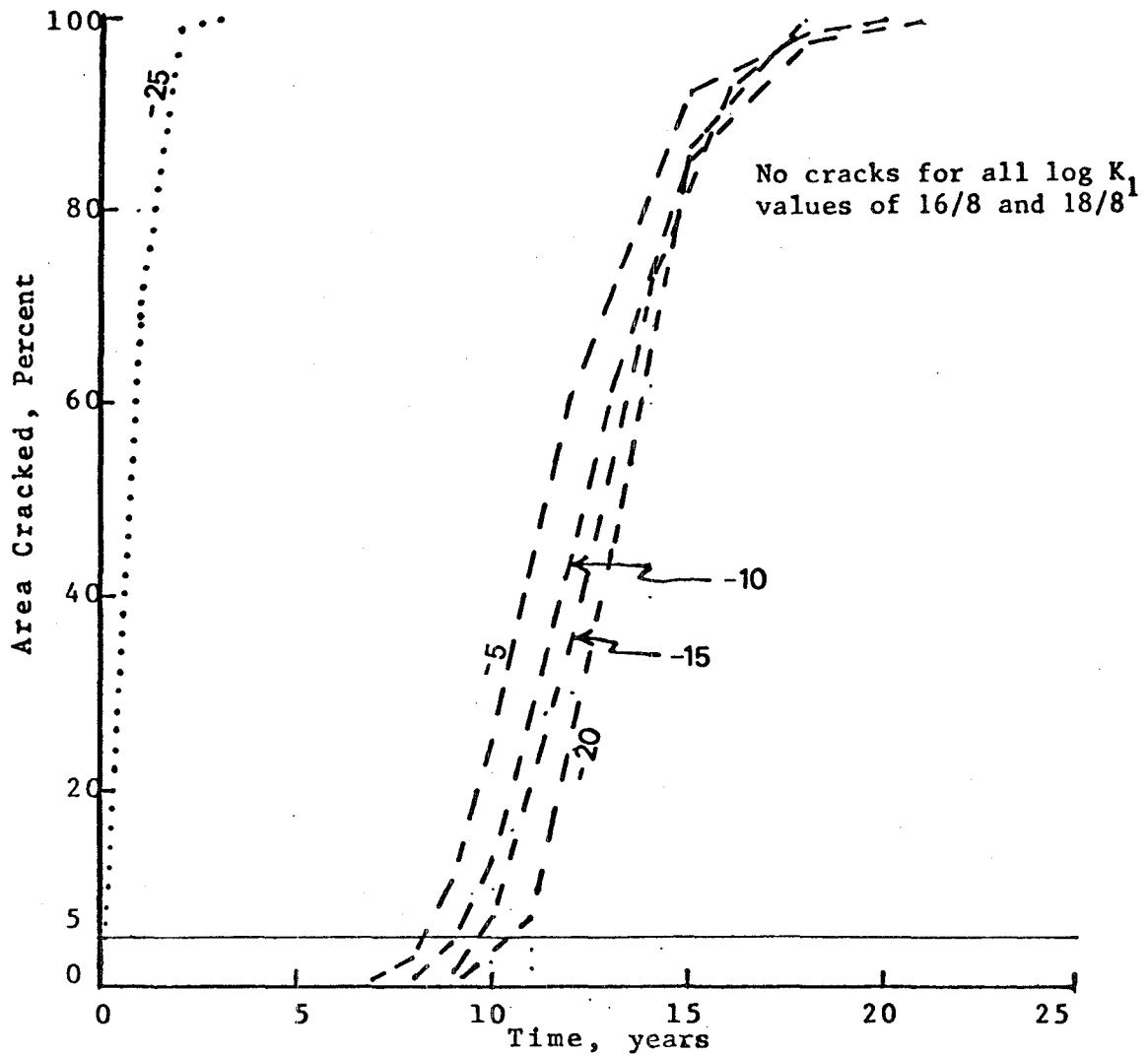


FIGURE 20. FATIGUE IN FLEXIBLE PAVEMENTS FOR VARIOUS K_1 , K_2 COMBINATIONS AND SURFACE THICKNESSES, ZONE: WET - NO FREEZE

- Legend:
- . . . 10 in ACP/8 in base
 - - - 13 in ACP/8 in base
 - . - 16 in ACP/8 in base
 - 18 in ACP/8 in base

Numbers on curves are $\log K_1$

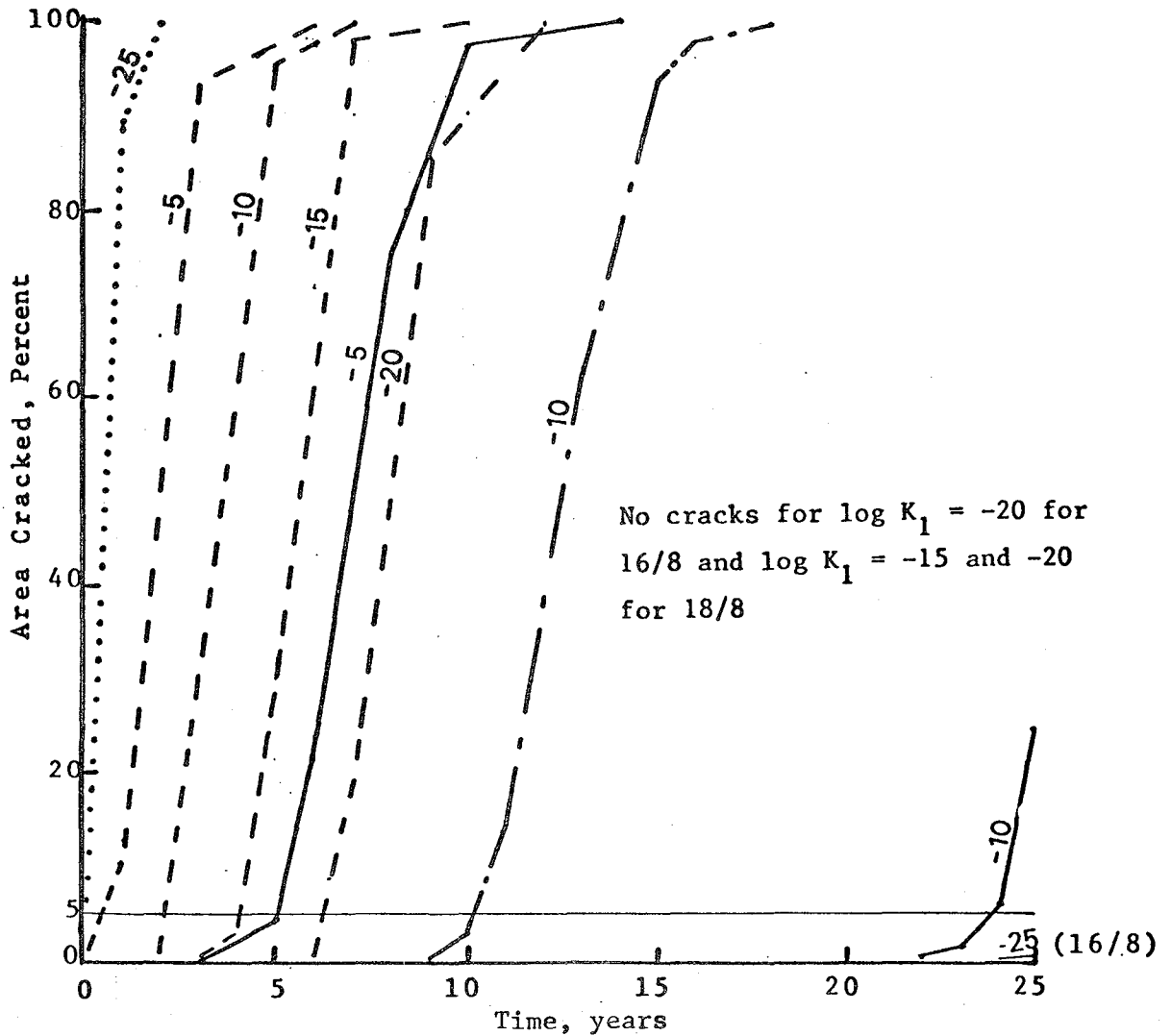


FIGURE 21. FATIGUE IN FLEXIBLE PAVEMENTS FOR VARIOUS K_1 , K_2 COMBINATIONS AND SURFACE THICKNESSES, ZONE: DRY - NO FREEZE

TABLE 24. TIME REQUIRED IN YEARS FOR 5 PERCENT FATIGUE CRACKING TO OCCUR

Zone	13 in (330 mm)				16 in (406 mm)		18 in (457 mm)			
	-5	-10	-15	-20	-10	-15	-5	-10	-15	-20
Wet Freeze	0.2	2.0	5.2	11.2	8.0	25	22	21.2	25	25
Dry Freeze	0.1	1.4	4.7	11.5	7.5	25	2.2	20.7	25	25
Wet No Freeze	6.7	7.4	7.4	8.7	25	25	25	25	25	25
Dry No Freeze	0.5	1.3	2.5	4.8	9.1	24.7	5.1	23.7	25	25

Shaded area satisfies zero maintenance requirements

1. It is possible to design a zero maintenance flexible pavement using currently available materials.
2. The material properties are not nearly as important as was the initial thickness, i.e., performance was affected more by thickness than was offset by improving the material properties for the normal range of properties available today for either conventional or new materials presently on the horizon.
3. Fatigue life is affected very significantly by the seasonal temperatures in the zone and design criteria for each should be developed to prevent the most prevalent distress occurring in the zone.

Figures 22 through 25 indicate the fatigue lives as a function of one of the accepted fatigue cracking criteria. These plots indicate the effect of material property on time from the beginning of the analysis period until five percent cracking had occurred. These plots clearly indicated that material properties have a significant impact on fatigue life but again demonstrated the overwhelming effect of thickness. As can be seen in Figure 22, the percent increase in fatigue life resulting from a change in the $\log K_1$ from -10 to -20 was 460 percent, however, the change in the fatigue life produced by increasing the thickness from 13 inches (330 mm) to 18 inches (457 mm) was 960 percent. Effects similar to those observed for the wet-freeze zone in Figure 22 were also observed for the dry-freeze and the dry-no freeze zones. For the wet-no freeze zone the effect of thickness was even more dramatic than for the other zones; an increase in thickness from 13 inches (330 mm) to either 16 inches (406 mm) or 18 inches (457 mm) produced a fatigue life compatible with zero maintenance requirements.

For the 18 inch (457 mm) pavement, a material with $\log K_1$ less than -10 would meet the requirement for no maintenance during the first 20 years. However, to ensure that the fatigue cracking was not a problem for 25 or more years, a $\log K_1$ equal to or less than -15 should be selected for a surface thickness of 18 inches (457 mm).

In developing criteria for selecting thickness requirements for zero maintenance the engineer must evaluate the uncertainties associated with obtaining the prescribed fatigue constants and the associated costs to ensure that those values are obtained. The costs and uncertainties associated with the more stringent material properties requirements must be compared with the cost and uncertainty of obtaining a thicker layer and the less stringent material property requirements for the thicker layer. These evaluations must be performed for each proposed zero maintenance project.

RUTTING

The relationships showing cumulative permanent deformation as a function of time are shown in Figures 26 through 29 for the wet-no freeze zone. Plots of data from other environmental zones were of similar form and summary information taken from those plots were included in subsequent analyses.

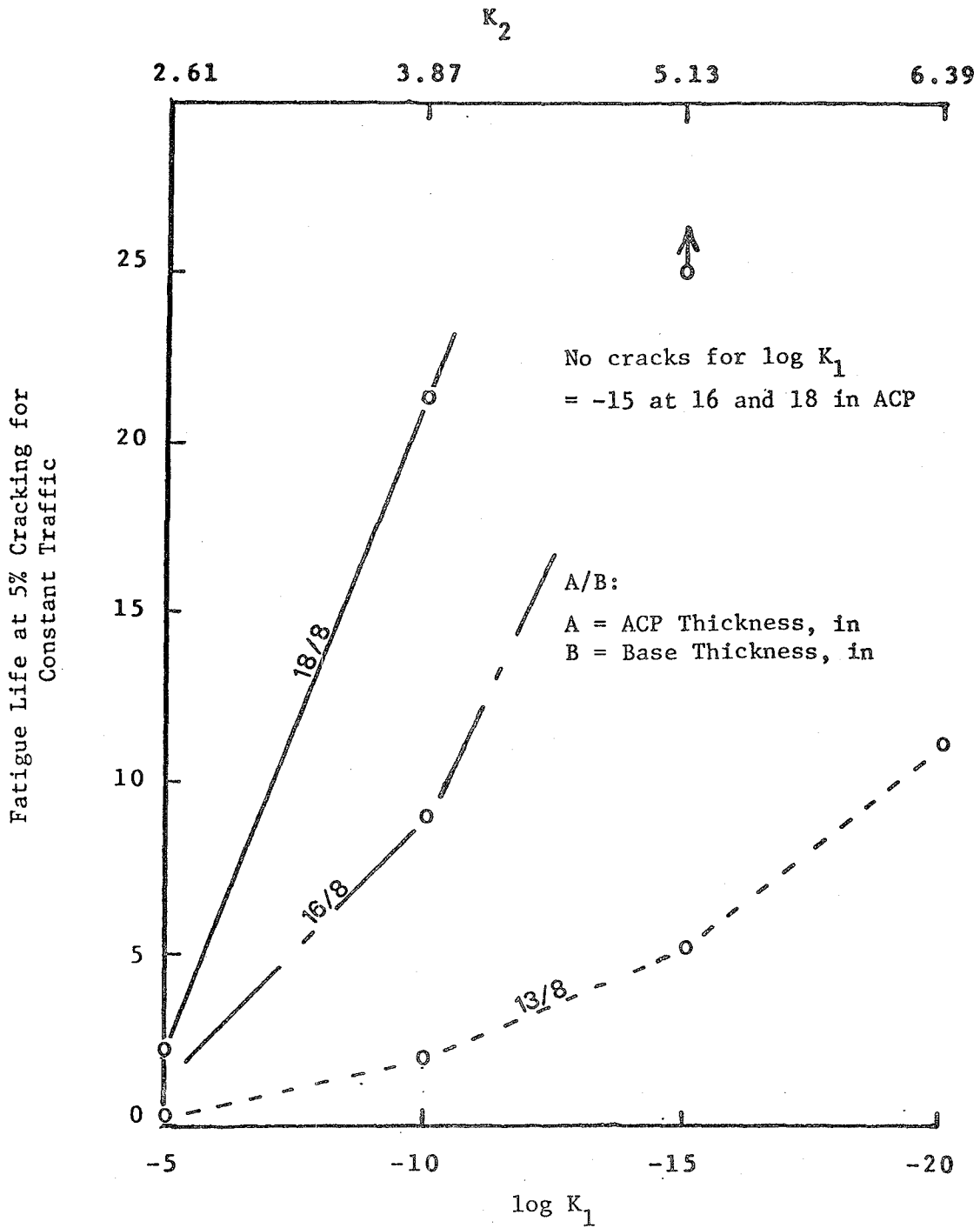


FIGURE 22. EFFECT OF FATIGUE CONSTANTS ON FATIGUE LIFE OF FLEXIBLE PAVEMENTS, -ZONE: WET - FREEZE

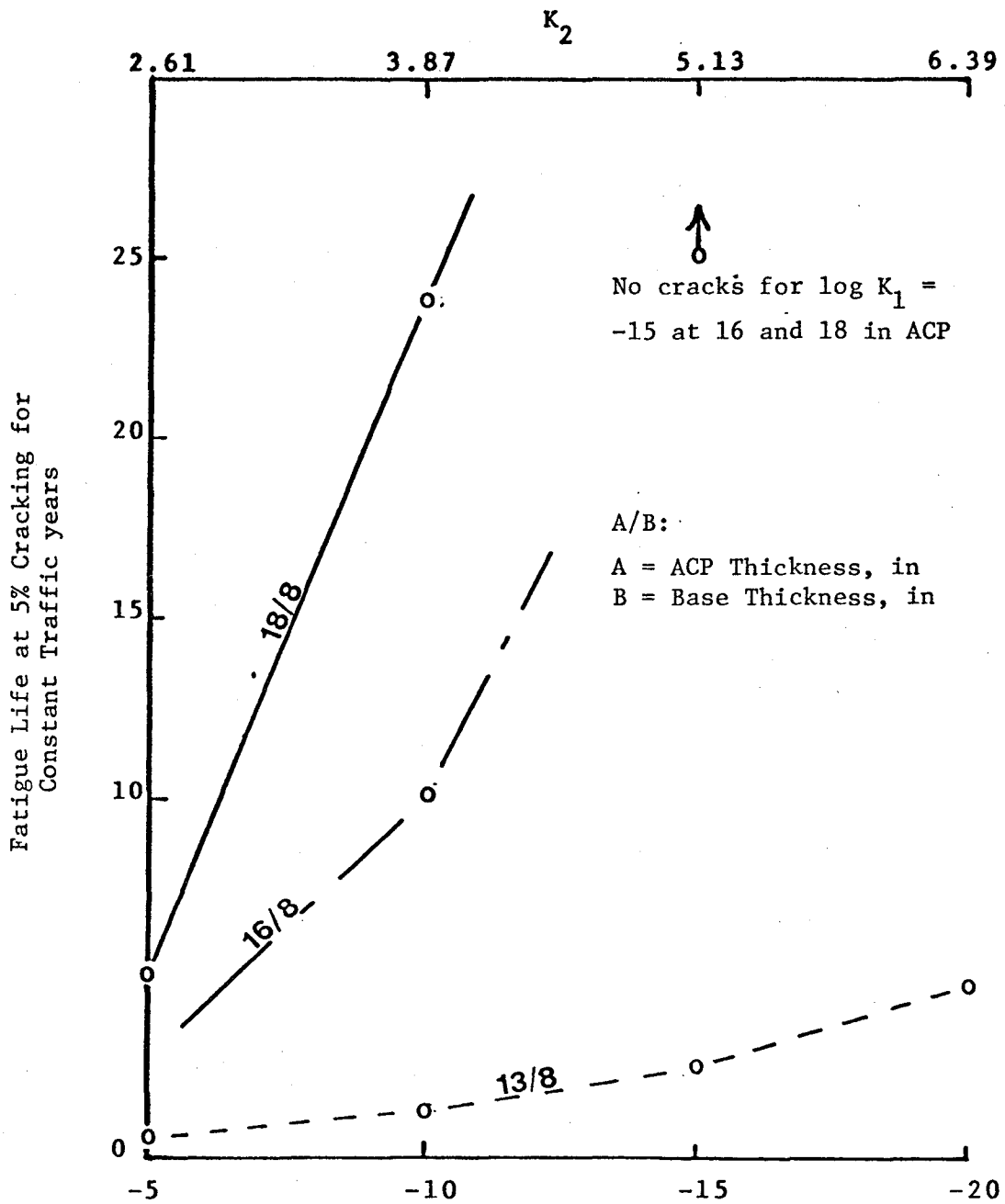


FIGURE 23. EFFECT OF FATIGUE CONSTANTS ON FATIGUE LIFE OF FLEXIBLE PAVEMENTS, -ZONE: DRY - NO FREEZE

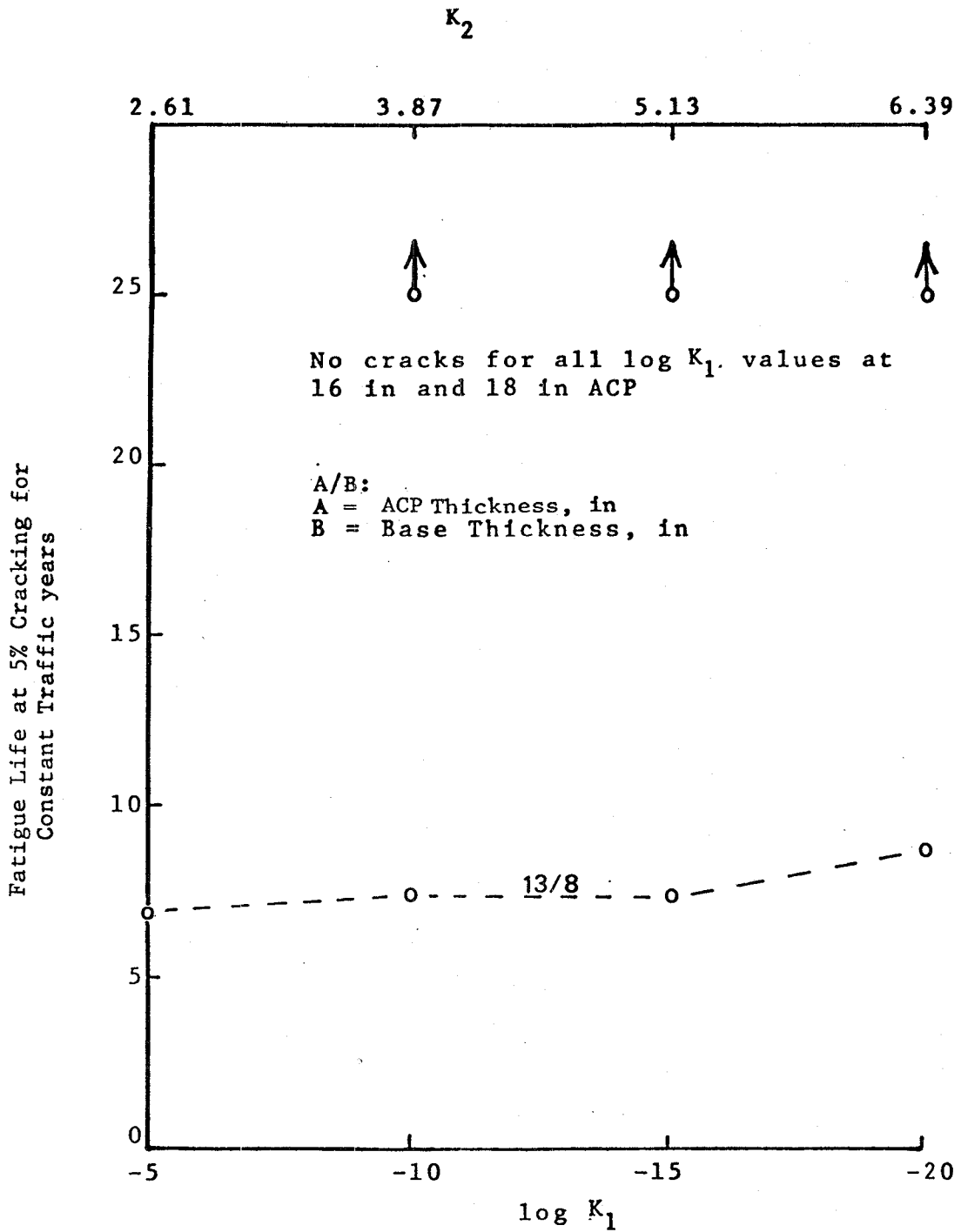


FIGURE 24. EFFECT OF FATIGUE CONSTANTS ON FATIGUE LIFE OF FLEXIBLE PAVEMENTS, -ZONE: WET - NO FREEZE

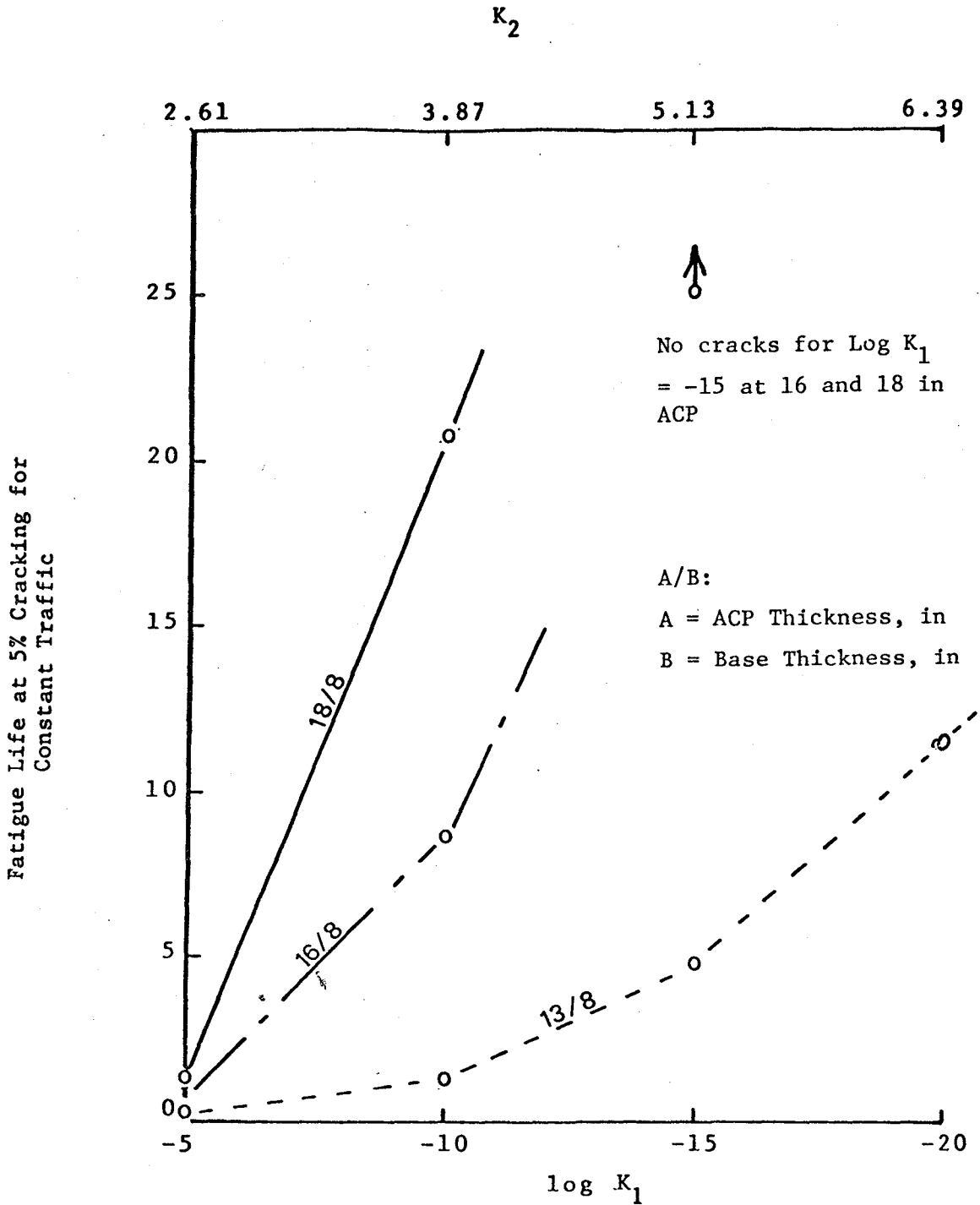


FIGURE 25. EFFECT OF FATIGUE CONSTANTS ON FATIGUE LIFE OF FLEXIBLE PAVEMENTS, - ZONE: DRY-FREEZE

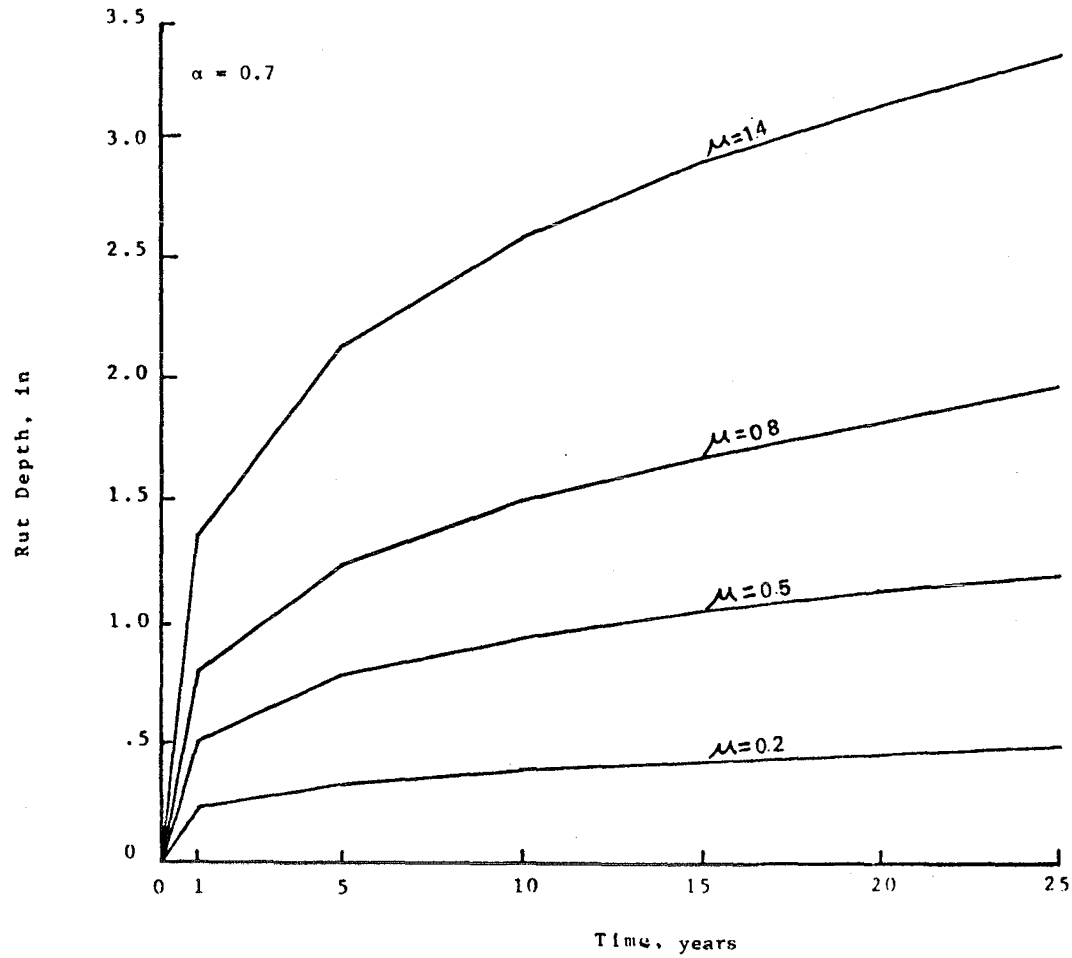


FIGURE 26. RUTTING VERSUS TIME FOR ALPHA 0.7, ALL GNUS, AND 13 in (330 mm) SURFACE

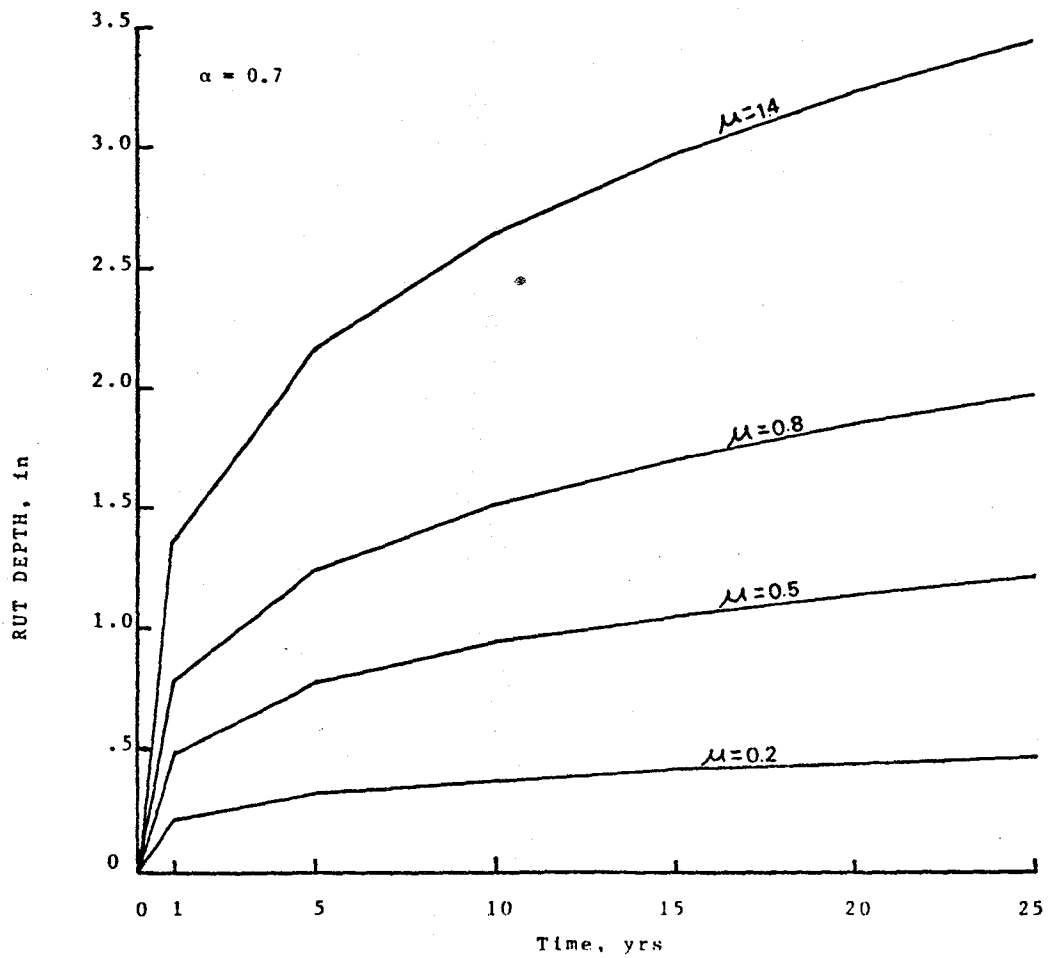


FIGURE 27. RUTTING VERSUS TIME FOR ALPHA 0.7, ALL GNUS,
AND 18 in (457 mm) SURFACE

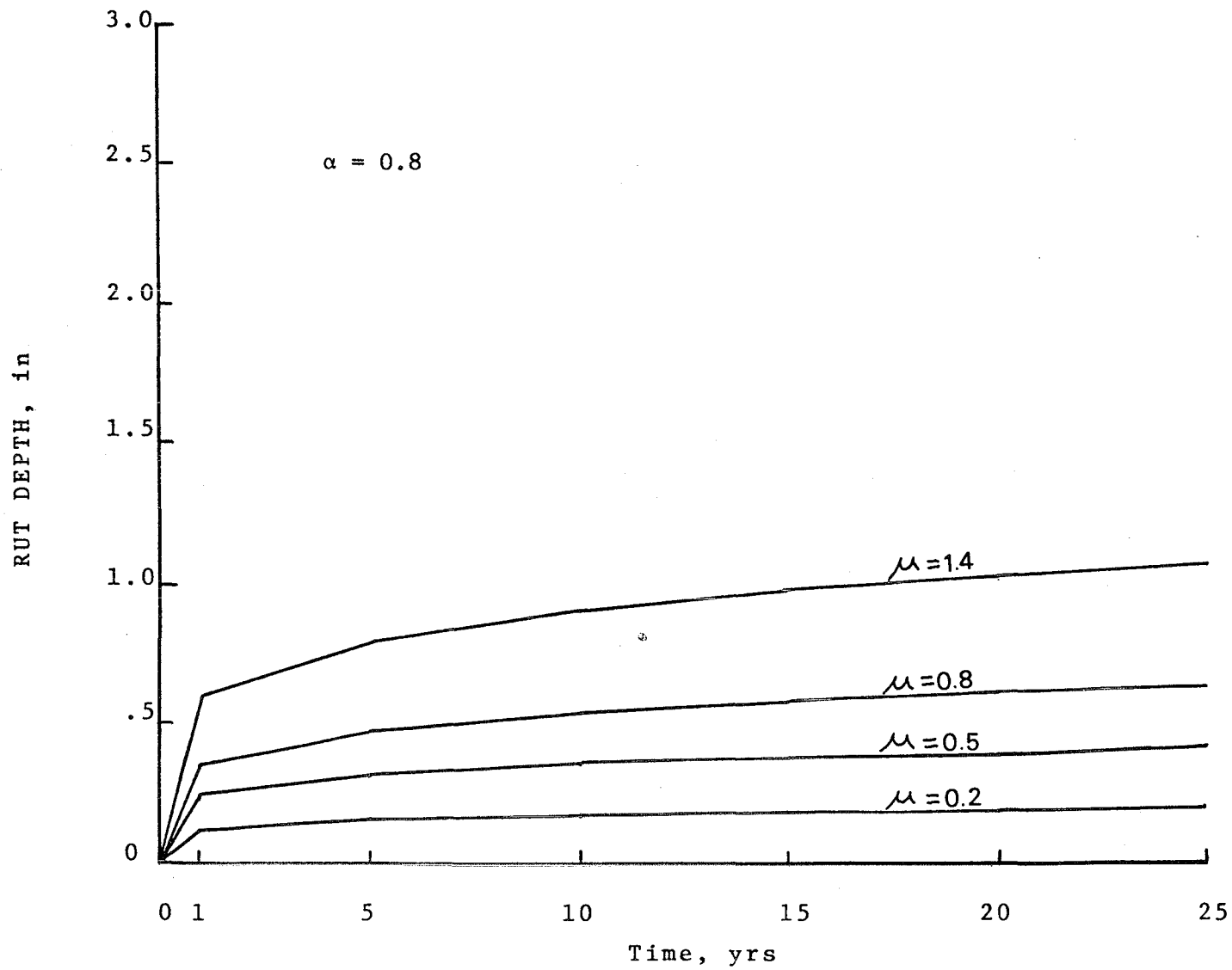


FIGURE 28. RUTTING VERSUS TIME FOR ALPHA 0.8, ALL GNUS, AND 13 in (330 mm) SURFACE

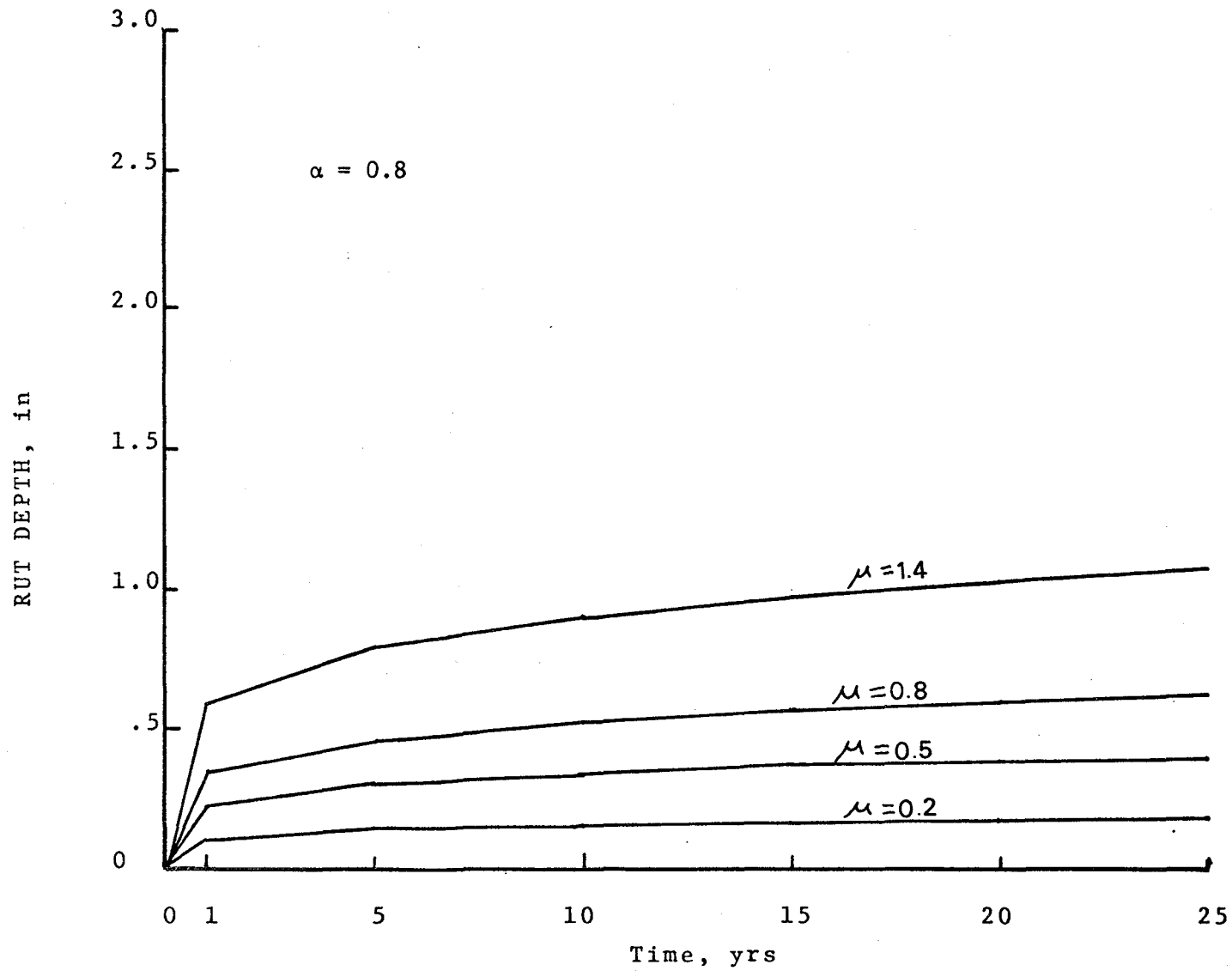


FIGURE 29. RUTTING VERSUS TIME FOR ALPHA 0.8, ALL GNUS, AND 18 in (457 mm) SURFACE

In establishing a limit for rutting, safety considerations have frequently been utilized. Generally, when rutting is 0.5 inches (13 mm) or less, the crossfall of a premium pavement is sufficient to prevent both significant water accumulation in the wheel paths and steering problems associated with moving out of the wheel path. Therefore, a rutting value of 0.5 inches (13 mm) was selected as a limiting value for use in this analysis. Any material providing a combination of permanent deformation parameters (ALPHA and GNU) that results in a rut depth of 0.5 inch (13 mm) or less after being subjected to 20 million 18-kip (80 kN) ESAL was considered to be acceptable for use in the design of zero-maintenance pavements.

As shown in Figures 26 through 29, the general shape of the cumulative permanent deformation versus time relationship is concave downward. According to the VESYS formulation, most of the rutting occurs early in the service life of the pavement with at least 50 percent occurring during the first 5 years. After 5 years, most combinations of ALPHA and GNU sustained very little additional cumulative permanent deformation.

From each of the plots of cumulative permanent deformation versus time, the time required for a 0.5 inch (13 mm) rut to develop was determined and the relationships between this time and the GNU values were developed for each ALPHA and each zone (Figures 30 through 33). Analysis of these relationships indicated that a GNU level of 1.4 was unsatisfactory for ALPHA values less than 0.8. Since most reported ALPHA values are less than 0.9, GNUs of 1.4 or greater were not expected to satisfy the zero maintenance requirements for rutting. However, for ALPHAs as high as 0.9, all value of GNU met the rutting criterion.

As shown in Figures 30, 31, and 33, the shape of the relationship between GNU and time to a 0.5 inch (13 mm) rut depth was similar for the wet-freeze, dry-freeze, and dry-no freeze zones. The interactive effects of temperature and stiffness produce a characteristically different response curve for the wet-no freeze zone. Again with the higher temperatures, lower stiffnesses, and increased deflections, the cumulative permanent deformations were more critical in that zone than in any of the other environmental zones.

The material combinations that produce acceptable rutting performance using the previously cited criteria are shown in Figure 34. Points represent the combinations of ALPHA and GNU for which VESYS solutions were obtained are shown in Figure 34. The numbers to the right of each point represent the zone for which the zero maintenance criteria were met for both the surface thicknesses of 13 inches (330 mm) and 18 inches (457 mm). It can be noted that all points within or to the right of the shaded area met the zero maintenance rutting performance criteria in more than one zone. The only combination that did not meet the established criteria was the ALPHA of 0.8 and GNU of 0.8 for the wet-no freeze environmental zone. This wet-no freeze zone was typically very warm and was the only zone where rutting and not fatigue cracking was the most prevalent distress.

LOW TEMPERATURE CRACKING

The results of the low temperature cracking analysis are presented in Table 25. For each combination of inputs presented in Chapter 3, the

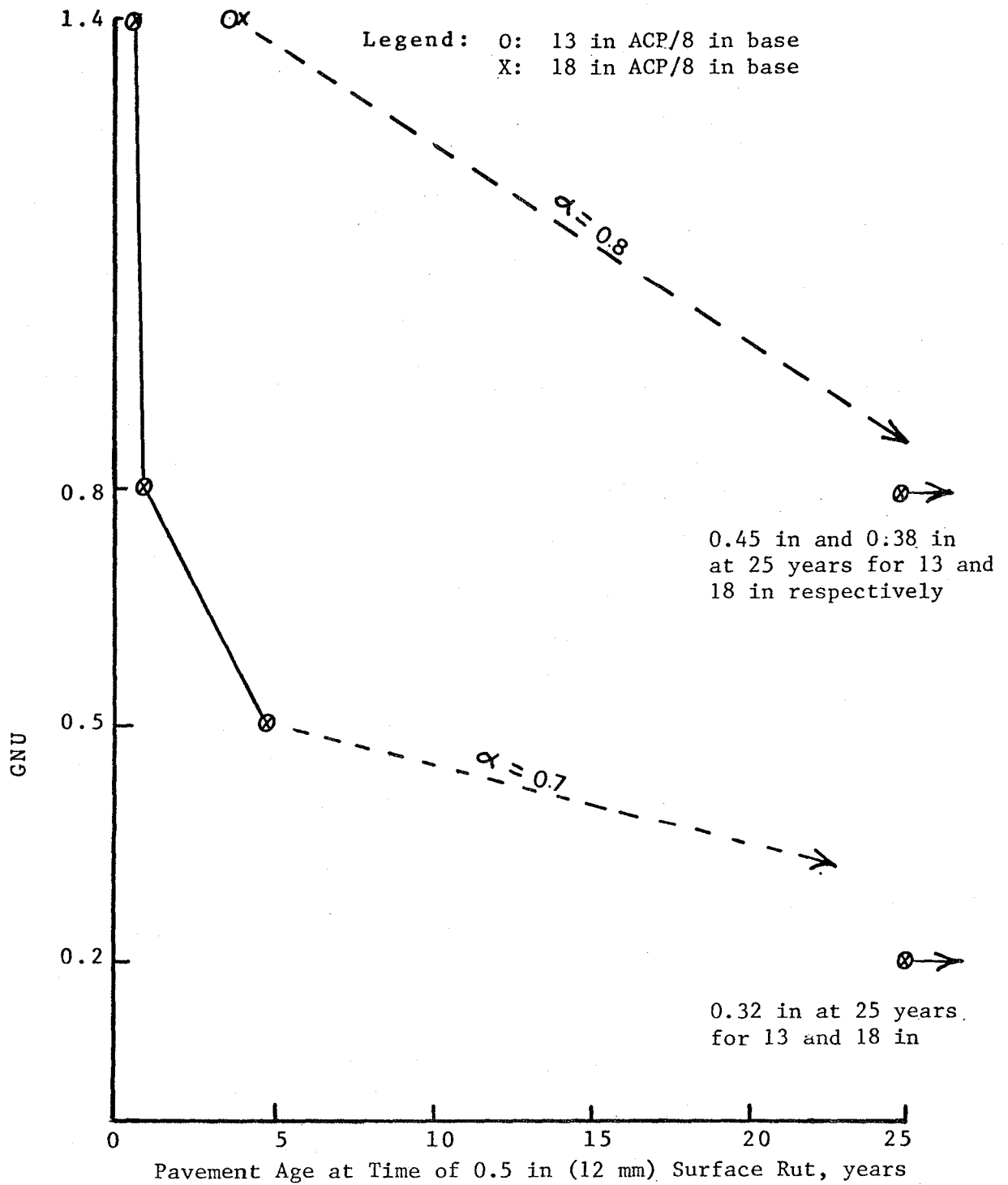


FIGURE 30. EFFECT OF PERMANENT DEFORMATION PARAMETERS ON RUTTING IN FLEXIBLE PAVEMENTS: ZONE: WET-FREEZE

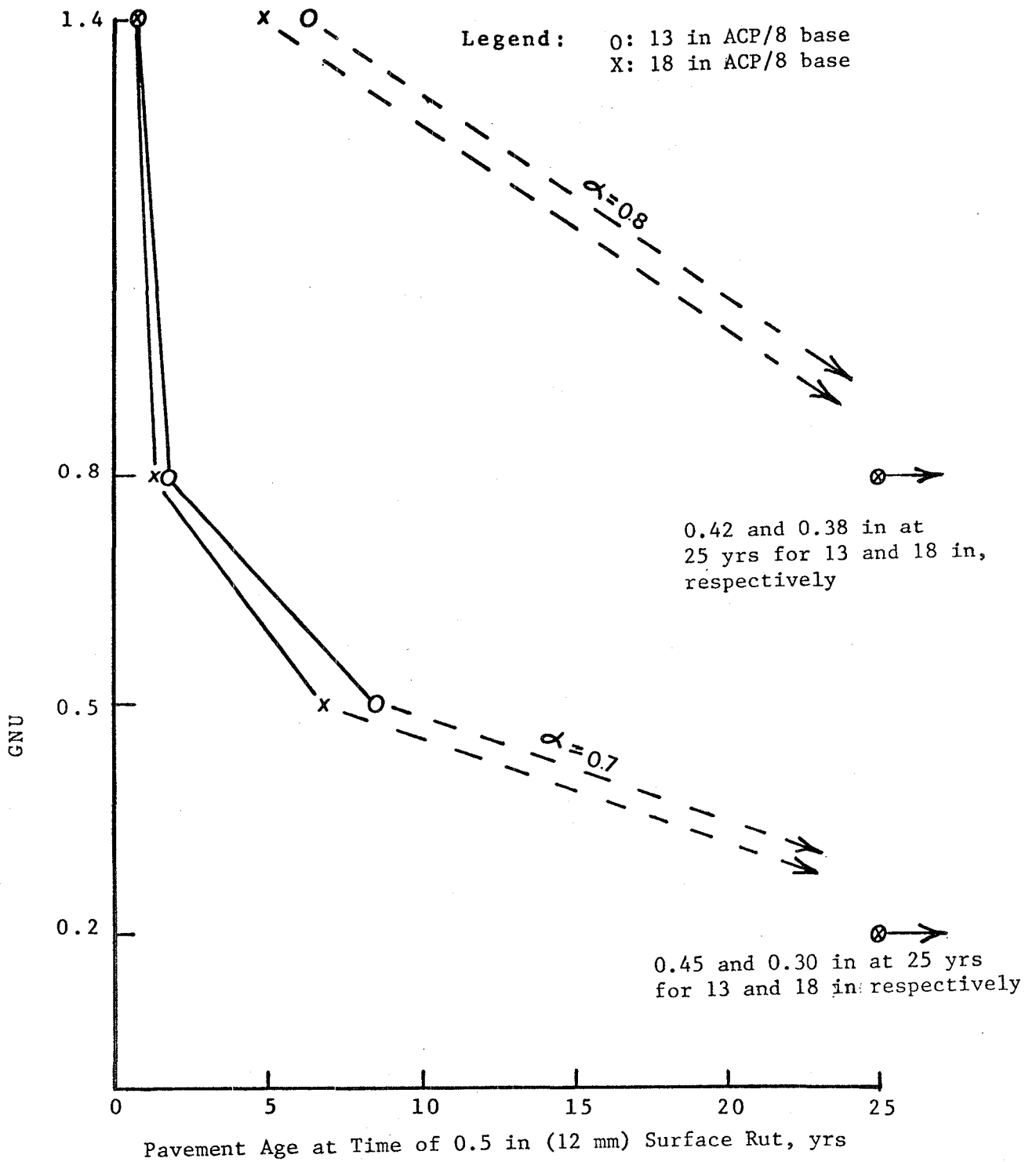


FIGURE 31. EFFECT OF PERMANENT DEFORMATION PARAMETERS ON RUTTING IN FLEXIBLE PAVEMENTS: ZONE: DRY-FREEZE

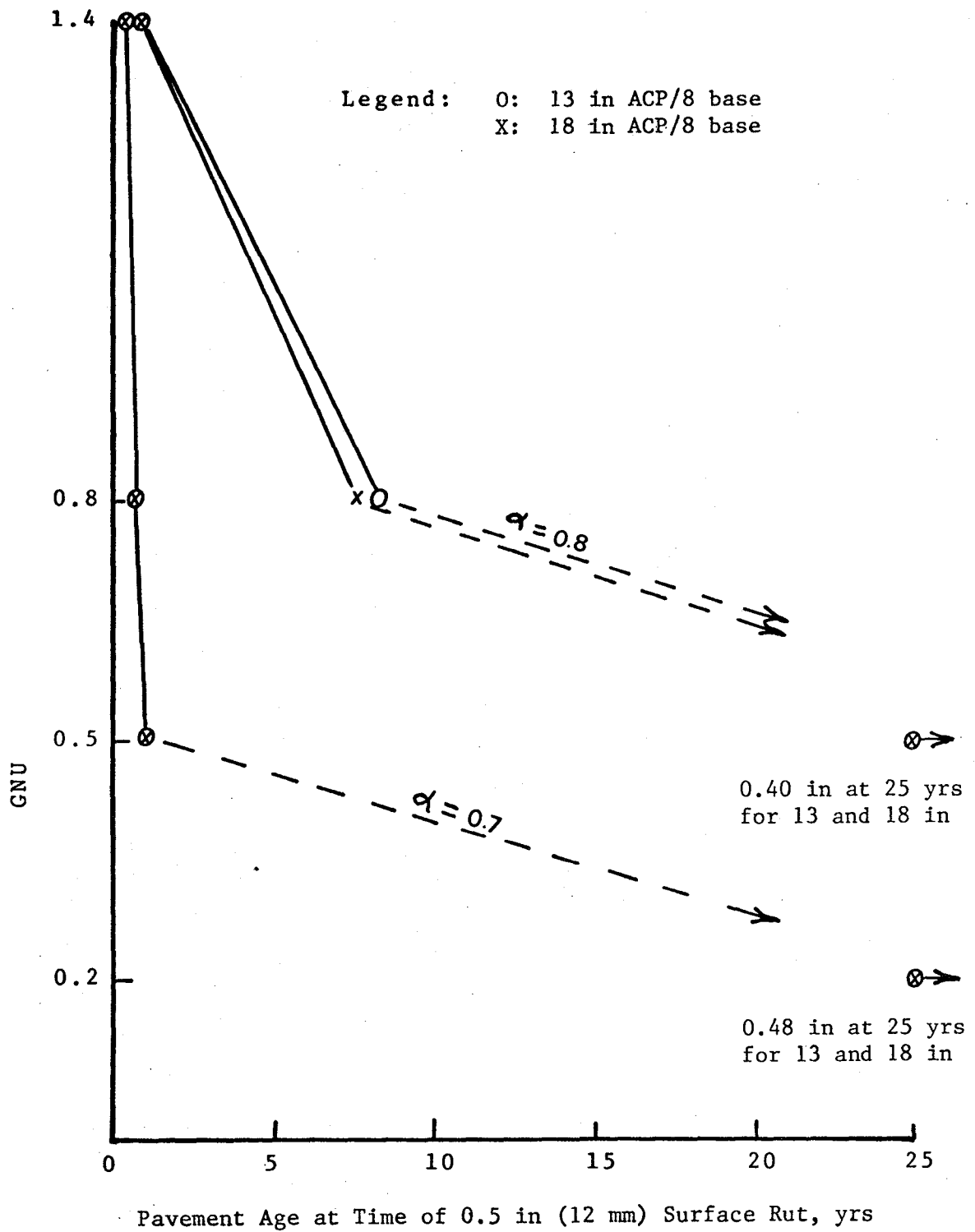


FIGURE 32. EFFECT OF PERMANENT DEFORMATION PARAMETERS ON RUTTING IN FLEXIBLE PAVEMENTS: ZONE: WET - NO FREEZE

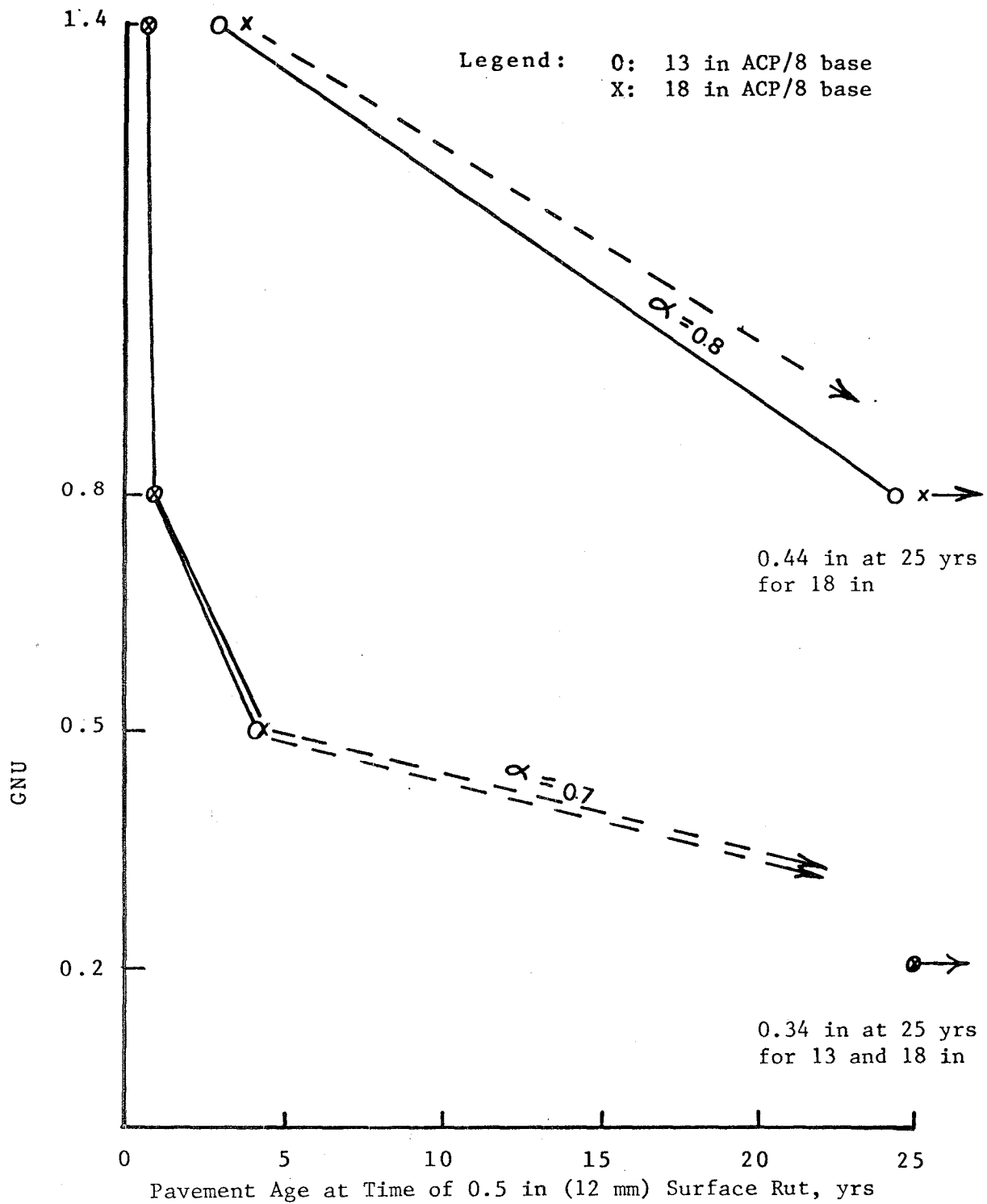
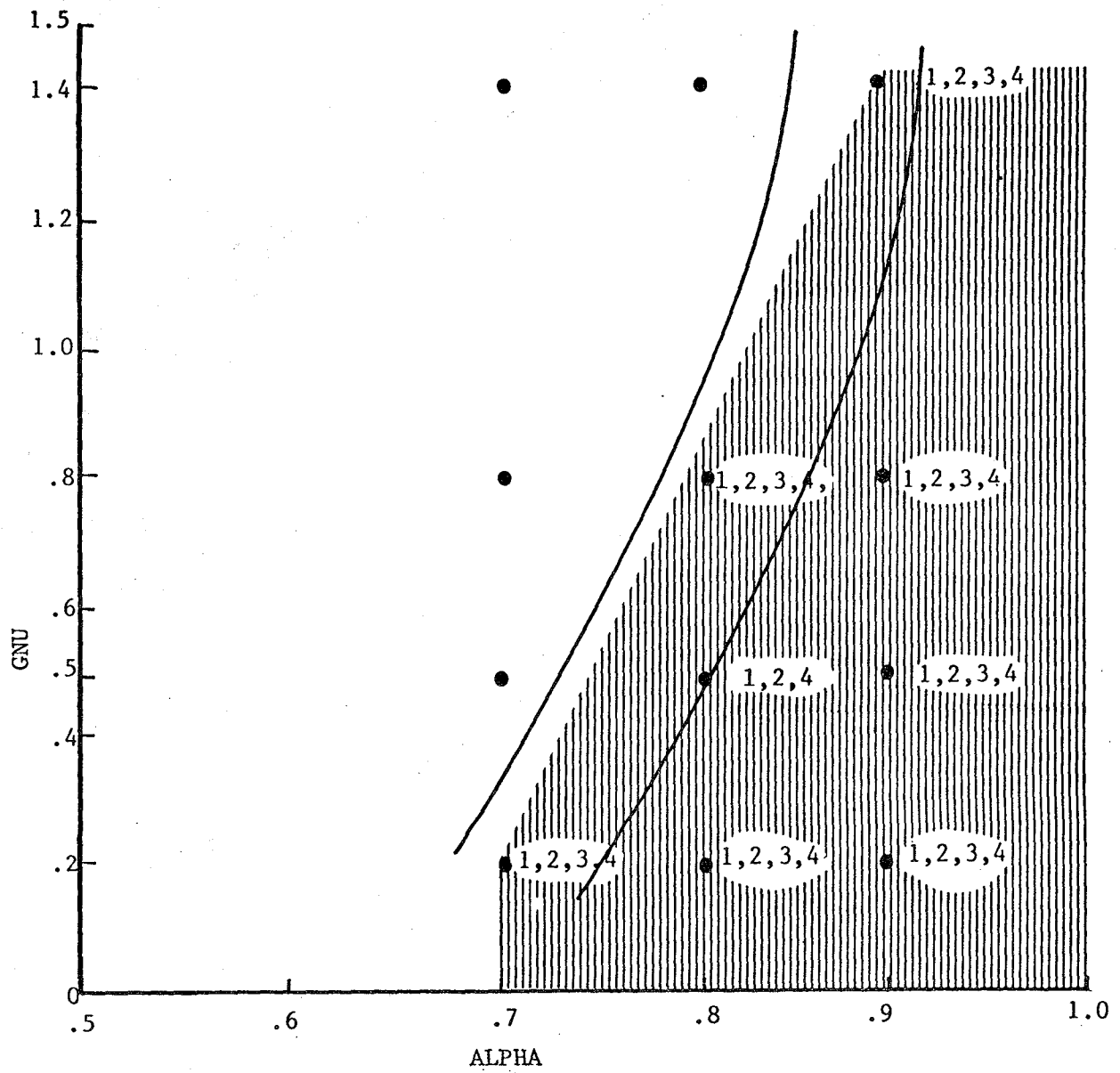


FIGURE 33. EFFECT OF PERMANENT DEFORMATION PARAMETERS ON RUTTING IN FLEXIBLE PAVEMENTS: ZONE: DRY-NO FREEZE

Legend: 1: WF 3: W-NF
 2: DF 4: D-NF



Shaded area satisfies zero maintenance requirements for both 13 in (330 mm) and 18 in (457 mm) surface thicknesses

FIGURE 34. PARAMETER COMBINATIONS MEETING ZERO MAINTENANCE CRITERIA BY ENVIRONMENTAL ZONE

TABLE 25. PREDICTED LOW TEMPERATURE CRACKING, ft/1000 ft²

Asphalt Type	PROPERTIES OF ASPHALT CEMENT	TENSILE STRENGTH OF MIXTURE psi (kPa)	THERMAL COEFFICIENT 10 ⁻⁶ /°F (10 ⁻⁶ /°C)	ENVIRONMENTAL ZONES			
				WET-FREEZE	DRY-FREEZE	WET-NO FREEZE	DRY-NO FREEZE
AC-10	Pen = 120 T _{Pen} = 77° T _{R&B} = 115°F TFOT = 67% SG _{Asp} = 1.040	300 (2,068)	11 (20)	14.70	67.44	.21	.11
			17 (31)	63.11	123.31	2.92	1.50
		600 (4,136)	11. (20)	.29	4.65	0	0
			17 (31)	3.93	33.20	.04	.02
AC-40	Pen = 50 T _{Pen} = 77° T _{R&B} = 125°F TFOT = 70% SG _{Asp} = 1.015	300 (2,068)	11. (20)	37.34	137.5	1.01	0.55
			17 (31)	98.39	167.0	11.40	7.02
		600 (4,136)	11 (20)	1.27	45.32	.01	.005
			17 (31)	13.61	107.1	.21	.12

$$1 \text{ ft}/1,000 \text{ ft}^2 = 3.3 \text{ m}/1,000\text{m}^2$$

$$^{\circ}\text{C} = (^{\circ}\text{F} - 32)/1.8$$

tabulated values represent the calculated amount of low temperature cracking expressed in terms of linear feet of cracking per 1,000 square feet.

Low temperature cracking data for mixtures containing AC-10 and AC-40 (Figure 35) indicated that the AC-40 mixtures experienced greater cracking than did the AC-10. These results imply that low temperature cracking increases as the bitumen stiffness increases for all environmental zones even though almost no cracking occurs in the no freeze zones.

Figure 36 indicated, as expected, that cracking increased as tensile strength decreased. The model predicted significantly lower cracking as the mixture strength increased from 300 psi (2,068 kPa) to 600 psi (4,136 kPa). In general, the effect of changes in strength on cracking were larger than the effect of changes in asphalt type. However, it should be pointed out that significant changes in strength are usually coupled with changes in asphalt type so that the effects of these two factors cannot be easily separated.

As shown in Figure 37, cracking decreased as the thermal coefficient was reduced from $17 \times 10^{-6}/^{\circ}\text{F}$ ($30 \times 10^{-6}/^{\circ}\text{C}$). The effect of changes in thermal coefficient on cracking are comparable to those of strength but probably are more controllable in design because of aggregate selection.

The asphalt cement grade that worked best to prevent low temperature cracking was one with low stiffness at low temperatures. For a particular grade of asphalt cement, lower stiffness at low temperatures can be obtained with a high penetration index. Penetration index is a measure of asphalt consistency developed by Shell researchers based on measurements of penetration at 77°F (25°C) and the ring and ball softening point.

Figure 38 was prepared for use in selecting material property levels to minimize low temperature cracking. At a mix stiffness of 500,000 psi (3,447,000 kPa), the predicted cracking was greater than 10 ft/1,000 ft² (33 m/1,000 m²) for a maximum tensile strength of 300 psi (2,068 kPa) and a thermal coefficient of $17 \times 10^{-6}/^{\circ}\text{F}$ ($31 \times 10^{-6}/^{\circ}\text{C}$). For these properties, the predicted cracking was approximately 20 ft/1,000 ft². As can be seen in Figure 38, the amount of thermal cracking at a stiffness of 500,000 psi (3,447,000 kPa) may be eliminated by either decreasing the thermal coefficient or increasing the tensile strength, the latter being more easily controlled. Based on extensive observations in Canada, McLeod (Reference 73¹) recommended a limiting stiffness of 500,000 psi (3,447,000 kPa) to prevent low temperature cracking for an expected low temperature of -40°F (-40°C).

This limiting stiffness of 500,000 psi (3,447,000 kPa) was used to generate original asphalt properties to characterize mixes for prevention of low temperature cracking. To produce the desired aged asphalt properties, the aging models used in this program were extrapolated outside the

¹McLeod, N.W., "A 4-Year Survey of Low Temperature Transverse Pavement Cracking on Three Ontario Test Roads", Proceedings, Association of Asphalt Paving Technologists, Vol 41, 1972.

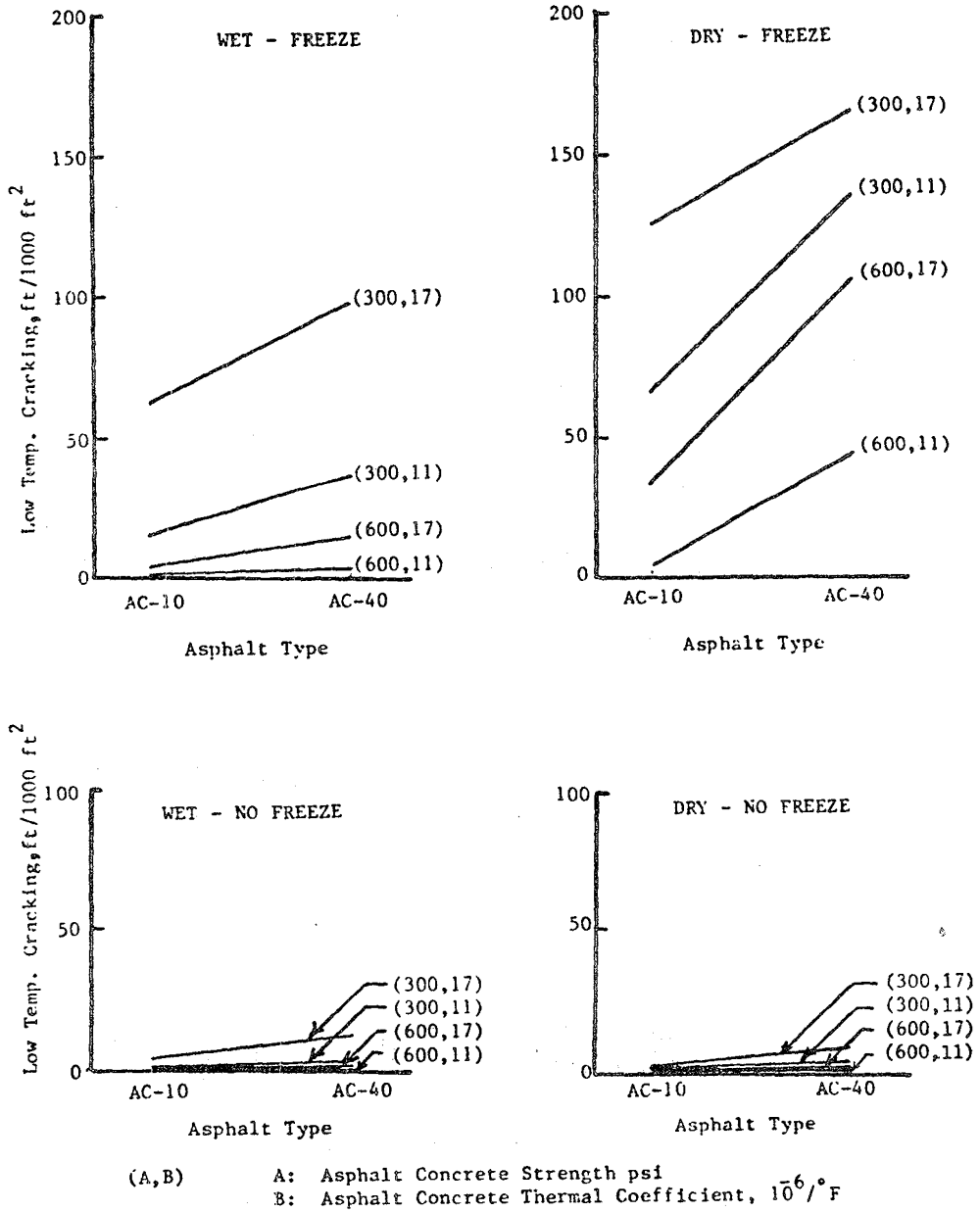


FIGURE 35. LOW TEMPERATURE CRACKING VERSUS THE ASSUMED ASPHALT CEMENT TYPE

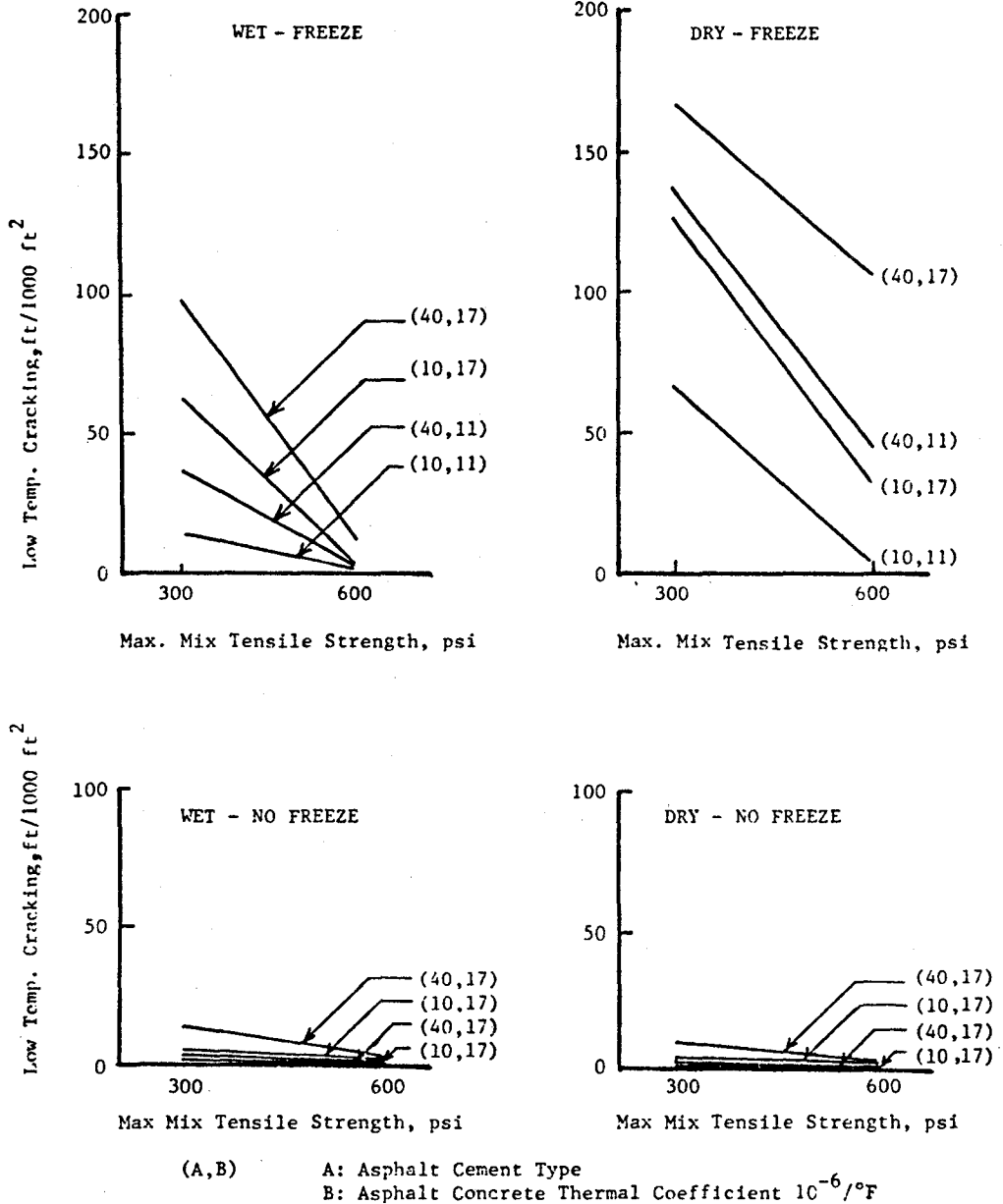
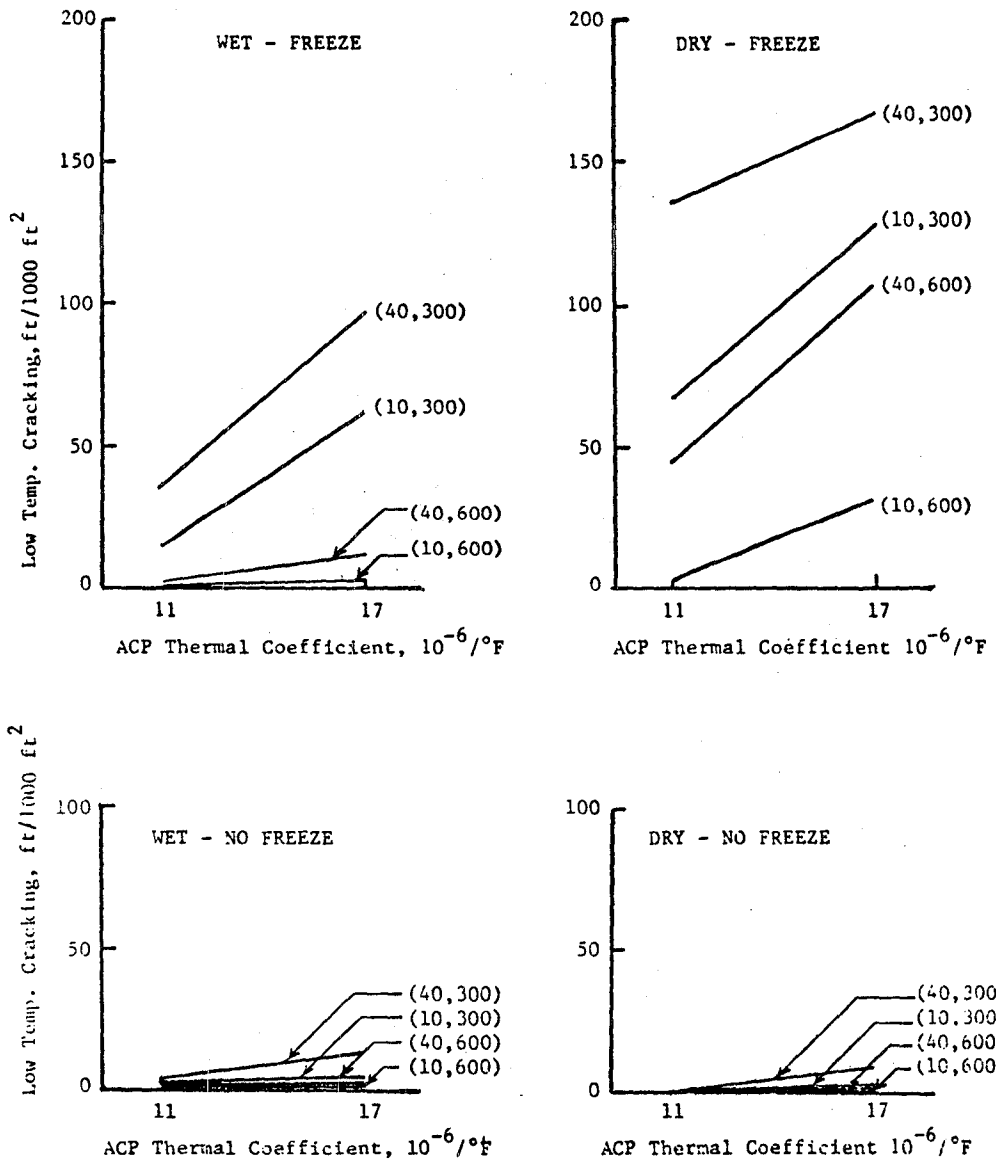


FIGURE 36. LOW TEMPERATURE CRACKING VERSUS MIX TENSILE STRENGTH



(A,B) A: Asphalt Cement Type
 B: Asphalt Concrete (ACP) Tensile Strength, psi

FIGURE 37. LOW TEMPERATURE CRACKING VERSUS AC THERMAL COEFFICIENT

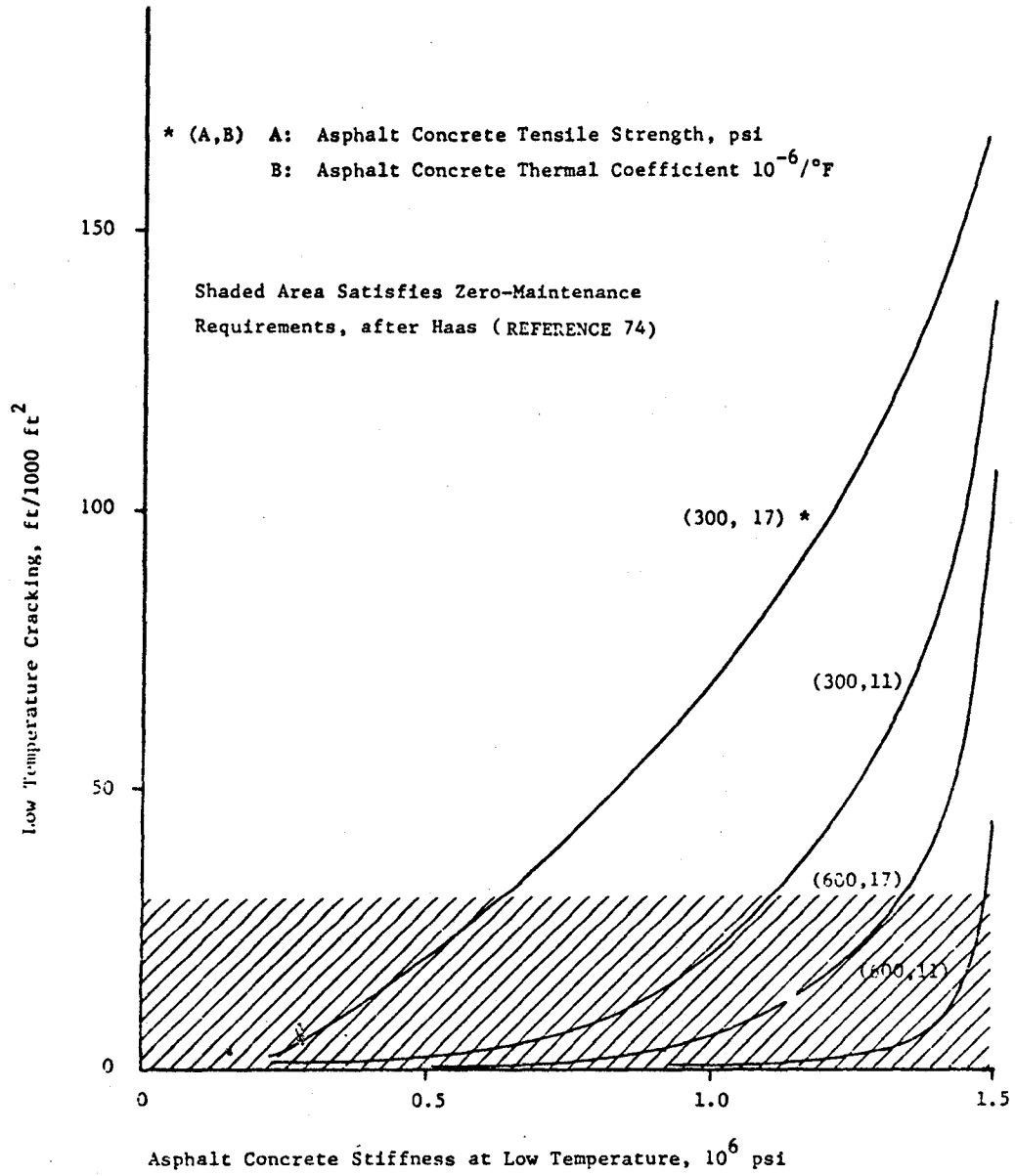


FIGURE 38. LOW TEMPERATURE CRACKING VERSUS ASPHALT CONCRETE STIFFNESS

inference space used during their development to generate the original asphalt cement properties. These properties and the resulting aged asphalt properties were calculated using the Shahin-McCullough model and are included in Table 26. The computer program predicted a negligible amount of transverse cracking for these inputs.

Due to the nature and background of the Shahin-McCullough model the study has several imposed limitations. The most severe limitation was the restriction on the length of the analysis period. The asphalt cement aging model was a regression model based on data for asphalt cements which were aged for 10 years or less. No basis exists for extrapolating the results to longer periods of aging. Thus, a 20 or 30 year analysis period could not be directly simulated to demonstrate zero maintenance pavement performance for the material properties under investigation. However, the material properties which minimize low temperature cracking over a ten year period were assumed to be applicable for the zero maintenance time period.

The results show that the amount of cracking predicted was a function of the lowest input temperature. The daily temperature drop for both the wet and dry environmental zones was approximately the same. The greatest amount of cracking was predicted for the wet-freeze zone where the low air temperature was -30°F (-34°C). The least amount of cracking was calculated for the dry-no freeze zone where the low air temperature was 8°F (-13°C).

The ideal asphaltic concrete for prevention of low temperature cracking was determined to be one with a minimum thermal coefficient of contraction, a high tensile strength, and a minimum stiffness at the expected low temperature.

It is difficult to infer the low temperature performance of conventional asphaltic paving materials for zero maintenance pavement criteria. Although conservative low temperatures were used, the effects of aging were not considered over the 20 year maintenance free period required for zero maintenance pavements. If additional aging was assumed to have no effect, then the results obtained in this analysis are equally applicable to a longer analysis period.

SKID RESISTANCE

To evaluate the acceptability of a surface material in meeting the zero maintenance materials criteria specified by the Steittle-McCullough model, Figure 39 was prepared. The shaded area in Figure 39 represents those values of initial skid number measured at 40 mph (64 kph) and exponent that were unacceptable according to this model and the criteria included for a minimum skid value from Reference 75¹ for a vehicle at 50 mph (80 kph). On the figure was plotted the results of a limited study on

¹Kummer, H.W. and W.E. Meyer, "Tentative Skid-Resistance Requirements for Main Rural Highways", NCHRP Report 37, National Cooperative Highway Research Program, 1967.

TABLE 26. REQUIRED ASPHALT PROPERTIES TO PREVENT LOW TEMPERATURE CRACKING USING THE SHAHIN-MCCULLOUGH AGING MODELS

ENVIRONMENTAL ZONES	ORIGINAL ASPHALT PROPERTIES			AGED ASPHALT PROPERTIES 10 yrs.	
	Pen. D mm	Softening Point, °F (°C)	Thin Film Oven Test	Pen. D mm	Softening Point, °F (°C)
Wet-Freeze	250	101 (38)	50	45	142 (61)
Dry-Freeze	800	82.1 (28)	45	160	118 (48)
Wet- No Freeze	150	110 (43)	61	37	146 (63)
Dry- No Freeze	120	109 (43)	61	31	150 (66)

Constant Material Properties used in Analysis

Maximum Tensile Strength = 450 psi (3,103 kPa)

Thermal Coefficient = $14 \times 10^{-6}/^{\circ}\text{F}$ ($25 \times 10^{-6}/^{\circ}\text{C}$)

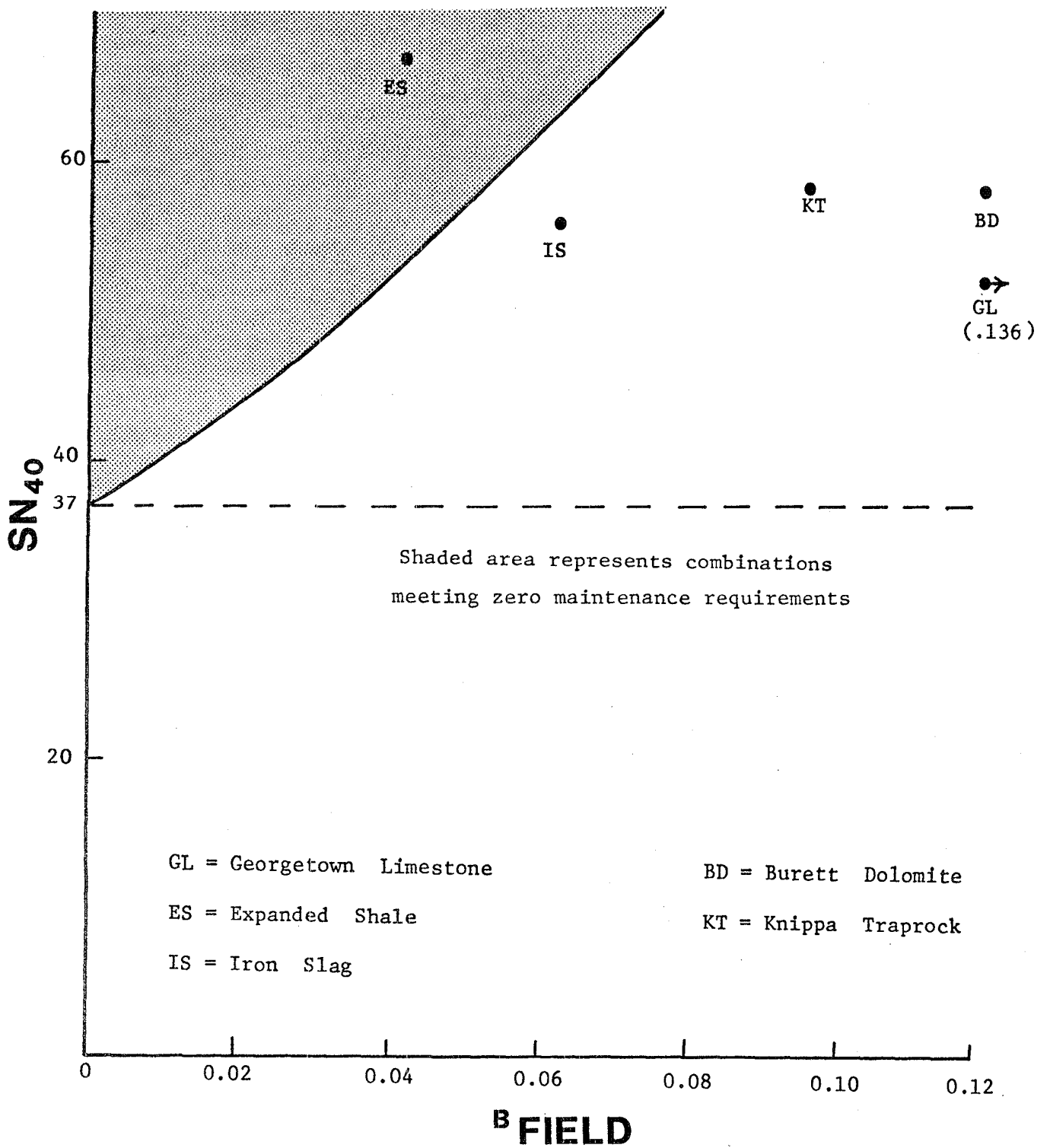


FIGURE 39. RANGE OF ACCEPTABLE COMBINATIONS OF SN_{40} AND B_{FIELD} FOR STEITLE - MC CULLOUGH SKID RESISTANCE MODEL

polishing conducted by Hankins at the Texas State Department of Highways and Transportation. For the five aggregates tested, only the expanded shale had a combination of material properties suitable for zero-maintenance application. The implication of this result was that the designer may be required to provide a surface lift with a very high initial skid number and a very low wear rate in order to meet the zero maintenance requirements for flexible pavements.

CHAPTER 5. RIGID PAVEMENT STUDY

The results of the rigid pavement distress studies are presented in this chapter. Pavement models used to study the relationship between material properties and distress were: (1) JRCP-2, (2) ELSYM5, and (3) CRCP-2. Due to the similarity in response, behavior, and method of modeling jointed pavements, the results for jointed reinforced concrete pavement (JRCP) and jointed concrete pavements (JCP) are discussed together, followed by a discussion of the results for continuously reinforced concrete pavement (CRCP).

DISTRESS STUDIES OF JRCP AND JCP

The significant distresses for jointed pavements were (1) fatigue cracking, (2) joint or crack faulting, (3) joint spalling, and (4) low temperature and shrinkage cracking.

Fatigue Cracking

The results of the fatigue cracking study on JRCP and JCP are summarized in Table 27 and the influence of the modulus of elasticity of the surface and subbase on fatigue life are illustrated in Figures 40 and 41.

The failure criterion used to determine the zero maintenance potential of various combinations of material properties was the abilities of the resulting pavements to carry 40 million 18 kip (80kN) ESAL applications without developing class 3 or 4 cracking. Treybig, et al (Reference 6) found that the structural response of a pavement changed significantly when class 3 and 4 cracking occurred and that routine maintenance was required.

Increased subbase stiffness, increased modulus of the concrete and fatigue characteristics of the concrete increased the number of loads required to produce fatigue cracking. A very stiff subbase greatly increased the traffic required to produce class 3 and 4 cracking. A concrete with better fatigue characteristics obviously improved the predicted fatigue performance - similarly a higher concrete modulus of elasticity increased the traffic applications required to produce class 3 and 4 cracking; however, the rate of increase was less in the higher modulus ranges. For the ranges investigated, increases of the subbase modulus produced larger improvements in fatigue performance than did increases in the modulus of elasticity of the concrete. For example, for the low fatigue level and subbase modulus the traffic carried increased by about 6 times as the concrete modulus varied from 3.5 to 7.0 million psi (24 to 48 million kPa); however, for the low concrete modulus, the traffic carried increased by a factor of almost 25 over the range of subbase moduli. Changes in the traffic carried at other concrete moduli were not as large but did vary by a factor of 6 or more. Since the values of subbase moduli used in this analysis are quite common, efforts to improve the subbase moduli should be given careful consideration.

TABLE 27. SUMMARY OF FATIGUE CRACKING RESULTS FOR JRCP AND JCP

Modulus of Elasticity		Predicted 18 kip (80 kN) ESAL Applications to produce class 3 and 4 cracking, Millions	
Concrete 10 ⁶ psi (10 ⁶ kPa)	Subbase 10 ³ psi (10 ³ kPa)	Low Fatigue Level*	High Fatigue Level*
	15 (103)	24.1	134
3.5 (24)	500 (3447)	147	817
	1000 (6895)	594	3,300
	15 (103)	91.4	508
5.25 (36.2)	500 (3447)	332	1,840
	1000 (6895)	935	5,190
	15 (103)	138	768
7.0 (48)	500 (3447)	382	2,120
	1000 (6895)	868	4,820

Shaded area satisfies zero-maintenance requirements of 40 million 18 kip (80 kN) ESAL

$$* \text{Low } N_f = 18,000 (f_r/\sigma)^{3.9}$$

$$\text{High } N_f = 100,000 (f_r/\sigma)^{3.9}$$

18-kip (80kN) ESAL Applications to Produce Class 3 and 4 Cracking, Millions

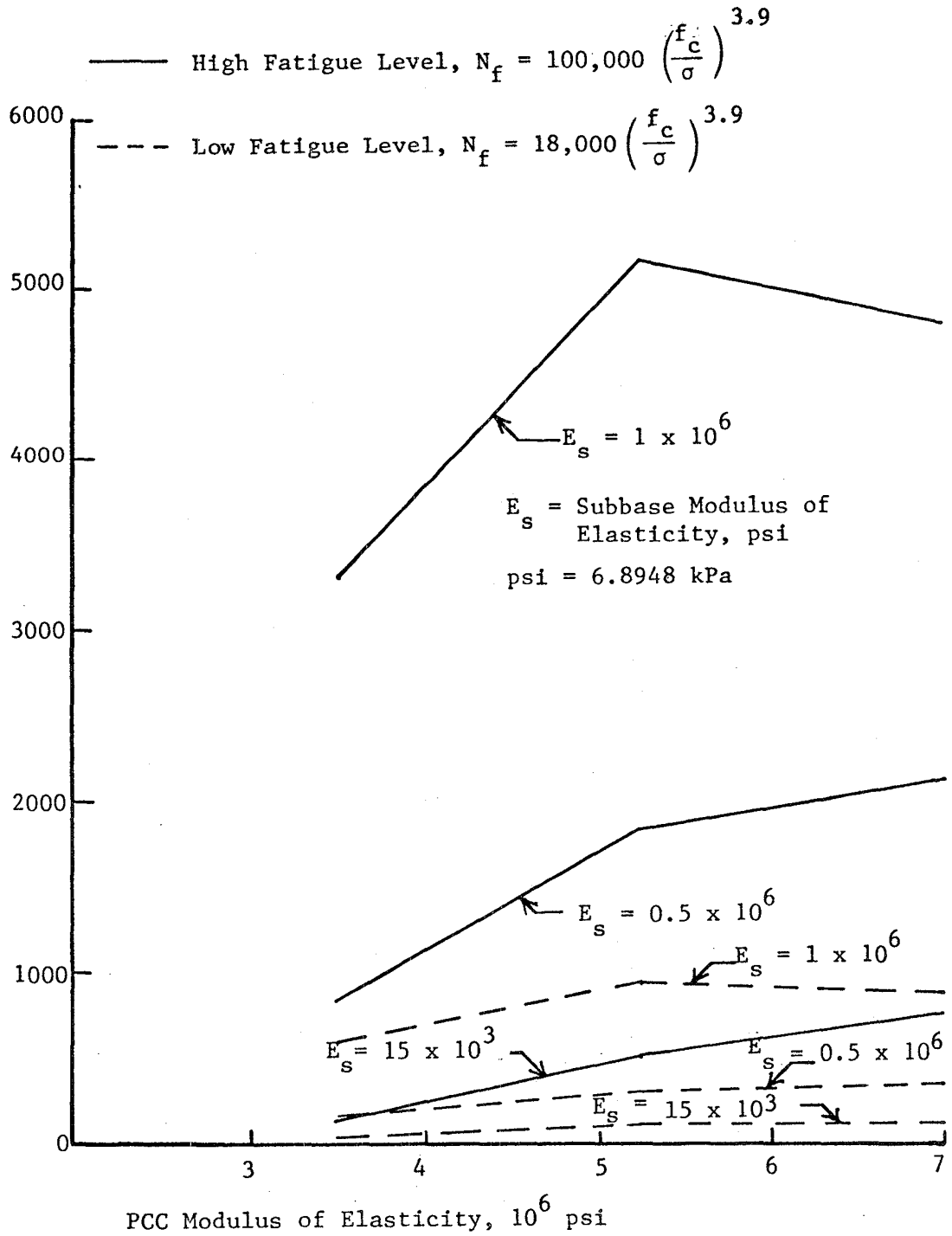


FIGURE 40. INFLUENCE OF CONCRETE MODULUS OF ELASTICITY ON JRCP and JCP FATIGUE CRACKING

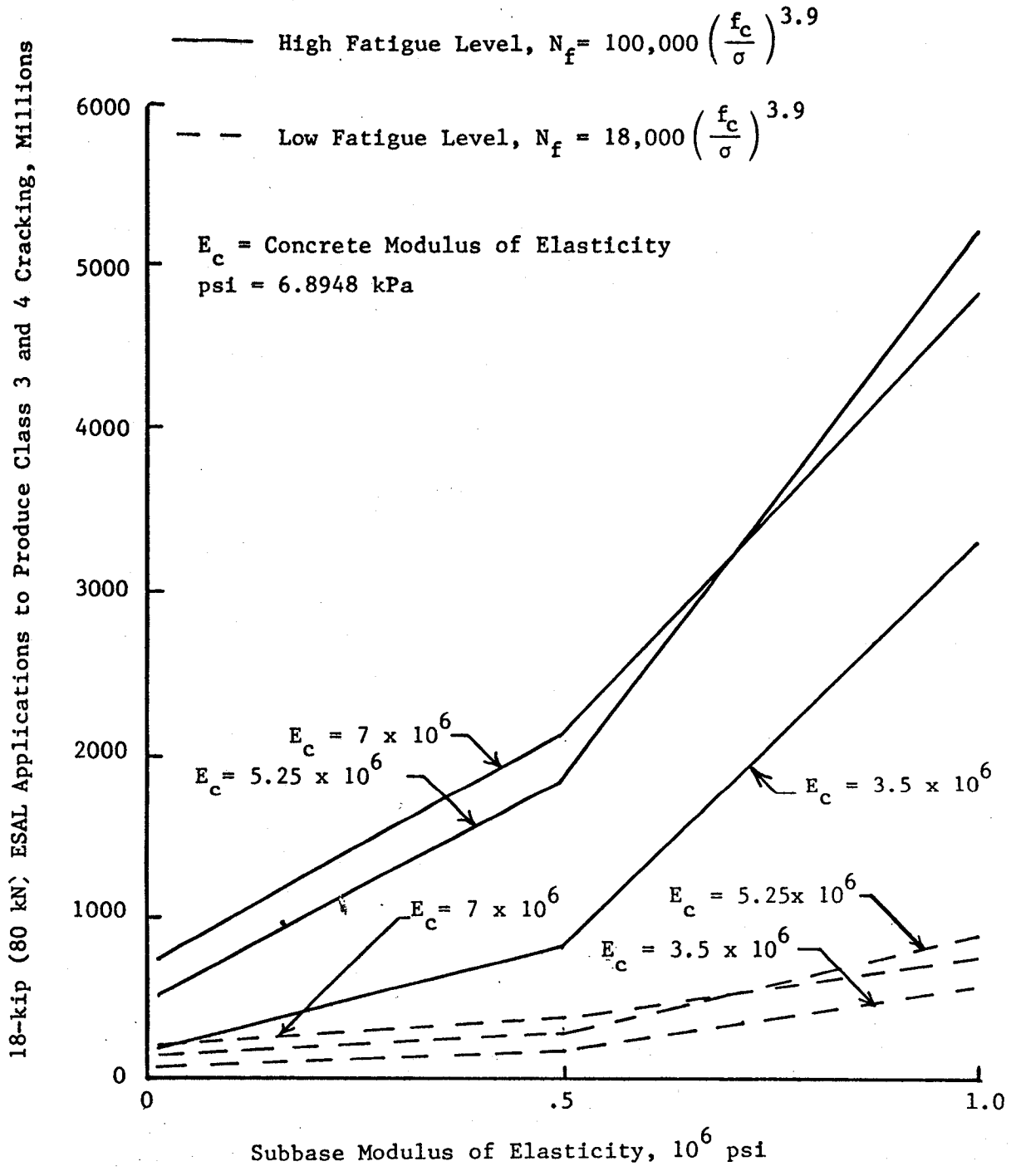


FIGURE 41. INFLUENCE OF SUBBASE MODULUS OF ELASTICITY ON JRCP and JCP FATIGUE CRACKING

For the values used in this study, the effect of varying the fatigue relationship on traffic was larger than the effect of varying the concrete modulus of elasticity. As shown in Figure 40, the fatigue life peaked at a concrete modulus of elasticity of 5.25 million psi (36.2 million kPa). This is probably not a significant observation since modulus and the fatigue characteristics are interrelated.

In summary, conventional concrete offers excellent resistance to fatigue cracking and it is quite capable of producing a zero maintenance pavement. All combinations of material properties except one were capable of carrying traffic for 20 years without the occurrence of class 3 and 4 cracking. In fact, the amount of traffic carried without cracking was substantially above that required. A missing element in this analysis was an evaluation of the effect of layer thickness. It is possible that fatigue performance is more effectively related to thicknesses than to material properties. Zero maintenance could be produced at smaller thicknesses, especially if the properties are improved. Nevertheless, this analysis shows that conventional materials have adequate material properties to meet the zero maintenance fatigue criterion for fatigue cracking.

Joint or Crack Faulting

Rauhut, et al (Reference 3) defined faulting as a difference in elevation of two adjacent rigid slabs at a joint or crack interface due to pumping, inadequate load transfer, or consolidation or swelling of the underlying material. Some faulting has been observed on most types of rigid pavement, but has generally occurred in the outer lanes which carry a high proportion of heavy truck traffic. To date, no quantitative faulting model has been developed; therefore, a quantitative analysis had to be conducted.

The primary cause of faulting is the buildup of material beneath the approach side of a joint or crack. Field investigations have detected these layers of material and other experimental investigations using tracer sand placed at various locations around joints have verified these observations (References 76¹, 77², 78³, 79⁴, and 80⁵). In all of these cases, the erosional and transport properties of water were identified as a necessary agent for creating the material buildup. In addition, the settlement of the subbase caused by infiltration of subgrade fines has been identified as a secondary cause of faulting (Reference 80).

¹Hveem, F.N., "A Report of an Investigation to Determine Causes for Displacement and Faulting at the Joints in Portland Cement Concrete Pavements on California Highways", State of California Division of Highways, Materials and Research Department, May 1949.

²Gessaman, J.D., "The Performance of Unbonded Concrete Resurfacing on Iowa Highways", Portland Cement Association, 1959.

³Neal, B.F. and J.H. Woodstrom, "Faulting of Portland Cement Concrete Pavements", Report No FHWA-CA-TL-5167-77-20, California Department of Transportation, July 1977.

Rigid pavement faulting can be alleviated or prevented by successfully controlling the erosional effects of water at the pavement-subbase interface. One method of control involves preventing water accumulation at this interface through (1) adequate surface drainage to prevent surface water from penetrating to this interface, (2) subsurface drainage for rapid removal of water that does penetrate, and (3) subsurface interceptor drains to intercept and divert lateral subsurface moisture movement as described in References 77 and 81¹.

Another technique that has been utilized to minimize this erosion problem involves improving the resistance of the subbase material to erosion. The use of cement or bituminous stabilized subbase material offers an excellent potential for control of faulting. However, some cement-treated bases or subbases under jointed pavements in California and Georgia have experienced erosion. Hydraulic transport of fines was identified as the cause of faulting on these pavements (References 78 and 79). California has subsequently developed specifications for a lean concrete base in an attempt to alleviate this problem. The use of an open-graded asphalt mixture appears to be an excellent candidate for use as a base or subbase to minimize rigid pavement faulting. In addition to removing a source of erodible fines through proper mix design, the open graded material would provide a drainage path for any water that does infiltrate into the pavement. Infiltration of fines into this layer can be prevented through use of construction fabrics or properly graded filter courses.

Joint Spalling

The primary causes of spalling are (1) entrapment of road debris in cracks, which causes stress concentrations when the cracks close with temperature increase, and (2) combined shear and tensile stresses at joints or cracks due to a combination of horizontal temperature loading and vertical traffic loading. A survey of major distresses in rigid pavements indicated that the problems with spalling are much more prevalent in JRCP and in CRCP. The higher incidence of spalling in reinforced pavements is related to the higher horizontal forces created by the additional restraint provided by the reinforcing steel.

⁴Gulden, W., "Pavement Faulting Study", Final Report, Georgia Department of Transportation, May 1975.

⁵Kalb, M.R., "Investigation of Slab Differential Movement on I-83 Baltimore-Harrisburg Expressway", Final Report, Maryland State Highway Administration, February 1972.

¹Cedergren, H.R., K.H. O'Brien, and J.A. Arman, "Guidelines for the Design of Subsurface Drainage Systems for Highway Structural Sections", Report FHWA-RD-72-30, Federal Highway Administration, 1972.

When a vertical load is applied near a joint or a crack, maximum shear and diagonal tensile stresses occur along an inclined surface running from the pavement surface to the vertical face of the joint or crack. McCullough, et al (Reference 2) found a relationship between spalling and tensile strength for CRCP as shown in Figure 42. The mean indirect tensile strength at the surface was found to be 540 psi (3720 kPa) for the nonspalled sections and 365 psi (2.51 kPa) for spalled sections. For tensile strengths higher than 425 psi (2930 kPa), no spalling was observed.

As previously indicated, spalling of JCP does not appear to be a problem. A combination of good design choices including joints every 15 feet (4.57 m) as recommended by Darter and Barenberg (Reference 1) well-designed and constructed dowel systems, and a concrete mix with high tensile strength should prevent spalling in JCP. Thus, material properties which minimize joint openings will decrease both the incidence and severity of spalling caused by entrapment of incompressible materials in the joints. Materials with relatively low drying shrinkage characteristics and thermal coefficients coupled with high tensile strength should reduce both cracking and spalling.

Low Temperature and Shrinkage Cracking

Since there was no workable computer code available, this distress was considered on a qualitative basis.

For a given joint spacing, relatively low thermal coefficients and shrinkage characteristics reduced the resulting crack widths as well as the horizontal stresses produced by the combined restraint provided by friction on the bottom of the slab and the steel reinforcement. Relatively high concrete tensile strengths also reduce formation of shrinkage cracks. Low temperature and shrinkage cracking was not a major consideration on JCP due to the mitigating effects of closely placed joints.

DISTRESS STUDIES OF CRCP

The important distresses for continuously reinforced concrete pavements were fatigue cracking, punchouts, crack spalling and low-temperature-shrinkage cracking.

Fatigue Cracking

The same material combinations used in the JRCP and JCP fatigue study were used in the CRCP analysis. The reinforcing steel was ignored in the fatigue analysis because of its close proximity to the neutral axis; therefore, the only difference between the continuous and jointed pavement was the thickness of the concrete layer. A concrete surface thickness of 11 inches (279 mm) was utilized in the CRCP study. The number of 18 kip (80 kN) ESAL required to produce class 3 and 4 cracking was compared against the total 20 year traffic to evaluate fatigue performance.

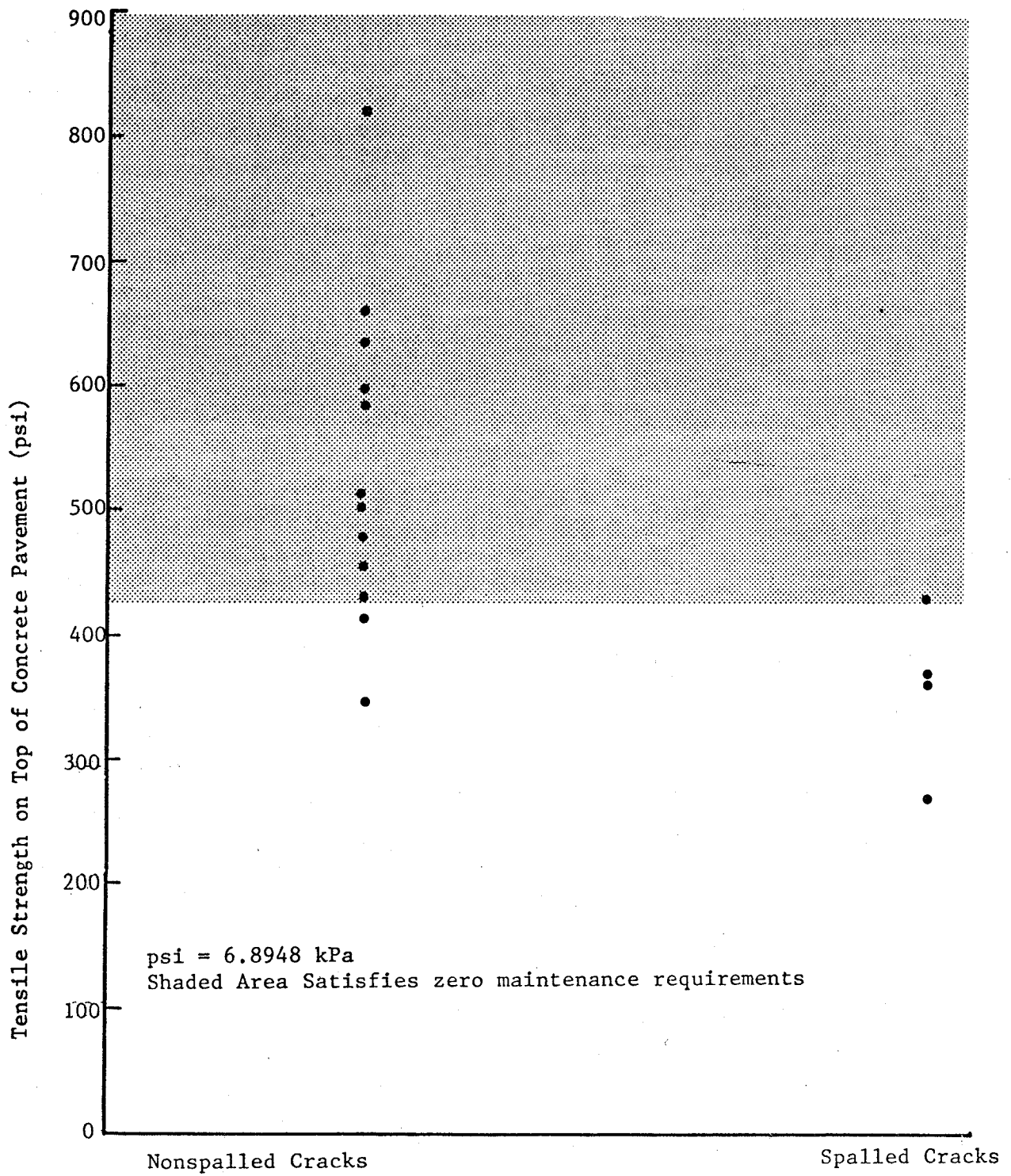


FIGURE 42. A COMPARISON BETWEEN THE TENSILE STRENGTH OF CONCRETE AT THE SURFACE FOR SPALLED AND NON-SPALLED AREAS (REFERENCE 2)

The combination of material properties used in the fatigue analysis and corresponding results are summarized in Table 28 and plotted in Figures 43 and 44, which are similar to those shown in Figure 40 and 41 for JRCP and JCP except that the CRCP did not carry as much traffic before class 3 and 4 cracking occurred because of the smaller thickness. All but two of the combinations of material properties produced pavements which easily satisfied the zero-maintenance requirements for fatigue cracking. The two material property combinations which were not satisfactory involved all low combination of material properties, and the low combination at the intermediate concrete modulus of elasticity of 5.25×10^6 psi (36.2×10^6 kPa). For the range of inputs considered, the subgrade modulus had a greater influence than the concrete modulus.

Punchouts and Crack Spalling

The occurrence of punchouts and spalled cracks can be controlled by setting limits on various response parameters, such as crack spacing. By relating these distress manifestations to the low temperature and shrinkage response parameters, the influence of material properties on these distresses were studied indirectly.

Punchouts. Transverse cracks in CRCP develop as a result of restrained volume change. As the transverse crack spacing becomes smaller and load transfer across the transverse crack deteriorates, the pavement slab begins to respond to load as a transverse beam instead of a longitudinal beam. This subsequently causes short longitudinal cracks to occur within the transverse beam sections which in turn produced small blocks of pavement that eventually lead to punchouts between the reinforcing steel. Thus, punchouts can be prevented by controlling the minimum crack spacing.

An analysis of crack spacing and the concrete stresses in the transverse and longitudinal direction was performed using the SLAB 49 computer program (References 82¹ and 83²). The results are shown in Figure 45 (Reference 84³). The intersection of the stress curves in the x and y directions defines the allowable crack spacing for zero load transfer condition, 5.2 feet (1.58 m). The intersection of the dashed line, drawn asymptotic to the maximum value on the x curve, with the y curve, defines

¹Panak, J.J. and H. Matlock, "A Discrete-Element of Analysis for Orthogonal Slab and Grid Bridge Floor Systems", Research Report 56-25, Center for Highway Research, The University of Texas at Austin, 1971.

²Hudson, W.R. and H. Matlock, "Discontinuous Orthotropic Plates and Pavement Slabs", Research Report 56-6, Center for Highway Research The University of Texas at Austin, 1966.

³Ma, J.C.M., C.S. Noble, and B.F. McCullough, "Design Criteria for Continuously Reinforced Concrete Pavements", Research Report 177-17, Center for Highway Research, The University of Texas at Austin, May 1979.

TABLE 28. SUMMARY OF FATIGUE CRACKING RESULTS FOR CRCP

PCC Modulus of Elasticity, 10 ⁶ psi	Subbase Modulus of Elasticity, 10 ³ psi	Predicted 18-kip ESAL Applications, in Millions, to produce class 3 and 4 cracking	
		Low Fatigue Potential *	High Fatigue Potential *
3.5	15	8.25	45.8
	500	68.4	380
	1000	342	1900
5.25	15	31.9	177
	500	149	827
	1000	493	2740
7.0	15	49	272
	500	166	924
	1000	438	2440

psi = 6.89 kPa

* Low Fatigue, $N_f = 18,000 (f_r/\sigma_t)^{3.9}$

kip = 4.45 kN

High Fatigue, $N_f = 100,000 (f_r/\sigma_t)^{3.9}$

Shaded areas satisfy zero-maintenance requirements of 40 million 18 kip (80 kN) ESAL applications.

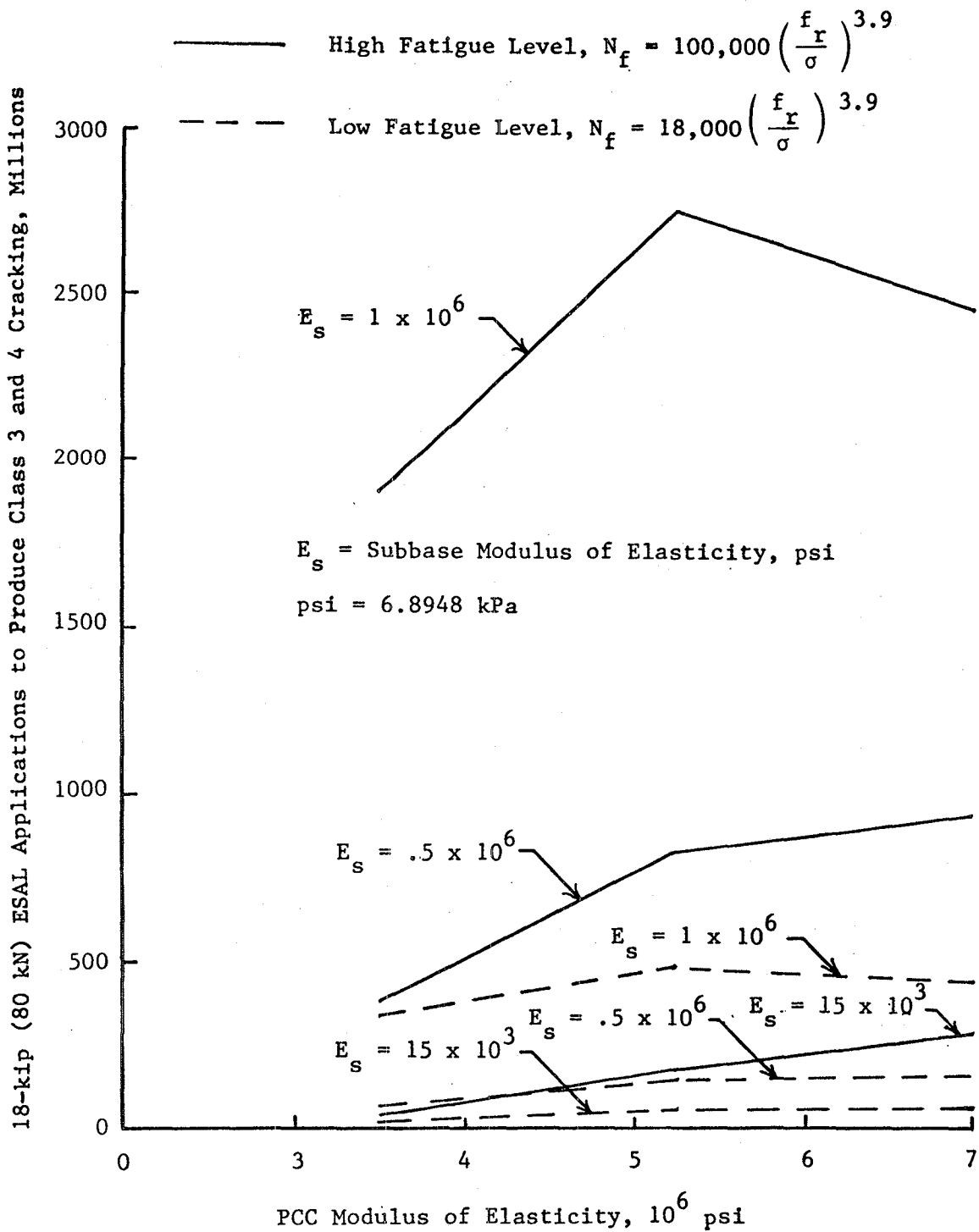


FIGURE 43. INFLUENCE OF CONCRETE MODULUS OF ELASTICITY ON CRCP FATIGUE CRACKING

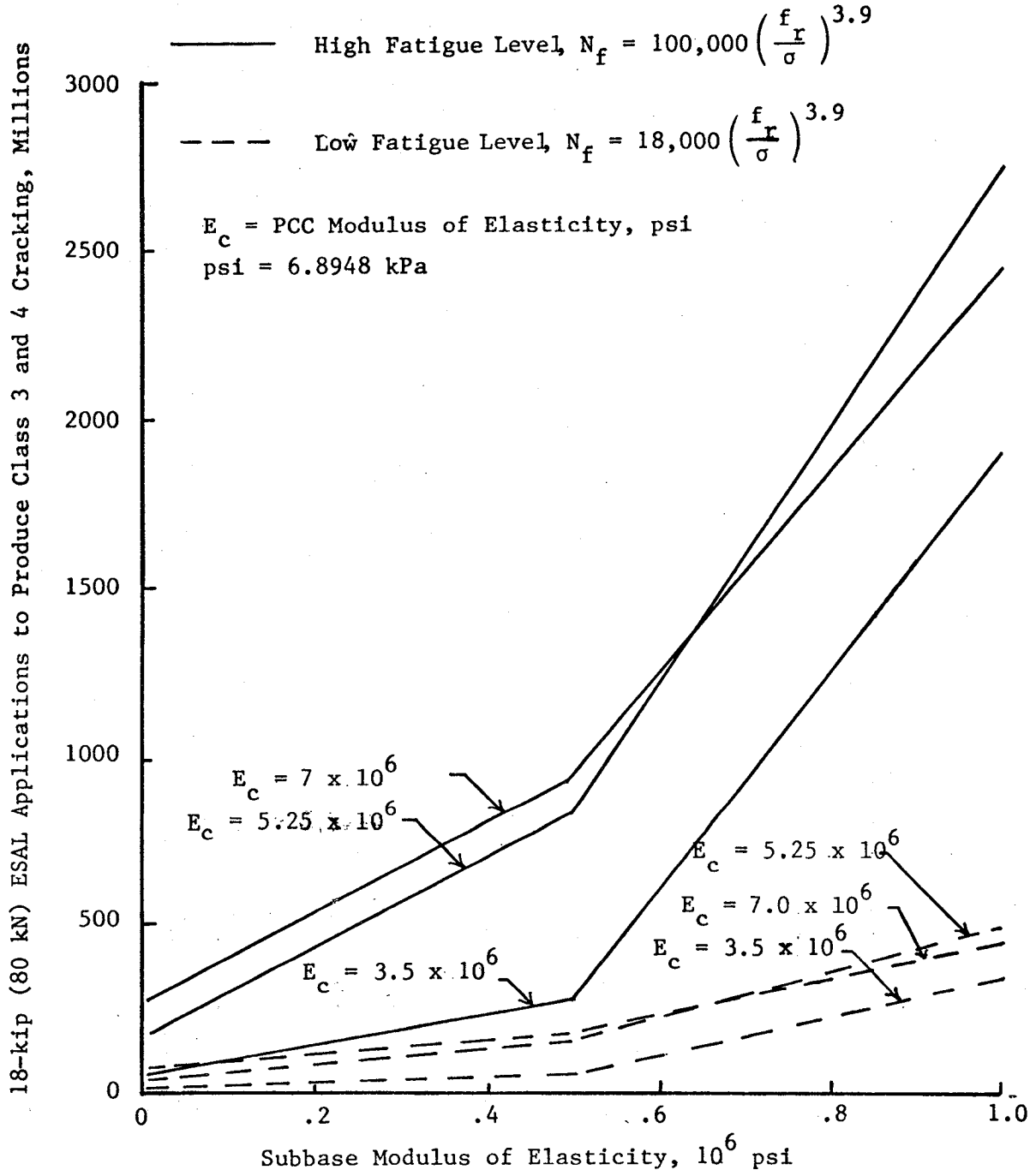


FIGURE 44. INFLUENCE OF SUBBASE MODULUS OF ELASTICITY ON CRCP FATIGUE CRACKING

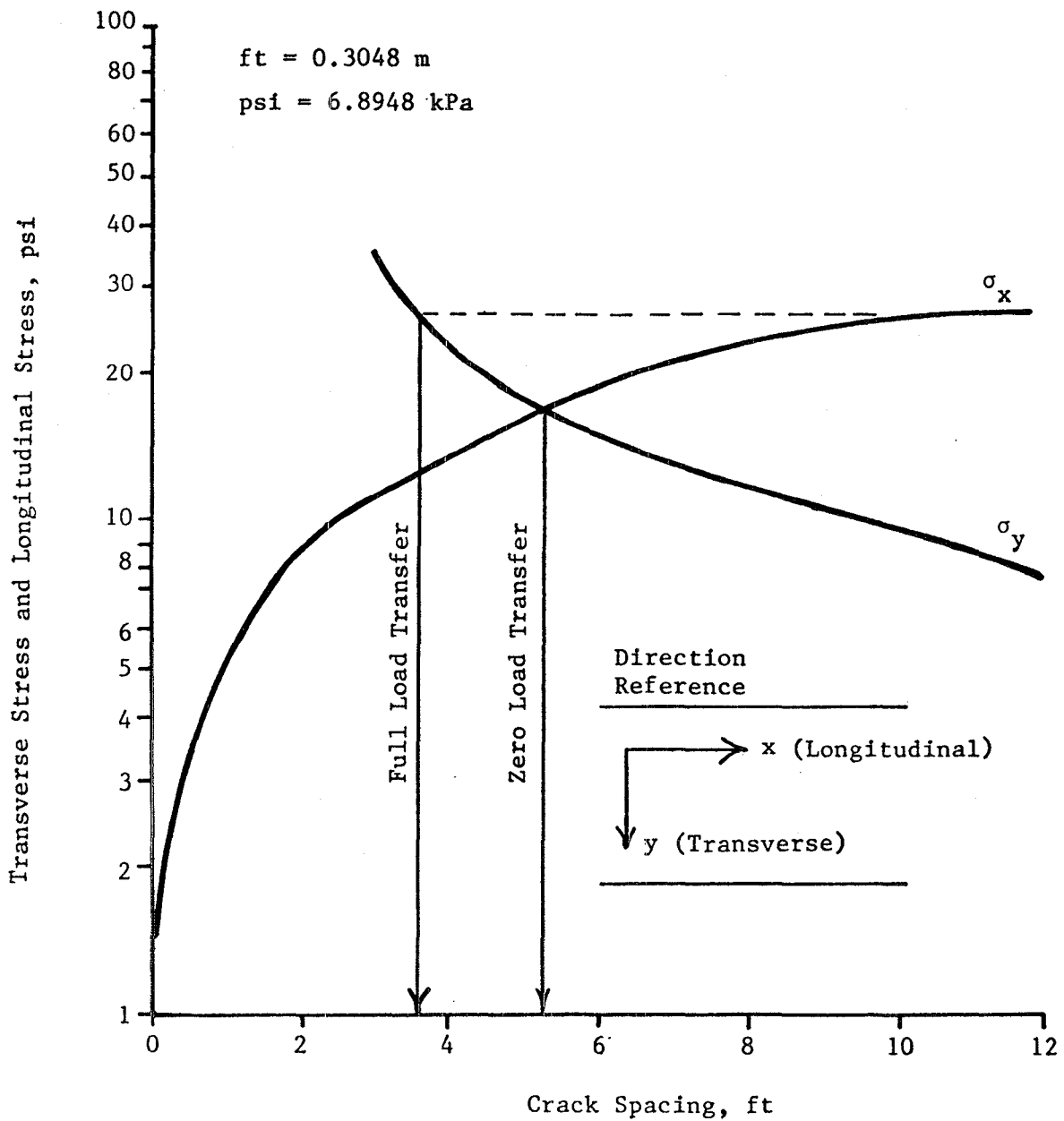


FIGURE 45. STRESS IN X AND Y DIRECTION VERSUS CRACK SPACING FOR A 279 mm (11 in) THICK SLAB (REFERENCE 26)

the allowable crack spacing for the full load transfer condition as 3.6 feet (1.10 m). The actual load transfer across a transverse crack will be somewhere between the no load transfer condition and the full load transfer condition. To determine a reasonable limit on crack spacing to minimize the occurrence of punchouts, a minimum load transfer across the transverse cracks of 50 percent was assumed. This corresponds to an interpolated value of crack spacing of 4.4 feet (1.34 m). This limit is slightly less than the 5 foot (1.52 m) optimum crack spacing determined by Majidzadeh (Reference 85¹), and the 5 feet (1.52 m) minimum suggested by McCullough (Reference 2) based on field observations of inservice pavements. Therefore, theoretically, crack spacings greater than 4.4 feet (1.34 m) should minimize the occurrence of punchouts on CRCP. This assumes that the concrete surface layer is in full contact with the subbase. Voids resulting from pumping of subbase material or non-uniform volume change can cause increased stresses with subsequent increased number of punchouts.

Crack Spalling. As with JRCP and JCP, the primary causes of spalling CRCP were: (1) entrapment of road debris in cracks which causes stress concentration when the cracks close with temperature increases and (2) combined shear and tensile stress at joints or cracks due to a combination of horizontal temperature loading and vertical traffic loading. However, based on a laboratory study, McCullough, et al (Reference 2) concluded that CRCP spalling caused by road debris entrapment was relatively insignificant, but that combined horizontal and vertical forces was the major cause of spalling. Since crack width and degree of spalling are both a function of horizontal stress, crack width and spalling are related. In a diagnostic study based on condition surveys data from Texas CRCP (Reference 2), crack widths and the occurrence of spalling were measured in the field. Results of these studies are shown in Figure 46 which indicates that spalling was more prevalent at larger cracks. A mean crack width of 0.021 inch (.53mm) was reported for the spalled sections and .0176 inch (.45mm) for the non-spalled sections. Cracks with widths less than 0.02 inch (.51mm) exhibited no spalling.

To control spalling, McCullough (Reference 84) established a maximum allowable crack width of 0.024 inches (.61mm). Since the crack widths were measured during the summer at relatively high temperatures, it was necessary to calculate the corresponding width at a lower temperature using the CRCP Program. Crack widths at the lowest temperatures during the analysis period were calculated and the results of such a calculation procedure were used to determine the allowable crack width versus temperature chart shown in Figure 47 (Reference 84).

Allowable crack widths corresponding to the temperature drops for the four environmental zones were determined to be:

¹Majidzadeh, K., "Observations of Field Performance of Continuously Reinforced Concrete Pavements in Ohio", Report No OHIO-DOT-12-77, Ohio Department of Transportation, September 1978.

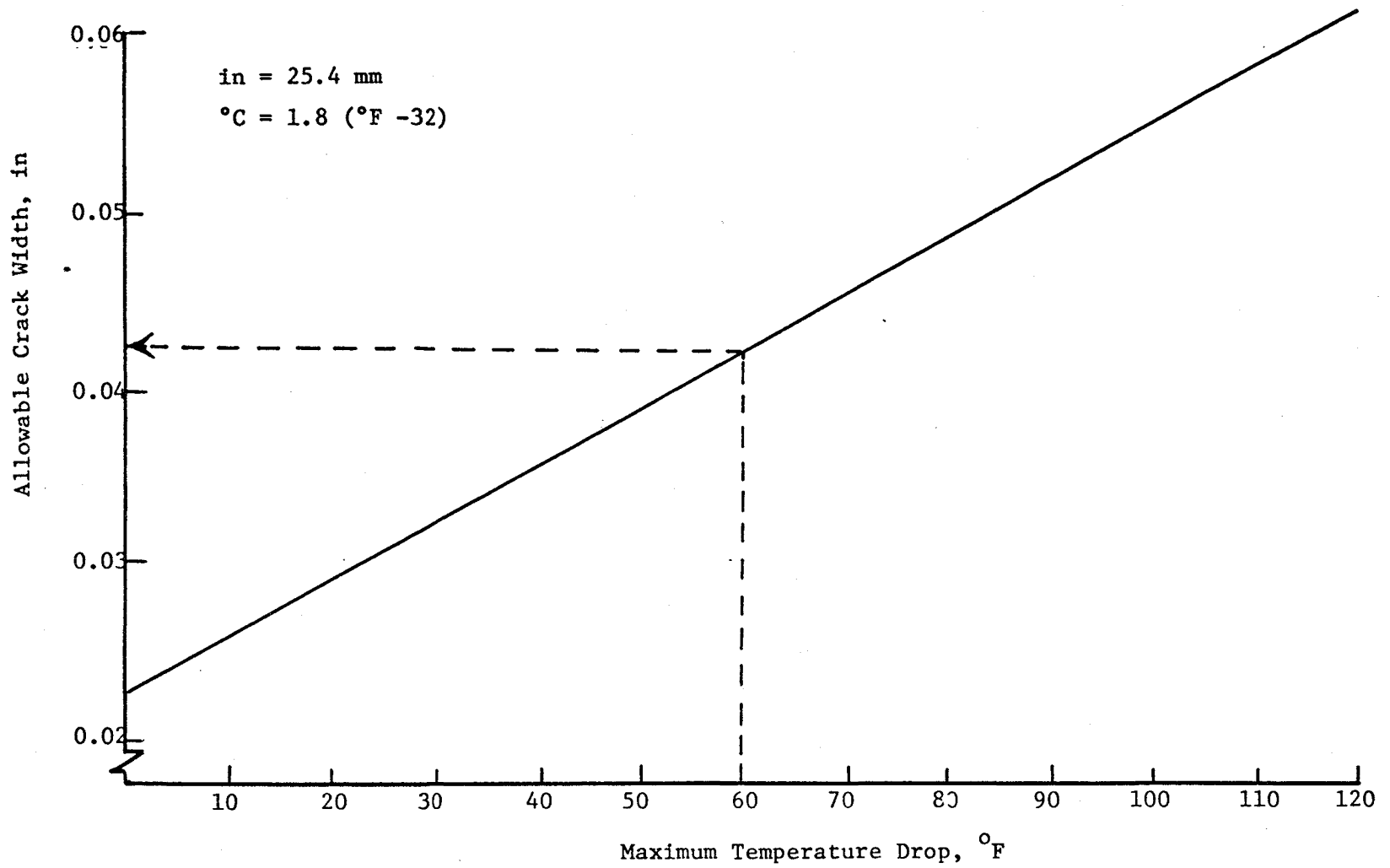


FIGURE 47. ALLOWABLE CRACK WIDTH FOR CONTROL OF SPALLING (REFERENCE 84)

Dry Freeze	.040 inches (1.02 mm)
Wet Freeze	.041 inches (1.04 mm)
Dry No Freeze	.034 inches (0.86)
Wet No Freeze	.030 inches (0.76 mm)

These recommended limits were used in the evaluation of the results of the low-temperature and shrinkage cracking study. Use of allowable crack widths smaller than these allowable values ensures prevention of spalling at joints and cracks.

Low Temperature and Shrinkage Cracking

The combination of material properties included in Tables 20 and 21 were utilized in the CRCP-2 computer model study.

First Stage Parameter Study. That analysis was performed in a sequential order beginning with the high and low values of tensile strength and 0.6 percent steel. The only variables changed in that study were the concrete thermal coefficient, ultimate concrete shrinkage, and tensile strength. The calculated crack spacing and crack widths in the wet and dry freeze environmental zones are shown in Figures 48 and 49. Relationships for the other environmental zones were similar.

The maximum desirable crack spacing for a CRC pavement determined from field observations has been set at 8 feet (2.44 m) (References 85). Crack spacings greater than 8 feet (2.44 m) produce (1) cracks that open widely, foreign materials enter the cracks and spalling results and (2) reduced load transfer as aggregate interlock decreases.

The relationship between steel stress is plotted in Figure 50 and concrete strength for two environmental zones is shown in Figure 50. For high strength concrete, the yield strength in the steel was exceeded. Thus, lower strength concrete would be desirable. If higher strength concrete is utilized, then a compatible yield strength steel should be selected.

For the range of values included in this analysis, concrete strength had the greatest effect on the CRCP predicted response parameters. At the low level of concrete strength, shrinkage exhibited greater effects than the thermal coefficient. At the high level of concrete strength the change in thermal coefficient produced a greater change in the predicted response than did the change in shrinkage.

In general, crack spacing increased as the concrete shrinkage and concrete thermal coefficient decreased and as the concrete strength increased. This result was reasonable since concrete shrinkage and thermal coefficients are the elements which produce the load on the system and since the concrete strength resists these induced stresses.

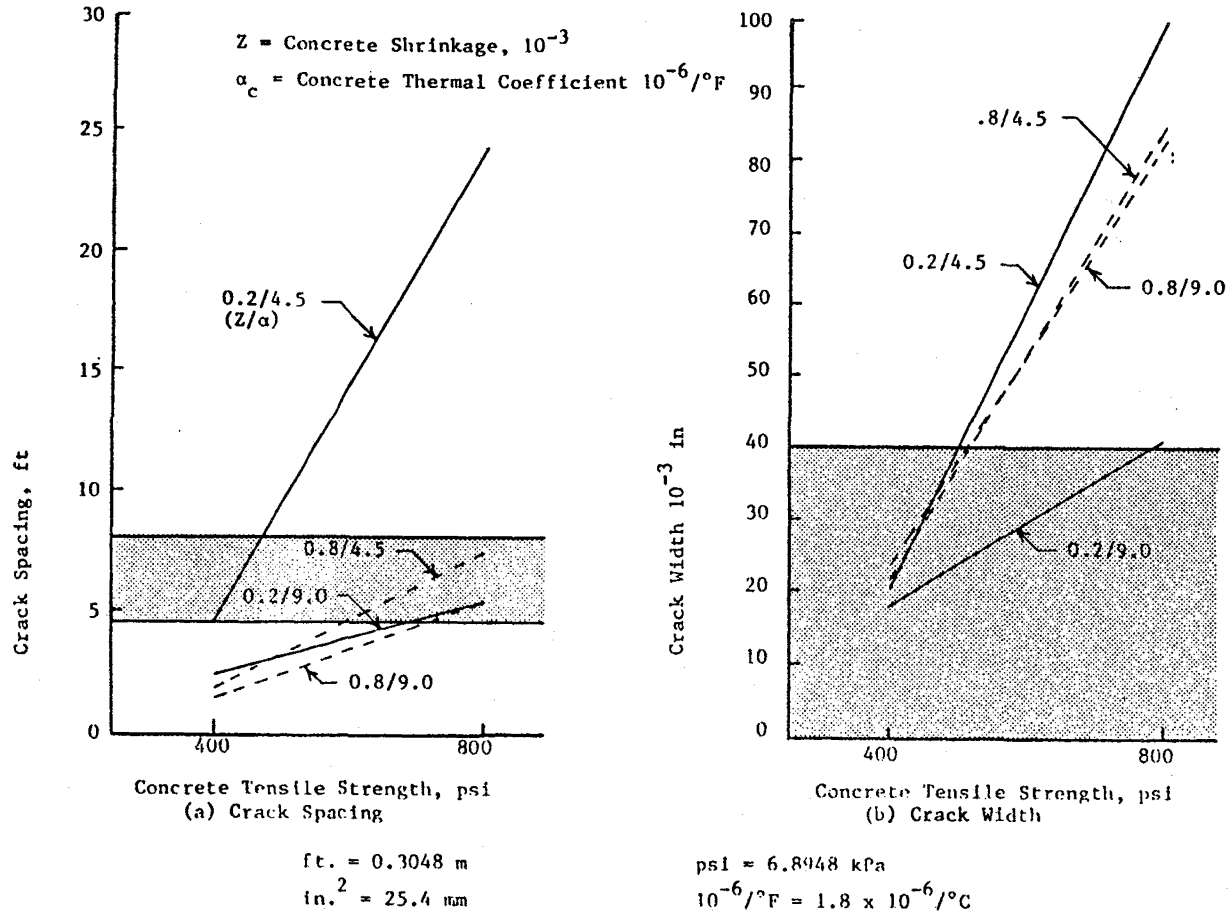


FIGURE 48. EFFECTS OF CONCRETE STRENGTH, SHRINKAGE CHARACTERISTICS AND THERMAL COEFFICIENTS ON CRACK SPACING AND CRACK WIDTH IN THE DRY - FREEZE ZONE

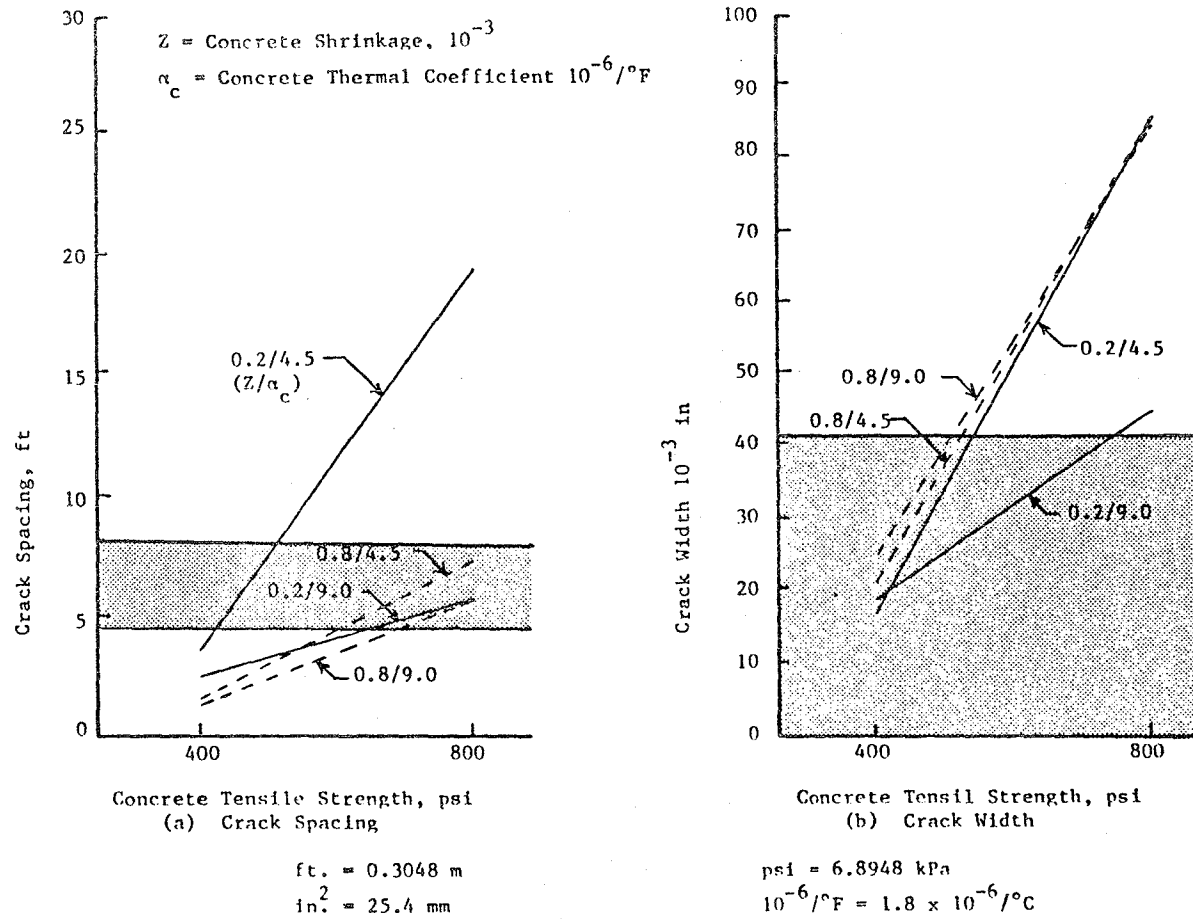
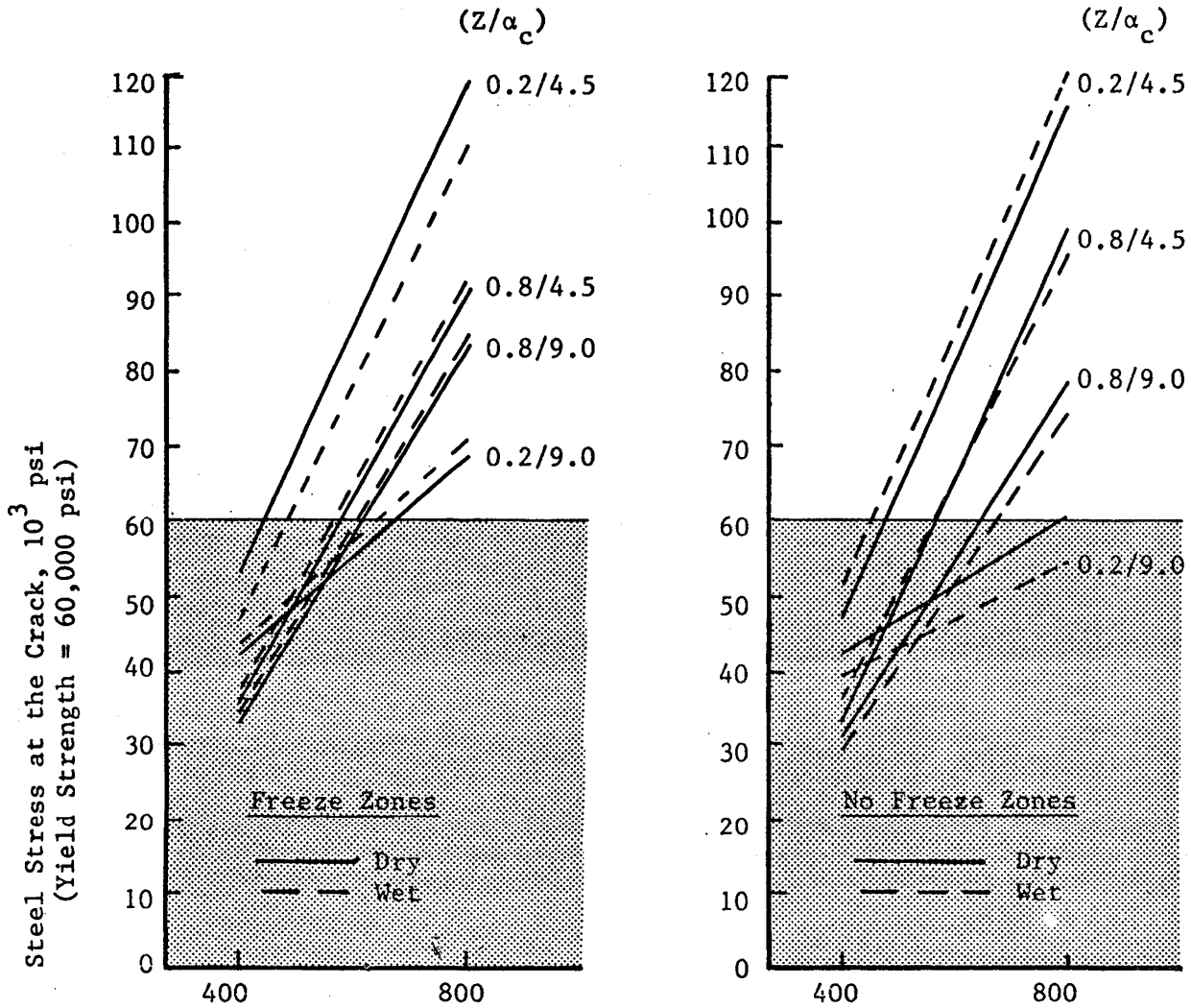


FIGURE 49. EFFECTS OF CONCRETE STRENGTH, SHRINKAGE CHARACTERISTICS AND THERMAL COEFFICIENTS ON CRACK SPACING AND CRACK WIDTH IN THE WET-FREEZE ZONE

Z = Concrete Shrinkage, 10^{-3}

α_c = Concrete Thermal Coefficient, $10^{-6}/^{\circ}\text{F}$

psi = 6.8948 kPa $10^{-6}/^{\circ}\text{F} = 1.8 \times 10^{-6}/^{\circ}\text{C}$



Concrete Tensile Strength
Shaded Areas Represent Stress Meeting Zero Maintenance Requirements

FIGURE 50. EFFECTS OF CONCRETE STRENGTH, SHRINKAGE AND THERMAL COEFFICIENTS ON STEEL STRESS AT THE CRACK FOR CRCP

Crack width increased as the concrete shrinkage and thermal coefficients decreased and as the concrete strength increased. This result may seem contrary to the reasoning that increasing concrete shrinkage and thermal coefficient causes the concrete to contract more, thus creating a wider crack. The phenomenon occurs because of the relationship between crack width and crack spacing.

To demonstrate the effect of these variables on crack width alone without the effect of crack spacing, the crack widths were divided by the corresponding crack spacings and plotted against the ultimate concrete strength for the dry freeze zone (Figure 51). These results which are typical of the other environmental zones indicate that the crack width per foot of slab increased as the concrete shrinkage and thermal coefficients increased. The insensitivity of predicted crack width to concrete strength was also noted in Figure 51.

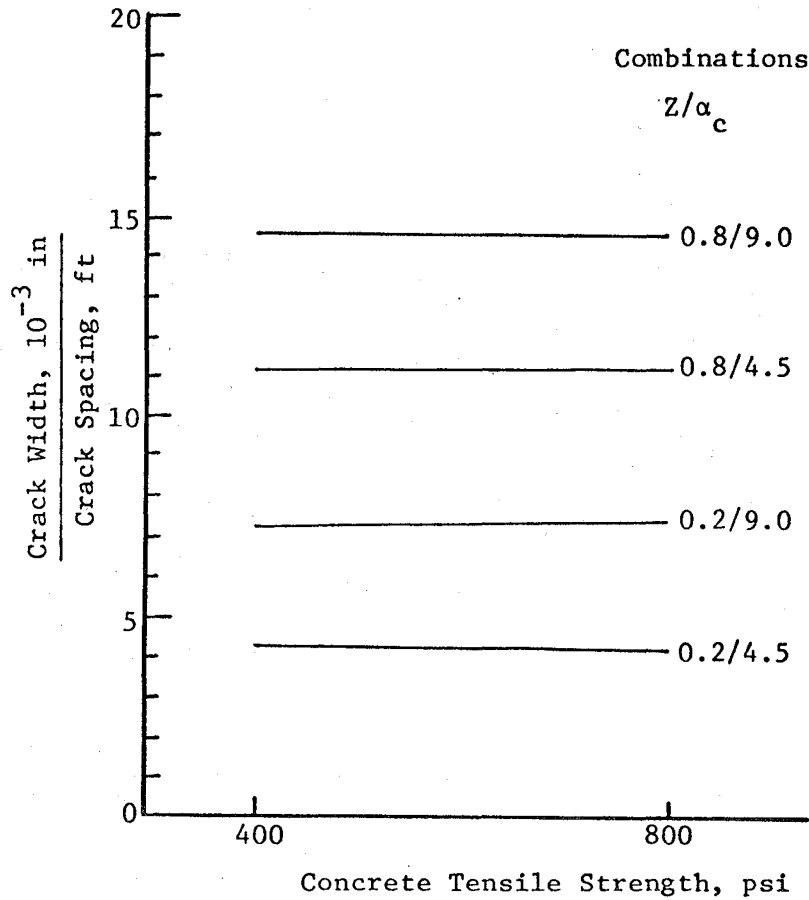
One other effect of crack spacing showed up in the analysis of steel stresses. As shown in Figure 50, the predicted steel stress at the crack was directly proportional to concrete strength. For a constant crack spacing, steel stress was expected to decrease as the concrete shrinkage and thermal coefficients decrease and to increase as the concrete strength increased. This result occurred for the variation in concrete shrinkage for the high concrete thermal coefficient value but not for the low value. These results occur because of the interaction of crack width and crack spacing as exhibited in Figures 48 and 49. In reviewing the results from these CRCP study runs, the interactive effects of crack spacing, crack width, and steel stress cannot be optimized separately to achieve a zero-maintenance pavement. This analysis indicated that crack spacing was a very influential response parameter for a CRCP. The effect of material properties were not separable from their effects on crack width and steel stress.

The effect of changes in temperature on the response of the CRCP system was illustrated in Figure 52. Crack spacing and crack widths were plotted as functions of temperature drop for 400 psi (2,758 kPa) concrete with low and high combinations of shrinkage and thermal coefficient. Note that the form of the relationship between temperature and both crack width and crack spacing were similar for the combination of low thermal and shrinkage coefficients. This combination of low coefficients is not the typical case for conventional PCC pavement. The more typical case consists of high shrinkage and thermal coefficient, where crack spacing was unacceptably small and remained essentially constant as the temperature dropped resulting in increased crack widths with decreasing temperature. Crack spacing generally decreases with increasing magnitudes of temperature drop to some minimum spacing, but the interactions between the concrete properties and the resistance of the subbase and steel to movement had an important effect on relative crack spacing and widths. The predicted steel stresses for all of the environmental zones were approximately equal, and varied slightly with variations in crack spacing and temperature drop.

In general, the material properties at the high level produced values of response parameters outside the recommended range developed from field studies to ensure zero maintenance service. The combination of high concrete

Z = Concrete Shrinkage, 10^{-3}

α_c = Concrete Thermal Coefficient, $10^{-6}/^{\circ}\text{F}$



in = 25.4 mm

ft = 0.3048 m

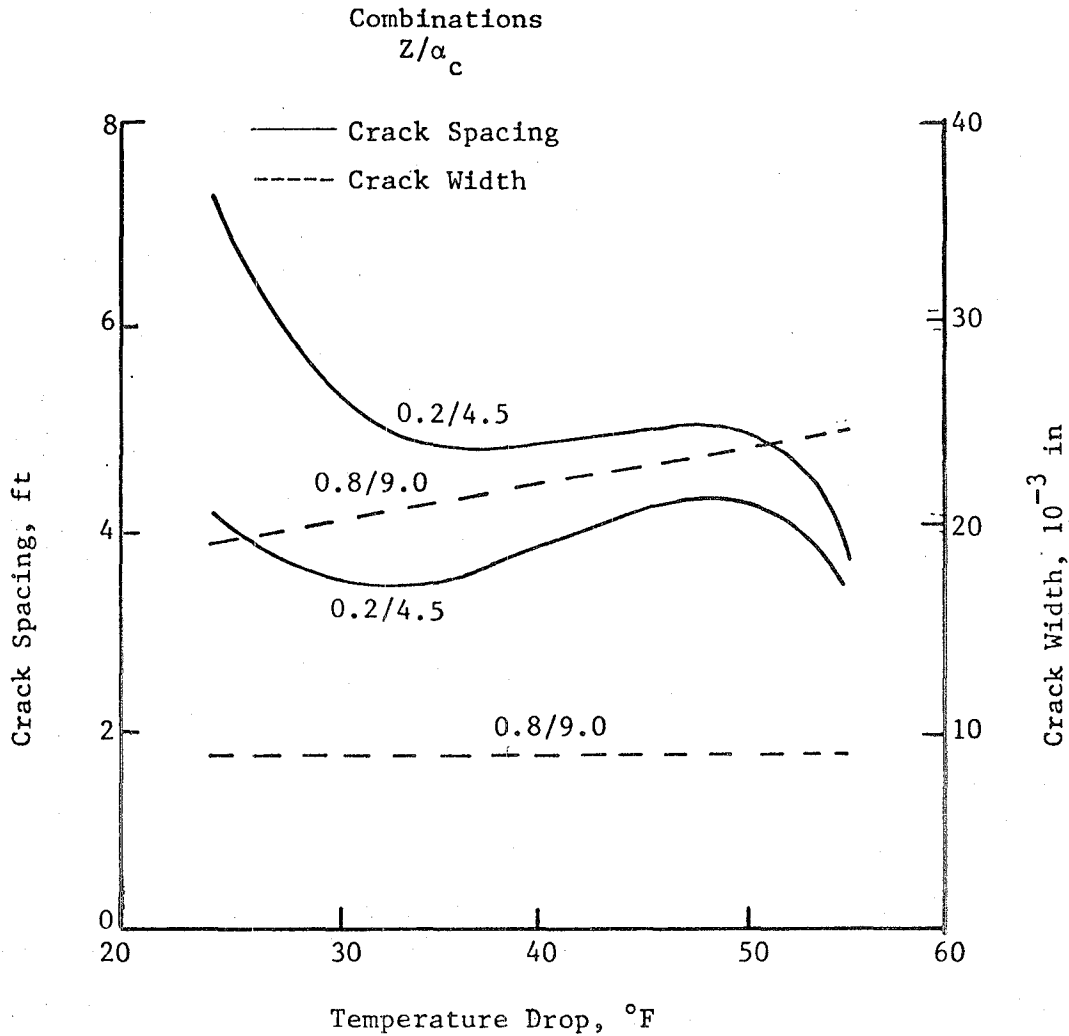
psi = 6.8948 kPa

$10^{-6}/^{\circ}\text{F} = 1.8 \times 10^{-6}/^{\circ}\text{C}$

FIGURE 51. EFFECTS OF MATERIAL PROPERTY VARIABLES ON CRACK WIDTH BY CRACK SPACING FOR THE DRY - FREEZE ZONE

Z = Concrete Shrinkage, 10^{-3}

α_c = Concrete Thermal Coefficient, $10^{-6}/^{\circ}\text{F}$



in = 25.4 mm

ft = 0.3048 m

$^{\circ}\text{C} = 1.8 (^{\circ}\text{F} - 32)$

$10^{-6}/^{\circ}\text{F} = 1.8 \times 10^{-6}/^{\circ}\text{C}$

FIGURE 52. CRACK SPACING AND CRACK WIDTH VERSUS MAGNITUDE OF TEMPERATURE DROP FOR LOW-STRENGTH CONCRETE

strength, low shrinkage, and low thermal coefficient resulted in crack spacings greater than 20 ft (6.1 m). The combinations of high concrete strength, high thermal coefficient, and both low and high levels of concrete shrinkage resulted in equal crack spacings in all environmental zones. However, the crack widths and steel stresses for these combinations with high shrinkage greatly exceeded the recommended limits in all environmental zones. The crack widths and steel stresses for the combination with low concrete shrinkage fell within the recommended limits in all but the wet-freeze zone.

For the combination with all material properties at the low level, the response criteria was not for all but the wet-freeze zone. The crack spacing in that zone was less than the recommended limit to prevent the occurrence of punchouts.

Second Stage Parameter Study. A second set of material property combinations were selected to span the limits of values used in current practice (Table 20).

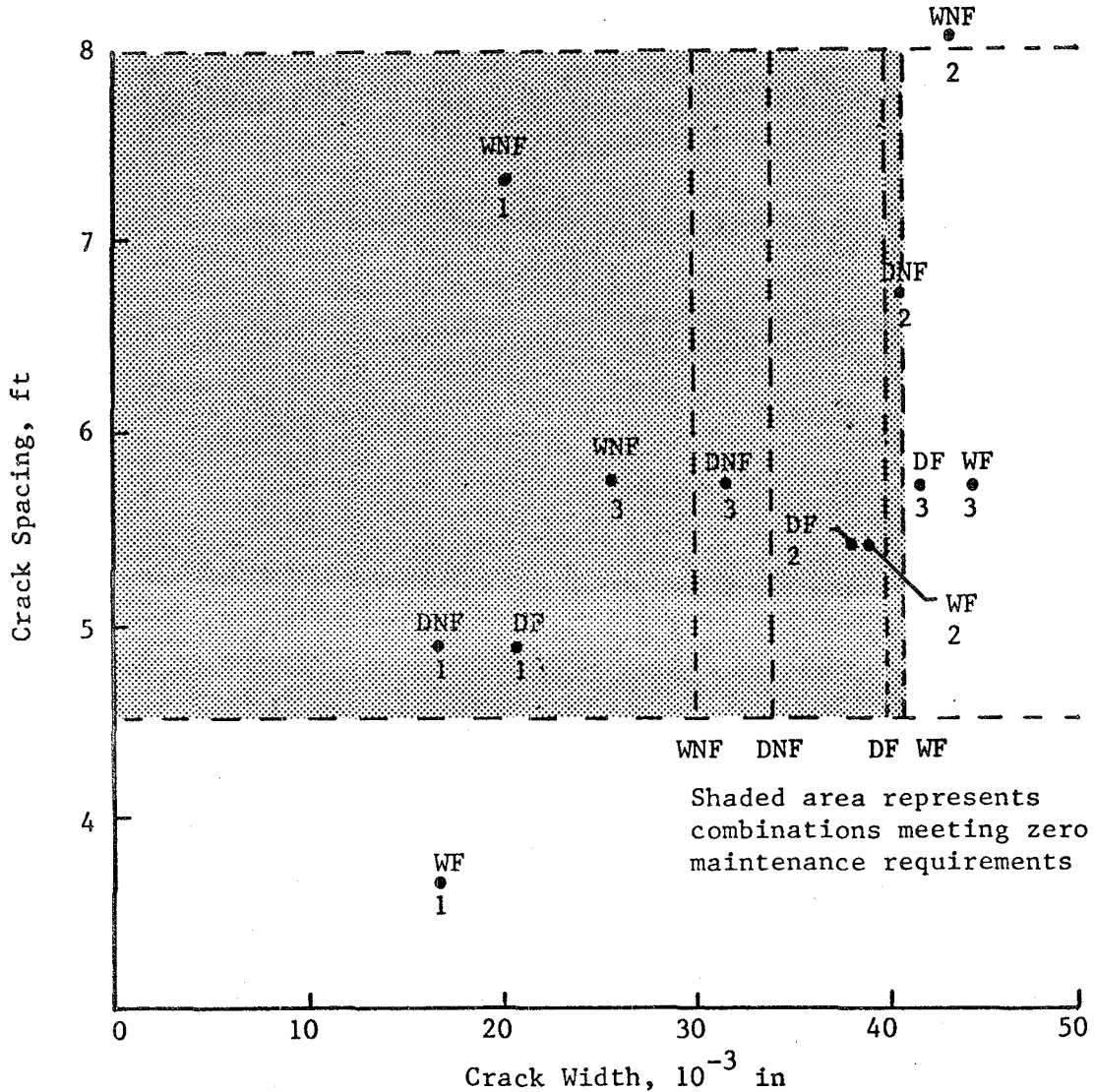
The effect of the inclusion of greater amounts of steel into a CRC pavement was shown by comparison of the 0.9 and 0.6 percent steel combinations with an ultimate concrete strength of 500 psi (3447 kPa). The crack spacing, crack width, and steel stress all decreased as the percent steel increased. Inspection of the results for higher percent steel showed that the calculated crack spacings were smaller than the punchout limiting criterion of 4.4 feet (1.34 m). The concrete strength was high enough to resist the higher stresses produced by the increased restraint provided by the additional steel. Thus, concrete strengths higher than those included in this analysis are required with the higher steel percentages.

The results from this first and second stage analysis along with the values of response parameters required for zero maintenance were plotted in Figures 53 and 54.

The results contained in these figures were all for a constant 0.6 percent steel reinforcement. No material property combination investigated produced acceptable results for all four environmental zones. The required criteria were developed from recommendations contained in Reference 84, such as that shown in Figure 47. Combination 1, which included low strength, low thermal, and low shrinkage met the required criteria in all but the wet-freeze zone. In that zone, the crack spacing dropped below the required level. Combination 2, Figure 53, met the crack spacing and width criteria for only the freeze zones. The steel stresses for combination 2 exceeded yield strength in all zones. Combination 3 met all three criteria only in the no freeze zones. Both crack width and steel stress exceeded the required limits in the freeze zones.

Several observations were made from these results. Combinations of material properties with a shrinkage greater than about 0.0004 yielded results outside the acceptable range. At the low concrete shrinkage, the

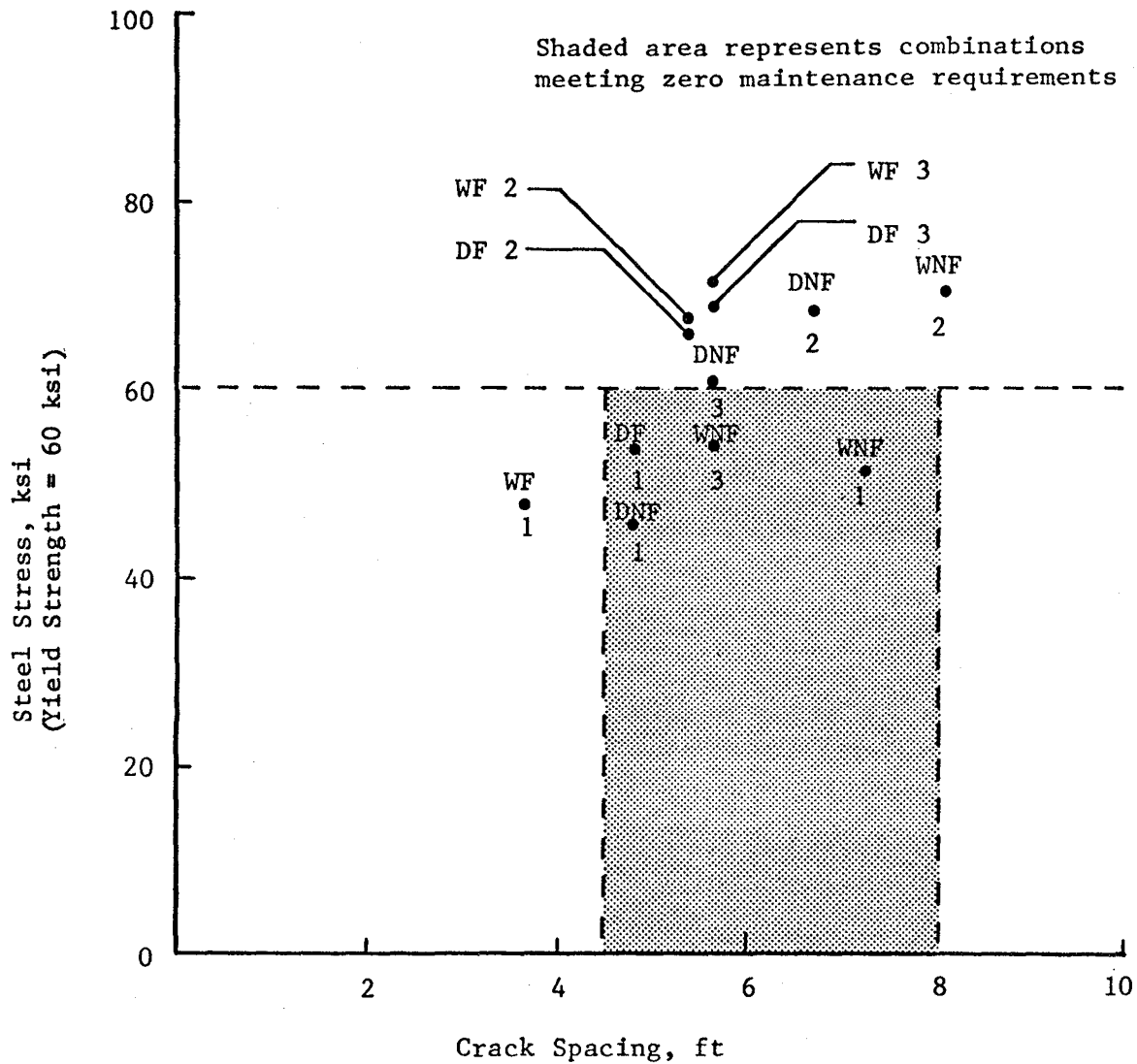
Material Properties	POINT NUMBERS		
	1	2	3
Tensile Strength, psi	400	550	800
Thermal Coefficient/°F	4.5×10^{-6}	5.0×10^{-6}	9.0×10^{-6}
Concrete Shrinkage	.0002	.0004	.0002



WF: Wet Freeze Zone in = 25.4 mm
 DF: Dry Freeze Zone ft = 0.3048 m
 WNF: Wet No Freeze Zone psi = 6.8948 kPa
 DNF: Dry No Freeze Zone $10^{-6}/^{\circ}\text{F} = 1.8 \times 10^{-6}/^{\circ}\text{C}$

FIGURE 53. SUMMARY OF CRACK SPACING AND CRACK WIDTH SHOWING REGIONS OF ACCEPTABILITY FOR ZERO MAINTENANCE PAVEMENTS

Material Properties	POINT NUMBERS		
	1	2	3
Tensile Strength, psi	400	550	800
Thermal Coefficient/°F	4.5×10^{-6}	5.0×10^{-6}	9.0×10^{-6}
Concrete Shrinkage	.0002	.0004	.0002



WF: Wet Freezing Zone ft = 0.3048 m
 DF: Dry Freezing Zone ksi = 6894.8 kPa
 WNF: Wet No Freezing Zone $10^{-6}/^{\circ}\text{F} = 1.8 \times 10^{-6}/^{\circ}\text{C}$
 DNF: Dry No Freezing Zone

FIGURE 54. SUMMARY OF CRACK SPACING AND STEEL STRESSES SHOWING REGION OF ACCEPTABILITY FOR ZERO MAINTENANCE PAVEMENTS

response parameters for the freeze regions approached the acceptable range when concrete strength was between 400 and 500 psi (2758 to 3447 kPa). The high strength concrete was better suited for application in the no freeze zones than in the freeze zones.

A subsequent analysis involved considering the effect on the response variables produced by changes in a material property. The response parameters utilized in this analysis were crack spacing and crack width. The effect on these two response parameters which was produced by the changes in the various material properties and percent steel are summarized in Table 29. The change in concrete strength produced the greatest change in both crack spacing and crack width. The second most influential material property was the thermal coefficient of concrete. Change in both crack spacing and crack width were inversely related to changes in this coefficient. The concrete shrinkage was inversely related to crack spacing and directly related to crack width. Changes in steel percentage produced greater changes in both crack width and spacing than did changes in either the thermal or coefficient shrinkage. Crack spacing and width were inversely related to steel percentage.

The order of influence of material properties investigated, starting with the most influential, were concrete strength, thermal coefficient, and shrinkage. A CRCP with 0.6 percent steel combined with a concrete of sufficient thickness and having:

- (a) a tensile strength of 500 to 550 psi (3447 to 3792 kPa)
- (b) a thermal coefficient of 4.5 to $5.0 \times 10^{-6}/^{\circ}\text{F}$ (8.1 to $9.0 \times 10^{-6}/^{\circ}\text{C}$)
- (c) a concrete shrinkage equal to or less than .0004

will provide performance compatible with zero maintenance requirements.

In this study, concrete tensile strengths greater than 550 psi (3792 kPa) produced steel stresses in excess of yield and should be avoided.

TABLE 29. EFFECTS OF UNIT CHANGES IN INPUT VARIABLES ON CRACK SPACING AND CRACK WIDTH

Property Causing Variation: (Percent Change)	Percent Steel	PCC Tensile Strength psi	PCC Thermal Coefficient $10^{-6}/^{\circ}\text{F}$	PCC Ultimate Shrinkage 10^{-4}	Change in Crack Spacing Percent	Change in Crack Width Percent
PCC Shrinkage (300%)	.6	400	4.5	2	-21	1.0
				8		
	.6	800	9.0	2	-11	32
				8		
PCC Thermal Coefficient (100%)	.6	400	4.5	2	-41	-1.4
			9.0			
	.6	800	4.5	8	-33	-16
			9.0			
PCC Tensile Strength (100%)	.6	400	4.5	2	400	373
		800				
	.6	400	9.0	8	210	206
		800				
Percent Steel (50%)	.6	500	5.5	5	-120	-99
	.9					
	.6	550	5.0	4	-100	-99
	.9					

psi = 6.89 kPa

$10^{-6}/^{\circ}\text{F} = 1.8 \times 10^{-6}/^{\circ}\text{C}$

CHAPTER 6. COMPOSITE PAVEMENT STUDY

Results from the studies of composite pavement using the distress models described in Chapter 2 and the inputs described in Chapter 3 are summarized in this chapter.

FATIGUE CRACKING

The relationships between percent fatigue cracking and time for each environmental zone are shown in Figure 55. Time was selected as the independent variable rather than equivalent axle loads, since the traffic was assumed to be uniform at 1.5 million 18-kip (80 kN) ESAL per year. These relationships show the percent cracking for each environmental zone and for the low level of concrete tensile strength and both fatigue relationships. It is quite apparent that the fatigue performance curves for each zone form a pattern similar to that reported in Chapter 4 for flexible pavements. There was a significant variation in fatigue performance from zone to zone.

These changes in fatigue performance were produced by the asphalt concrete temperature-stiffness modeling in VESYS. As the seasonal temperatures increased, the stiffness of the asphalt concrete surface decreased and the load transmitted to the underlying PCC pavement increased. This increase in load produced higher stresses and strains in the concrete with attendant lower fatigue performance. As the temperature decreased, the opposite effect occurred. As can be noted in Figure 55, the zone exhibiting the earliest appearance of class 3 and 4 cracking was the warmest zone while pavements in the colder zones took longer. As the fatigue characteristics were improved, significant increases occurred in the fatigue performance. In fact, the time required to produce the initiation of class 3 and 4 cracking doubled as the fatigue relationship was changed from low to high for a concrete tensile strength of 500 psi (3,447 kPa). At a concrete tensile strength of 1,000 psi (6,895 kPa) the fatigue performance was sufficient to meet the zero maintenance criteria for all zones for both the high and low fatigue relationship.

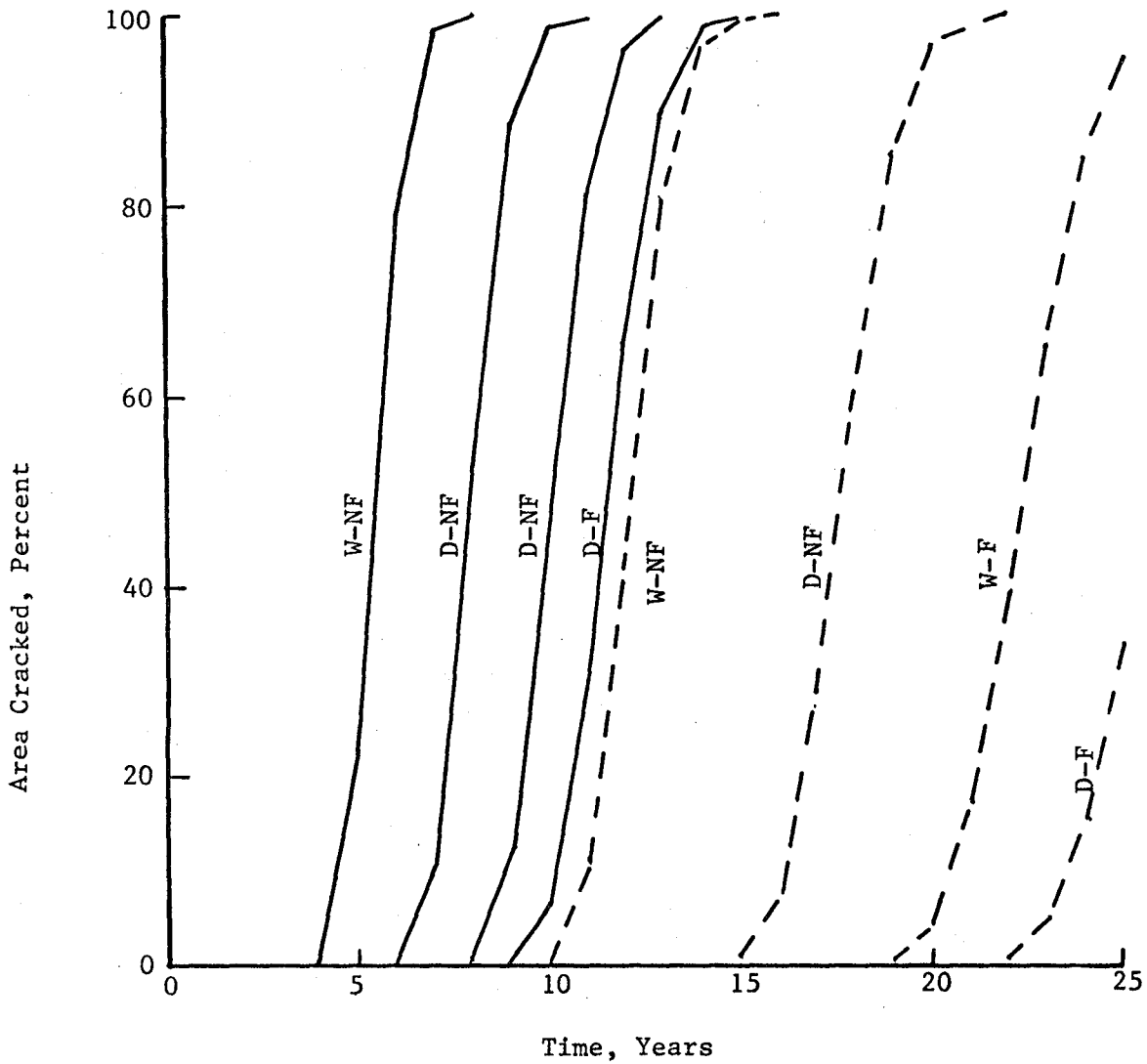
From this analysis it was concluded that:

1. It is possible to design a zero maintenance composite pavement using currently available concrete and asphalt materials. Improved materials will provide even a better possibility for zero-maintenance performance.
2. Fatigue life is affected very significantly by the seasonal temperatures in the zone, and design criteria for each should be developed to prevent the most prevalent distress occurring in the zone.

In developing criteria for selecting material requirements for zero maintenance pavements, the engineer must evaluate the uncertainties associated with obtaining the selected strength and fatigue relationship and

Legend: ——— $N_f = 18,000 (f/\sigma)^{3.9}$
 - - - - - $N_f = 40,000 (f/\sigma)^{3.9}$

f = Concrete Tensile Strength = 500 psi (3447 kPa)



W-NF: Wet-No Freeze
 D-NF: Dry-No Freeze

W-F: Wet-Freeze
 D-F: Dry-Freeze

FIGURE 55. COMPOSITE PAVEMENT FATIGUE CRACKING RESULTS FOR A 6 INCH (152 mm) ASPHALT CONCRETE OVER AN 8 INCH (203 mm) SLAB AND AN 8 INCH (203 mm) BASE

the associated costs to insure that those values are obtained. The costs and uncertainties associated with the more stringent material properties requirement must be compared with the cost and uncertainty of obtaining a thicker layer and the less stringent material property requirements for the thicker sections. Such evaluations must be performed for each proposed zero maintenance project in order to select the most cost effective combination of materials and thicknesses.

RUTTING

A limited rutting study was conducted to determine the extent of rutting in the selected composite pavement configurations. The combinations of permanent deformation characteristics selected were shown in Table 30 along with the time required to develop a 0.5 in (13 mm) rut under a loading rate of 1.5 million 18 kip (80 kN) ESAL per year. An example of the relationship between cumulative permanent deformation (rut depth) and time for the wet-freeze environmental zone is shown in Figure 56. In order to compare the rutting results from the flexible and composite studies, a summary of the flexible pavement rutting results was prepared (Table 31).

As can be noted from a comparison of the time required to produce a 0.5 in (13 mm) rut depth, rutting of surface material was not as serious in composite pavements as it was in flexible pavements. Notice that for the ALPHA/GNU combination of 0.8/1.4, (Table 31) none of the flexible pavements met the zero-maintenance rutting criteria while all composite pavements in all environmental zones met the zero-maintenance criterion (Table 30). One must remember that in the VESYS formulation, total deformation is a function of surface deflection, total thickness of the asphalt concrete layer, and the value of the permanent deformation characteristics. Since both the surface deflection and thickness of the asphalt concrete layer are smaller for the composite than for the flexible pavements, these results are not unexpected. It can be concluded that if a particular asphalt concrete mixture meets the rutting requirements for flexible pavements, it will also meet the rutting requirements for composite pavements.

REFLECTION CRACKING

Program RFLCR1 predicts tensile and shear strains in the asphaltic concrete surface resulting from the action of a joint in the underlying layer. RFLCR1 does not directly consider the formation of cracking. An elastic model of the asphalt concrete was used in RFLCR1 calculate the induced strains; therefore, the results were presented in terms of both stress and strain. The principal material properties in the study of reflection cracking were the thermal coefficient of the underlying concrete layer and the stiffness modulus of the asphalt concrete surface layer for both dynamic and thermal loading, the latter was referred to in this report as the creep modulus (Reference 6).

TABLE 30. SUMMARY OF TIMES AT WHICH RUTTING REACHED 0.5 IN (13mm)
FOR COMPOSITE PAVEMENTS THICKNESS AND MATERIAL
COMBINATIONS

Surface Thickness, in (mm)	Environmental Zone	ALPHA/GNU COMBINATION*		
		0.7/1.4	0.7/0.8	0.8/1.4
6(152)	W-F	1.7	10.8	25
	D-F	2.8	17.9	25
	W-NF	0.7	2.1	21.5
	D-NF	1.5	9.3	25
9(229)	W-F	-	3.9	-
	D-F	-	6.5	-
	W-NF	-	0.9	-
	D-NF	-	3.4	-

*Surface layers with these material combinations were placed over a portland cement concrete slab with tensile strength of 1000 psi (6,895 kPa)

Shaded area represents combinations satisfying zero-maintenance rutting criterion.

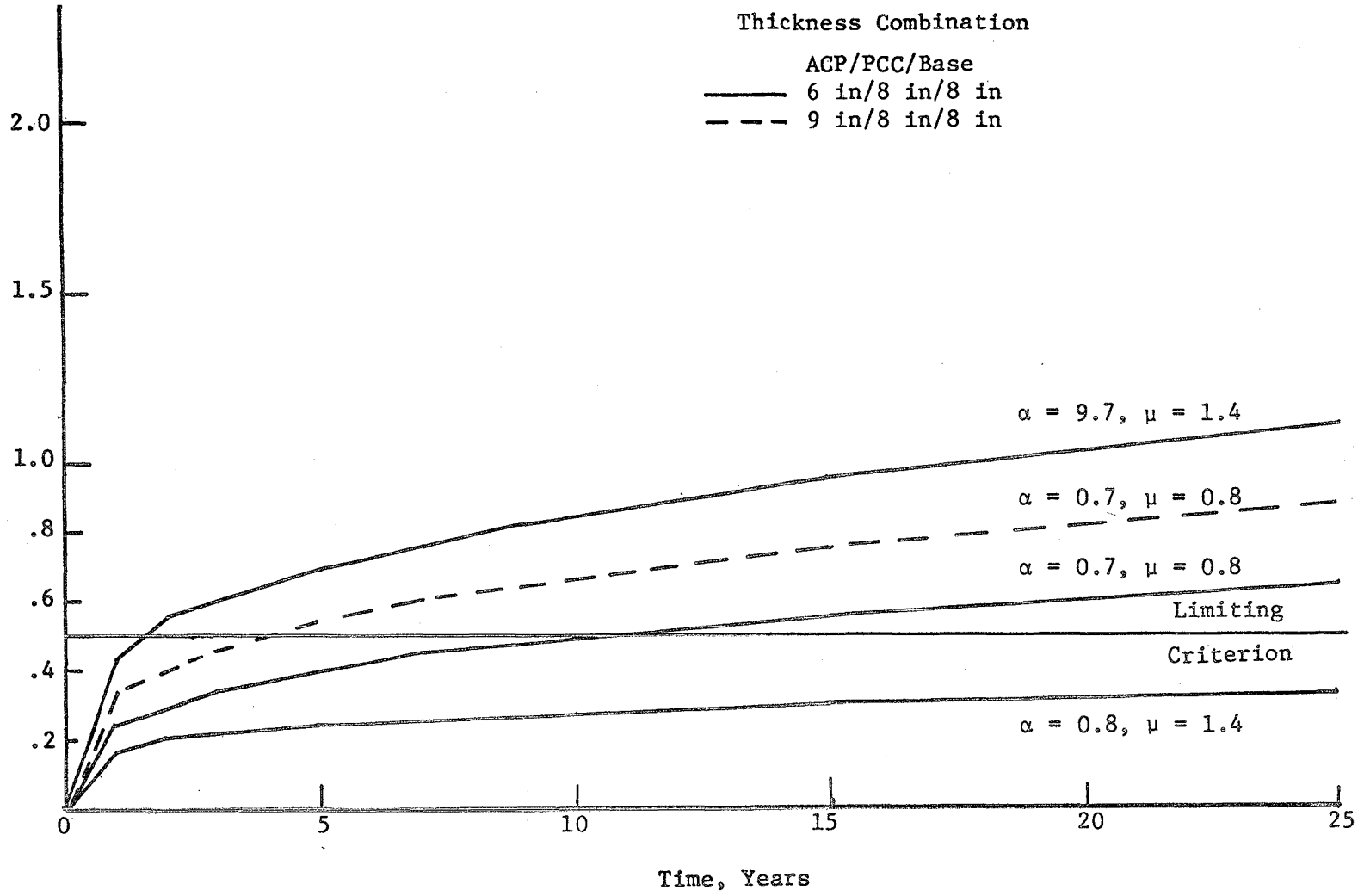


FIGURE 56. RUTTING VERSUS TIME FOR ALPHA, GNU COMBINATIONS - COMPOSITE PAVEMENT IN WET - FREEZE ZONE

TABLE 31. SUMMARY OF TIMES AT WHICH RUTTING REACHED
0.5 IN (13mm) FOR FLEXIBLE PAVEMENT
MATERIAL PROPERTY COMBINATIONS

Surface Thickness in (mm)	MATERIAL PROPERTY		ENVIRONMENTAL ZONE			
	ALPHA	GNU	Wet Freeze	Dry Freeze	Wet-No Freeze	Dry-No Freeze
13 (330)	0.7	0.2	25	25	25	19.0
		0.5	4.7	6.7	1.0	4.0
		0.8	0.9	1.2	0.6	0.9
		1.4	0.6	0.6	0.3	0.5
	0.8	0.2	25	25	25	25
		0.5	25	25	25	25
		0.8	25	25	8.0	25
		1.4	3.6	4.7	0.8	2.7
18 (457)	0.7	0.2	25	25	25	25
		0.5	4.8	8.4	1.0	4.3
		0.8	0.9	1.7	0.6	0.9
		1.4	0.6	0.6	0.3	0.6
	0.8	0.2	25	25	25	25
		0.5	25	25	25	25
		0.8	25	25	7.4	25
		1.4	4.0	6.3	0.8	3.7

Shaded areas represent combinations satisfying
zero-maintenance rutting criterion.

Horizontal Tensile Strain

Characterization of the temperature induced horizontal joint movement was required as a part of the pavement model calibration procedure. The joint movements input were selected to be consistent with the values chosen for concrete thermal coefficient, slab length, and temperature variations in each zone. These selections were made based on previous experience with the model.

The results of the model calibration were presented in Table 32 in terms of strain and Table 33 in terms of stress (the product of strain and creep modulus). Tensile strains decreased as asphalt concrete stiffness increased and increased as concrete thermal coefficient and bond stress increased. The tensile stress increased as asphalt concrete stiffness, concrete thermal coefficient, and bond stress increased.

Figure 57 illustrates the influence of asphalt concrete stiffness on induced stress in the wet freeze zone for the condition of no bond between the asphalt and portland cement concrete layers. For the selected properties, the maximum tensile strength occurred at a stiffness of approximately 400,000 psi (2,758,000 kPa). The critical stresses, where induced stress equalled tensile strength, generally occurred at high stiffness values. The concrete tensile strength required to keep the induced stress below the limiting stress at a stiffness of 5,000 psi (34,470 kPa) was less than that required at 500,000 psi (3,447,000 kPa). Also, even though the strains were much greater at the 5,000 psi (34,470 kPa) stiffness than at the 500,000 psi (3,447,000 kPa) stiffness, Table 32, the induced stresses at the 500,000 psi (3,447,000 kPa) stiffness were much greater than at 5,000 psi (34,470 kPa).

The effect of changes in the bond condition between the asphalt concrete and the portland cement concrete on horizontal tensile stress was shown in Figure 58. The induced stresses for the full bond condition were significantly greater than for other levels of bond. At intermediate bond levels, the stress at the high asphalt concrete stiffness for both low and high concrete thermal coefficients was greater than at the low asphalt concrete stiffness. At the full bond condition, the combination of low asphalt concrete stiffness and high concrete thermal coefficient yielded a higher stress than did the combination of high stiffness and low concrete thermal coefficient. Such a result indicates that as the bond stress increased toward full bond, changes in the concrete thermal coefficient produced significant changes in tensile stress.

Vertical Shear

The equation used to calculate vertical shear strain in the asphaltic concrete surface over a joint was:

TABLE 32. HORIZONTAL STRAIN RESULTS FROM REFLECTION CRACKING STUDY

Creep Modulus (@ 20,000 sec loading), psi (kPa)	Concrete Thermal Coefficient, $10^{-6}/^{\circ}\text{F}$ ($10^{-6}/^{\circ}\text{C}$)	Bond Stress between ACP and PCC, psi (kPa)	Environmental Zones			
			Wet Freeze	Dry Freeze	Wet-No Freeze	Dry-No Freeze
5,000 (34,474)	4.5 (8.1)	50 (345)	.00626	.00665	.00634	.00681
		500 (3450)	.0183	.0197	.0161	.0176
	9.0 (16.2)	50 (345)	.00937	.00975	.00816	.00789
		500 (3450)	.0276	.0283	.0259	.0261
500,000 (3,447,400)	4.5 (8.1)	50 (345)	.00126	.00137	.00114	.00112
		500 (3450)	.00215	.00231	.00194	.00196
	9.0 (16.1)	50 (345)	.00129	.00138	.00199	.00116
		500 (3450)	.00277	.0029	.00258	.00255

TABLE 33. STRESS RESULTS FROM REFLECTION CRACKING STUDY, PSI

Creep Modulus (@ 20,000 sec loading), psi (kPa)	PCC Thermal Coefficient, $10^{-6}/^{\circ}\text{F}$ ($10^{-6}/^{\circ}\text{C}$)	Bond Stress between ACP and PCC, psi (kPa)	Environmental Zones			
			Wet Freeze	Dry Freeze	Wet-No Freeze	Dry-No Freeze
5,000 (34,474)	4.5 (8.1)	50 (345)	3.13	33.2	31.7	34.1
		500 (3450)	91.5	98.5	80.5	88.0
	9.0 (16.2)	50 (345)	46.8	48.7	40.8	39.4
		500 (3450)	138	142	129	139
500,000 (3,447,400)	4.5 (8.1)	50 (345)	630	685	570	560
		500 (3450)	1075	1155	970	980
	9.0 (16.1)	50 (345)	645	690	595	580
		500 (3450)	1385	1450	1290	1275

psi = 6.8948 kPa

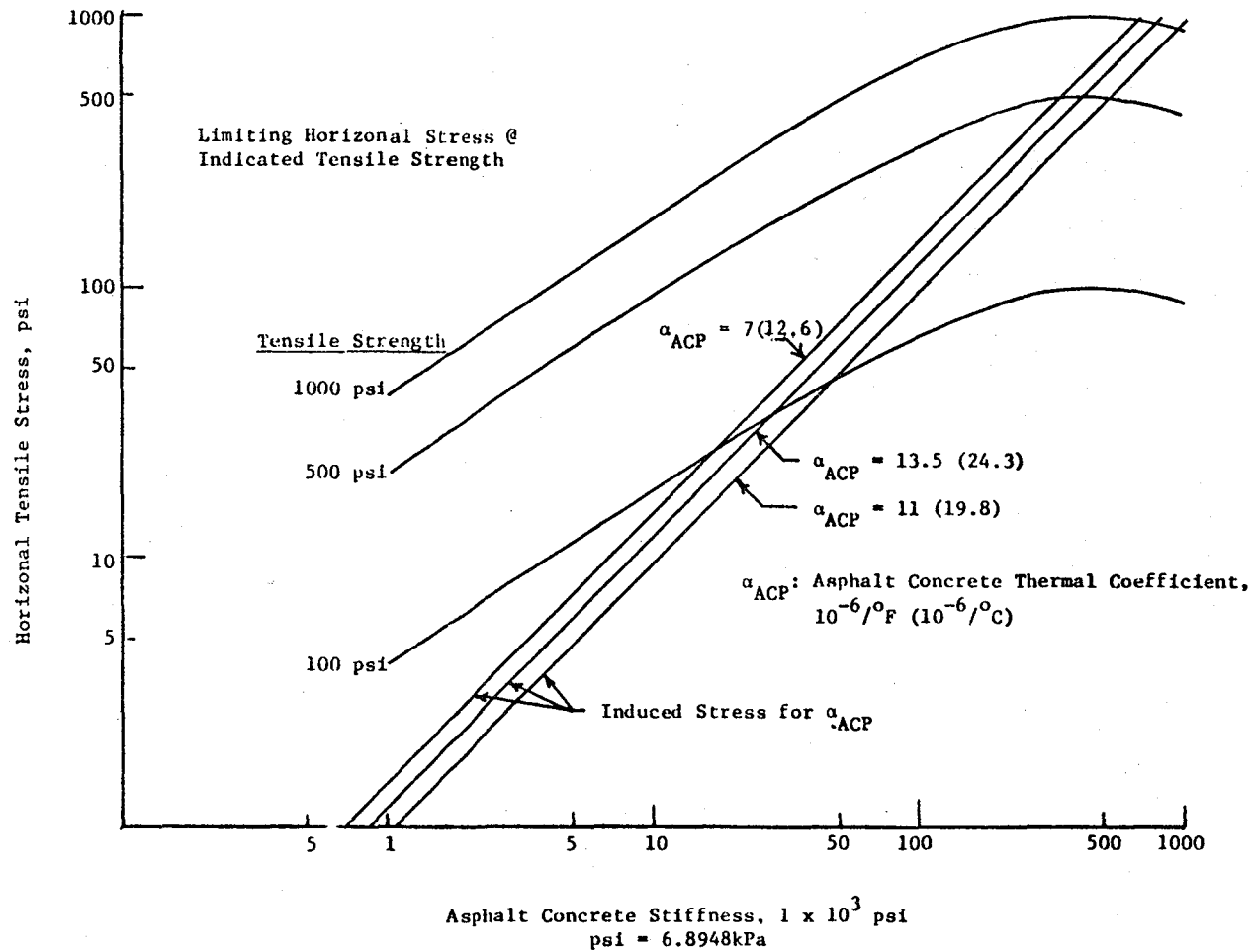


FIGURE 57. INDUCED HORIZONTAL TENSILE STRESS IN UNBOUND ASPHALT CONCRETE LAYER: ZONE: WET - FREEZE

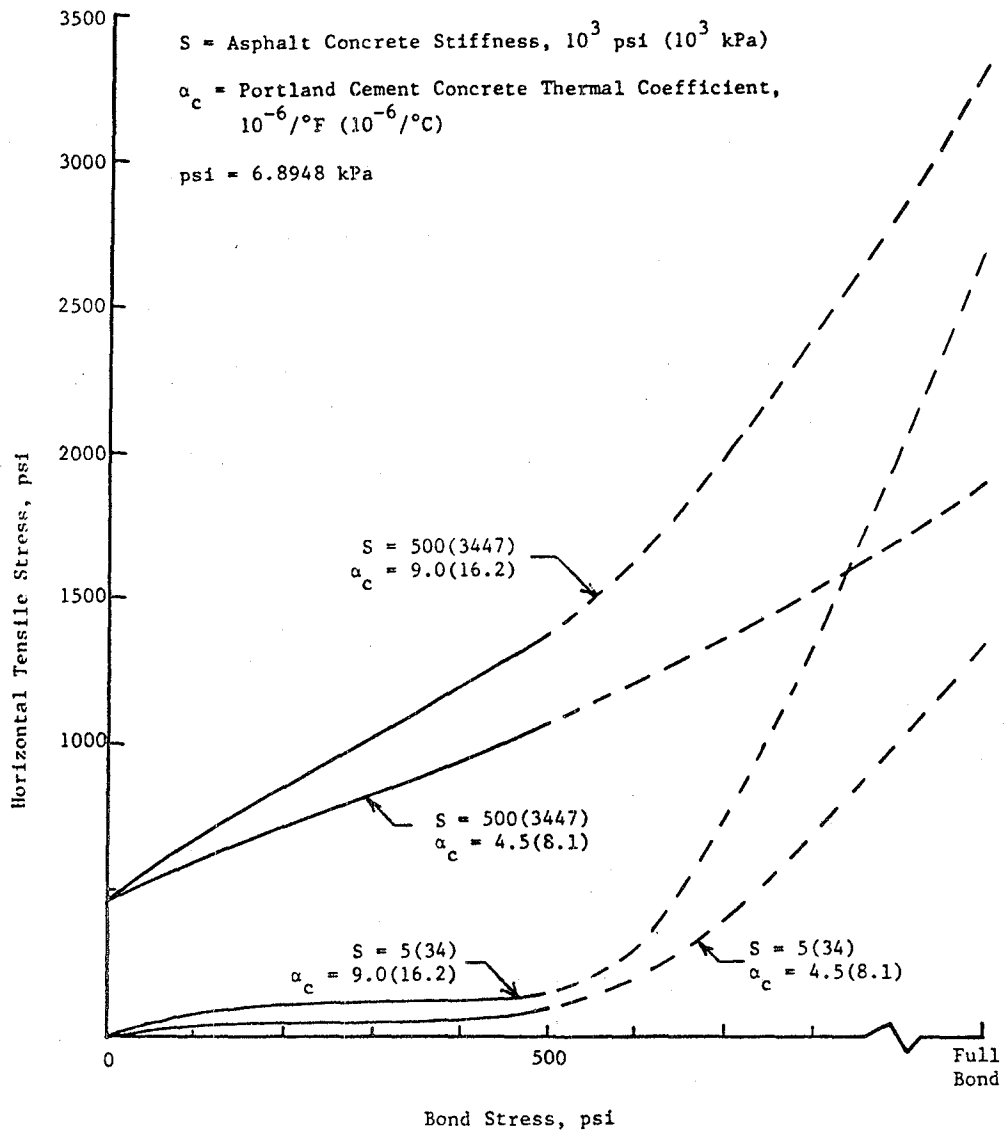


FIGURE 58. EFFECT OF BOND ON HORIZONTAL TENSILE STRESS: ZONE: WET-FREEZE

$$\gamma_o = \frac{2 \frac{L_D}{W_D} (1 - L_T) (1 + V_{ov})}{D_{ov} E_{ov}}$$

where

- γ_o = Vertical shear strain in the overlay,
- L_D = Design load = 9,000 lb (40 kN)
- W_D = Width of design load = 24 in (610 mm)
- L_T = Load transfer = $1 - \frac{W_d}{W_1}$
- W_d = Differential vertical deflection between two adjoining slabs, in
- W_1 = Deflection measured at the joint on the loaded slab, in
- V_{ov} = Poisson's ratio of overlay material = 0.3
- D_{ov} = Effective overlay thickness = 6 in (152 mm)
- E_{ov} = Dynamic modulus of overlay material, psi.

The numerical values included in the definition of variables were held constant throughout the analysis. Substituting these values into the equation produced:

$$\gamma_o = 162.5 \frac{1 - L_T}{E_{ov}}$$

Both percent load transfer and the dynamic modulus were varied over a range of values. The relationships between calculated shear strains and dynamic moduli are shown in Figure 59 for three levels of load transfer. The load transfer can vary from zero to one. The maximum shear force occurs under the load or where the maximum deflection occurs, and will vary transversely along the joint according to the deflection basin.

The evaluation of vertical shear strain was complicated by the fact that no data or test method existed which could be used to evaluate acceptable levels of shear strain in the asphalt concrete. Two indirect approaches for selecting allowable shear strains were attempted. An investigation was conducted to determine the level of shear occurring in indirect tensile and beam fatigue test specimens and to relate these shear strains to the number of applications to failure. Because the specimen fails in tension and not shear, the level of shear is below the failure level but could be used as a limiting shear strain value.

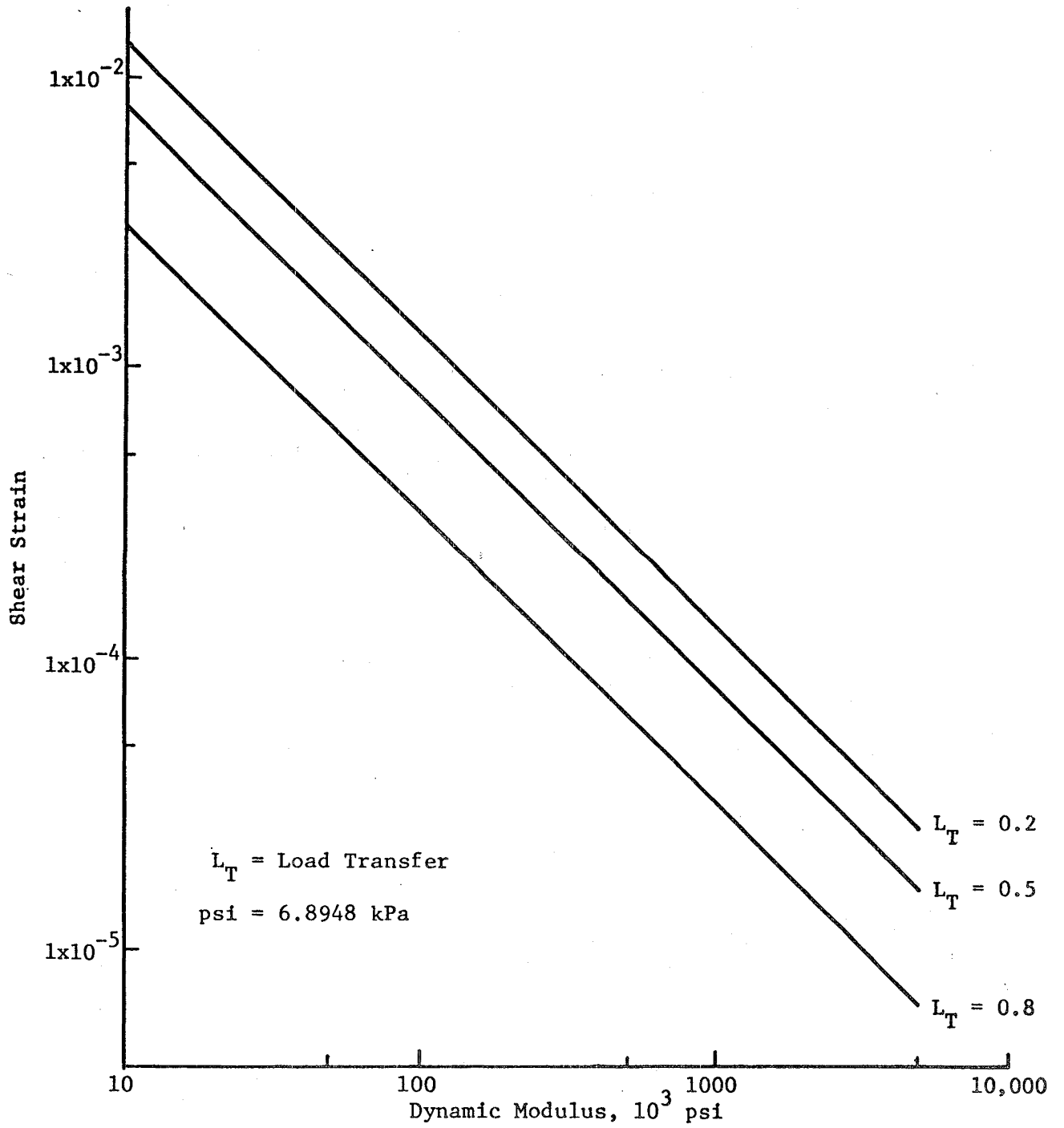


FIGURE 59. SHEAR STRAIN IN ASPHALT CONCRETE SURFACE LAYER AS A FUNCTION OF ACP DYNAMIC MODULUS AND PERCENT LOAD TRANSFER OF THE UNDERLYING JOINT

The relationship between tensile strain and shear strain in a specimen tested in indirect tension was reported by Schnitter (Reference 86¹) as:

$$\gamma = 4(1 + \mu)\epsilon$$

where:

γ = Maximum shear strain,

μ = Poisson's ratio,

ϵ = Indirect tensile strain.

The shear strain equation was substituted into a fatigue relationship developed using indirect tensile test material characterizations and observed field performance to provide an estimate of the maximum strain level at the number of repetitions required for satisfactory zero-maintenance service for composite pavements.

The relationship between the maximum shear strain and horizontal tensile strain in beam test specimen is:

$$\gamma = (1 + \mu)\epsilon_t$$

where:

γ = Maximum shear strain,

μ = Poisson's ratio,

ϵ_t = Tensile strain in beam specimen.

This shear strain equation was substituted into a fatigue relationship developed using beam tests and field observations to establish an allowable level of shear strain to eliminate fatigue at the required traffic level.

The fatigue equations based on indirect tensile and beam specimen are included in Table 34. The indirect tensile fatigue equations were those developed by Austin Research Engineers (Reference 87²) based on regression on AASHO Road Test data recorded at the time that cracking appeared at the surface. The range in fatigue coefficients selected were based on temperature

¹Schnitter, O., B.F. McCullough, and W.R. Hudson, "A Rigid Pavement Overlay Design Procedure for Texas SDHPT", Research Report 177-13, Center for Highway Research, The University of Texas at Austin, May 1978.

²"Development of New Design Criteria for Asphalt Concrete Overlays of Flexible Pavement", Vol 1, Report No. FHWA-RD-75-75, June 1975.

TABLE 34. FATIGUE EQUATIONS BASED ON INDIRECT
TENSILE AND BEAM SPECIMENS

Indirect Tensile Fatigue Specimen (References 87, 88)

$$N = K_1 \left(\frac{1}{\epsilon} \right)^{K_2} \quad \text{where:}$$

$$K_1: 2.6 \times 10^{-8} \text{ to } 3.1 \times 10^{-15} \text{ and}$$

$$K_2: 4.82 \quad \text{to } 5.16$$

Beam Fatigue Equation (Reference 89)

Initial Crack

$$\log N_f = 14.82 - 3.291 \log \frac{\epsilon}{10^{-6}} - .854 \log \frac{|E^*|}{10^3}$$

10% Cracking

$$\log N_f = 15.95 - 3.291 \log \frac{\epsilon}{10^{-6}} - .854 \log \frac{|E^*|}{10^3}$$

ϵ = tensile strain

$|E^*|$ = dynamic modulus, psi

dependent transformations presented by Rauhut and Jordahl (Reference 88¹). The beam test fatigue equation was developed by Finn, et al (Reference 89²) and was also based on observations from the AASHO Road Test. The equation by Finn, et al, was prepared because of the inclusion of a modulus term and the desire to reflect the effect of modulus changes in fatigue results. The importance of the modulus on the induced stress state was shown in Figure 57. The allowable strain levels calculated from these equations are shown in Figure 60.

Figure 60 indicates that low values of dynamic modulus are more critical than the high values. The strains developed from the beam test were one to two orders of magnitude lower than those shown from the indirect tensile test. The curve labeled Finn indicates the approximate influence of the dynamic modulus on the allowable strain. The shear strains exceed the allowable limits for a range of dynamic modulus values of 100,000 to 10,000 psi (689,480 to 68,948 kPa).

The actual allowable shear strains can be expected to be larger than indirectly derived strains shown on Figure 60 due to the tensile fatigue failure limitation for which they were derived. Thus, a conservative value of dynamic modulus may be selected at 50,000 psi (344,740 kPa), below which a greater potential for vertical shear induced reflection cracking exists.

¹Rauhut, B. and P. Jordahl, "Effects on Flexible Pavement of Increased Legal Vehicle Weights Using VESYS IIM", Report No FHWA-RD-79-116, Federal Highway Administration, January 1978.

²Finn, F.N., C. Saraf, and R. Kulkarni, "Development of Pavement Structural Subsystems", Final Report NCHRP 1-10B, National Cooperative Highway Research Program, July 1976.

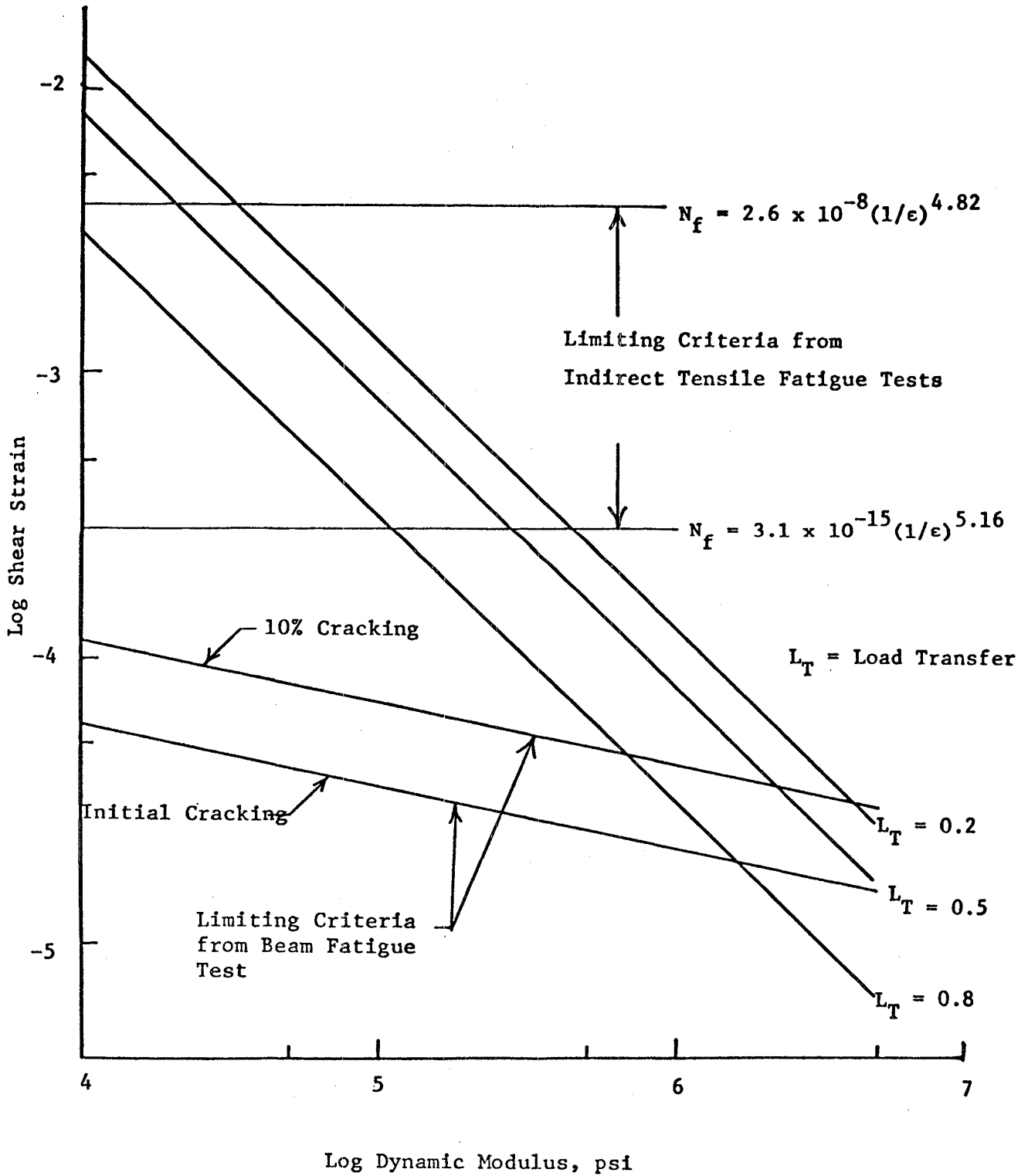


FIGURE 60. SHEAR STRAIN IN ASPHALT CONCRETE SURFACE LAYER AS A FUNCTION OF THE ACP DYNAMIC MODULUS AND PERCENT LOAD TRANSFER OF THE JOINT

CHAPTER 7. DISCUSSION, RECOMMENDATIONS, AND CONCLUSIONS

The zero-maintenance potential for materials used in each pavement type have been discussed for each major distress encountered. The range of material properties that satisfied the specified zero-maintenance criteria were identified in Chapters 4, 5, and 6 for the flexible, rigid, and composite pavements, respectively. The purpose of this chapter is to discuss the interactions of material properties on two or more distresses and to discuss the tradeoffs for those properties in terms of distress and to present the overall conclusions derived from this study.

DISCUSSION AND RECOMMENDATIONS

Flexible Pavements

The material properties utilized in the study of skid resistance were not included in any of the other studies. Therefore, the recommended values of the initial skid number and the field determined exponent suggested in Figure 39 of Chapter 4 should provide a minimum skid resistance that remains above the minimum suggested in Reference 75.

In the VESYS formulation there is no connection between the rutting and the fatigue equations, and no relationship between the material characteristic used to model the two types of distress, therefore, the studies were conducted independently and the recommended values were developed without interaction consideration. The recommended values for each environmental zone are included in Figure 34. For the pavement thicknesses utilized in this study, materials properties had a significant effect on rutting and in fact only a small range of values of ALPHA and GNU produced acceptable results. In addition, if the full-depth asphalt concrete thickness exceeding 18 inches (457 mm) is considered, additional rutting calculations should be performed to define the range of properties required to prevent excessive rutting. To establish the rutting potential of an asphalt concrete mixture that has been proposed for use in a zero-maintenance pavement, laboratory testing should be performed to determine the values of ALPHA and GNU for each mixture. Kenis (Reference 25) has proposed laboratory testing procedures for determining values for ALPHA and GNU. As can be observed from review of Figures 30 through 33, a significant difference in the rutting performance was observed for the various environmental zones. Results from VESYS showed that rutting was a significant problem in the wet-no freeze zone at values of ALPHA and GNU that did not produce significant problems in the other zones.

The fatigue cracking criterion was satisfied for several of the material property combinations included in the study. The range of material properties used in the fatigue cracking study was not wide enough for the zero maintenance fatigue criterion to be met for the 13 inch (330 mm) surface over an 8 inch (203 mm) base for any environmental zone. All combinations failed quickly even when the $\log K_1$ was changed to -25, which

corresponds to a material similar to a sulfur asphalt. Thus, the improvement in material property was not sufficient to overcome the effects of high strain in the thinner 10 inch (25 mm) and 13 inch (330 mm) pavements. However, when the thickness was increased to 16 inches (406 mm), the strains were reduced enough for variations in the material properties over the range included in this study to significantly affect the initiation of fatigue cracking as shown in Figures 18 through 21 and as summarized in Table 24. As the pavement thickness increased to 18 inches (457 mm), more than 75 percent of the material property combinations included in the study were adequate to meet the zero-maintenance fatigue criterion. The shaded area of Table 24 indicates the material property combinations that provided zero-maintenance performance.

As observed in Table 25, the occurrence of low temperature cracking for the no freeze zones was minimal. In the freeze zones, the high tensile strength and low thermal coefficient were satisfactory for an AC-10, but a crack spacing of about 20 feet (6 m) resulted for the AC-40 with the same mixture characteristics. For the freeze zones, the AC-10 with high tensile strength and low thermal coefficient minimized or prevented the formation of low temperature cracking.

Material property combinations that will prevent low temperature cracking do not necessarily correspond to the same combinations of values required to minimize fatigue and rutting. To minimize low temperature cracking, the mixture stiffness at the design low temperature should be low. In order to secure these effects, a low viscosity asphalt is required. However, low viscosity asphalts also produce a low stiffness during the warmer seasons with an attendant change in pavement stresses and strains that produce a reduction in fatigue life and an increase in rutting. McLeod (Ref. 73) has suggested values of stiffness at various temperatures that will eliminate low temperature cracking. These stiffnesses were determined at a loading time of 20,000 seconds and are included in Table 35. Applying the temperature shift techniques (Reference 74) to the 500,000 psi (3,447,000 kPa) stiffness used in the low temperature cracking study indicates that at 35°F (2°C) and a loading time of 10 cps, a stiffness of 500,000 psi (3,447,000 kPa) results instead of the value of 2×10^6 psi (13.8×10^6 kPa) used in the fatigue analysis.

As shown in Figure 38, increasing the stiffness in order to increase fatigue life also increased the stiffness at low temperature. It should be noted that reasonable stiffnesses at higher temperatures can be obtained by using the high tensile strength materials. The shaded area in Figure 38 defines the recommended design cracking index proposed by Haas (Reference 74). For primary highways, Haas recommended a maximum cracking index of 12.5 which corresponds to a crack spacing of approximately 30 feet (9.1m). Haas also indicated that results from the St. Anne road test showed that increasing the thickness of the asphalt concrete layer from 4 inches (102 mm) to 10 inches (254 mm) reduced the cracking frequency by one half. As a result, a suggested criterion for low temperature cracking of 30 ft/1,000 ft² (98 m/1,000 m²) was included in Figure 38 and adopted for use in this analysis.

TABLE 35. MAXIMUM MIX STIFFNESS FOR SELECTING ASPHALT
CEMENT GRADE (AFTER MCLEOD, REFERENCE 73)

Minimum Temperature at 2 in(51mm)Depth, °F (°C)	Stiffness Modulus, 10^6 psi (10^6 kPa)	
	Cracking Expected	Cracking Eliminated
-40 (-40)	1.0 (6.9)	0.5 (3.4)
-25 (-32)	0.7 (4.8)	0.3 (2.1)
-10 (-23)	0.4 (3.4)	0.2 (1.4)
10 (-12)	0.2 (1.4)	0.05 (0.3)

One other consideration should be mentioned relative to low temperature cracking, the type of subgrade was very important in considering the effect of the low temperature cracking on performance and maintenance. Studies by Haas have shown that if the subgrade has a very low swell potential, then the low temperature cracking will have little effect on performance and subsequent maintenance. However, if the subgrade soil is a clay, then the designer should carefully consider a choice of materials that will prevent formation of low temperature cracking. Water infiltration through the low temperature cracks may produce subsequent movements in the subgrade soil either through swelling or frost action.

Rigid Pavements

Discussion of the results for rigid pavements have been divided into sections that include common analysis for all types and those involving different models for the same analyses.

All rigid pavements. The only difference between the fatigue analyses for the JRC and JC pavements and the CRC pavements was the thickness of the concrete surface layer. As can be seen in Tables 27 and 28, the only combination of material properties failing to meet the zero-maintenance requirements for the JCP and JRCP was the low subbase modulus, low fatigue, and low concrete modulus and for the CRCP the low subbase modulus, low fatigue, and both the low and intermediate concrete moduli. In summary, conventional concrete pavements offer excellent resistance to fatigue cracking and can produce a zero-maintenance pavement. Most combinations of material properties were capable of carrying traffic for 20 years without the occurrence of class 3 and 4 cracking. In fact, the amount of traffic carried without cracking was substantially above that required. The analyses indicated that the subgrade modulus had a more significant effect on fatigue cracking than did the improvement in concrete material properties for the range of properties evaluated. In addition, the fatigue performance was more effectively increased, at the higher levels of material property, by increasing the thickness than by improving the material properties. However, zero-maintenance pavements could be produced at lesser thicknesses with improvements in the material properties and quality control. Nevertheless, material property levels of conventional concretes are adequate to meet the zero-maintenance criterion for fatigue cracking for all types of rigid pavements.

The results of the fatigue analysis indicated an optimum performance potential for a concrete with a modulus of elasticity around 5 million psi (34 million kPa) supported by a subbase with a modulus in the 1 million psi (7 million kPa) range. The indirect tensile strength corresponding to a modulus of elasticity of 5 million psi (34 million kPa) is about 500 psi (3447 kPa). This value matches very well with a tensile strength requirement for concrete at the top of the slab to prevent spalling.

JC and JRC Pavement. The erosional effects of water at the pavement-subbase interface has been identified as a primary factor in producing faulting in rigid pavements where inadequate load transfer occurs. From a

material standpoint, this problem can be minimized by designing the surface of the subbase to be resistant to those erosional effects. Control of this problem has basically been proposed through stabilization of the subbase, adequate drainage, or a combination of the two.

Joint spalling has been related to the concrete tensile strength at the surface of the pavement at the joint. The suggested minimum value for concrete tensile strength of 425 psi (2930 kPa) agrees well with the values required to maximize fatigue performance.

CRC Pavements. Several distress manifestations studied for CRCP were combined in the low-temperature and shrinkage cracking study. For this study, the development of punchouts was one of the considerations that omits the minimum crack spacing while spalling was controlled by limiting the extent of crack width. Therefore, by setting the proper limits on the low temperature and shrinkage model study, control of all these distresses were obtained.

The results from the model studies have been summarized for each environmental zone in Figures 53 and 54. The study of fatigue identified a minimal level of the modulus of elasticity of concrete. A corresponding tensile strength, using the relationships developed in Reference 90¹, was identified on the basis of the analysis. The material properties recommended for a CRC pavement are summarized in Chapter 5.

Composite Pavements

ALPHA and GNU are determined from laboratory test that are independent from other material property test and have not been directly coupled with other test results, they have been isolated from tradeoff analyses. Predicted rutting values of Tables 30 and 31 indicates that total rutting for composite pavements was not as severe as for flexible pavements for the combinations of ALPHA and GNU used in this study. Because the asphalt concrete layer is thinner for the composite than for the flexible pavement sections, less total rutting occurred in the surface layer, and no rutting occurred below the asphalt concrete surface for the composite pavement while some rutting did occur below the surface for the flexible sections. Therefore, results of these studies indicate that an asphalt concrete mixture that will perform adequately in a flexible pavement should perform adequately in a composite pavement.

No fatigue cracking occurred in the asphalt concrete surfacing because that layer was in compression, however, the underlying concrete layer was subjected to tensile strains and some fatigue cracking occurred. In the analysis using VESYS, the time to develop class 3 and 4 cracking was that for cracking to occur in the concrete itself and did not include the time

¹"ACI Standard Building Code Requirements for Reinforced Concrete", American Concrete Institute, ACI318-71, 1971.

for cracks to propagate through the asphalt concrete to the surface. For the 8 inch (203 mm) slab utilized in the studies, a tensile strength of 1000 psi (6895 kPa) was required to satisfy the zero-maintenance criteria at either the high or low fatigue relationship. However, if the slab thickness was increased slightly, a lower tensile strength concrete could be utilized in all environmental zones as verified in the rigid pavement study.

The reflection cracking study indicated that the stiffnesses required to prevent low temperature cracking in asphalt concrete surfaces was about the same as that required to prevent reflection cracking in composite pavements (Figure 57). For the range of asphalt concrete thermal coefficients, the limiting tensile stress was greater than the induced stress if the tensile strength of the asphalt concrete was above 500 psi (3447 kPa). For the lower thermal coefficient, a stiffness in the range of 500,000 psi (3447 kPa) represented a point where the induced and limiting stresses were equal. The induced stress can be reduced by providing a thin layer between the asphalt concrete and portland cement concrete that acts as a bond breaker. The effect of a bond breaker in reducing tensile strain was shown in Figure 58. If the bond stress can be reduced significantly below 500 psi (3447 kPa), then all combinations of material properties should prevent the occurrence of reflection cracking. However, as the bond stress nears 500 psi (3447 kPa), some of the combinations experienced induced tensile stresses higher than the limiting value shown in Figure 57 with the result that reflection cracking occurred.

CONCLUSIONS

From this study utilizing computer models to predict the effects of various material properties on distress, the following conclusions have been made:

1. Conventional paving materials can be utilized to produce zero-maintenance pavements, however, there are several restrictions and trade-offs that must be evaluated. Not all mixtures combinations investigated in this study can be used to design flexible, composite, and rigid pavements to meet the developed zero-maintenance performance criteria.
2. For jointed rigid pavements, performance problems center around difficulties associated with interfaces such as at the joints and at the pavement edge and between the concrete and subbase layer, and not with the concrete slab itself.
3. For continuously reinforced concrete pavements, a delicate balance exists between the material properties that control crack spacing and crack widths. These factors control the particular mixture characteristics but material property combinations are available to produce zero-maintenance CRC pavements.

4. For flexible pavements, the trade-off between stiffness at low and high temperatures presents some difficulties in developing material properties that will perform adequately in all environmental zones. However, the results from those model studies indicated that materials were available for flexible pavements that could meet the zero-maintenance criteria when the thicknesses are at the higher end used in the study.

Generally, the variability of material properties selected for the models that were based on statistical formulations corresponded to very good quality control. For these very severe traffic levels, a high variability would produce localized failures that would require maintenance. Since the primary design criterion for these roadways was no maintenance for twenty years, very high quality control was deemed appropriate and, in fact, was the only way for the predicted performance to meet the selected criteria.

The significance of surface thickness on the fatigue results obtained in this study cannot be over emphasized, especially for the flexible and composite pavement study results. For flexible pavements, the materials with the best fatigue properties included in this study were not able to overcome the high strains induced by marginal pavement thickness. Once an adequate thickness was obtained, several of the material property combinations began to provide zero maintenance performance. It is desirable to determine if there are material properties outside the range included in this investigation that might meet the zero maintenance properties. These properties may not have been measured in currently available materials but would be especially valuable for use in the thinner pavement sections. Such studies could identify sets of material properties that could serve as targets for future materials research studies.

Currently there is no technique that allows the engineer to select a set of desirable mixture properties and then design a pavement material mixture to produce those properties. Rather, the mixtures designs are made first and then specimens are tested to determine the material property values to be used in pavement model studies. Therefore, a significant need exists to develop mixture design procedures that can be used to produce mixtures with desirable engineering properties.

REFERENCES

1. Darter, M.I. and E.J. Barenberg, "Zero-Maintenance Pavements Requirements and Capabilities of Conventional Pavement Systems", Interim Report No FHWA-RD-76-105, Federal Highway Administration, April 1976.
2. McCullough, B.F., A. Abou-Ayyash, W.R. Hudson, and J.P. Randall, "Design of Continuously Reinforced Concrete Pavements for Highways", NCHRP 1-15, National Cooperative Highway Research Program, 1975.
3. Rauhut, J.B., F.L. Roberts, and T.W. Kennedy, "Material Properties to Minimize Distress in Zero-Maintenance Pavements, Volume 1. Models," Report No. FHWA/RD-80/155, Federal Highway Administration, September 1980.
4. Rauhut, J.B. and P.R. Jordahl, "Effects on Flexible Highways of Increased Legal Vehicle Weights Using VESYS IIM", Final Report No FHWA-RD-77-116, Federal Highway Administration, January 1978.
5. Finn, F.N., C. Saraf, R. Kulkarni, K. Nair, W. Smith, and A. Abdullah, "Development of Pavement Structural Subsystems", Final Report, NCHRP Project 1-10B, National Cooperative Highway Research Program, February 1977.
6. Treybig, H.J., B.F. McCullough, P. Smith, and H. Von Quintus, "Overlay Design and Reflection Cracking Analysis for Rigid Pavements, Volume 1, Development of New Design Criteria", Final Report No FHWA-RD-77-66, Federal Highway Administration, January 1978.
7. Darter, M.I., "Design of Zero-Maintenance Plain Jointed Concrete Pavement, Vol 1 - Development of Design Procedures", Report ZM-2-77, prepared by the Department of Civil Engineering, University of Illinois at Urbana-Champaign, prepared for the FHWA, June 8, 1977.
8. Shahin, M.Y., "Prediction of Low-Temperature and Thermal Fatigue Cracking of Bituminous Pavements", University of Texas, Ph.D. Dissertation, August 1972.
9. Crawford, J.E. and M.G. Katrona, "State-of-the-Art for Prediction of Pavement Response", Report No FAA-RD-75-183, U.S. Army Engineer Waterways Experiment Station, September 1975.
10. Schnitter, O., "Comparison of Stresses, Strains, and Deflections Calculated with Various Layer Programs", Pavement Design Course Term Project, University of Texas at Austin, Spring 1977.
11. Monismith, C.L., K. Inkabi, C.R. Freena, and D.E. McLean, "A Subsystem to Predict Rutting in Asphalt Concrete Pavement Structures", Proceedings, Fourth International Conference on Structural Design of Asphalt Pavements, Vol 1, August 1977.

12. Claessen, A.I.M., J.M. Edwards, P. Sommer, and P. Uge, "Asphalt Pavement Design - The Shell Method", Proceedings, Fourth International Conference on Structural Design of Asphalt Pavement, Vol 1, August 1977.
13. Kirwan, R.W., M.N. Snaith, and T.E. Glynn, "A Computer-Based Subsystem for the Prediction of Pavement Deformation", Proceedings, Fourth International Conference on Structural Design of Asphalt Pavements, Vol 1, August 1977.
14. Meyer, F.R.P. and R.C.G. Haas, "A Working Design Subsystem for Pavement Deformation in Asphalt Pavements", Proceedings, Fourth International Conference on Structural Design of Asphalt Pavements, Vol 1, August 1977.
15. Meyer, F.R.P., A. Cheetham, and R.C.G. Haas, "A Coordinated Method for Structural Distress Predictions in Asphalt Pavements", Proceedings, Meeting of the Association of Asphalt Paving Technologists, Vol 47, February 1978.
16. Huschek, S., "Evaluation of Rutting Due to Viscous Flow in Asphalt Pavements", Proceedings, Fourth International Conference on Structural Design of Asphalt Pavements, Vol 1, August 1977.
17. Shahin, M.Y., "Design System for Minimizing Asphalt Concrete Thermal Cracking", Proceedings, Fourth International Conference on Structural Design of Asphalt Pavements, August 1977.
18. Steitle, D.C. and B.F. McCullough, "Skid Resistance Considerations in the Flexible Pavement Design System", Research Report 123-9, published jointly by Texas Highway Department; Texas Transportation Institute; Texas A&M University; and Center for Highway Research, The University of Texas at Austin, April 1972.
19. Rauhut, J.B. and B.F. McCullough, "Development of Guideway Skid Control Requirements for Dual Mode Vehicle Systems", submitted to ABAM Engineers by ARE Inc, January 1974.
20. Uge, P. and P.J. Van de Loo, "Permanent Deformation of Asphalt Mixes", Proceedings, Canadian Technical Asphalt Association, Vol 19, 1974.
21. Pfeiffer, J. and P.M. Van Doormaal, "The Rheological Properties of Asphaltic Bitumen", Journal, Institution of Petroleum Technologists, No 22, 1963.
22. Van Dijk, W., "Practical Fatigue Characterization of Bituminous Mixes", Proceedings, Association of Asphalt Paving Technologists, Vol 44, February 1975.

23. Van Dijk, W. and W. Visser, "The Energy Approach to Fatigue for Pavement Design", Proceedings, Association of Asphalt Paving Technologists, Vol 46, February 1977.
24. Rauhut, J.B., J.C. O'Quin, and W.R. Hudson, "Sensitivity Analysis of FHWA Structural Model VESYS II", Report No FHWA-RD-76-23 and FHWA-RD-76-24, Federal Highway Administration, March 1976.
25. Kenis, W.J., "Predicted Design Procedures - Design Method for Flexible Pavements Using the VESYS Structural Subsystem", Proceedings, Fourth International Conference on Structural Design of Asphalt Pavements, Vol 1, August 1977.
26. Christison, J.T., "Response of Asphalt Pavements to Low Temperature", Ph.D. Dissertation, University of Alberta, 1972.
27. Hofstra, A. and A.J.G. Klomp, "Permanent Deformation of Flexible Pavements Under Simulated Road Traffic Conditions", Proceedings, Third International Conference on the Structural Design of Asphalt Pavements, Vol 1, London, 1972.
28. Heukelom, W. and A.J.G. Klomp, "Road Design and Dynamic Loading", Proceedings, Association of Asphalt Paving Technologists, Vol 33, February 1964.
29. Treybig, H.J., B.F. McCullough, P. Smith, and H. Von Quintus, "Overlay Design and Reflection Cracking Analysis for Rigid Pavements, Vol 2, Design Procedures", Report No FHWA-RD-77-67, Federal Highway Administration, August 1977.
30. Rivero-Vallejo and B.F. McCullough, "Drying Shrinkage and Temperature Drop Stresses in Jointed Reinforced Concrete Pavement", Report 177-1, Center for Highway Research, The University of Texas at Austin, August 1975.
31. Ma, J.C.M., "CRCP-2, An Improved Computer Program for the Analysis of Continuously Reinforced Concrete Pavement", University of Texas at Austin, Master Thesis, August 1977.
32. Strauss, P., B.F. McCullough, and W.R. Hudson, "Continuously Reinforced Concrete Pavements; Structural Performance and Design Construction Variables", Research Report 177-7, Center for Highway Research, The University of Texas at Austin, May 1977.
33. Huang, Y.H. and S.T. Wang, "Finite-Element Analysis of Concrete Slabs and Its Implications for Rigid Pavement Design", Highway Research Record 466, Highway Research Board, 1973.

34. Darter, M.I., E.J. Barenberg, and J.S. Sarvan, "Maintenance-Free Life of Heavily Trafficked Flexible Pavements", a paper presented at the 55th Annual Meeting of the Transportation Research Board, January 1976.
35. "Drainage of Asphalt Pavement Structures", MS-15, The Asphalt Institute, May 1966.
36. Cedergren, H.R., J.A. Arman, and K.H. O'Brien, "Development of Guidelines for the Design of Subsurface Drainage Systems for Highway Pavement Structural Sections", Report No FHWA-RD-73-14, Federal Highway Administration, February 1973.
37. "Implementation Package for a Drainage Blanket in Highway Pavement Systems", Federal Highway Administration, May 1972.
38. Cedergren, H.R., Drainage of Highway and Airfield Pavements, John Wiley and Sons, 1974.
39. Snethen, D.R., L.D. Johnson, and D.M. Patrick, "An Evaluation of Expedient Methodology for Identification of Potentially Expansive Soils", Report No FHWA-RD-77-94, Federal Highway Administration, June 1977.
40. McKeen, R.G., "Design and Construction of Airport Pavement on Expansive Soils", Report No FAA-RD-76-66, Federal Aviation Administration, June 1976.
41. Soils and Geology - Pavement Design for Frost Conditions, TM 5-818-2, Department of the Army Technical Manual, Headquarters, Department of the Army, July 1965.
42. McKeen, R.G. and J.P. Nielsen, "Characterization of Expansive Soils for Airport Pavement Design", Interim Report No FAA-RD-78-59, Federal Aviation Administration, August 1978.
43. Smith, N., R.A. Eaton, and J.M. Stubstab, "Repetitive Loading Tests on Membrane-Enveloped Road Sections During Freeze-Thaw Cycles", CRREL Report 78-12, Cold Regions Research and Engineering Laboratory, May 1978.
44. Sayward, J.M., "Evaluation of MESL Membrane-Puncture, Stiffness, Temperature, Solvents", CRREL Report 76-22, Cold Regions Research and Engineering Laboratory, June 1976.
45. Smith, N. and D.A. Pazzint, "Field Test of a MESL (Membrane-Enveloped Soil Layer) Road Section in Central Alaska", CRREL Technical Report 260, Cold Regions Research and Engineering Laboratory, July 1975.
46. Webster, S.L., "Implementation Package 74-2, Users' Manual for Membrane Encapsulated Pavement Sections (MEPS)", Federal Highway Administration, June 1974.

47. Penner, E., "Insulated Road Study", Transportation Research Record No 612, Transportation Research Board, 1976.
48. Lytton, R.L., W.F. McFarland, and D.L. Schaefer, "Flexible Pavement Design and Management, Systems Approach Implementation", NCHRP Report 160, National Cooperative Highway Research Program, 1975.
49. Adedimila, A.S. and T.W. Kennedy, "Fatigue and Resilient Characteristics of Asphalt Mixtures by Repeated-Load Indirect Tensile Test", Research Report 183-5, Center for Highway Research, The University of Texas at Austin, August 1975.
50. Monismith, C.L., J.A. Epps, D.A. Kasianchuk, and D.B. McLean, "Asphalt Mixture Behavior in Repeated Flexure", Report No. TE-70-5, Office of Research Services, University of California, Berkeley, December 1970.
51. Kallas, B.F. and V.P. Puzinauskas, "Flexural Fatigue Tests on Asphalt Paving Mixtures", ASTM STP 508, American Society for Testing and Materials, 1972.
52. Pell, P.S. and K.E. Cooper, "The Effect of Testing and Mix Variables on the Fatigue Performance of Bituminous Materials", Proceedings, Association of Asphalt Paving Technologists, Vol 44, 1975.
53. Navarro, D. and T.W. Kennedy, "Fatigue and Repeated-Load Elastic Characteristics of In-Service Asphalt-Treated Materials", Research Report 183-2, Center for Highway Research, The University of Texas at Austin, January 1975.
54. Witczak, M.W., "Development of Regression Models for Asphalt Concrete Modulus for Use in MS-1 Study", unpublished report dated January 1978, The Asphalt Institute, College Park, Maryland.
55. Hudson, W.R. and T.W. Kennedy, "An Indirect Tensile Test for Stabilized Materials", CFHR Research Report 98-1, Center for Highway Research, The University of Texas at Austin, January 1968.
56. Vallejo, J., T.W. Kennedy, and R. Haas, "Permanent Deformation Characteristics of Asphalt Mixtures by Repeated-Load Indirect Tensile Test", Research Report 183-7, Center for Highway Research, The University of Texas at Austin, June 1976.
57. Moavenzadeh, F., J.E. Soussou, H.K. Findakly, and B. Brademeyer, "Synthesis for Rational Design of Flexible Pavements", Part III, Massachusetts Institute of Technology, Cambridge, February 1974.
58. Hveem, F.N., E. Zube, and J. Skog, "Progress Report on the Zaca-Wigmore Experimental Asphalt Test Project", Symposium on Paving Materials, American Society for Testing Materials, Special Technical Publication No 277, 1959.

59. Witczak, M.W., "Development of Regression Model for Asphalt Concrete Modulus for Use in MS-1 Study", January 1978.
60. Gotolski, W.H., S.K. Ciesielski, and L.N. Heagy, "Progress Report on Changing Asphalt Properties of In-Service Pavements in Pennsylvania", Proceedings, Association of Asphalt Paving Technologists, Vol 33, February 1964.
61. Kenis, W.J., Sr., "Progress Report on Changes in Asphaltic Concrete in Service", Bulletin 333, Highway Research Board, 1962.
62. Simpson, W.C., R.L. Griffin, and T.K. Miles, "Correlation of the Microfilm Durability Test with Field Hardening Observed in the Zaca-Wigmore Experimental Project", Symposium on Paving Materials, Publication No 277, 1959.
63. Skog, J., "Results of Cooperative Test Series on Asphalts from the Zaca-Wigmore Experimental Project", Symposium on Paving Materials, American Society for Testing Materials, Special Technical Publication No 277, 1959.
64. Zube, E. and J. Skog, "Final Report on the Zaca-Wigmore Asphalt Test Road", a progress report presented to the Materials and Research Department of the California Division of Highways, 1959.
65. Corbett, L.W. and R.E. Merz, "Asphalt Binder Hardening in the Michigan Test Road after 18 Years of Service", Transportation Research Record No 544, Transportation Research Board, 1975.
66. Schmidt, R.J., "Use of ASTM Tests to Predict Low-Temperature Stiffness of Asphalt Mixes", Transportation Research Record No 544, Transportation Research Board, 1975.
67. Johnson, T.C., M.Y. Shahin, B.J. Dempsey, and J. Ingersoll, "Projected Thermal and Load-Associated Distress in Pavements Incorporating Different Grades of Asphalt Cement", Proceedings, Association of Asphalt Paving Technologists, Vol 48, February 1979.
68. National Oceanic and Atmospheric Administration, et al, "Local Climatological Data: Annual Summaries for 1977."
69. "The AASHO Road Test, Proceedings of a Conference held May 16-18, 1962, St. Louis, Mo.", Special Report 73, Highway Research Board, 1962.
70. Hudson, W.R. and F.H. Scrivner, "AASHO Road Test Principal Relationships-Performance with Stress, Rigid Pavements", Special Report 73, Highway Research Board, 1962.
71. Treybig, H.J., B.F. McCullough, and W.R. Hudson, "Tests on Existing Pavements and Synthesis of Design Methods", Vol I, CRC Airfield Pavements, Air Force Weapons Laboratory, December 1973.

72. Vesic, A.S. and S.K. Saxena, "Analysis of Structural Behavior of Road Test Rigid Pavements", NCHRP Project 1-4 (1), National Cooperative Highway Research Program, 1968.
73. McLeod, N.W., "A 4-Year Survey of Low Temperature Transverse Pavement Cracking on Three Ontario Test Roads", Proceedings, Association of Asphalt Paving Technologists, Vol 41, 1972.
74. Haas, R.C.G., "A Method for Designing Asphalt Pavements to Minimize Low-Temperature Shrinkage Cracking", Research Report 73-1, The Asphalt Institute, January 1973.
75. Kummer, H.W. and W.E. Meyer, "Tentative Skid-Resistance Requirements for Main Rural Highways", NCHRP Report 37, National Cooperative Highway Research Program, 1967.
76. Hveem, F.N., "A Report of an Investigation to Determine Causes for Displacement and Faulting at the Joints in Portland Cement Concrete Pavements on California Highways", State of California Division of Highways, Materials and Research Department, May 1949.
77. Gessaman, J.D., "The Performance of Unbonded Concrete Resurfacing on Iowa Highways", Portland Cement Association, 1959.
78. Neal, B.F. and J.H. Woodstrom, "Faulting of Portland Cement Concrete Pavements", Report No FHWA-CA-TL-5167-77-20, California Department of Transportation, July 1977.
79. Gulden, W., "Pavement Faulting Study", Final Report, Georgia Department of Transportation, May 1975.
80. Kalb, M.R., "Investigation of Slab Differential Movement on I-83 Baltimore-Harrisburg Expressway", Final Report, Maryland State Highway Administration, February 1972.
81. Cedergren, H.R., K.H. O'Brien, and J.A. Arman, "Guidelines for the Design of Subsurface Drainage Systems for Highway Structural Sections", Report FHWA-RD-72-30, Federal Highway Administration, 1972.
82. Panak, J.J. and H. Matlock, "A Discrete-Element of Analysis for Orthogonal Slab and Grid Bridge Floor Systems", Research Report 56-25, Center for Highway Research, The University of Texas at Austin, 1971.
83. Hudson, W.R. and H. Matlock, "Discontinuous Orthotropic Plates and Pavement Slabs", Research Report 56-6, Center for Highway Research, The University of Texas at Austin, 1966.
84. Ma, J.C.M., C.S. Noble, and B.F. McCullough, "Design Criteria for Continuously Reinforced Concrete Pavements", Research Report 177-17, Center for Highway Research, The University of Texas at Austin, May 1979.

85. Majidzadeh, K., "Observations of Field Performance of Continuously Reinforced Concrete Pavements in Ohio", Report No OHIO-DOT-12-77, Ohio Department of Transportation, September 1978.
86. Schnitter, O., B.F. McCullough, and W.R. Hudson, "A Rigid Pavement Overlay Design Procedure for Texas SDHPT", Research Report 177-13, Center for Highway Research, The University of Texas at Austin, May 1978.
87. "Development of New Design Criteria for Asphalt Concrete Overlays of Flexible Pavement", Vol 1, Report No FHWA-RD-75-75, June 1975.
88. Rauhut, B. and P. Jordahl, "Effects on Flexible Pavement of Increased Legal Vehicle Weights Using VESYS IIM", Report No FHWA-RD-79-116, Federal Highway Administration, January 1978.
89. Finn, F.N., C. Saraf, and R. Kulkarni, "Development of Pavement Structural Subsystems", Final Report NCHRP 1-10B, National Cooperative Highway Research Program, July 1976.
90. "ACI Standard Building Code Requirements for Reinforced Concrete", American Concrete Institute, ACI318-71, 1971.



FEDERALLY COORDINATED PROGRAM (FCP) OF HIGHWAY RESEARCH AND DEVELOPMENT

The Offices of Research and Development (R&D) of the Federal Highway Administration (FHWA) are responsible for a broad program of staff and contract research and development and a Federal-aid program, conducted by or through the State highway transportation agencies, that includes the Highway Planning and Research (HP&R) program and the National Cooperative Highway Research Program (NCHRP) managed by the Transportation Research Board. The FCP is a carefully selected group of projects that uses research and development resources to obtain timely solutions to urgent national highway engineering problems.*

The diagonal double stripe on the cover of this report represents a highway and is color-coded to identify the FCP category that the report falls under. A red stripe is used for category 1, dark blue for category 2, light blue for category 3, brown for category 4, gray for category 5, green for categories 6 and 7, and an orange stripe identifies category 0.

FCP Category Descriptions

1. Improved Highway Design and Operation for Safety

Safety R&D addresses problems associated with the responsibilities of the FHWA under the Highway Safety Act and includes investigation of appropriate design standards, roadside hardware, signing, and physical and scientific data for the formulation of improved safety regulations.

2. Reduction of Traffic Congestion, and Improved Operational Efficiency

Traffic R&D is concerned with increasing the operational efficiency of existing highways by advancing technology, by improving designs for existing as well as new facilities, and by balancing the demand-capacity relationship through traffic management techniques such as bus and carpool preferential treatment, motorist information, and rerouting of traffic.

3. Environmental Considerations in Highway Design, Location, Construction, and Operation

Environmental R&D is directed toward identifying and evaluating highway elements that affect

the quality of the human environment. The goals are reduction of adverse highway and traffic impacts, and protection and enhancement of the environment.

4. Improved Materials Utilization and Durability

Materials R&D is concerned with expanding the knowledge and technology of materials properties, using available natural materials, improving structural foundation materials, recycling highway materials, converting industrial wastes into useful highway products, developing extender or substitute materials for those in short supply, and developing more rapid and reliable testing procedures. The goals are lower highway construction costs and extended maintenance-free operation.

5. Improved Design to Reduce Costs, Extend Life Expectancy, and Insure Structural Safety

Structural R&D is concerned with furthering the latest technological advances in structural and hydraulic designs, fabrication processes, and construction techniques to provide safe, efficient highways at reasonable costs.

6. Improved Technology for Highway Construction

This category is concerned with the research, development, and implementation of highway construction technology to increase productivity, reduce energy consumption, conserve dwindling resources, and reduce costs while improving the quality and methods of construction.

7. Improved Technology for Highway Maintenance

This category addresses problems in preserving the Nation's highways and includes activities in physical maintenance, traffic services, management, and equipment. The goal is to maximize operational efficiency and safety to the traveling public while conserving resources.

0. Other New Studies

This category, not included in the seven-volume official statement of the FCP, is concerned with HP&R and NCHRP studies not specifically related to FCP projects. These studies involve R&D support of other FHWA program office research.

* The complete seven-volume official statement of the FCP is available from the National Technical Information Service, Springfield, Va. 22161. Single copies of the introductory volume are available without charge from Program Analysis (HRD-3), Offices of Research and Development, Federal Highway Administration, Washington, D.C. 20590.

B342

11

